AD-A146 538

AD

CURRENT STATUS OF

BLAST WAVE THEORY

AND COMPUTATIONS

Vol.II The quasi-similar solution

by

Mostafa M. Kamel and Amr M. Abdel Raouf

Faculty of Engineering
Cairo University, Egypt

OCT 5 1984

A

March, 1984

This document has been approved
for public release and sale; its
distribution is unlimited.

BEST
AVAILABLE COPY

84 10 01 146

CURRENT STATUS OF BLAST WAVE
THEORY AND COMPUTATIONS
VOLUME II. THE QUASI-SIMILAR SOLUTIONS

by

Mostafa M. Kamel and Amr M. Abdel Raouf
Faculty of Engineering
Cairo University, Egypt

March, 1984

PREFACE

The first volume of this monograph included the formulation and self-similar solutions to blast waves. The next step in our exposition of **Blast Wave Theory and Computations** then expresses the need for presenting analytical solutions that, in effect, extend the range of validity of self-similar ones. The authors found that the one analytical method that is most amenable to solving different classes of problems is the Quasi-Self-Similar Method developed by Oshima. It was then decided to devote the second volume of this series to presenting a complete exposition to this method that includes solutions to several types of problems, most are included here for the first time.

In this volume, after a concise introduction in Chapter I, the basic blast wave equations are presented in Chapter II. A novel treatment of the quasi-similar formulation, presenting it as a zero order solution to a double Taylor's series expansion is presented in Chapter III. Applications are then presented in Chapter IV which is divided into six parts. The first two parts include solutions to the adiabatic point explosion problem, the latter being an analytical closed form solution. The third part deals with blast waves in real gases, where the formulation is presented here in more details than that presented in Volume I. Blast waves in a detonating medium is included in the fourth part, with energy added in the front. Blast waves in reactive media where the detonation energy is released in a spacially varying fashion, are given in the fifth part. Finally, in the sixth part, the effects of viscosity, heat conduction and radiation on detonation are presented.

The authors are greatly indebted to Mrs. Ellen Kamel, Mrs. Janie Abdel Aziz and Mr. Taher Nour for their ability to produce this neatly typed monograph. The efforts of Eng. Salah Roushdy in producing the graphs can only make one wonder at the extent of human endurance.

This work is supported in part by the U.S. Army Office of Scientific Research - European Research Office under

Accession For

ii

CONTENTS

CHAPTER I

NON-SELF-SIMILAR BLAST WAVES

I.1 INTRODUCTION

Blast waves considered here are geometrically symmetrical, non-steady flow fields of a compressible medium that are bounded by gasdynamic discontinuities. Generally they are formed by explosions. The process is governed by spatially one-dimensional time dependent equations expressing the conservations of mass, momentum and energy, subject to the appropriate boundary conditions at the center and at the front for the particular problem under consideration.

I.2 SELF-SIMILAR BLAST WAVES

In Volume I of this report, it has been shown that under certain conditions the blast wave equations may be reduced to a set of ordinary differential equations in terms of a single similarity variable, thus making them amenable to simple analysis. This may occur, in general, when the dependence of the gasdynamic parameters on the front coordinate is anihilated. Such self-similar problems are, as a rule, characterized either by a constant front velocity, or by a negligible, essentially zero, counter-pressure that causes the Mach number of the wave to remain infinite, irrespective of its actual velocity. In addition, the specific heat ratio of the gas, as well as any existing source terms of mass, momentum or energy, may only be admitted as functions of the non-dimensional similarity variable. If the wave front were moving into a variable density atmosphere, then the ambient density dependence should be restricted only to a constant power of the distance from the center of symmetry.

The power and versatility of the concept of self-similarity have been demonstrated in Volume I by a wide variety of possible applications.

In many physical situations, however, especially when one is interested in the interpretation of experimental records, wave front Mach numbers are finite and the waves either accelerate or decay. Under such circumstances similarity conditions are inapplicable. One then has to take into account the dependence of the gasdynamic parameters of the problem on the change in conditions at the

front, as well as their change within the flow field. It thus becomes necessary to contend with a system of non-linear, coupled, non-homogeneous set of partial differential equations.

I.3 THE QUASI-SIMILAR METHOD

An analytical solution to this set of equations utilizing the so-called "quasi-similar" method developed by Oshima (1960, 1962, 1964). By postulating a "separation of variables" relation between the dependent and the independent variables, then, due to the logarithmic nature of the governing equations, all the terms containing the front coordinate may take their values at the front. The equations, thus, are reduced to a system of ordinary differential equations, identical to the self-similar ones, with the dependence on the front coordinate included only as an additive algebraic term that has the front coordinate as a parameter. An explanation of the theoretical basis of the quasi-similarity method was given later by Kamel (1971). He proved that the quasi-similarity approximation is the zeroth-order solution of a double Taylor's series expansion of the dependent variables.

The numerical solution to the quasi-similar equations, for constant energy blast waves, has been tabulated by Lewis (1961) for the plane, cylindrical, and spherical symmetries with a variety of specific heat ratios, while Oshima (1960, 1964) obtained an approximate closed form solution. This method was then used by Lee (1967) to study the non-uniform propagation of imploding shocks and detonations, while Oshima (1967) attempted to apply it to the decoupled shock-deflagration system. Rae (1963, 1965, 1968), on the other hand, used it in conjunction with his meteoroid impact solutions. Attia (1974) used this method to obtain a non-self-similar solution of blast waves in adiabatic point explosions based on the criterion of zero particle velocity at the center of symmetry. In Chapter XI of Volume I of this report, the quasi-similar method was used to obtain a solution to blast waves taking into account real gas effects (Ghuneim, 1975; Kamel et al., 1977b). The problem of non-self-similar detonation waves was solved by Abdel-Raouf (1982) and that with transport phenomena taken into account was also solved by the same author (1982) Ohyagi et al. (1981) took into account the distribution of fuel concentration in a reactive medium by an exponential model of heat release, in terms of the front coordinate, and ob-

tained a solution for the spherical wave by utilizing the quasi-similar technique.

In this volume, the quasi-similar method of Oshima is analyzed and discussed briefly, since it is a simple and qualitatively accepted analytical method of solution which has a wide range of applicability. A wide range of possible applications are included. These applications deal with blast waves: in an adiabatic medium; with conduction and radiation effects and with real gas effects, as well as flame and detonation induced blast waves.

CHAPTER II

BASIC EQUATIONS

II.1. INTRODUCTION

The phenomenon of wave propagation in gases constitutes unsteady motion of the flowing medium, which is governed by the conservation equations, namely the conservation of mass, momentum, and energy. When the condition of symmetry is satisfied, the flow field behind the shock wave is one-dimensional, i.e., the gasdynamic parameters will then depend only on one spatial coordinate r, measured from the center of explosion, and the time t, measured from the instant of explosion.

In this chapter, the fundamental conservation equations are formulated applicable for the three geometrical symmetries; planar, cylindrical and spherical, without restrictions imposed by a specific form of an equation of state and including any possible source terms of mass, momentum or energy that may affect the flow field. The fundamental equations are thus, accordingly, transformed, with the use of appropriate non-dimensional variables and parameters, to a most concise non-dimensional form, of Eulerian space profiles, for an arbitrary equation of state relating the internal energy with pressure and density. The formulation of the problem is then completed by the specification of the boundary conditions imposed by a gasdynamic discontinuity at the wave front.

The integral relations, which are the global conservation equations of mass, momentum and energy, are also formulated in their general form. These relations serve a dual purpose; in addition to providing a check on the accuracy of the flow field obtained by solving the conservation equations, they also provide means for the determination of the front trajectory.

Finally, the reduction of the conservation equations, boundary conditions and integral relations to their simplest forms for a medium which behaves as a perfect gas with constant specific heats as well as in the case of strong explosion, or self-similar motion, is determined.

II.2. THE CONSERVATION EQUATIONS

The governing equations, when taking into account possible sources of mass, momentum or energy that may affect the flow field, are expressed, as given by Oppenheim et al. (1971) as follows:

$$\frac{\partial}{\partial t}(\rho r^j) + \frac{\partial}{\partial r}(\rho u r^j) = \rho r^j \lambda_M \tag{II.1}$$

$$\frac{\partial}{\partial t}(\rho u r^j) + \frac{\partial}{\partial r}\left[(u^2 + \frac{P}{\rho})\rho r^j\right] = \rho r^j (\frac{jP}{\rho r} + \lambda_F) \tag{II.2}$$

$$\frac{\partial}{\partial t}\left[(e + \frac{u^2}{2})\rho r^j\right] + \frac{\partial}{\partial r}\left[(e + \frac{u^2}{2} + \frac{P}{\rho})\rho u r^j\right] = \rho r^j \lambda_E \tag{II.3}$$

where u is the particle velocity, ρ is the density, P is the pressure and e is the specific internal energy. The index j is a geometrical factor defined in terms of the variation of the flow cross-sectional area A with distance as:

$$j \equiv \frac{d \ln A}{d \ln r} = 0, 1, 2$$

for plane, cylindrical and spherical symmetrical flow, respectively. The symbols λ_M, λ_F and λ_E represent the mass, momentum and energy source terms, respectively, per unit mass of the flowing medium.

II.3. **THE EQUATION OF STATE**

The governing equations, Eqs. (II.1) - (II.3), are completed by the equation of state that expresses the internal energy in terms of pressure and density. Thus, since $e = e (P , \rho)$ it follows that

$$de = \left(\frac{\partial e}{\partial \ln P}\right)_\rho d \ln P + \left(\frac{\partial e}{\partial \ln \rho}\right)_\rho d \ln \rho \qquad (II.4)$$

from the above equation, one has

$$\left(\frac{\partial e}{\partial \ln P}\right)_S = \left(\frac{\partial e}{\partial \ln P}\right)_\rho + \left(\frac{\partial e}{\partial \ln \rho}\right)_\rho \left(\frac{\partial \ln \rho}{\partial \ln P}\right)_S$$

where subscript S denotes entropy.
While for a constant entropy process, the first law of thermodynamics requires that

$$di = \frac{dP}{\rho}$$

where i is the specific enthalpy.
Thus

$$di = d\left(e + \frac{\rho}{\rho}\right) = de + \frac{dP}{\rho} - \frac{P d\rho}{\rho^2} = \frac{dP}{\rho}$$

or

$$de = \frac{P d\rho}{\rho^2}$$

from the above equation, one has in general

$$\left(\frac{\partial e}{\partial \ln P}\right)_S = \frac{P}{\rho}\left(\frac{\partial \ln \rho}{\partial \ln P}\right)_S$$

Hence it follows that

$$\left(\frac{\partial e}{\partial \ln P}\right)_\rho = \left[\frac{P}{\rho} - \left(\frac{\partial e}{\partial \ln \rho}\right)_P\right]\left(\frac{\partial \ln \rho}{\partial \ln P}\right)_S \qquad (II.5)$$

defining now a non-dimensional isentropic compressibility, or velocity of sound modulus

$$\Gamma \equiv \left(\frac{\partial \ln P}{\partial \ln \rho}\right)_S = \frac{\rho}{P} a^2 \qquad (II.6)$$

and a non-dimensional internal energy factor

$$\mathcal{K} \equiv -\frac{\rho}{P}\left(\frac{\partial e}{\partial \ln \rho}\right)_P \qquad (II.7)$$

Thus, Eq. (II.5) reduces to

$$\left(\frac{\partial e}{\partial \ln P}\right)_\rho = \frac{\mathcal{K}+1}{\Gamma}\cdot\frac{P}{\rho} \qquad (II.8)$$

and Eq. (II.4) becomes

$$de = \frac{\mathcal{K}+1}{\Gamma}\frac{P}{\rho}\,d\ln P - \mathcal{K}\frac{P}{\rho}\,d\ln \rho \qquad (II.9)$$

Equation (II.9) represents the general equation of state in a differential form.

Taking partial derivatives of the above with respect to the space coordinate, r, and the time, t, respectively, one obtains finally:

$$\frac{\partial e}{\partial r} = \frac{k+1}{\Gamma} \frac{P}{\rho} \frac{\partial \ln P}{\partial r} - k. \frac{P}{\rho} \frac{\partial \ln \rho}{\partial r} \qquad (II.10)$$

and

$$\frac{\partial e}{\partial t} = \frac{k+1}{\Gamma} \frac{P}{\rho} \frac{\partial \ln P}{\partial t} - k \frac{P}{\rho} \frac{\partial \ln \rho}{\partial t} \qquad (II.11)$$

II.4. NON-DIMENSIONAL VARIABLES AND PARAMETERS

The next step is to cast the governing equations, Eqs. (II.1) - (II.3), in their most convenient non-dimensional form. The various non-dimensional variables and parameters can be properly specified by referring to Fig.II.1 which represents the various blast wave coordinates in the time-space domain. The origin of the system is, as a rule, at $t = 0$ and $r = 0$, and the coordinates of the front are t_n and r_n. With reference to Fig. II.1, the Eulerian space profiles are obtained by seeking a solution along $t = t_n$ or $\tau = 1$, where

$$\tau \equiv \frac{t}{t_n} \qquad (II.12)$$

Therefore, the following groups of non-dimensional variables and parameters will be used:

i) Physical space coordinates, the independent variables of the problem:

$$\chi \equiv \frac{r}{r_n} \qquad ; \qquad \zeta \equiv \frac{r_n}{r_o} \qquad\qquad (II.13)$$

where the first is referred to as the field coordinate and the second as the front coordinate. The symbol (r) denotes the space coordinate of a point in the flow field while (r_n) is the radius of the front at the same instant of time, subscript (o) specifying a reference value. It should be noted that when the front trajectory is known, ζ becomes a measure of time.

ii) Front parameters, i.e. variables pertaining uniquely to the front motion and, therefore, are functions of only the front coordinate, ζ :

$$y \equiv \frac{a_a^2}{w_n^2} = \frac{1}{M^2} \quad ; \quad \gamma \equiv \frac{t_n}{t_o} \quad ; \quad \lambda \equiv -2\frac{d\ln w_n}{d\ln r_n} = \frac{d\ln y}{d\ln \zeta} - 2\frac{d\ln a_a}{d\ln \zeta}$$

$$\mu \equiv \frac{d\ln r_n}{d\ln t_n} = \frac{d\ln \zeta}{d\ln t_n} = \frac{w_n t_n}{r_n} \quad ; \quad \rho_a' \equiv \frac{d\ln \rho_a}{d\ln r_n} = \frac{d\ln \rho_a}{d\ln \zeta} \quad (II.14)$$

where $w_n \equiv \frac{dr_n}{dt}$ is the front propagation velocity, λ is the decay coefficient which expresses the deceleration of the wave front, a is the velocity of sound, M is the Mach number of the wave front, μ is the front velocity modulus, and ρ_a' is the ambient density parameter, while subscript (a) denotes conditions of the ambient atmosphere into which the front of the blast wave propagates.

iii) Gasdynamic parameters of the flow field, the dependent variables describing the structure of the flow field:

$$f \equiv \frac{u}{w_n} \quad ; \quad h \equiv \frac{\rho}{\rho_a} \quad ; \quad g \equiv \frac{p}{\rho_a w_n^2} \quad \text{and} \quad \sigma \equiv \frac{e}{w_n^2} \qquad (II.15)$$

iv) Reduced variables; coordinates of the phase plane:

$$F \equiv \frac{f}{x} = \left(\frac{t}{r} \cdot \frac{u}{\mu}\right) \qquad ; \qquad Z \equiv \frac{rg}{x^2 h} = \left(\frac{t}{r} \cdot \frac{\mu}{a}\right)^2 \qquad \text{(II.16)}$$

v) The source term parameters:

$$\omega_M \equiv \Lambda_M \frac{r_n}{w_n} \qquad ; \qquad \omega_F \equiv \Lambda_F \frac{r_n}{w_n^2} \qquad \text{and} \qquad \omega_E \equiv \Lambda_E \frac{r_n}{w_n^3} \qquad \text{(II.17)}$$

II.5. TRANSFORMATION TO NON-DIMENSIONAL FORM

1. Transformation of variables

The independent variables of the problem in non-dimensional form will be $x = x(r, t)$ and $f = f(r, t)$. This, consequently, means that $r = r(x, f)$ and $t = t(x, f)$, and with the aid of the definitions of Eq. (II.13), one has for the non-dimensional transformation

$$\frac{\partial}{\partial r} = \frac{\partial x}{\partial r} \frac{\partial}{\partial x} + \frac{\partial f}{\partial r} \frac{\partial}{\partial f}$$

But for the Eulerian space profiles, $\frac{\partial f}{\partial r} = 0$. Thus:

$$\frac{\partial}{\partial r} = \frac{1}{r_n} \frac{\partial}{\partial x} \qquad \text{(II.18)}$$

and

$$\frac{\partial}{\partial t} = \frac{\partial x}{\partial t} \frac{\partial}{\partial x} + \frac{\partial f}{\partial t} \frac{\partial}{\partial f}$$

$$= \frac{\partial x}{\partial r_n} \cdot \frac{dr_n}{dt} \cdot \frac{\partial}{\partial x} + \frac{\partial f}{\partial r_n} \cdot \frac{dr_n}{dt} \cdot \frac{\partial}{\partial f}$$

where

$$\frac{\partial x}{\partial r_n} = \frac{\partial x}{\partial r} \cdot \frac{\partial r}{\partial r_n} = \frac{1}{r_n} \cdot x$$

$$\frac{\partial f}{\partial r_n} = \frac{1}{r_o} = \frac{1}{r_n} \cdot f$$

Thus

$$\frac{\partial}{\partial t} = \frac{w_n}{r_n} \left[\frac{\partial}{\partial \ln x} + \frac{\partial}{\partial \ln f} \right] \tag{II.19}$$

2. Conservation equations in non-dimensional form

Substitution from Eqs. (II.13) - (II.19) into Eqs. (II.1) - (II.3) yield the following non-linear partial differential equations for the conservation of mass, momentum and energy, respectively, in non-dimensional form, as given by Oppenheim et al. (1971):

$$\frac{\rho'}{a} + \frac{\partial \ln h}{\partial \ln f} + (\frac{f}{x} - 1) \frac{\partial \ln h}{\partial \ln x} + \frac{f}{x} (\frac{\partial \ln f}{\partial \ln x} + j) = \Phi_M \tag{II.20}$$

where

$$\Phi_M \equiv \omega_M \tag{II.21}$$

$$-\frac{\lambda}{2} + \frac{\partial \ln f}{\partial \ln f} + (\frac{f}{x} - 1) \frac{\partial \ln f}{\partial \ln x} + \frac{g}{h x f} \frac{\partial \ln g}{\partial \ln x} = \Phi_F \tag{II.22}$$

wher-

$$\Phi_F \equiv \frac{1}{f}\,\omega_F - \omega_M \qquad\qquad (II.23)$$

and

$$-\lambda\sigma + \frac{\partial\sigma}{\partial\ln\tilde{f}} + \left(\frac{f}{x}-1\right)\frac{\partial\sigma}{\partial\ln x} - \frac{g}{h}\left[\rho_a' + \frac{\partial\ln h}{\partial\ln\tilde{f}} + \left(\frac{f}{x}-1\right)\frac{\partial\ln h}{\partial\ln x}\right]$$

$$= \omega_E - f\,\omega_F - \left(\sigma + \frac{g}{h} - \frac{f^2}{2}\right)\omega_M \qquad (II.24)$$

Equations (II.10) and (II.11) are also, respectively, reduced to

$$\frac{\partial\sigma}{\partial\ln x} = \frac{k+1}{\Gamma}\,\frac{g}{h}\,\frac{\partial\ln g}{\partial\ln x} - k\,\frac{g}{h}\,\frac{\partial\ln h}{\partial\ln x} \qquad (II.25)$$

and

$$\frac{\partial\sigma}{\partial\ln\tilde{f}} = \lambda\sigma' + \frac{k+1}{\Gamma}\,\frac{g}{h}\left[\rho_a' - \lambda + \frac{\partial\ln g}{\partial\ln\tilde{f}}\right] - k\,\frac{g}{h}\left[\rho_a' + \frac{\partial\ln h}{\partial\ln\tilde{f}}\right] \qquad (II.26)$$

Using Eqs. (II.25) and (I1.26) to eliminate σ from Eq. (II.24), one gets

$$\rho_a' - \lambda + \frac{\partial\ln g}{\partial\ln\tilde{f}} + \left(\frac{f}{x}-1\right)\frac{\partial\ln g}{\partial\ln x} - \Gamma\left[\rho_a' + \frac{\partial\ln h}{\partial\ln\tilde{f}} + \left(\frac{f}{x}-1\right)\frac{\partial\ln h}{\partial\ln x}\right] = \Phi_E \qquad (II.27)$$

where

$$\Phi_E \equiv \frac{\Gamma}{k+1}\cdot\frac{h}{g}\left[\omega_E - f\,\omega_F - \left(\sigma + \frac{g}{h} - \frac{f^2}{2}\right)\omega_M\right] \qquad (II.28)$$

Equations (II.20), (II.22) and (II.27) together with the definitions of Eqs. (II.21), (II.23) and (II.28) represent the governing equations in their general form without restrictions imposed by specific equation of state and including any possible sources of mass, momentum or energy that may affect the flow field.

3. Reduced autonomous form

The governing equations, Eqs. (II.20), (II.22) and (II.27) may be expressed in terms of the reduced variables defined in Eq. (II.16). When these variables are substituted in Eqs. (II.20), (II.22) and (II.27) yield, respectively:

$$\rho'_a + \frac{\partial \ln h}{\partial \ln \zeta} + (F-1)\frac{\partial \ln h}{\partial \ln x} + F\left(\frac{\partial \ln F}{\partial \ln x} + j + 1\right) = \Phi_M \tag{II.29}$$

$$-\frac{\lambda}{2} + \frac{\partial \ln F}{\partial \ln \zeta} + (F-1)\left(\frac{\partial \ln F}{\partial \ln x} + 1\right) + \frac{Z}{\Gamma F}\frac{\partial \ln g}{\partial \ln x} = \Phi_F \tag{II.30}$$

and

$$\rho'_a - \lambda + \frac{\partial \ln g}{\partial \ln \zeta} + (F-1)\frac{\partial \ln g}{\partial \ln x} - \Gamma\left[\rho'_a + (F-1)\frac{\partial \ln h}{\partial \ln x} + \frac{\partial \ln h}{\partial \ln \zeta}\right] = \Phi_E \tag{II.31}$$

The above equations can be considered as a set of three algebraic equations for three unknowns that represent the logarithmic gradients with respect to x of F, h and g, respectively. Solving them algebraically for these gradients, one obtains the following autonomous form of the blast wave equations:

$$D\frac{\partial \ln F}{\partial \ln x} = F_x + F_\zeta + F_\omega \tag{II.32}$$

$$D \frac{\partial \ln h}{\partial \ln x} = H_x + H_z + H_\omega \qquad (II.33)$$

$$D \frac{\partial \ln g}{\partial \ln x} = G_x + G_z + G_\omega \qquad (II.34)$$

As a consequence of the definition of Z, one has also from the above

$$D \frac{\partial \ln Z}{\partial \ln x} = Z_x + Z_z + Z_\omega \qquad (II.35)$$

where

$$D(F, Z) \equiv Z - (1 - F)^2 \qquad (II.36)$$

$$F_x = (F - 1)\left(F - \frac{\lambda + 2}{2}\right) + \frac{Z}{\Gamma F}\left[\lambda - (j + 1)\Gamma F - \ell_a'\right] \qquad (II.37)$$

$$H_x \equiv \frac{1}{(1 - F)}\left\{F F_x + \left[(j + 1)F + \ell_a'\right] D\right\} \qquad (II.38)$$

$$G_x \equiv \frac{1}{(1 - F)}\left\{\Gamma F F_x + \left[\Gamma F(j + 1) - \lambda + \ell_a'\right] D\right\} \qquad (II.39)$$

$$Z_x \equiv G_x - H_x - 2D \tag{II.40}$$

and

$$F_\zeta \equiv (F-1)\frac{\partial \ln F}{\partial \ln \zeta} - \frac{Z}{\Gamma F}\frac{\partial \ln g}{\partial \ln \zeta} \tag{II.41}$$

$$H_\zeta \equiv \frac{1}{(1-F)}\left[F F_\zeta + \frac{\partial \ln h}{\partial \ln \zeta}\cdot D\right] \tag{II.42}$$

$$G_\zeta \equiv \frac{1}{(1-F)}\left[\Gamma F F_\zeta + \frac{\partial \ln g}{\partial \ln \zeta}\cdot D\right] \tag{II.43}$$

$$Z_\zeta \equiv G_\zeta - H_\zeta \tag{II.44}$$

while

$$F_\omega \equiv (1-F)\Phi_F + \frac{Z}{\Gamma F}(\Gamma \Phi_M + \Phi_E) \tag{II.45}$$

$$H_\omega \equiv \frac{1}{(1-F)}(\dot{F} F_\omega - \Phi_M \cdot D) \tag{II.46}$$

$$G_\omega \equiv \frac{1}{(1-F)} \left[\Gamma F F_\omega - (\Gamma \phi_M + \phi_E) D \right]$$

(II.47)

$$Z_\omega \equiv G_\omega - H_\omega$$

(II.48)

II.6 **BOUNDARY CONDITIONS**

In addition to the conservation equations and the equation of state, the formulation of a blast wave problem is completed by the boundary conditions which can be found by solving simultaneously the equations of continuity, momentum and energy across the shock front. Accordingly, the boundary conditions depend on the problem under study. Generally, there are two types of boundary conditions:

i) for adiabatic point explosion problem, or when the heat of reaction, in the case of reactive medium, is distributed inside the flow field, the boundary conditions or the Rankine-Hugoniot relations will be determined as follows:

Consider the shown control volume, Fig. II.2, which contains discontinuity in flow variables at the shock front. Applying the conservation principles of mass, momentum and energy between states 1 and 2, ahead and behind the wave front immediately, one gets, respectively

$$\rho_1 u_1 = \rho_2 u_2$$
$$P_1 + \rho_1 u_1^2 = P_2 + \rho_2 u_2^2$$

and

$$i_1 + \frac{u_1^2}{2} = i_2 + \frac{u_2^2}{2}$$

Changing to a frame of reference in which the shock wave is at rest, the above equations yield, respectively

$$\rho_a W_n = \rho_n (W_n' - u_n)$$

(II.49)

$$P_a + \rho_a W_n^2 = P_n + \rho_n (W_n' - u_n)^2$$

(II.50)

$$e_a + \frac{P_a}{\rho_a} + \frac{W_n^2}{2} = e_n + \frac{P_n}{\rho_n} + \frac{(W_n - u_n)^2}{2}$$

(II.51)

where W_n is the front propagation velocity, and subscripts a and n denote conditions of the ambient atmosphere into which the front of the blast wave propagates and conditions immediately behind the wave front, respectively.

ii) in the case of reactive medium, the heat released may be applied to the blast wave at its front due to laser irradiation or chemical reaction. The boundary conditions in this case, or the Hugoniot relations, are determined exactly as above, except for the energy equation which takes the form

$$e_a + \frac{P_a}{\rho_a} + \frac{W_n^2}{2} + q = e_n + \frac{P_n}{\rho_n} + \frac{(W_n - u_n)^2}{2}$$

(II.52)

where q is the energy deposited at the front per unit mass of the medium. Defining the non-dimensional chemical energy parameter

$$\bar{q} \equiv \frac{q}{a_a^2}$$

(II.53)

Therefore, the boundary conditions, Eqs. (II.49) - (II.52), will take the following non-dimensional form, respectively

$$h_n = \frac{1}{1 - f_n} \tag{II.54}$$

$$g_n = f_n + \frac{y}{\Gamma_a} \tag{II.55}$$

$$\sigma_n = \sigma_a + \frac{y}{\Gamma_a} f_n + \frac{1}{2} f_n^2 \tag{II.56}$$

and

$$\sigma_n = \sigma_a + \frac{y}{\Gamma_a} f_n + \frac{1}{2} f_n^2 + y \bar{q} \tag{II.57}$$

For adiabatic point explosions or for reactive medium with distributed heat release inside the flow field, Eq. (II.56) is applied, while for reactive medium with instantaneous heat release at the front, Eq. (II.57) is applied.

II.7   INTEGRAL RELATIONS

The integral relations for a blast wave are the expressions of the principles of global mass, momentum, and energy conservation.

1.   Mass integral equation

The mass integral states that, at any moment, the amount of mass distributed inside the flow field should equal that engulfed by the front plus that of any other source that may affect the flow field.   Thus:

$$\frac{M_j}{n_j} = \int_0^{r_n} \rho r^j dr = M_a + M_{\lambda} \tag{II.58}$$

where M_j is the total mass content inside the flow field, while n_j is a geometrical factor, defined by

$$n_j = {}'2\pi j + \tfrac{1}{2}(j-1)(j-2)$$

M_a is the mass of the ambient medium engulfed by the front, thus:

$$M_a = \int_0^{r_n} \ell_a\, r_n^j\, dr_n = \frac{\ell_a\, r_n^{j+1}}{j+1} - \int_0^{r_n} \frac{r_n^{j+1}}{j+1}\, d\ell_a$$

with the aid of Eq. (II.14)

$$d\ell_a = \frac{\ell_a\, \ell_a'}{r_n}\, dr_n$$

thus

$$M_a = \frac{1}{j+1}\left[\ell_a\, r_n^{j+1} - \int_0^{r_n} \ell_a\, \ell_a'\, r_n^j\, dr_n\right] \tag{II.59}$$

and

M_{Ω} is the mass that may be added to the flow field by a source from the instant of explosion till the instant under consideration, thus

$$M_{\Omega} = \int_0^{t_n}\int_0^{r_n} \rho r^j\, \Omega_M\, dr\, dr \tag{II.60}$$

Therefore, the substitution of Eqs. (II.59) and (II.60) into Eq. (II.58) yields the mass integral

$$\frac{M_j}{n_j} = \int_0^{r_n} \rho r^j\, dr$$

$$= \frac{1}{j+1}\left[\ell_a\, r_n^{j+1} - \int_0^{r_n} \ell_a\, \ell_a'\, r_n^j\, d\bar{r}_n\right] + \int_0^{t_n}\int_0^{r_n} \rho r^j\, \Omega_M\, dr\, dt \tag{II.61}$$

which for a sourceless flow and uniform ambient density, ρ_a = constant, re-duces to the simple form

$$\frac{M_j}{n_j} = \frac{\rho_a \, r_n^{j+1}}{(j+1)} \tag{II.62}$$

On the other hand, the mass integral may be obtained directly by integrating Eq. (II.1), the mass conservation equation, with respect to r, from the center of symmetry to the shock front, to yield

$$\int_o^{r_n} \frac{\partial}{\partial t}(\rho r^j)\, dr + \rho_n \, u_n \, r_n^j = \int_o^{r_n} \rho r^j \lambda_M \, dr \tag{II.63}$$

By utilizing Leibnitz rule, the first term gives

$$\int_o^{r_n} \frac{\partial}{\partial t}(\rho r^j)\, dr = \frac{d}{dt}\int_o^{r_n} \rho r^j \, dr - \rho_n \, r_n^j \frac{dr_n}{dt}$$

which may be substituted into Eq. (II.63) to yield, noting that $\frac{dr_n}{dt} = W_n$.

$$\frac{d}{dt}\int_o^{r_n} \rho r^j \, dr + \rho_n \, r_n^j (u_n - W_n) = \int_o^{r_n} \rho r^j \lambda_M \, dr$$

But, from Eq. (II.49), one has

$$\rho_n (u_n - W_n) = -\rho_a \, W_n = -\rho_a \frac{dr_n}{dt}$$

then

$$\frac{d}{dt}\int_o^{r_n} \rho r^j \, dr - \rho_a \, r_n^j \frac{dr_n}{dt} = \int_o^{r_n} \rho r^j \lambda_M \, dr$$

The last equation may now be integrated with respect to time to yield

$$\int_0^{r_n} \rho r^j \, dr = \int_0^{r_n} \rho_a \, r_n^j \, dr_n + \int_0^t \int_0^{r_n} \rho r^j \, \omega_M \, dr \, dt$$

which, after integrating the first term on the right hand side by part, reduces to the required mass integral, exactly as given by Eq. (II.61).

Now, for ρ_a = constant, and noting the definitions of μ Eq. (II.14), and ω_M , Eq. (II.17), Eq. (II.61) may be non-dimensionalized to yield

$$\mathcal{J}_1 = \frac{M_j}{\eta_j \, \rho_a \, r_n^{j+1}} = \int_0^1 h \, x^j \, dx$$

$$= \frac{1}{j+1} + \int_0^1 \int_0^1 h \, x^j \, \omega_M \, \mu \, dx \, d\tau \qquad (II.64)$$

which, in turn, for a sourceless flow reduces to

$$\mathcal{J}_1 = \int_0^1 h \, x^j \, dx = \frac{1}{j+1} \qquad (II.65)$$

2. Momentum integral equation

The momentum integral may be obtained by integrating Eq. (II.2), the momentum conservation equation, with respect to r , from $r = 0$ to $r = r_n$, as follows

$$\int_0^{r_n} \frac{\partial}{\partial t} (\rho u \, r^j) \, dr + (\rho_n u_n^2 + P_n) r_n^j = \int_0^{r_n} \rho r^j (\frac{\partial P}{\partial r} + \omega_F) \, dr \qquad (II.66)$$

The first term yields, after utilizing Leibnitz rule,

$$\int_0^{r_n} \frac{\partial}{\partial t}(\rho u r^j)\,dr = \frac{d}{dt}\int_0^{r_n} \rho u r^j\,dr - \rho_n u_n r_n^j \frac{dr_n}{dt}$$

Substituting the above equation in Eq. (II.66), to yield

$$\frac{d}{dt}\int_0^{r_n}\rho u r^j\,dr + r_n^j\left[P_n + \rho_n u_n(u_n - w_n)\right] = \int_0^{r_n}\rho r^j\left(\frac{jP}{\rho r} + \Lambda_F\right)dr$$

By solving Eqs. (II.49) and (II.50) simultaneously, one obtains

$$P_n + \rho_n u_n(u_n - w_n) = P_a = \frac{P_a}{w_n}\cdot\frac{dr_n}{dt}$$

then

$$\frac{d}{dt}\int_0^{r_n}\rho u r^j\,dr + \frac{r_n^j P_a}{w_n}\cdot\frac{dr_n}{dt} = \int_0^{r_n}\rho r^j\left(\frac{jP}{\rho r} + \Lambda_F\right)dr$$

Integrating the above equation with respect to time, one gets

$$\frac{P_j}{n_j} = \int_0^{r_n}\rho u r^j\,dr$$

$$= -\int_0^{r_n}\frac{P_a r_n^j}{w_n}\,dr_n + \int_0^t\int_0^{r_n}(jP r^{j-1} + \rho r^j \Lambda_F)\,dr\,dt \qquad (II.67)$$

where P_j is the momentum of blast wave.

Hence, for constant P_a Eq. (II.67) may be non-dimensionalized to give

$$J_2 = \frac{P_j}{n_j P_a r_n^{j+1} w_n} = \int_0^1 hf x^j\,dx$$

$$= -\frac{\mu y}{3^j 3\sqrt{a}}\int_0^3 \frac{3}{\mu}3^{j+1}\,d3$$

$$+ \int_0^1\int_0^1 \mu x^j(jg + h\omega_F)\,dx\,d\tau \qquad (II.68)$$

3. Energy integral equation:

The energy integral states that the total energy of a blast wave, E_j , should equal the summation of the energy deposited initially to generate the wave, E_i , the ambient internal energy engulfed by the front, E_a , the chemical energy liberated in the case of reactive medium, E_{ch} , and the energy due to sources within the wave, E_{λ} . Thus, for ρ_a = constant:

$$\frac{E_j}{n_j} = E_i + E_a + E_{ch} + E_{\lambda} = \int_0^{r_n} (e + \frac{u^2}{2}) \, \rho \, r^j \, dr \qquad (II.69)$$

where

$$E_a = \int_0^{r_n} e_a \, \rho_a \, r_n^j \, dr_n = \frac{e_a \, \rho_a \, r_n^{j+1}}{(j+1)}$$

if the heat liberated is considered at the front, thus

$$E_{ch} = \int_0^{r_n} q \, \rho_a \, r_n^j \, dr_n = \frac{q \, \rho_a \, r_n^{j+1}}{j+1}$$

while, in the case of distributed heat release, E_{ch} will be obtained as E_{λ}, where

$$E_{\lambda} = \int_0^{t_n} \int_0^{r_n} \rho \, r^j \, \lambda_E \, dr \, dt$$

Therefore the energy integral will be, in general

$$\frac{E_j}{n_j} = \int_0^{r_n} (e + \frac{u^2}{2}) \, \rho \, r^j \, dr = E_i + \frac{e_a \, \rho_a \, r_n^{j+1}}{j+1}$$

$$+ \frac{q \, \rho_a \, r_n^{j+1}}{j+1} + \int_0^{t_n} \int_0^{r_n} \rho \, r^j \, \lambda_E \, dr \, dt \qquad (II.70)$$

For a sourceless flow and heat released at the front, the energy integral reduces to

$$\frac{E_j}{n_j} = \int_0^{r_n} (e + \frac{u^2}{2}) \rho r^j \, dr = E_i + \frac{e_a \rho_a r_n^{j+1}}{(j+1)} + \frac{q \rho_a r_n^{j+1}}{j+1} \qquad \text{(II.71)}$$

We are going to use the definition of r_0 , the reference radius, as that given by Oppenheim et al. (1971) which includes the two most important initial parameters (E_i and P_a) of the problem:

$$r_0 \equiv \left(\frac{E_i}{P_a}\right)^{\frac{1}{j+1}} \qquad \text{(II.72)}$$

Using the definition of r_0 to replace E_i in Eq. (II.70) by

$$E_i = P_a \, r_0^{\,j+1}$$

Thus, the energy integral equation in its general form, Eq. (II.70), can be expressed in non-dimensional form as follows

$$J_3 \equiv \frac{E_j}{n_j \rho_a r_n^{j+1} w_n^2} = \int_0^1 (\sigma + \frac{f^2}{2}) h \, x^j \, dx = \frac{y}{\sqrt{a} \, \zeta^{j+1}} + \frac{\sigma_a}{j+1}$$

$$+ \frac{y\bar{q}}{j+1} + \int_0^1 \int_0^1 h \, x^j \omega_E \, \mu \, dx \, d\tau \qquad \text{(II.73)}$$

which, for a sourceless flow field, reduces to

$$J_3 = \int_0^1 (\sigma + \frac{f^2}{2}) h \, x^j \, dx$$

$$= \frac{\sigma_a}{j+1} + y\left[\frac{1}{\sqrt{a} \, \zeta^{j+1}} + \frac{\bar{q}}{j+1}\right]$$

$$= y\left[\frac{e_a}{a_a^2(j+1)} + \frac{1}{\sqrt{a} \, \zeta^{j+1}} + \frac{\bar{q}}{j+1}\right] \qquad \text{(II.74)}$$

where

$$\tilde{\sigma_a} = \frac{e_a}{W_n^2} = y \frac{e_a}{a_a^2}$$

Differentiating the above equation with respect to y and using the definition of λ, one can easily obtain an expression for the decay coefficient

$$\lambda = \frac{(j+1)\mathcal{J}_3 - \tilde{\sigma_a} - \bar{q}\, y}{\mathcal{J}_3 - y\frac{d\mathcal{J}_3}{dy}} \tag{II.75}$$

while, for adiabatic point explosion, the above equation reduces to

$$\lambda = \frac{(j+1)\mathcal{J}_3 - \tilde{\sigma_a}}{\mathcal{J}_3 - y\frac{d\mathcal{J}_3}{dy}} \tag{II.76}$$

II.8 CASE OF PERFECT GASES

As formulated above, the introduction of a general equation of state, $e = e(P,\rho)$, leads to two thermodynamic properties, namely the internal energy σ and the speed of sound factor Γ, which include essentially the characteristics of real gases. However, due to the complexity of the governing equations in their general form, the assumption that the flow field behaves as a perfect gas with mean specific heat ratio has a wide popularity in most literature.

1. Properties of perfect gases

The equation of state of a perfect gas is

$$P = \rho R T \tag{II.77}$$

where R is the gas constant and T is the temperature. One has also the following relations:

$$e = C_v T = \frac{RT}{\gamma - 1} = \frac{P}{\rho(\gamma - 1)} \tag{II.78}$$

where C_v is the specific heat at constant volume, and γ is the specific heat ratio.

$$\Gamma = \gamma \tag{II.79}$$

$$\mathcal{K} = \frac{1}{\gamma - 1} \tag{II.80}$$

$$\tilde{\sigma}_a = \frac{y}{\gamma(\gamma - 1)} \tag{II.81}$$

and

$$\sigma = \frac{1}{\gamma - 1} \cdot \frac{g}{h} \tag{II.82}$$

2. Governing equations

The mass and momentum equations, Eqs. (II.20) and (II.22) remain unchanged, while energy equation, Eq. (II.27), becomes, for $\mathcal{L}_a$ = constant and noting that $\frac{\partial}{\partial \ln \tilde{\mathcal{F}}} = \lambda \frac{\partial}{\partial \ln y}$

$$-\lambda + \frac{\lambda y}{g} \frac{\partial g}{\partial y} + \frac{(f - x)}{g} \frac{\partial g}{\partial x} - \gamma \left[\frac{f - x}{h} \frac{\partial h}{\partial x} + \frac{\lambda y}{h} \frac{\partial h}{\partial y} \right] = \Phi_E \tag{II.83}$$

where

$$\Phi_E = (\gamma - 1) \frac{h}{g} \left[\omega_E - f \omega_F - \left(\frac{\gamma}{\gamma - 1} \cdot \frac{g}{h} - \frac{f^2}{2} \right) \omega_M \right] \tag{II.84}$$

3. Boundary conditions

Equation (II.54) of the boundary conditions remains unchanged, while Eqs. (II.55) - (II.57) reduce, respectively, to

$$g_n = f_n + \frac{y}{\gamma} \tag{II.85}$$

$$\frac{1}{(\gamma-1)} \cdot \frac{g_n}{h_n} = \frac{y}{\gamma(\gamma-1)} + \frac{y}{\gamma} f_n + \frac{f_n^2}{2} \tag{II.86}$$

$$\frac{1}{(\gamma-1)} \cdot \frac{g_n}{h_n} = \frac{y}{\gamma(\gamma-1)} + \frac{y}{\gamma} f_n + \frac{f_n^2}{2} + y\bar{q} \tag{II.87}$$

For adiabatic point explosion problem, Eqs. (II.54), (II.85) and (II.86) yield the familiar boundary conditions for blast waves, namely

$$f_n = \frac{2}{\gamma+1} (1 - y) \tag{II.88}$$

$$h_n = \frac{\gamma+1}{\gamma-1+2y} \tag{II.89}$$

and

$$g_n = \frac{2\gamma - y(\gamma-1)}{\gamma(\gamma+1)} \tag{II.90}$$

while, for the reactive medium with heat released takes place instantaneously at the front, Eqs. (II.54), (II.85) and (II.87) yield

$$f_n = (\frac{1-y}{\gamma+1}) \pm \left[(\frac{1-y}{\gamma+1})^2 - 2(\frac{\gamma-1}{\gamma+1}) y\bar{q} \right]^{1/2} \tag{II.91}$$

For any given shock strength y , there exist two possible solutions represented by the two signs in Eq. (II.91). The plus sign denotes the overdriven detonation solution, and the minus sign the weak detonation solution. The unique Chapman-Jouguet solution is obtained when the two solutions coincide, i.e. when the terms between square brackets in Eq. (II.91) equal zero, yielding

$$y_{CJ} = \left[(\gamma^2 - 1)\bar{q} + 1 \right] \pm \sqrt{\left[(\gamma^2 - 1)\bar{q} + 1 \right]^2 - 1} \tag{II.92}$$

with the minus sign applying for detonation, while the plus one for deflagration. In general, only the overdriven detonation solutions are of interest; and one may discard the bottom sign in Eq. (II.91) for weak detonations. Thus:

$$f_n = \frac{1 - y}{\gamma + 1} + \left[\left(\frac{1 - y}{\gamma + 1} \right)^2 - 2 \left(\frac{\gamma - 1}{\gamma + 1} \right) y \bar{q} \right]^{1/2} \tag{II.93}$$

and

$$y_{CJ} = \left[(\gamma^2 - 1)\bar{q} + 1 \right] - \sqrt{\left[(\gamma^2 - 1)\bar{q} + 1 \right]^2 - 1} \tag{II.94}$$

The other two boundary conditions for h_n and g_n are still applied through Eqs. (II.54) and (II.85).

4. Integral relations

The mass and momentum integrals in the case of perfect gases are not changed and have the same forms, given by Eqs. (II 64) and (II.68), except for the momentum integral, Eq. (II.68), Γ_a changes to γ . While the energy integral, Eq. (II.73), reduces to

$$\mathcal{J}_3 = \int_0^1 \left[\frac{1}{(\gamma-1)} \cdot \frac{g}{h} + \frac{f^2}{2} \right] h \, x^j \, dx$$

$$= \frac{y}{\gamma} \left[\mathcal{J}^{-(j+1)} + \frac{1}{(j+1)(\gamma-1)} + \frac{\gamma\bar{q}}{(j+1)} \right] + \int_0^1 \int_0^1 h \, x^j \, \omega_E \mu \, dx \, dt \quad \text{(II.95)}$$

which, for a sourceless flow field, becomes

$$\mathcal{J}_3 = \frac{y}{\gamma} \left[\mathcal{J}^{-(j+1)} + \frac{1}{(j+1)(\gamma-1)} + \frac{\gamma\bar{q}}{(j+1)} \right] \quad \text{(II.96)}$$

and, the decay coefficient takes the form

$$\lambda = \frac{(j+1)\mathcal{J}_3 - \dfrac{y}{\gamma(\gamma-1)} - \bar{q}y}{\mathcal{J}_3 - y \dfrac{d\mathcal{J}_3}{dy}} \quad \text{(II.97)}$$

which, for adiabatic point explosions, reduces to

$$\lambda = \frac{(j+1)\mathcal{J}_3 - \dfrac{y}{\gamma(\gamma-1)}}{\mathcal{J}_3 - y \dfrac{d\mathcal{J}_3}{dy}} \quad \text{(II.98)}$$

II.9 CASE OF SELF-SIMILARITY

The self-similar motion of a medium is one in which the number of independent variables in the fundamental system of equations is reduced from two to one, thus, the system of non-linear partial differential equations is reduced to a system of ordinary differential equations. However, the value of this solution is confined to the early time regime when the shock wave is strong enough to neglect the effect of counter-pressure. This, consequently, means that the

front propagation velocity is very large approaching infinity. Thus,

$$y = 0 \tag{II.99}$$

1. Governing equations

Substituting this condition of self-similarity into governing equations, Eqs. (I1.20), (II.22) and (II.27) yield respectively

$$\frac{(f-x)}{h} \frac{dh}{dx} + \frac{df}{dx} + j\frac{f}{x} = \Phi_M \tag{II.100}$$

$$-\frac{\lambda}{2} + \frac{(f-x)}{f} \frac{df}{dx} + \frac{1}{hf} \frac{dg}{dx} = \Phi_F \tag{II.101}$$

$$-\lambda + \frac{(f-x)}{g} \frac{dg}{dx} - \Gamma\left[\frac{(f-x)}{h} \frac{dh}{dx}\right] = \Phi_E \tag{II.102}$$

For a perfect gas, the energy equation reduces to

$$-\lambda + \frac{(f-x)}{g} \frac{dg}{dx} - \gamma\left[\frac{(f-x)}{h} \frac{dh}{dx}\right] = \Phi_E \tag{II.103}$$

where Φ_E is given by Eq. (II.84).

The above set of equations is an ordinary differential one, which can be solved numerically once the source terms are specified.

2. Boundary conditions

The boundary conditions in this case are simply obtained by putting $y = 0$ in Eqs. (II.55) - (II.57), while Eq. (II.54) is still applied without any restric-

tions. Thus, one has the following relations

$$g_n = f_n \qquad \qquad (II.104)$$

$$\tilde{\sigma}_n = \frac{f_n^2}{2} \qquad \qquad (II.105)$$

where Eqs. (II.56) and (II.57) reduce to a single equation given by Eq. (II.105). This means that the heat released at the front is negligible in the self-similar solution compared to the initiation energy, E_i , which is the predominant parameter governing the flow field.

For a perfect gas, the boundary conditions, Eqs. (II.54), (II.104) and (II.105), yield the following relations:

$$f_n = \frac{2}{\gamma+1} \qquad \qquad (II.106)$$

$$h_n = \frac{\gamma+1}{\gamma-1} \qquad \qquad (II.107)$$

$$g_n = \frac{2}{\gamma+1} \qquad \qquad (II.108)$$

3. Integral relations

The mass integral, in this case, is given by Eq. (II.65), since for strong explosions the double integration in the right side of Eq. (II.64), which includes the effect of mass source term, will equal to zero. On the other hand, the

energy integral still takes the form

$$\mathfrak{J}_3 = \int_0^1 (\sigma + \frac{f^2}{2}) \, h \, x^j \, dx \tag{II.109}$$

while the right side of Eq. (II.73) leads to a trivial solution of $\mathfrak{J}_3 = 0$.
Thus, the energy integral is obtained by numerical integration of Eq. (II.109)
from the flow field solution.

Equation (II.109) is reduced to the following relation in the case of perfect
gases

$$\mathfrak{J}_3 = \int_0^1 \left[\frac{1}{(\gamma-1)} \frac{g}{h} + \frac{f^2}{2}\right] h \, x^j \, dx \tag{II.110}$$

while the decay coefficient takes the following simple form

$$\lambda = j + 1 \tag{II.111}$$

II.10. **COMPATIBILITY EQUATION**

At any time, the particle velocity at the center of symmetry must be equal to
zero, that is

$$u(0, t) = 0$$

This represents a compatibility equation which must be satisfied by the correct
solution. This equation in non-dimensional form can be written as:

$$f(0, y) = 0 \tag{II.112}$$

Figure Captions

Fig. II.1.   Blast wave coordinates

Fig. II.2.   Control volume of a blast wave

$\tau=\infty$
$X=1$

$r=r_n$
$(X=1)$

ψ ϕ η $\phi=\left\{\dfrac{X}{\tau}\right\}=1$

t

t_n $t=t_n$
$(\tau=1)$

$X=\dfrac{r}{r_n}$

$\tau=\dfrac{t}{t_n}$

t_0

$\tau=0$
$X=\infty$

0 r r_n r
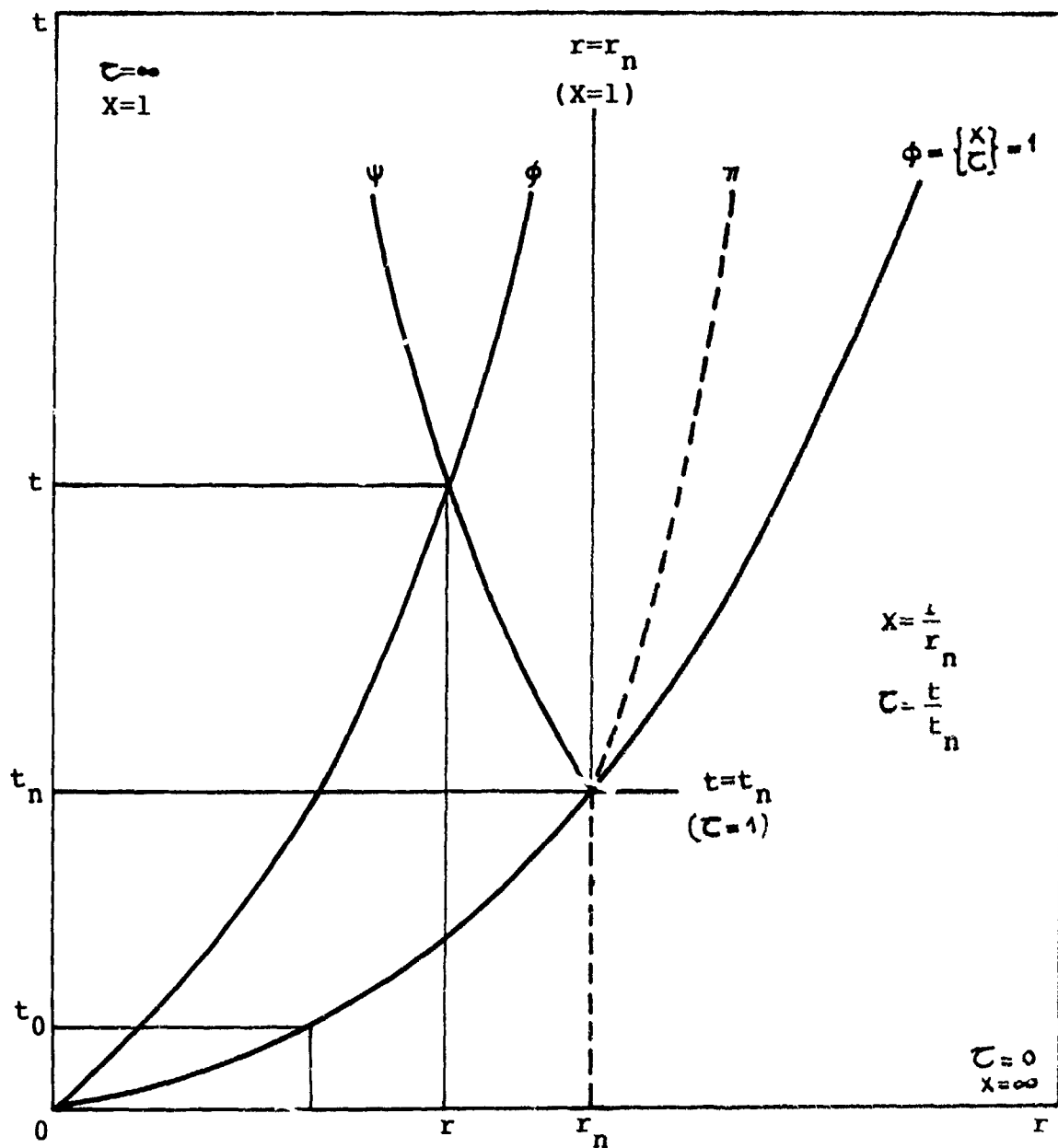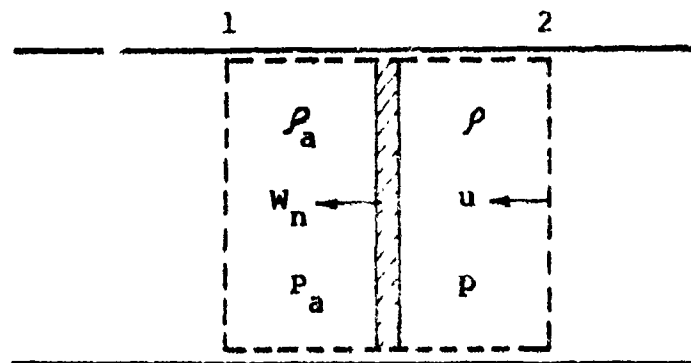
Fig. II.1

Fig. II.2

CHAPTER III

THE QUASI-SIMILAR SOLUTION

III.1. INTRODUCTION

The conservation equations, as derived previously, are highly non-linear, non-homogeneous, coupled, partial differential equations. Therefore, a closed form solution is so far impossible, and approximate solutions appear to be essential. Mainly, three analytical techniques are used for predicting the non-self-similar flow field of a blast wave, the perturbation method of Sakurai (1965), the quasi similar method of Oshima (1960, 1964) and the power density law of Bach and Lee (1970).

In this chapter, the quasi-similar technique will be discussed briefly with a complete description and derivation of this method of solution to be applicable for any type of problems.

III.2. TAYLOR'S SERIES EXPANSION

To obtain the approximate quasi-similar solution, one has to perform, firstly, a double Taylor's series expansion on the dependent variables. As mentioned previously, any dependent variable of the problem is a function of the two independent variables x and y. Thus, for any dependent variable $\mathcal{F}$, the application of the double Taylor's series expansion yields

$$
\begin{aligned}
\mathcal{F}(x,y) &= \mathcal{F}(a,b) + \left[(x-a)\left(\frac{\partial \mathcal{F}}{\partial x}\right)_{a,b} + (y-b)\left(\frac{\partial \mathcal{F}}{\partial y}\right)_{a,b} \right] + \frac{1}{2!}\left[(x-a)^2 \left(\frac{\partial^2 \mathcal{F}}{\partial x^2}\right)_{a,b} \right. \\
&\quad + 2(x-a)(y-b)\left(\frac{\partial^2 \mathcal{F}}{\partial x \partial y}\right)_{a,b} + (y-b)^2\left(\frac{\partial^2 \mathcal{F}}{\partial y^2}\right)_{a,b} \left.\right] + \frac{1}{3!}\left[(x-a)^3\left(\frac{\partial^3 \mathcal{F}}{\partial x^3}\right)_{a,b} \right. \\
&\quad + 3(x-a)^2(y-b)\frac{\partial^3 \mathcal{F}}{\partial x^2 \partial y} + 3(x-a)(y-b)^2\left(\frac{\partial^3 \mathcal{F}}{\partial x \partial y^2}\right)_{a,b} \\
&\quad + (y-b)^3\left(\frac{\partial^3 \mathcal{F}}{\partial y^3}\right)_{a,b} \left.\right] + \cdots \cdots
\end{aligned}
\tag{III.1}
$$

where a and b are the values of x and y, respectively, in the neighborhood of which the solution is to be obtained, provided that the function $\mathcal{F} = \mathcal{F}(x,y)$ together with its partial derivatives up to the nth order are continuous in the neighborhood of the point (a, b).

Since one's interest centers upon the region of the flow field near the wave front, for any value of Mach number, one may set

$$a = 1$$

and

$$b = y$$

Eq. (III.1) then reduces to

$$\mathcal{F}(x,y) = \mathcal{F}(1,y) - (1-x)\left(\frac{\partial \mathcal{F}}{\partial x}\right)_{1,y} + \frac{1}{2!}(1-x)^2\left(\frac{\partial^2 \mathcal{F}}{\partial x^2}\right)_{1,y}$$

$$- \frac{1}{3!}(1-x)^3\left(\frac{\partial^3 \mathcal{F}}{\partial x^3}\right)_{1,y} + \cdots \qquad (III.2)$$

It now becomes possible to substitute the above equation, of course with $\mathcal{F} = F$, h, and g, in the equations of motion and proceed to obtain the expansion solution in the normal fashion.

With reference to the autonomous equations (II.32) - (II.34), only the quantities subscripted by $\mathcal{J}$ will be expanded, thus yielding a set of first-order ordinary differential equations identical to those of the self-similar case except that the dependence of $\mathcal{J}$, or y, is included only as additive algebraic terms. For any dependent variable $\mathcal{F}$, the autonomous equations give

$$D \frac{\partial \ln \mathcal{F}}{\partial \ln x} = \mathcal{F}_x + \mathcal{F}_{\mathcal{J}} + \mathcal{F}_\omega \qquad (III.3)$$

where D, $\mathcal{F}_x$, $\mathcal{F}_{\zeta}$ and $\mathcal{F}_{\omega}$ are defined in Eqs. (II.36) - (II.48). The above equation may now be put in the form

$$\frac{\partial \ln \mathcal{F}}{\partial x} = \frac{\mathcal{F}_x + \mathcal{F}_{\zeta} + \mathcal{F}_{\omega}}{x D}$$

which, by differentiating with respect to $\ln \zeta$, yields

$$\frac{\partial}{\partial x}\left(\frac{\partial \ln \mathcal{F}}{\partial \ln \zeta}\right) = \frac{\partial}{\partial \ln \zeta}\left[\frac{\mathcal{F}_x + \mathcal{F}_{\zeta} + \mathcal{F}_{\omega}}{x D}\right] \tag{III.4}$$

where the order of differentiation of the term on the right hand side has been interchanged. Thus, with the aid of Eq. (III.2), one has

$$\frac{\partial \ln \mathcal{F}}{\partial \ln \zeta} = \left(\frac{\partial \ln \mathcal{F}}{\partial \ln \zeta}\right)_{x=1} - (1-x)\left[\frac{\partial}{\partial \ln \zeta}\left(\frac{\mathcal{F}_x + \mathcal{F}_{\zeta} + \mathcal{F}_{\omega}}{x D}\right)\right]_{x=1} + \cdots \tag{III.5}$$

or

$$\frac{\partial \ln F}{\partial \ln \zeta} = \left(\frac{\partial \ln F}{\partial \ln \zeta}\right)_{x=1} - (1-x)\left[\frac{\partial}{\partial \ln \zeta}\left(\frac{F_x + F_{\zeta} + F_{\omega}}{x D}\right)\right]_{x=1} + \cdots \tag{III.5a}$$

$$\frac{\partial \ln h}{\partial \ln \zeta} = \left(\frac{\partial \ln h}{\partial \ln \zeta}\right)_{x=1} - (1-x)\left[\frac{\partial}{\partial \ln \zeta}\left(\frac{H_x + H_{\zeta} + H_{\omega}}{x D}\right)\right]_{x=1} + \cdots \tag{III.5b}$$

and

$$\frac{\partial \ln g}{\partial \ln \zeta} = \left(\frac{\partial \ln g}{\partial \ln \zeta}\right)_{x=1} - (1-x)\left[\frac{\partial}{\partial \ln \zeta}\left\{\frac{(G_x + G_{\zeta} + G_{\omega})}{x D}\right\}\right]_{x=1} + \cdots \tag{III.5c}$$

where, denoting $\dfrac{\partial}{\partial \ln \zeta}$ by a prime,

$$\frac{\partial}{\partial \ln \mathfrak{Z}}\left(\frac{F_x + F_\mathfrak{Z} + F_\omega}{\chi D}\right) = \left(\frac{1}{\chi D}\right)\left(F_x' + F_\mathfrak{Z}' + F_\omega'\right) + \left(\frac{1}{\chi D}\right)'\left(F_x + F_\mathfrak{Z} + F_\omega\right) \tag{III.6a}$$

$$\frac{\partial}{\partial \ln \mathfrak{Z}}\left(\frac{H_x + H_\mathfrak{Z} + H_\omega}{\chi D}\right) = \left(\frac{1}{\chi D}\right)\left(H_x' + H_\mathfrak{Z}' + H_\omega'\right) + \left(\frac{1}{\chi D}\right)'\left(H_x + H_\mathfrak{Z} + H_\omega\right) \tag{III.6b}$$

and

$$\frac{\partial}{\partial \ln \mathfrak{Z}}\left(\frac{G_x + G_\mathfrak{Z} + G_\omega}{\chi D}\right) = \left(\frac{1}{\chi D}\right)\left(G_x' + G_\mathfrak{Z}' + G_\omega'\right) + \left(\frac{1}{\chi D}\right)'\left(G_x + G_\mathfrak{Z} + G_\omega\right) \tag{III.6c}$$

with

$$F_x' \equiv \frac{\partial F_x}{\partial \ln \mathfrak{Z}} = F'\left(F - \frac{\lambda+2}{2}\right) + (F-1)\left(F' - \frac{\lambda'}{2}\right)$$

$$+ \frac{Z}{\Gamma F}\left[\lambda' - (j+1)(\Gamma F' + F \Gamma') - \rho_a''\right]$$

$$+ \frac{1}{\Gamma F}\left[\lambda - (j+1)\Gamma F - \rho_a'\right]\left[Z' - Z\left(\frac{\Gamma'}{\Gamma} + \frac{F'}{F}\right)\right] \tag{III.7}$$

$$F_\mathfrak{Z}' \equiv \frac{\partial F_\mathfrak{Z}}{\partial \ln \mathfrak{Z}} = \left(\frac{F-1}{F}\right)F'' + \left(\frac{F'}{F}\right)^2 - \frac{1}{\Gamma F g}\left\{Z g''\right.$$

$$\left. + g'\left[Z' - Z\left(\frac{\Gamma'}{\Gamma} + \frac{g'}{g} + \frac{F'}{F}\right)\right]\right\} \tag{III.8}$$

$$F'_\omega \equiv \frac{\partial F_\omega}{\partial \ln \mathfrak{z}} = (1-F)\,\Phi'_F - F'\Phi_F + \frac{z}{\Gamma F}(\Gamma\Phi'_M + \Gamma'\Phi_M + \Phi'_E)$$

$$+ \left(\frac{\Gamma\Phi_M + \Phi_E}{\Gamma F}\right)\left[z' - z\left(\frac{\Gamma'}{\Gamma} + \frac{F'}{F}\right)\right] \tag{III.9}$$

while

$$H'_x \equiv \frac{\partial H_x}{\partial \ln \mathfrak{z}} = \frac{1}{(1-F)}\left\{F\,F'_x + F_x\,F' + \left[(j+1)F + \rho'_a\right]D'\right.$$

$$+ D\left[(j+1)\,F' + \rho''_a\right] + H_x\,\frac{F'}{(1-F)} \tag{III.10}$$

$$H'_\mathfrak{z} \equiv \frac{\partial H_\mathfrak{z}}{\partial \ln \mathfrak{z}} = \frac{1}{(1-F)}\left[F\,F'_\mathfrak{z} + F'\,F_\mathfrak{z} + \frac{D}{h}\left(h'' - \frac{h'^2}{h}\right)\right.$$

$$+ \frac{h'}{h}\,D'\right] + H_\mathfrak{z}\left(\frac{F'}{1-F}\right) \tag{III.11}$$

$$H'_\omega \equiv \frac{\partial H_\omega}{\partial \ln \mathfrak{z}} = \frac{1}{(1-F)}\left[F\,F'_\omega + F'\,F_\omega - \Phi_M\,D' - \Phi'\,D\right]$$

$$+ H_\omega\left(\frac{F'}{1-F}\right) \tag{III.12}$$

and

$$G'_x \equiv \frac{\partial G_x}{\partial \ln \mathfrak{z}} = \frac{1}{(1-F)}\left\{\Gamma(F'\,F_x + F\,F'_x) + \Gamma'F\,F_x + \left[\Gamma F(j+1)\right.\right.$$

$$\left. -\dot{\lambda} + \rho'_a\right]D' + D\left[(j+1)(\Gamma F' + \Gamma'F) - \lambda' + \rho''_a\right] + \frac{G_x F'}{1-F} \tag{III.13}$$

$$G_{\mathfrak{z}}' \equiv \frac{\partial G_{\mathfrak{z}}}{\partial \ln \mathfrak{z}} = \frac{1}{(1-F)} \left\{ \Gamma(F'F_{\mathfrak{z}} + FF_{\mathfrak{z}}') + \Gamma' F F_{\mathfrak{z}} + \frac{D}{g}\left(g'' - \frac{g'^2}{g}\right) \right.$$

$$\left. + \frac{g'}{g} D' \right\} + G_{\mathfrak{z}} \left(\frac{F'}{1-F}\right) \qquad \text{(III.14)}$$

$$G_{\omega}' \equiv \frac{\partial G_{\omega}}{\partial \ln \mathfrak{z}} = \frac{1}{(1-F)} \left\{ \Gamma(F F_{\omega}' + F' F_{\omega}) + \Gamma' F F_{\omega} - (\Gamma \Phi_M + \Phi_E) D' \right.$$

$$\left. - (\Gamma \Phi_M' + \Gamma' \Phi_M + \Phi_E') D + G_{\omega}\left(\frac{F'}{1-F}\right) \right. \qquad \text{(III.15)}$$

where

$$\left(\frac{1}{\chi D}\right)' \equiv \frac{\partial \left(\frac{1}{\chi D}\right)}{\partial \ln \mathfrak{z}} = -\left(\frac{1}{\chi D^2}\right)\left[Z' + 2(1-F)F'\right] \qquad \text{(III.16)}$$

Now, for simplicity, consider the case of perfect gas with constant specific heats and constant ρ_a . For adiabatic point explosion, the boundary conditions are given by Eqs. (II.88) - (II.90), and since

$$\mathcal{F}' \equiv \frac{\partial \mathcal{F}}{\partial \ln \mathfrak{z}} = \lambda y \frac{\partial \mathcal{F}}{\partial y}$$

one may then evaluate Eqs. (III.7) - (III.16) at $\chi = 1$, by noting that

$$F_n = f_n = \frac{2}{\gamma+1}(1-y)$$

$$F_n' = f_n' = -\lambda y \left(\frac{2}{\gamma+1}\right)$$

$$F_n'' = f_n'' = \left(\frac{-2}{\gamma+1}\right)(\lambda y)\left(\lambda + y\frac{d\lambda}{dy}\right)$$

$$h_n = \frac{\gamma+1}{\gamma-1+2y}$$

$$h_n' = (\lambda y)\frac{[-2(\gamma+1)]}{(\gamma-1+2y)^2}$$

$$h_n'' = \frac{-2(\gamma+1)\lambda y}{(\gamma-1+2y)^2}\left[\frac{-4\lambda y}{\gamma-1+2y} + \lambda + y\frac{d\lambda}{dy}\right]$$

$$g_n = \frac{2\gamma - (\gamma-1)y}{\gamma(\gamma+1)}$$

$$g_n' = -\frac{(\gamma-1)}{\gamma(\gamma+1)}\lambda y$$

$$g_n'' = -\frac{(\gamma-1)}{\gamma(\gamma+1)}(\lambda y)\left(\lambda + y\frac{d\lambda}{dy}\right)$$

$$Z_n = \frac{\gamma g_n}{h_n} = \frac{1}{(\gamma+1)^2}\left[2\gamma - (\gamma-1)y\right]\left[\gamma-1+2y\right]$$

$$Z_n' = \frac{\lambda y}{(\gamma+1)^2}\left\{2\left[2\gamma - (\gamma-1)y\right] - (\gamma-1)(\gamma-1+2y)\right\}$$

The above equations, then, give, for any order of the expansion, algebraic expressions for $\frac{\partial F}{\partial \ln\zeta}$, $\frac{\partial h}{\partial \ln\zeta}$, and $\frac{\partial g}{\partial \ln\zeta}$. These may be substituted in F_ζ , H_ζ , and G_ζ , respectively, to yield a set of first-order autonomous differential equations with respect to the field coordinate χ , where y , λ and its derivatives appear as parameters. The gasdynamic flow fields may now be obtained for each value of y , where λ and its derivatives are found either from experiment or from the energy integral, by integrating these auto-

nomous equations.

III.3. QUASI-SIMILAR METHOD OF SOLUTION

The concept of the so-called Oshima's "quasi-similar" solution states that the derivatives of all dependent variables with respect to the front coordinate, ζ or y , are considered constants in all of the flow field and equal to those corresponding to $x = 1$. This concept arises from the fact that the variations of the dependent variables f , h , and g are not sensitive to the independent variable ζ , or y , as compared to their variations with the other independent variable x . However, this assumption causes the solution to be accurate for high Mach numbers, corresponding to small values of y , and just behind the wave front.

From the mathematical point of view, this method of solution may be considered as the zeroth order of the Taylor's series expansion of a function of two independent variables. It follows from Eqs. (III.5) that

$$\frac{\partial f}{\partial y} = \left(\frac{\partial f}{\partial y}\right)_{x=1} \tag{III.17a}$$

$$\frac{\partial h}{\partial y} = \left(\frac{\partial h}{\partial y}\right)_{x=1} \tag{III.17b}$$

$$\frac{\partial g}{\partial y} = \left(\frac{\partial g}{\partial y}\right)_{x=1} \tag{III.17c}$$

This leads Oshima to express the non-dimensional dependent variables in the following form

$$f(x,y) = f_1(x) \cdot f_2(y)$$

$$h(x,y) = h_1(x) \cdot h_2(y)$$

and

$$g(x,y) = g_1'(x) \cdot g_2(y)$$

Differentiating the above equations with respect to y, one obtains

$$\frac{\partial f(x,y)}{\partial y} = \frac{f(x,y)}{f_2(y)} \cdot \frac{d f_2'(y)}{dy} \qquad \text{(III.18a)}$$

$$\frac{\partial h(x,y)}{\partial y} = \frac{h(x,y)}{h_2(y)} \cdot \frac{d h_2(y)}{dy} \qquad \text{(III.18b)}$$

$$\frac{\partial g(x,y)}{\partial y} = \frac{g(x,y)}{g_2(y)} \cdot \frac{d g_2(y)}{dy} \qquad \text{(III.18c)}$$

Taking the values of $f_2(y)$, $h_2(y)$ and $g_2(y)$ as their values at the wave front, yields to the required solution.

For constant ρ_a and when the medium may be considered as a perfect gas with constant specific heats, Eqs. (III.18) may be obtained simply from the boundary conditions of adiabatic point explosion, Eqs. (II.88) - (II.90), or from the boundary conditions of reactive detonating blast waves, Eqs. (II.54), (II.85) and (II.93).

1. Adiabatic point explosion

In this case, one obtains from Eqs. (II.88) - (II.90)

$$\frac{d f_a(y)}{d y} = \frac{d f_n}{d y} = \frac{-2}{\gamma + 1} \tag{III.19a}$$

$$\frac{d h_a(y)}{d y} = \frac{d h_n}{d y} = - \frac{2(\gamma + 1)}{(\gamma - 1 + 2y)^2} \tag{III.19b}$$

$$\frac{d g_a(y)}{d y} = \frac{d g_n}{d y} = - \frac{(\gamma - 1)}{\gamma(\gamma + 1)} \tag{III.19c}$$

Substituting Eqs. (II.88) - (II.90) as well as Eqs. (III.19) into Eqs. (III.18) yields, respectively

$$\frac{\partial f}{\partial y} = - \frac{f}{(1 - y)} \tag{III.20}$$

$$\frac{\partial h}{\partial y} = - \frac{2h}{\gamma - 1 + 2y} \tag{III.21}$$

and

$$\frac{\partial g}{\partial y} = - \frac{(\gamma - 1) g}{2\gamma - (\gamma - 1) y} \tag{III.22}$$

Substitution of Eqs. (III.20) - (III.22) into governing equations, Eqs. (II.20), (]I.22) and (II.83), yields, respectively

$$\frac{(f - x)}{h} \cdot \frac{dh}{dx} + \frac{df}{dx} + j \frac{f}{x} + \lambda A = \Phi_M \tag{III.23}$$

$$\frac{(f - x)}{f} \frac{df}{dx} + \frac{1}{hf} \frac{dg}{dx} + \lambda B = \Phi_F \tag{III.24}$$

$$\frac{(f-x)}{g} \frac{dg}{dx} - \gamma \frac{(f-x)}{h} \frac{dh}{dx} + \lambda C = \Phi_E \qquad \text{(III.25)}$$

where

$$A \equiv - \frac{2y}{(\gamma-1) + 2y}$$

$$B \equiv - \frac{y+1}{2(1-y)}$$

$$C \equiv - \left[\frac{2\gamma}{2\gamma - (\gamma-1)y} + \gamma A \right]$$

Thus, the quasi-similarity assumption has reduced the set of non-linear partial differentail equations to a set of ordinary differential equations without making the strong shock approximation.

Solving for the derivatives $\frac{df}{dx}$, $\frac{dh}{dx}$ and $\frac{dg}{dx}$ in Eqs. (III.23) - (III.25), one obtains

$$\frac{df}{dx} = \frac{\frac{i\gamma gf}{x} + \lambda gC + f(f-x)h(\Phi_F - \lambda B) - \gamma g(\Phi_M - \lambda A) - g\Phi_E}{h(f-x)^2 - \gamma g} \qquad \text{(III.26)}$$

$$\frac{dh}{dx} = \frac{-h}{(f-x)} \left[\frac{df}{dx} + j\frac{f}{x} + \lambda A - \Phi_M \right] \qquad \text{(III.27)}$$

$$\frac{dg}{dx} = -h \left[(f-x)\frac{df}{dx} + \lambda f B - f\Phi_F \right] \qquad \text{(III.28)}$$

2. Detonating blast waves

Applying the same previous procedure, one arrives finally at the same Eqs. (III.26) - (III.28), except for the parameters A, B and G, which will, with the aid of Eqs. (II.54), (II.85) and (II.93), take the following form

$$A \equiv \frac{\varphi}{1 - f_n}$$

$$B \equiv \frac{\varphi}{f_n} - 0.5$$

$$G \equiv \frac{\gamma \varphi + y}{\gamma f_n + y} - 1 - \gamma A$$

where

$$\varphi \equiv y \frac{df_n}{dy} = \left(\frac{-y}{\gamma+1} \right) \left[1 + \frac{\left(\frac{1-y}{\gamma+1} \right) + (\gamma-1)\bar{q}}{\sqrt{\left(\frac{1-y}{\gamma+1} \right)^2 - 2 \left(\frac{\gamma-1}{\gamma+1} \right) y \bar{q}}} \right]$$

III.4. ADIABATIC INTEGRAL

In order to find a check on the numerical method used for solving the governing equations of the quasi-similar solutions in the case of sourceless adiabatic flow fields, one may derive an intermediate integral, the so-called adiabatic integral. The continuity and energy equations, Eqs. (III.23) and (III.25), can be rewritten for sourceless flow fields as

$$(f - x) \frac{d \ln h}{dx} + \frac{df}{dx} + j \frac{f}{x} + \lambda A = 0 \tag{III.29}$$

$$(f-x)\frac{d\ln g}{dx} - \gamma(f-x)\frac{d\ln h}{dx} + \lambda C = 0 \qquad \text{(III.30)}$$

with

$$A = -\frac{2y}{\gamma - 1 + 2y}$$

and

$$C = -2\gamma\left[\frac{1}{2\gamma - (\gamma-1)y} - \frac{y}{\gamma - 1 + 2y}\right]$$

To find the adiabatic integral from the above two equations, one may multiply the first of them by an integration factor ψ and then subtract Eq. (III.30) from it, one obtains

$$(f-x)\left[(\psi + \gamma)\frac{d\ln h}{dx} - \frac{d\ln g}{dx}\right] + (\frac{df}{dx} - 1)\psi + j\frac{f}{x}\psi$$
$$+ \psi' + \lambda(\psi A - C) = 0 \qquad \text{(III.31)}$$

For the above equation to be integrated, the value of the integration factor ψ will be chosen as to satisfy the condition

$$j\psi = -\lambda(\psi A - C) - \psi$$

from which one gets

$$\psi = \frac{\lambda C}{j+1 + \lambda A}$$

Or, with the use of the definitions of ψ and C ,

$$\Psi = \frac{2\gamma\lambda\left[y/(\gamma-1+2y)-i/(2\gamma+y-\gamma y)\right]}{j+1-2\lambda y/(\gamma-1+2y)} \qquad \text{(III.32)}$$

Therefore, Eq. (III.31) will be

$$(\Psi+\gamma)\frac{d\,\ell_n h}{dx} - \frac{d\,\ell_n g}{dx} + \Psi\left(\frac{\frac{df}{dx}-1}{f-x}\right) + \frac{j\gamma}{x} = 0$$

which yields upon integration

$$\frac{h^\gamma}{g}\left[h\,x^j(x-f)\right]^\Psi = K$$

where K is a constant of integration which can be determined from the boundary conditions, Eqs. (II.88) - (II.90), one gets

$$K = \frac{h_n^{\Psi+\gamma}}{g_n}(1-f_n)^\Psi$$

$$= \frac{\gamma(\gamma+1)\left[(\gamma+1)/(\gamma-1+2y)\right]^\gamma}{(2\gamma-\gamma y+y)}$$

Therefore, the adiabatic integral will be

$$\frac{h^\gamma}{g}\left[h\,x^j(x-f)\right]^{\frac{2\gamma\lambda\left[y/(\gamma-1+2y)-1/(2\gamma+y-\gamma y)\right]}{j+1-2\lambda y/(\gamma-1+2y)}} = \frac{\gamma(\gamma+1)\left[(\gamma+1)(\gamma-1+2y)\right]^\gamma}{(2\gamma-\gamma y+y)} \qquad \text{(III.33)}$$

In the case of strong explosions, $y = 0$ and $\lambda = j+1$, the above integral reduces to

$$\frac{h^{\gamma}}{g} \left[h \, x^{j} (x-f) \right]^{-1} = \left(\frac{\gamma+1}{2}\right) \left(\frac{\gamma+1}{\gamma-1}\right)^{\gamma} \tag{III.34}$$

The adiabatic integral, Eq. (III.33), has been used as a check on the precision of machine computations. The step size Δx in the Runge-Kutta method was assigned different values until the values of f, h and g, obtained from the numerical calculations, satisfied Eq. (III.33) in a desired accuracy.

III.5. SINGULARITY ANALYSIS

In order to analyse the singularities of the governing equations, it is more convenient to transform them into the phase plane, i.e. in terms of the reduced variables F and Z defined by Eq. (III.16), which are, for a perfect gas

$$Z(x,y) = \frac{\gamma g}{x^2 h} \qquad \text{and} \qquad F(x,y) = \frac{f}{x} \tag{III.35}$$

In the governing equations for quasi-similar solutions, one has derivatives with respect to x only while the variable y appears as a parameter. Therefore, one can write

$$\frac{1}{Z} \frac{dZ}{dx} = \frac{1}{g} \frac{dg}{dx} - \frac{1}{h} \frac{dh}{dx} - \frac{2}{x}$$

and

$$\frac{1}{F} \frac{dF}{dx} = \frac{1}{f} \frac{df}{dx} - \frac{1}{x}$$

The above two equations combined with Eq. (III.35) when substituted in Eqs. (III.23) through (III.25) give for a sourceless flow field

$$(F-1)\frac{d\ln h}{dF} + F\frac{d\ln x}{dF}\left(j+1+\frac{q\lambda}{F}\right) + 1 = 0 \qquad \text{(III.36)}$$

$$\frac{Z}{\delta}\frac{d\ln h}{dF} + \frac{d\ln x}{dF}\left[F(F-1)+\frac{2Z}{\delta}+\lambda FB\right] + \frac{Z}{\delta}\frac{d\ln Z}{dF} + (F-1) = 0 \qquad \text{(III.37)}$$

$$(1-\delta)(F-1)\frac{d\ln h}{dF} + \frac{d\ln x}{dF}\left[2(F-1)+\lambda C\right] + (F-1)\frac{d\ln Z}{dF} = 0 \qquad \text{(III.38)}$$

Solving for the logarithmic derivatives $\dfrac{d\ln h}{dF}$, $\dfrac{d\ln x}{dF}$ and $\dfrac{d\ln Z}{dF}$, one gets

$$\frac{d\ln h}{dF} = \frac{(F-1)^2(A\lambda + jF) - \lambda F(F-1)B + Z(\lambda C/\delta)}{(F-1)\left\{F(F-1)^2 + \lambda F(F-1)B - Z\left[F(j+1)+A\lambda+\lambda C/\delta\right]\right\}} \qquad \text{(III.39)}$$

$$\frac{d\ln x}{dF} = \frac{Z-(1-F)^2}{F(F-1)^2 + \lambda F(F-1)B - Z\left[F(j+1)+A\lambda+\lambda C/\delta\right]} \qquad \text{(III.40)}$$

$$\frac{d\ln Z}{dF} = \frac{(\delta-1)\left\{(F-1)^2(A\lambda+jF)-\lambda F(F-1)B+Z\lambda C/\delta\right]-\left[2(F-1)+\lambda C\right]\left[Z-(1-F)^2\right]}{(F-1)\left\{F(F-1)^2+\lambda F(F-1)B-Z\left[F(j+1)+A\lambda+\frac{\lambda C}{\delta}\right]\right\}} \qquad \text{(III.41)}$$

The Rankine-Hugoniot conditions at the shock front can be rewritten in terms

of the variables Z and F by combining Eqs. (II.88) through (II.90) with Eq. (II.16)

$$Z_n = Z(1,y) = \frac{[2\gamma - (\gamma-1)y](\gamma-1+2y)}{(\gamma+1)^2} \qquad \text{(III.42)}$$

$$F_n = F(1,y) = \left(\frac{2}{\gamma+1}\right)(1-y) \qquad \text{(III.43)}$$

Eliminating y from the above two equations, one obtains a relation between Z_n and F_n . It is

$$Z_n = (1 - F_n)\left(1 + \frac{\gamma-1}{2}F_n\right) \qquad \text{(III.44)}$$

It is obvious that the solution of Eqs. (III.26) through (III.28) will diverge when the denominators vanish. This will happen at the values of x given by:

$$x = 0 \qquad \text{(III.45a)}$$

$$x = f \qquad \text{(III.45b)}$$

$$x = f \pm \sqrt{\frac{\gamma g}{h}} \qquad \text{(III.45c)}$$

The divergence of the solution at $x = 0$ may be avoided by expanding the fluid properties in terms of x near the center of symmetry. The continuity and momentum equations for a sourceless flow field, after some algebraic manipula-

tions, can be written as

$$\frac{\partial}{\partial t}(\rho r^j) + \frac{\partial}{\partial r}(\rho u r^j) = 0 \qquad \text{(III.46)}$$

$$\frac{\partial}{\partial t}(\rho u) + \frac{j}{r}(\rho u^2) + \frac{\partial}{\partial r}(\rho u^2) + \frac{\partial P}{\partial r} = 0 \qquad \text{(III.47)}$$

Integrating Eq. (III.46) with respect to r, one obtains

$$\rho u r^j = -\int_0^r r^j \left(\frac{\partial \rho}{\partial t}\right) dr + Const_1$$

under the condition that $u = 0$ at $r = 0$, the constant in the above equation will be zero, and this equation becomes

$$u(r,t) = -\frac{1}{\rho r^j} \int_0^r r^j \left(\frac{\partial \rho}{\partial t}\right) dr \qquad \text{(III.48)}$$

In a similar manner, Eq. (III.47) upon integration with respect to r, yields

$$P(r,t) = -\rho u^2 - \int_0^r \frac{\partial(\rho u)}{\partial t} dr - \int_0^r \frac{j}{r} \rho u^2 dr + Const_2$$

Also, in order to determine the constant in the above equation, we use the condition that $u = 0$ at $r = 0$. Hence, the above equation becomes

$$P(r,t) = P(o,t) - \rho u^2 - \int_0^r \frac{\partial(\rho u)}{\partial t} dr - \int_0^r \frac{j \rho u^2}{r} dr \qquad \text{(III.49)}$$

Differentiating Eq. (III.48) with respect to time and substituting into the above equation, one gets

$$P(r,t) = P(o,t) - \rho u^2 - j \int_o^r \frac{\rho u^2}{r} \, dr + \int_o \frac{1}{r^j} \int_o^r r^j \left(\frac{\partial^2 \rho}{\partial t^2}\right) dr \qquad \text{(III.50)}$$

Assuming that the density $\rho(r,t)$ can be expanded in the following power series near the center of symmetry

$$\rho(r,t) = r^\alpha \left[\rho_o(t) + \rho_1(t) \, r + \rho_2(t) \, r^2 + \text{----} \right] \qquad \text{(III.51)}$$

where α is a constant and the coefficients ρ_o, ρ_1, ρ_2, ... are functions of time only.

Substituting the preceeding series into Eq. (III.48) and integrating with respect to r, one obtains the velocity profile represented as a series of the form

$$u(r,t) = r \left[u_o(t) + u_1(t) \, r + u_2(t) \, r^2 + \text{---} \right] \qquad \text{(III.52)}$$

where the coefficients u_o, u_1, u_2, -- are functions of time only.

Substituting from Eqs. (III.51) and (III.52) into Eq. (III.50), one finds that the pressure can also be represented as a series of the form

$$P(r,t) = P(o,t) + r^{\alpha+2} \left[P_o(t) + P_1(t) \, r + P_2(t) \, r^2 + \text{--} \right] \qquad \text{(III.53)}$$

where $P(o,t)$, P_o, P_1, P_2, --- are functions of the time only.

For convenience, the three series for the density, velocity and pressure can be rewritten in a non-dimensional form as

$$h = x^{\alpha}(h_0 + h_1' x + h_2 x^2 + \text{---}) \qquad \text{(III.54)}$$

$$f = x(f_0 + f_1 x + f_2 x^2 + \text{----}) \qquad \text{(III.55)}$$

$$g = g(o,y) + x^{\alpha+2}(g_0 + g_1 x + g_2 x^2 + \text{---}) \qquad \text{(III.56)}$$

where the coefficients h_0, h_1, h_2, ----, f_0, f_1, f_2, --- and $g(o,y)$, g_0, g_1, g_2, ---- are functions of y only.

It is evident that for small values of x, i.e., $x \ll 1$, the following asymptotic formulae hold

$$f = f_0 x \qquad \text{(III.57)}$$

$$h = h_0 x^{\alpha} \qquad \text{(III.58)}$$

$$g = g(o,y) + g_0 x^{\alpha+2} \qquad \text{(III.59)}$$

The fact that the velocity profile is linear near the center of symmetry indicates that the value of f/x will be finite and no divergence of the solution will occur.

Because one cannot proceed with the numerical solution till the center of symmetry, the solution will be based on matching the numerical solution, from $x = 1$ to $x = \bar{x}$, with the asymptotic formulae for f, h and g given by Eqs. (III.57) - (III.59), provided that the value of $\bar{x}$ must be as small as possible.

In terms of the reduced variables F and Z, the other two singularities,

given by Eqs. (III.45), correspond to

$$F = 1.0 \tag{III.60}$$

$$Z = (1 - F)^2 \tag{III.61}$$

The value of the variable F at the shock front is given from Eq. (III.43) while its value at the center of symmetry is obtained by substituting $x = 0$ in Eq. (III.55). It gives

$$F\big)_{x=0} = \left(\frac{f}{x}\right)_{x=0} = f_0$$

Therefore, the range of variation of F is given by the inequality

$$f_0 \leq F \leq \left(\frac{2}{\gamma+1}\right)(1-y)$$

The relationship between Z and F has been obtained by solving Eq. (III.41) numerically as F ranged over its value at $x = 1$ to its value at $x = 0$.

Since the value of λ is not known a priori, an iteration procedure is performed to search for the correct λ. The correct λ may be obtained based on satisfaction of the energy integral equation, Eq. (II.98), or it may be found when it satisfies the condition of zero velocity at the center of symmetry, Eq. (II.112). When the value of λ is greater or less than the correct one, the solution will diverge at some non-zero values of x corresponding to the singularity $F = 1$ or $Z = (1-F)^2$.

Furthermore, from the theory of ordinary differential equations, the slope $\frac{dZ}{dF}$ will take the indetermined value $\frac{0}{0}$ when both the numerator and denominator on the right hand side of Eq. (III.41) vanish simultaneously. This will correspond to a number of singular points given as the intersection of the isocline of zero slope with the isocline of infinite slope.

The isocline of zero slope is given from the following equation

$$Z\left[(F-1)\left\{(\gamma-1)\left[jF(F-1)-\lambda FB\right]-2Z+2(F-1)^2+(F-1)\lambda G\right\}\right]=0 \qquad \text{(III.62)}$$

while the equation of the isocline of infinite slope is

$$(F-1)\left\{F(F-1)^2+\lambda F(F-1)B-ZF(j+1)-Z\lambda(A+G/\gamma)\right\}=0 \qquad \text{(III.63)}$$

Solving for Z from Eq. (III.63), one gets

$$Z=\frac{F(F-1)^2+\lambda F(F-1)B}{F(j+1)+\lambda(A+G/\gamma)}$$

Substituting the value of Z from the above equation, one obtains an expression for the values of F at the singular points. These values are obtained from the roots of the equation

$$(F-1)\left[(\gamma-1)\left\{jF(F-1)-\lambda FB\right\}+2(F-1)^2+\lambda(F-1)G\right]$$
$$-2\frac{F(F-1)^2+\lambda F(F-1)B}{F(j+1)+\lambda(A+G/\gamma)}=0 \qquad \text{(III.64)}$$

At each value of y, the roots of the above equation can be obtained numerically using a root search technique. Depending on the value of λ, singular points may exist inside the field $f_0 \leq F \leq (\frac{2}{\gamma+1})(1-y)$. With the correct value of λ satisfying the condition $f(0,y)=0$, the roots of the above equation lie outside the field and the solution is free from singularities.

APPLICATIONS

IV.1. ADIABATIC POINT EXPLOSIONS*

i) Introduction

In this section, a detailed solution for the non-self-similar blast waves in an adiabatic medium is obtained. The three geometrical symmetries of blast waves: spherical, cylindrical and planar are considered. The flow field is considered as a sourceless one, while the medium is treated as a perfect gas with constant specific heats. The solution is based on satisfying the condition of zero particle velocity at the center of symmetry rather than the constant energy criterion. Using this condition, a considerable saving in the numerical solution steps is achieved. Finally, the accuracy of the present solution is discussed by comparing it with other solutions.

ii) Problem Formulation

The basic equations governing any gasdynamic problem are given by Eqs. (II.20), (II.22) and (II.27). For a perfect gas with constant specific heats, a sourceless flow field and uniform ambient density, these equations may be represented as:

$$(f-x)\frac{\partial h}{\partial x} + \lambda y\frac{\partial h}{\partial y} + h\left(\frac{\partial f}{\partial x} + j\frac{f}{x}\right) = 0$$

$$(f-x)\frac{\partial f}{\partial x} + \lambda y\frac{\partial f}{\partial y} + \frac{1}{h}\frac{\partial g}{\partial x} - \frac{1}{2}f\lambda = 0 \qquad \text{(IV.1.1)}$$

and

$$(f-x)\frac{\partial g}{\partial x} + \lambda y\frac{\partial g}{\partial y} + \gamma g\left(\frac{\partial f}{\partial x} + j\frac{f}{x}\right) - \lambda g = 0$$

The boundary conditions of the problem are given by the Rankine-Hugoniot rela-

---

*This application is based on Attia (1974).

tions, Eqs. (II.88) - (II.90), which may be rewritten as follows

$$f_n = f(1, y) = (1 - \beta)(1 - y)$$

$$h_n = h(1, y) = \frac{1}{\beta + (1 - \beta)y} \qquad \qquad (IV.1.2)$$

and

$$g_n = g(1, y) = (1 - \beta)\left(1 - \frac{\beta}{1 + \beta} y\right)$$

where

$$\beta \equiv \frac{\gamma - 1}{\gamma + 1}$$

The application of the quasi-similar approximation on the governing equations, Eqs. (IV.1.1), yields the following ordinary differential equations, as given by Eqs. (III.23) - (III.25) when all ϕ 's vanish

$$(f - x)\frac{dh}{dx} + h\left(\frac{df}{dx} + j\frac{f}{x}\right) + \lambda h A = 0$$

$$(f - x)\frac{df}{dx} + \frac{1}{h}\frac{dg}{dx} + \lambda f B = 0 \qquad \qquad (IV.1.3)$$

and

$$(f - x)\frac{dg}{dx} + \gamma g\left(\frac{df}{dx} + j\frac{f}{x}\right) + \lambda g C = 0$$

where

$$A \equiv - \frac{(1-\beta)\, y}{\beta + (1-\beta)\, y}$$

$$B \equiv - \frac{y+1}{2(1-y)}.$$

and

$$C \equiv - \frac{1}{1 - \frac{\beta}{1+\beta}\, y}$$

Equations (IV.1.3) may be put in the following autonomous form, as given by Eqs. (III.26) - (III.28), with all ϕ 's set to equal zero

$$\frac{df}{dx} = \frac{\frac{j\gamma gf}{x} + \lambda g\, C - \lambda f(f-x)B}{h\,(f-x)^2 - \gamma g}$$

$$\frac{dh}{dx} = \frac{-h}{(f-x)}\left(\frac{df}{dx} + j\frac{f}{x} + \lambda A\right) \qquad\qquad \text{(IV.1.4)}$$

and

$$\frac{dg}{dx} = - h \left[(f-x)\frac{df}{dx} + \lambda f B\right]$$

An overall check for the denisty profiles is the mass integral, Eq. (III.65), which can be rewritten as

$$J_1 = \int_0^1 h\, x^j\, dx = \frac{1}{j+1} \qquad\qquad \text{(IV.1.5)}$$

Furthermore, multiplying the first of Eqs. (IV.1.3) by x^j and arranging terms, one has

$$x^j \frac{d}{dx}(fh) - x^{j+1} \frac{dh}{dx} + j x^{j-1} fh + \lambda hA x^j = 0$$

Integrating the above equation with respect to x from $x = 0$ to $x = 1$, one gets after some algebraic manipulations

$$\int_0^1 d(x^j fh) - \int_0^1 d(x^{j+1} h) + (j+1 + A\lambda) \int_0^1 h x^j \, dx = 0$$

which gives

$$h_n (f_n - 1) + (j+1 + A\lambda) \int_0^1 h x^j \, dx = 0$$

Using Eqs. (IV.1.2), one obtains

$$\int_0^1 h x^j \, dx = \frac{1}{j+1 + A\lambda} \qquad\qquad \text{(IV.1.6)}$$

Consequently, the density profile obtained by the quasi-similar solution does not satisfy the global mass conservation. However, it should satisfy the quasi-similar mass integral given by Eq. (IV.1.6).

The difference, ϵ , between the two mass integral equations, which represents the inherent deviation introduced by the quasi-similar approximation, can be obtained from Eqs. (IV.1.5) and (IV.1.6) as

$$\epsilon = \frac{1}{j+1 + A\lambda} - \frac{1}{j+1}$$

or

$$\epsilon = \frac{-A\lambda}{(j+1)(j+1 + A\lambda)}$$

Since both A and λ are functions of y, the error in the mass integral is also a function of y. It is obvious that the error is zero when $A = 0$ and this corresponds to $y = 0$ which is the self-similar case.

The energy integral, Eq. (II.95), is reduced to

$$\mathcal{J}_3 = \int_0^1 \left(\frac{h f^2}{2} + \frac{g}{\gamma - 1} \right) x^j \, dx = \frac{y}{\gamma} \left[\mathcal{J}^{-(j+1)} + \frac{1}{(j+1)(\gamma-1)} \right] \qquad \text{(IV.1.7)}$$

while the decay coefficient λ takes the form given by Eq. (II.98), which is

$$\lambda = \frac{(j+1)\,\mathcal{J}_3 - \frac{y}{\gamma(\gamma-1)}}{\mathcal{J}_3 - y \frac{d\mathcal{J}_3}{dy}} \qquad \text{(IV.1.8)}$$

THe adiabatic integral, Eq. (III.33), which is used as a check on the precision of the numerical solution, may be rewritten as follows

$$\frac{h^\gamma}{g} \left[h\, x^j (x - f) \right]^y = \frac{1}{(\beta - 1)\left(1 - \frac{\beta y}{\beta + 1}\right) \left[\beta + (1-\beta)y\right]^\gamma} \qquad \text{(IV.1.9)}$$

with

$$y = \frac{\lambda (G - \gamma A)}{j + 1 + \lambda A}$$

The solution is considered to be correct when it satisfies the compatibility equation, Eq. (II.112), that is

$$f(0, y) = 0 \tag{IV.1.10}$$

iii) Solution

The governing equations of the quasi-similar solution in their autonomous form, Eqs. (IV.1.4), which are coupled ordinary differential ones, are subject to the boundary conditions given by Eqs. (IV.1.2). These equations can be easily integrated numerically, once the correct value of λ at a specific y is determined. There are two criteria for evaluating the shock decay coefficient λ. One is based on the conservation of total energy behind the shock and the other is based on satisfying the condition of symmetry, namely, $f = 0$ at the center of symmetry. Although only the latter is used in these calculations, it may be interesting to summarize the steps of calculations which one may follow to determine the correct λ based on each criterion.

First of all, one should chose the values of step sizes of both x and y. The whole range of y ($0 < y < 1$) is divided into small intervals, not necessarily equal. The step size Δx is kept constant throughout the integration intervals, and assigned different values until the values of f, h and g, obtained from the numerical calculations, satisfied the adiabatic integral, Eq. (IV.1.9), with the desired accuracy.

If the solution at $y = y_i$ is known, then the solution at $y = y_{i+1}$ ($y_{i+1} = y_i + (\Delta y)_i$), based on the constant energy criterion, may be computed as follows

a) At the value of $y = y_{i+1}$, the boundary conditions f (1, y_{i+1}), h (1, y_{i+1}) and g (1, y_{i+1}) can be computed from Eqs. (IV.1.2).

b) A trial value of the decay coefficient λ is then chosen and Eqs. (IV.1.4) can be solved numerically.

c) The value of the energy integral function $J_3)_{i+1}$ can then be determined from Eq. (IV.1.7) using any numerical integration method, for example, the Simpson's rule.

d) For small intervals in y, the derivative $\dfrac{dJ_3}{dy}$ in Eq. (IV.1.8) can be

put in a finite difference form as

$$\frac{d\mathcal{J}_3}{dy} = \frac{\Delta\mathcal{J}_3}{\Delta y} = \frac{\mathcal{J}_3)_{i+1} - \mathcal{J}_3)_i}{y_{i+1} - y_i} = \frac{\mathcal{J}_3)_{i+1} - \mathcal{J}_3)_i}{(\Delta y)_i}$$

Thus a calculated value of λ is given by

$$\lambda_{i+1} = \frac{(j+1)(\mathcal{J}_3)_{i+1} - [y_{i+1} / \sigma(\sigma+1)]}{\mathcal{J}_3)_{i+1} - y_{i+1}[\mathcal{J}_3)_{i+1} - \mathcal{J}_3)_i] / (\Delta y)_i}$$

e) The above procedure is repeated for other trial values of λ and a curve between the calculated values and the assumed ones may be drawn. The correct value of λ will be obtained as the intercept of the 45° line with the above curve and, with this correct value, the profiles of the various fluid properties are then determined.

f) Having computed everything at $y = y_{i+1}$, one can proceed further until the solution is obtained for the whole range of y.

To obtain the starting conditions for this computational procedure, one simply substitues $y = 0$ at the system of Eqs. (IV.1.4). They become

$$\frac{df}{dx} = \frac{\frac{j\sigma f}{x} - \lambda g + \frac{\lambda}{2} f(f-x)}{h(f-x)^2 - \sigma g}$$

$$\frac{dh}{dx} = \frac{-h}{(f-x)}\left(\frac{df}{dx} + j\frac{f}{x}\right)$$

and

$$\frac{dg}{dx} = -h\left[(f-x)\frac{df}{dx} - \frac{\lambda f}{2}\right]$$

Similarly, the substitution of $y = 0$ into Eq. (IV.1.8) yields

$$\lambda = j + 1$$

The boundary conditions, Eqs. (IV.1.2), become

$$f_n = 1 - \beta = \frac{2}{\gamma+1}$$

$$h_n = \frac{1}{\beta} = \frac{\gamma+1}{\gamma-1}$$

and

$$g_n = 1 - \beta = \frac{2}{\gamma+1}$$

Fortunately, this system of equations has been solved exactly using the concept of self-similarity. Thus, the value of $\sigma_3)_0$ (a $y = 0$) can be determined and is used as the starting value for the computational procedure.

On the other hand, the solution based on zero particle velocity at the center of symmetry, which is applied here, required the following calculation steps:

a) At any value of y , the boundary conditions $f(1,y)$, $h(1,y)$ and $g(1,y)$ can be computed from Eqs. (IV.1.2).

b) A trial value of the decay coefficient λ is assumed and Eqs. (IV.1.4) can be integrated numerically. Due to the singularity at the center of symmetry, the integration is stopped at $x = \bar{x}$ which is arbitrarily close to $x = 0$.

c) The velocity at the center of symmetry can then be obtained using linear extrapolation from $x = \bar{x}$ to $x = 0$.

d) The above procedure is repeated for several values of assumed decay coefficient and a curve is plotted between the assumed value of λ and the velo-

city at the center of symmetry. The correct value of λ is obtained as the intercept of the above curve with the line $f = 0$.

e) With the correct value of λ determined, the flow field parameters are to be obtained by matching the numerical solution, as x ranges over from $x = 1$ to $x = \bar{x}$, with appropriate asymptotic formulae valid from $x = \bar{x}$ to $x = 0$, as that given by Eqs. (III.57) - (III.59), which are

$$f = f_0 \, x$$

$$h = h_0 \, x^{\alpha}$$

and

$$g = g(0,y) + g_0 \, x^{\alpha+2}$$

The value of f_0 is determined as

$$f_0(y) = \frac{f(\bar{x},y)}{\bar{x}}$$

consequently, the velocity at any value of $x \leqslant \bar{x}$ is given by

$$f(x,y) = \frac{f(\bar{x},y)}{\bar{x}} \cdot x$$

One may now proceed to determine the density and pressure profiles near the center. The exponent α can be determined from the following relation

$$\frac{h(\bar{x}, y)}{h(\bar{x} - \Delta x, y)} = \left(\frac{\bar{x}}{\bar{x} - \Delta x}\right)^{\alpha}$$

where Δx is the step size used in the numerical iterative integration.

Having computed α from the preceeding equation, the value of the function h_o can be determined from

$$h_o(y) = \frac{h(\bar{x}, y)}{\bar{x}^{\alpha}}$$

Thus, the density at any value of $x \leq \bar{x}$ can be obtained as

$$h(x, y) = h_o(y) \, x^{\alpha}$$

In order to find the pressure profile near the center, one must first determine the functions $g(o, y)$ and $g_o(y)$. They can be obtained as the solution of the two simultaneous equations

$$g(\bar{x}, y) = g(o, y) + g_o(y) \, \bar{x}^{\alpha+2}$$

and

$$g(\bar{x} - \Delta x, y) = g(o, y) + g_o(y) (\bar{x} - \Delta x)^{\alpha+2}$$

Solving for the unknown functions $g_o(y)$ and $g(o, y)$, one obtains

$$g_o(y) = \frac{g(\bar{x} - \Delta x, y) - g(\bar{x}, y)}{(\bar{x} - \Delta x)^{\alpha+2} - \bar{x}^{\alpha+2}}$$

and

$$g(o,y) = \frac{(\bar{x}-\Delta x)^{\alpha+2} \, g(\bar{x},y) - \bar{x}^{\alpha+2} \, g(\bar{x}-\Delta x,y)}{(\bar{x}-\Delta x)^{\alpha+2} - \bar{x}^{\alpha+2}}$$

consequently the pressure at any value of $x \leqslant \bar{x}$ is given by

$$g(x,y) = g(o,y) + g_o(y) \, \bar{x}^{\alpha+2}$$

iv)   Results and Conclusions

The self-similar solution is illustrated in Figs. IV.1.1 to Fig. IV.1.4 $_j$ $\gamma=1.4$.
It is seen that the pressure immediately behind the shock wave is a maximum
and falls off quite rapidly near the shock wave to a nearly constant value for
$x < 0.5$. As expected, the fall-off in pressure is greatest for the spherical
case, with its greatest freedom for expansion, and least for the planar case.
The same tendency is even more accentuated in the density profiles, where it is
seen that nearly all of the mass of the gas engulfed by the blast is concentra-
ted close to the shock front itself. The effects of pressure and density chan-
ges are reflected in the temperature profiles, since $T \propto P/\rho$. It is seen
that, subject to the assumption of an inviscid, non-conducting and non-radia-
ting gas, enormous temperatures are developed towards the center of the blast,
as a result of the prevailing vanishingly small densities and finite pressure.
This is particularly marked in the spherical case. The particle velocities de-
crease from their maximum values immediately behind the shock front to zero at
the origin of the blast. It is observed that the curves differ only slightly
in the range $0.5 < x < 1$. At any given x , the spherical flow velocity is the
lowest and the planar velocity the largest.

During the decay of the shock front from its strong limit, self-similar case,
to a sound wave ($M = 1$), the quasi-similar model is used to predict the non-

self-similar case based on satisfying the condition of zero particle velocity at the center. This criterion is, of course, not new. It was used previously in finding higher order terms in the perturbation technique (Korobeinikov and Mel'nikova (1962); Bach and Lee (1969)).

Conditions behind the shock, as given by the solution based on the above mentioned criterion, are shown for air (γ = 1.4) in Figs. IV.1.5 - IV.1.16: they define the motion and the changes of the state of the gas in the three cases for j = 0, 1, 2 and for different values of the shock wave Mach number. It is observed that the decrease in the shock Mach number causes the pressure to be uniform in the whole range until the Mach number approaches unity where the pressure becomes vanishingly different from the ambient pressure. It is also seen that at high values of the shock Mach number ($M \geq$ 3) the density falls off very rapidly behind the shock. At low values of the shock Mach number, the mass engulfed by the front becomes equally distributed inside the wave and the density approaches the ambient density ρ_a everywhere except at x = 0. Particle velocities decrease as the time passes and tend to zero when the shock wave attenuates to a sound wave.

The usefulness of the derived asymptotic formulae, Eqs. (III.57) - (III.59), is apparent in the neighbourhood of x = 0, where the original equation shows a singularity. In this region, the velocity distribution is linear. Close to zero, the pressure is finite and asymptotically constant to the x coordinate. The density approaches zero very rapidly indicating that the gas is displaced from the center of the explosion. The temperature distribution $T \propto P/\rho$ shows a steep increase to infinite values.

In the course of high temperature processes within the blast the specific heat ratio, γ , differs from its initial value of 1.4. Therefore, the solution is also obtained, when assuming air to behave as a perfect gas with a constant average value of specific heat ratios of 1.2 and 1.3. Figures IV.1.17-IV.1.20 show a comparison between the distribution of fluid properties behind the wave front for the special case of j = 1, M = 5. The trend is the same for other values of M as well as for other types of blast waves (i.e. j = 0 and 2).

The accuracy of satisfying the adiabatic integral, Eq. (IV.1.9) is the criterion for the choice of the step size Δx in the Runge-Kutta iterative inte-

gration. Figure IV.1.21 shows that for Δx = 0.01, the adiabatic integral is satisfied within 1×10^{-7}. It is also seen that at first the error decreases quite rapidly with the step size and then becomes almost constant for $\Delta x \leqslant$ 0.005.

The integral curves in $Z - F$ phase plane where $Z \equiv \frac{xg}{x^2 h}$ and $F \equiv \frac{f}{x}$, are shown in Figs. (IV.1.22) - (IV.1.24) for different values of the shock Mach number. All the curves start from the Rankine-Hugoniot curve and all of them tend to infinity corresponding to x = 0. It is seen that the locii of the singularity $Z = (1 - F)^2$, Eq. (III.61), and the singularity F = 1, Eq. (III.80), do not intersect with any of the integral curves, i.e. the solutions are singularity free. Of course, all the integral curves are drawn with the correct value of λ satisfying the condition $f(o, y) = 0$.

The effect of inserting values of λ in the differential equation that are less or greater than the correct one is indicated in Fig. (IV.1.25) where it is seen that for λ less than the correct one, the singularity F = 1 is encountered while for λ greater than the correct value, the singularity $Z = (1 - F)^2$ is reached.

It may be observed from Fig. IV.1.26 that a considerable error is obtained in the mass integral which means that the density profiles are not accurate. However, the comparison made in Fig. IV.1.27 between the present solution and the solution of Bach and Lee (1969) indicates that the present solution has a wider range of applicability and, therefore, it gives a reasonable description of the shock trajectory.

The Rankine-Hugoniot shock conditions, which represent the maximum damage occurring due to the passage of the blast wave, are shown in Figs. IV.1.28 - IV.1.31. It is observed that when the blast expands, the pressure, temperature and density behind the shock wave approach the atmospheric conditions while the velocity behind the shock wave tends to zero. The relation of the shock wave attenuation is shown in Fig. IV.1.32, where it is seen that the shock Mach number approaches unity when the shock radius tends to infinity. The relation between the shock radius and the time is shown in Fig. IV.1.33. The decay coefficient obtained by the present criterion is shown in Fig. IV.1.34 as a function of y for the three types of blast waves: spherical, cy-

lindrical and planar.

The present calculation is compared with that of Oshima (1964) in the $\lambda - y$ curve, as shown in Fig. IV.1.35. It is seen that the present results give a slightly greater value for the decay coefficient. However, since the flow field is very sensitive to λ , this slight change may change the flow field considerably.

It should be noted that either the zero particle velocity criterion, or the energy integral criterion is sufficient in iterating for the correct solution. However, it was found that the solution based on zero particle velocity at the center is by far more sensitive than the energy integral to very small variations in λ as it approaches its correct value. Hence, higher accuracies in the solutions can be obtained using the zero particle velocity criterion. Figure IV.1.36 shows the variation of the particle velocity at the center $f(o,y)$ with the assumed value of λ . It is observed that any small change in the value of the decay coefficient produces a considerable change in the velocity at the center. In the present calculations the velocity at the center is considered zero when $|f(o,y)| \leq 10^{-4}$.

The iteration by the energy integral criterion is not rapidly convergent. Furthermore, when λ approaches its correct values, the properties of the solution by the zero particle velocity criterion, such as the position of the singular points and whether the velocity at the center is positive or negative, may indicate the direction for the correct values of the decay coefficient. In addition, reducing the step of the numerical integration, results in a considerable saving in machine time.

The difference between the results obtained from the two criteria is due to the quasi-similar approximation which reduced the partial differential equations to ordinary differential ones. It should be noted that if the governing equations were solved exactly, the two criteria would result in the same values of the decay coefficient and the flow field variables.

Figure Captions

Fig. IV.1.1   Self-similar pressure profiles for intense planar, cylindrical
             and spherical blast waves with γ = 1.4.

Fig. IV.1.2   Self-similar density profiles for intense planar, cylindrical
             and spherical blast waves with γ = 1.4.

Fig. IV.1.3   Self-similar temperature profiles for intense planar, cylindri-
             cal and spherical blast waves with γ = 1.4.

Fig. IV.1.4   Self-similar velocity profiles for intense planar, cylindrical
             and spherical blast waves with γ = 1.4.

Fig. IV.1.5   Pressure distribution behind the wave front for spherical blast
             waves at different values of the shock Mach number M while
              γ = 1.4.

Fig. IV.1.6   Density distribution behind the wave front for spherical blast
             waves at different values of the shock Mach number M while
              γ = 1.4.

Fig. IV.1.7   Temperature distribution behind the wave front for spherical
             blast waves at different values of the shock Mach number M
             while γ = 1.4.

Fig. IV.1.8   Particle velocity profile behind the wave front for spherical
             blast waves at different values of the shock Mach number M
             while γ = 1.4.

Fig. IV.1.9   Pressure distribution behind the wave front for cylindrical
             blast waves at different values of the shock Mach number M
             while γ = 1.4.

Fig. IV.1.20   Comparison between the particle velocity profiles for diffe-
                rent values of the specific heat ratio while $\dot{\jmath}$ = 1 and
                M = 5.

Fig. IV.1.21   Error in the machine computations as a function of the step
                size Δx in the Runge-Kutta iterative integration in the
                case of $\dot{\jmath}$ = 1, M = 2 and x = 0.1.

Fig. IV.1.22   Effect of variation of the shock Mach number M on the loca-
                tion of the integral curves with respect to the locii of the
                singularities F = 1 and Z = $(1 - F)^2$ for $\dot{\jmath}$ = 2 and
                γ = 1.4.

Fig. IV.1.23   Effect of variation of the shock Mach number M on the loca-
                tion of the integral curves with respect to the locii of the
                singularities F = 1 and Z = $(1 - F)^2$ for $\dot{\jmath}$ = 1 and
                γ = 1.4.

Fig. IV.1.24   Effect of variation of the shock Mach number M on the loca-
                tion of the integral curves with respect to the locii of the
                singularities F = 1 and Z = $(1 - F)^2$ for $\dot{\jmath}$ = 0 and
                γ = 1.4.

Fig. IV.1.25   Location of the singular points F = 1 and Z = $(1 - F)^2$ at
                values of λ rather than the exact one in the case of $\dot{\jmath}$ = 2
                and M = 2.

Fig. IV.1.26   The mass integral $(\dot{\jmath} + 1)\ \tilde{U}_1$ as a function of y in the
                case of γ = 1.4.

Fig. IV.1.27   Comparison between the present solution with the first order
                perturbation solution (Sakurai, 1954) and the second pertur-
                bation solution (Bach and Lee, 1969).

76

Fig. IV.1.1

Fig. IV.1.2

Fig. IV.1.3

Fig. IV.1.4
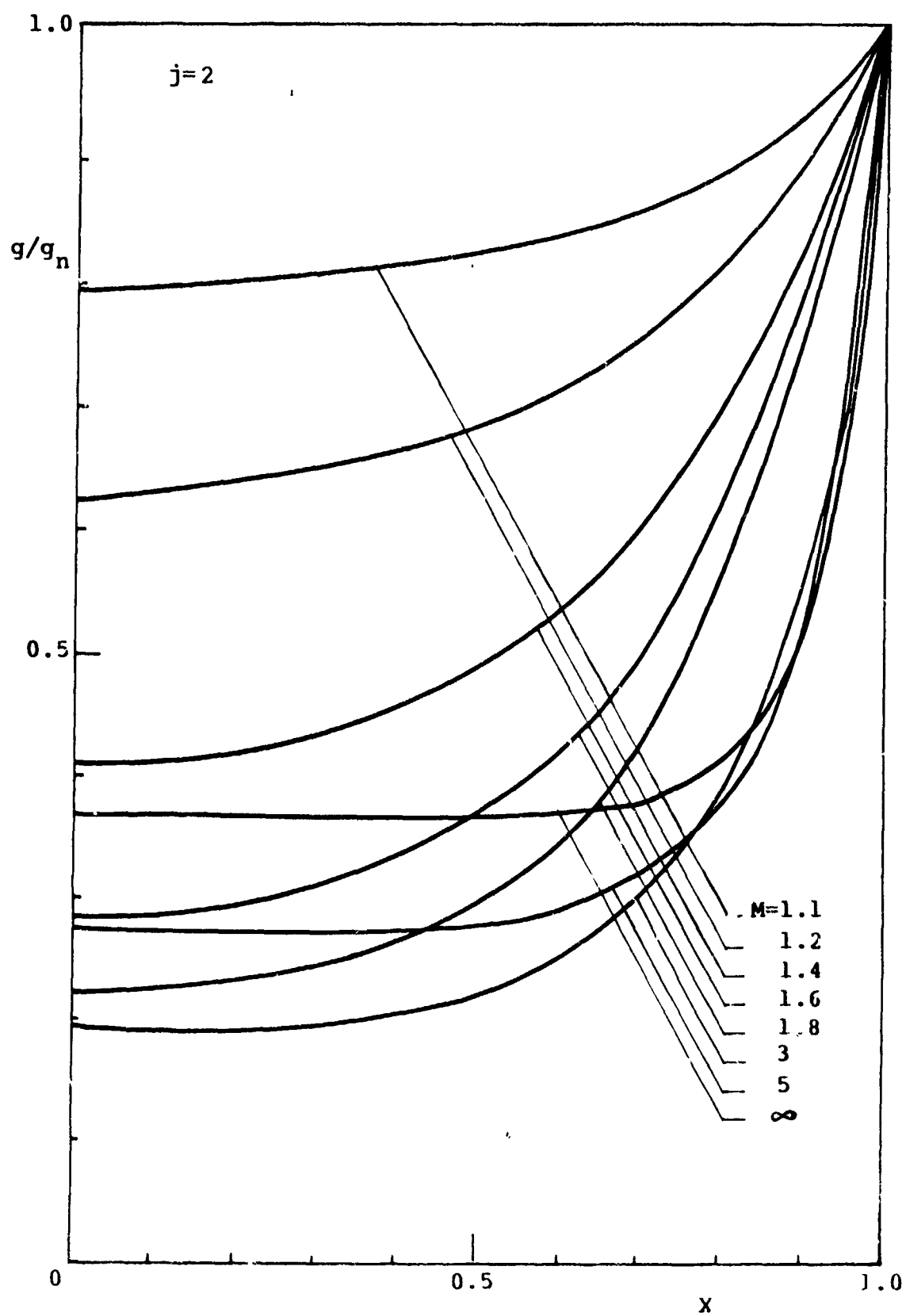
Fig. IV.1.5
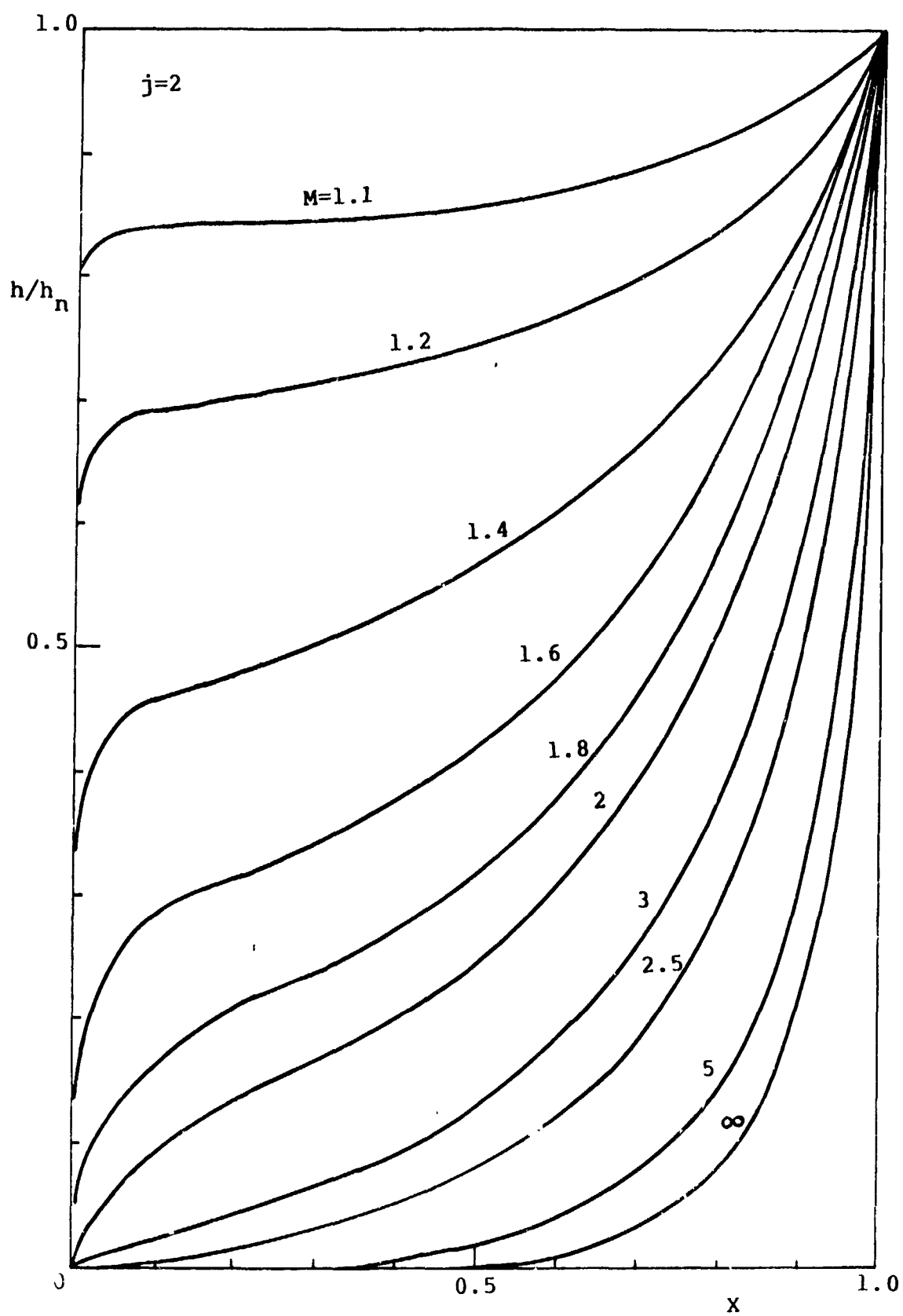
Fig. IV.1.6
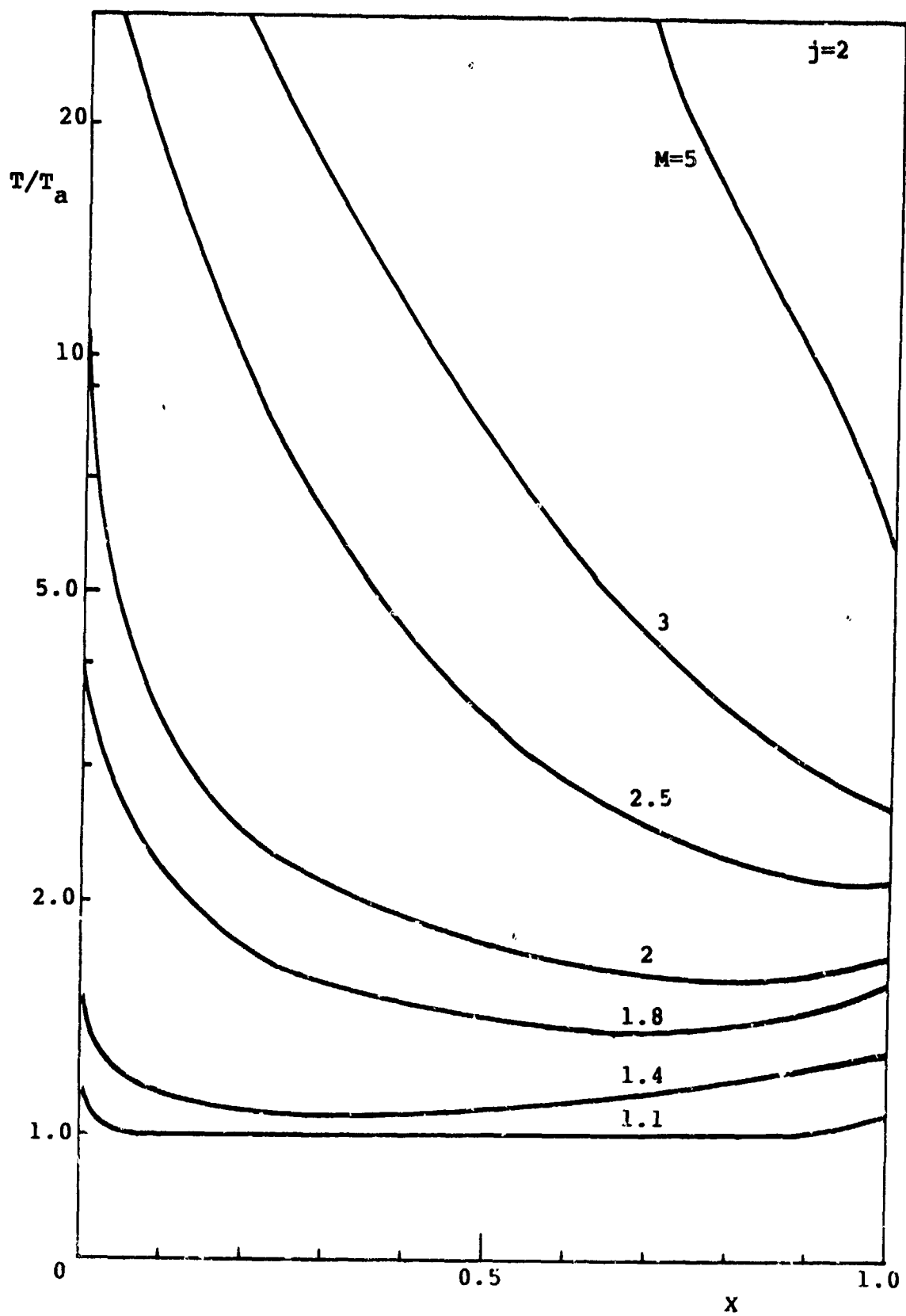
Fig. IV.1.7
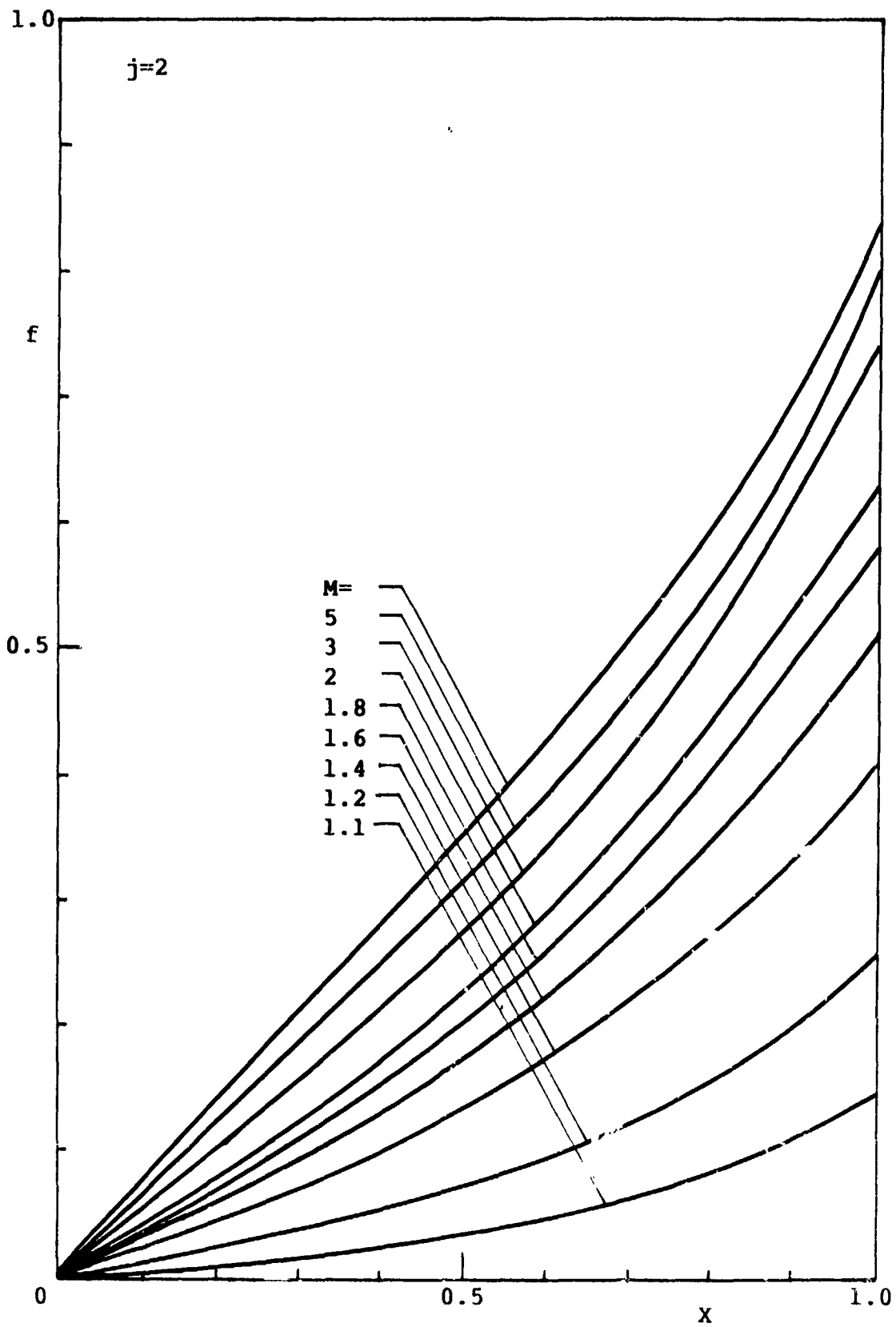
Fig. IV.1.8
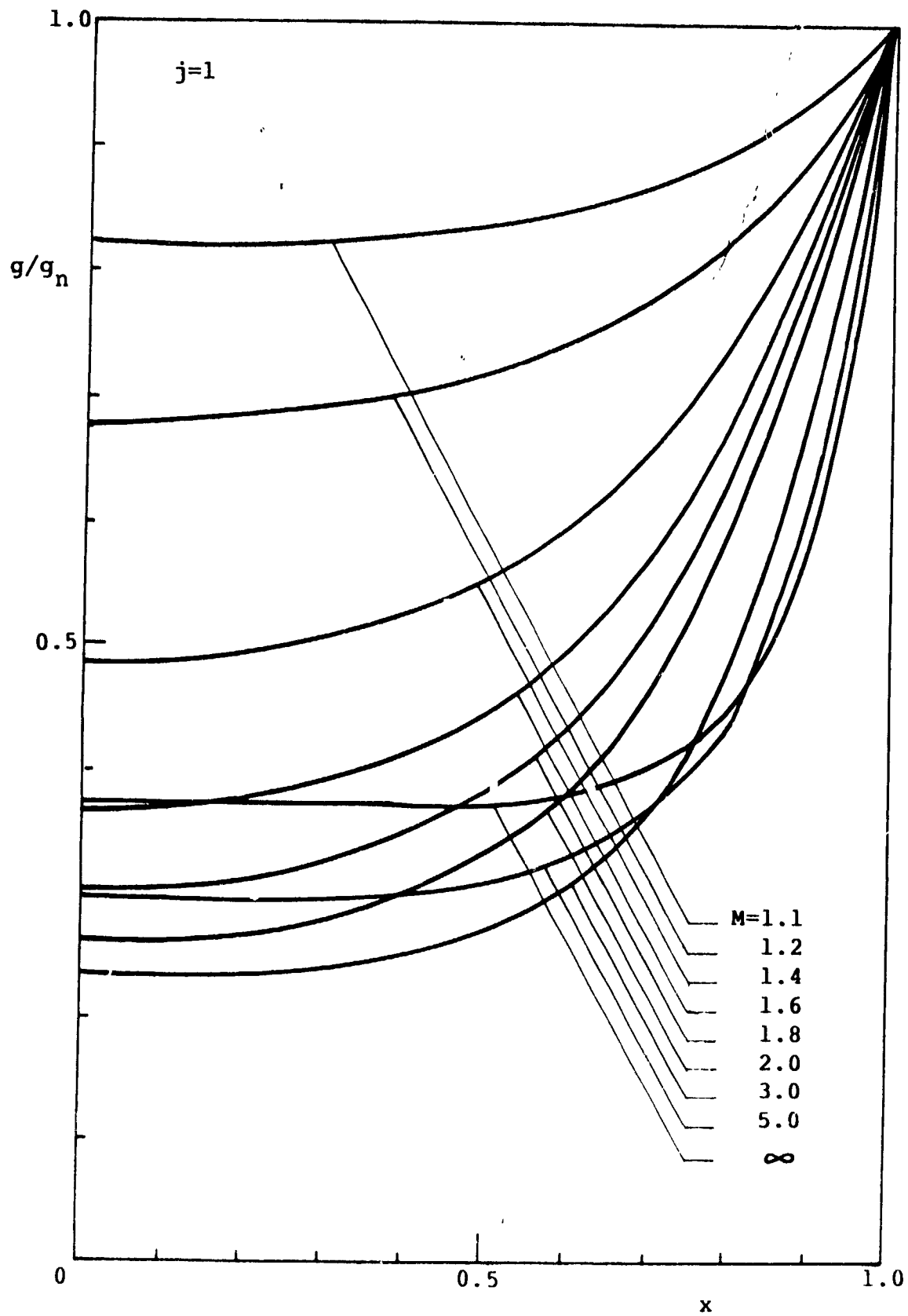
Fig. IV.1.9
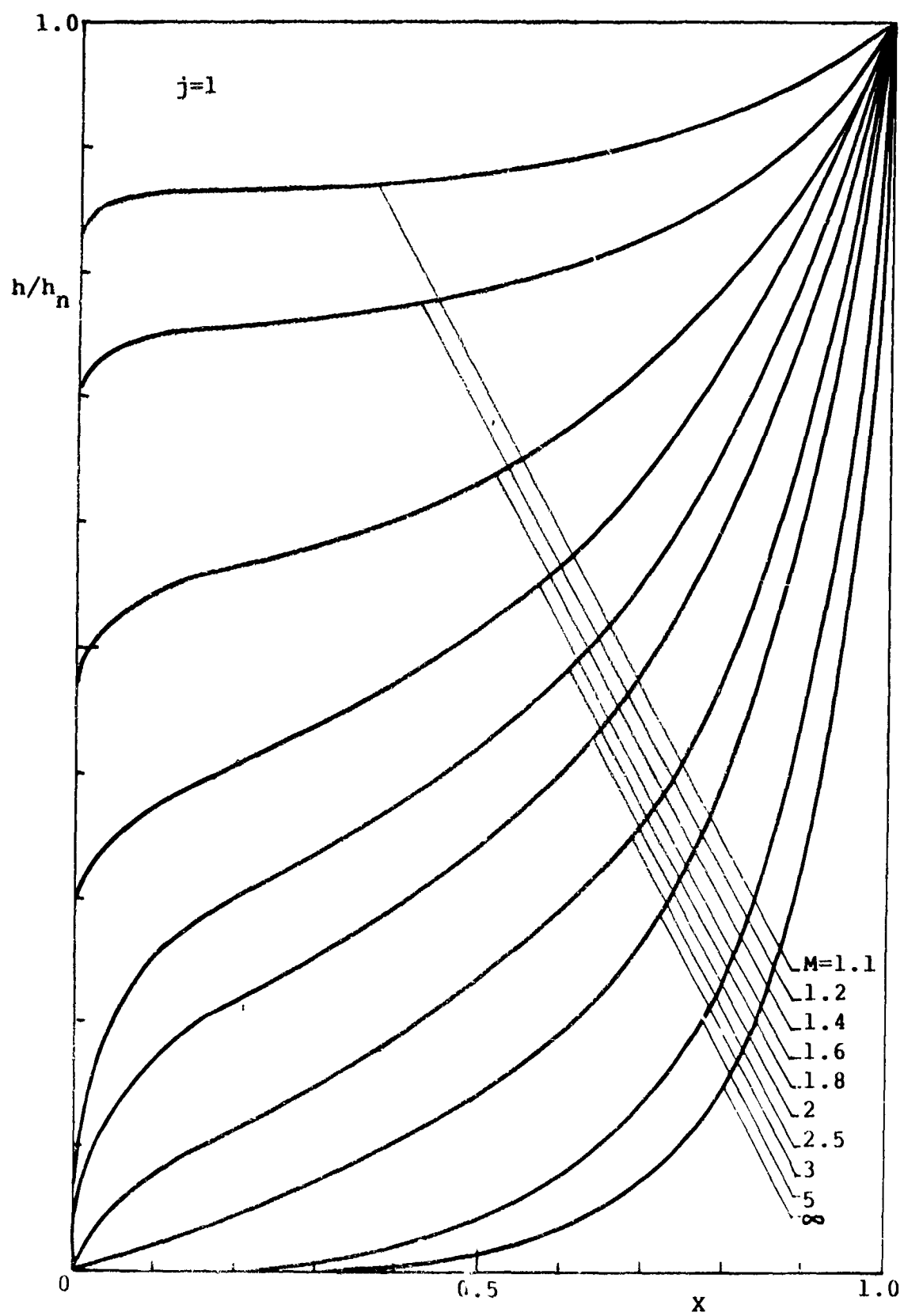
Fig. IV.1.10
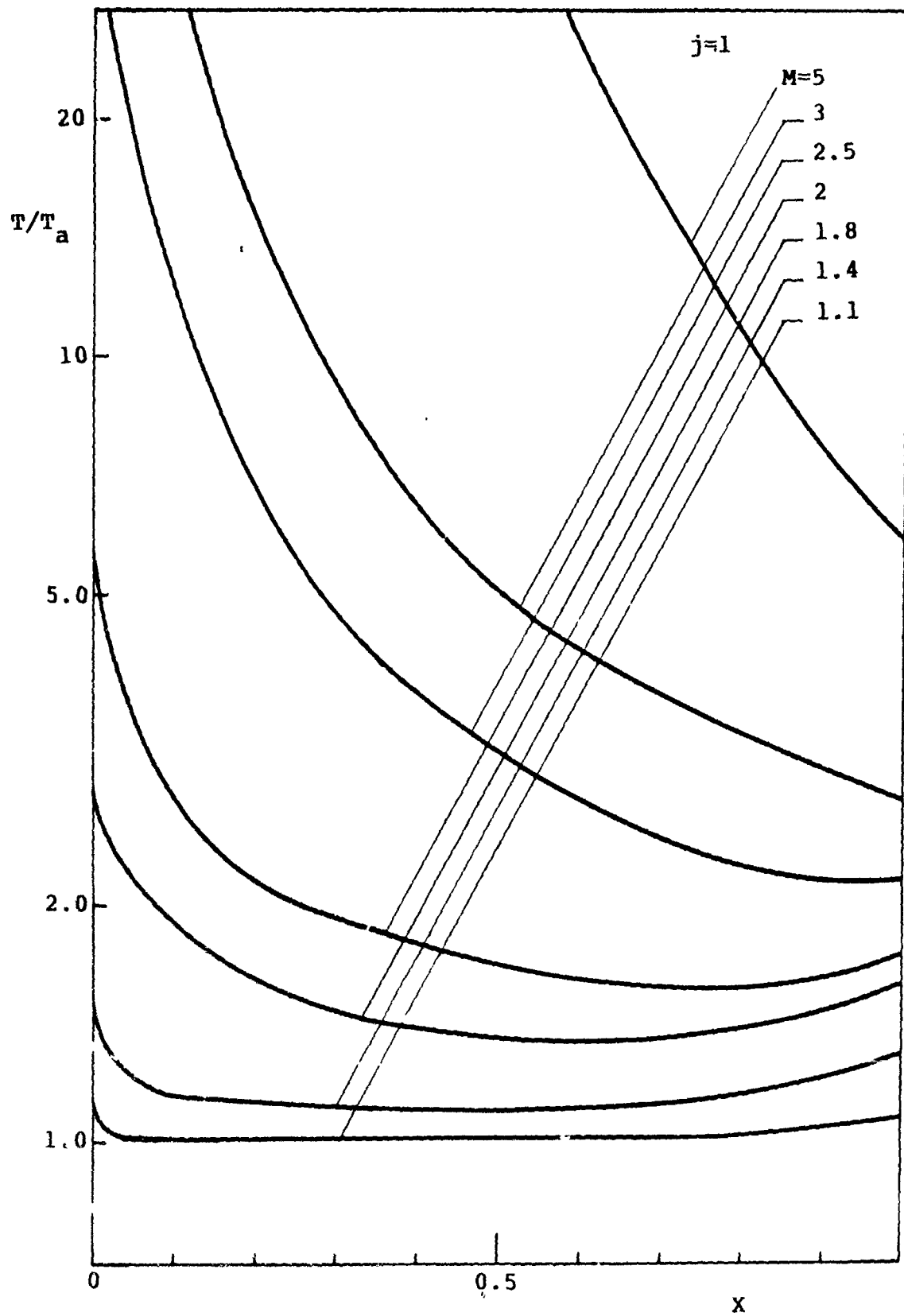
Fig. IV.1.11
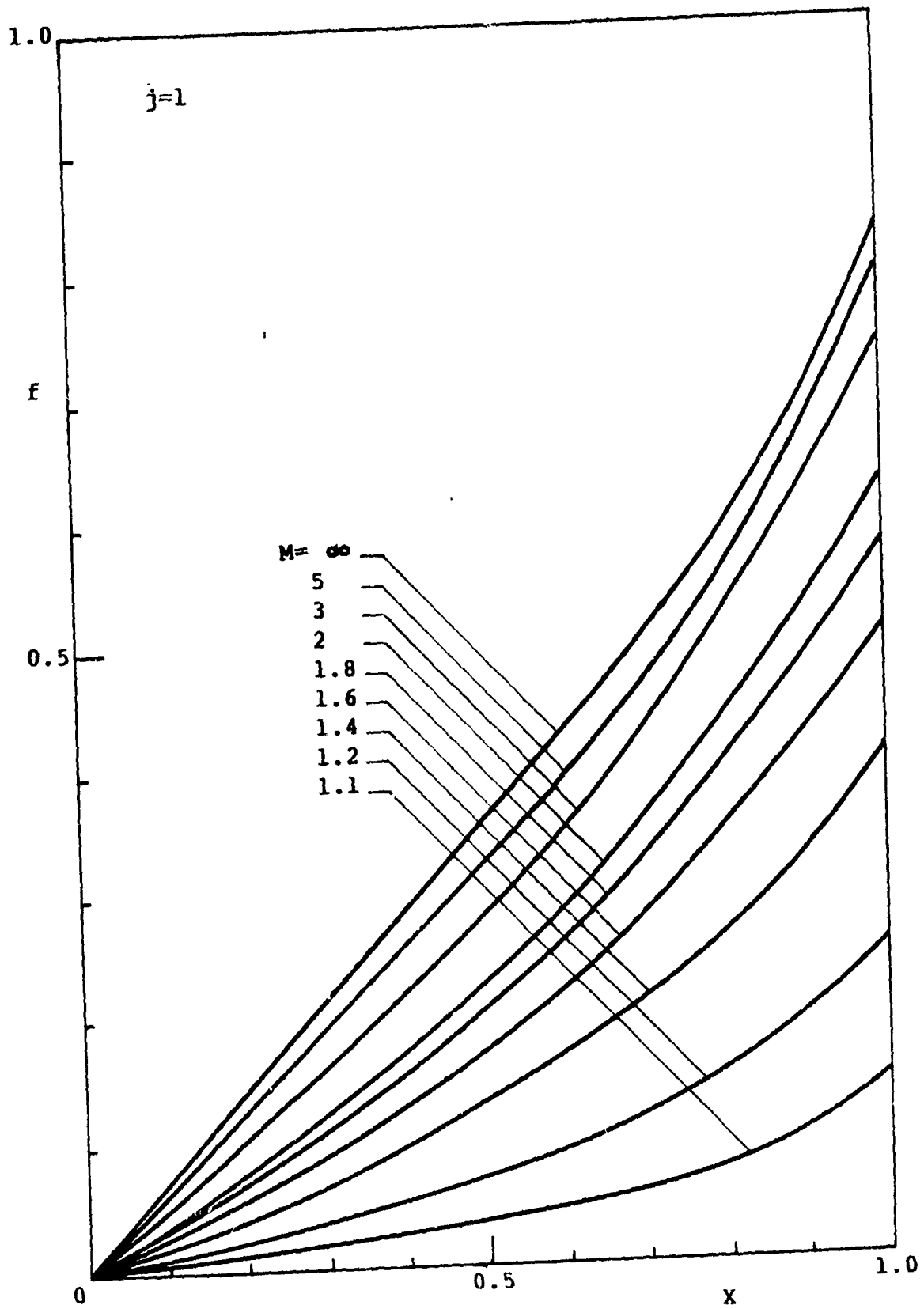
Fig. IV.1.12
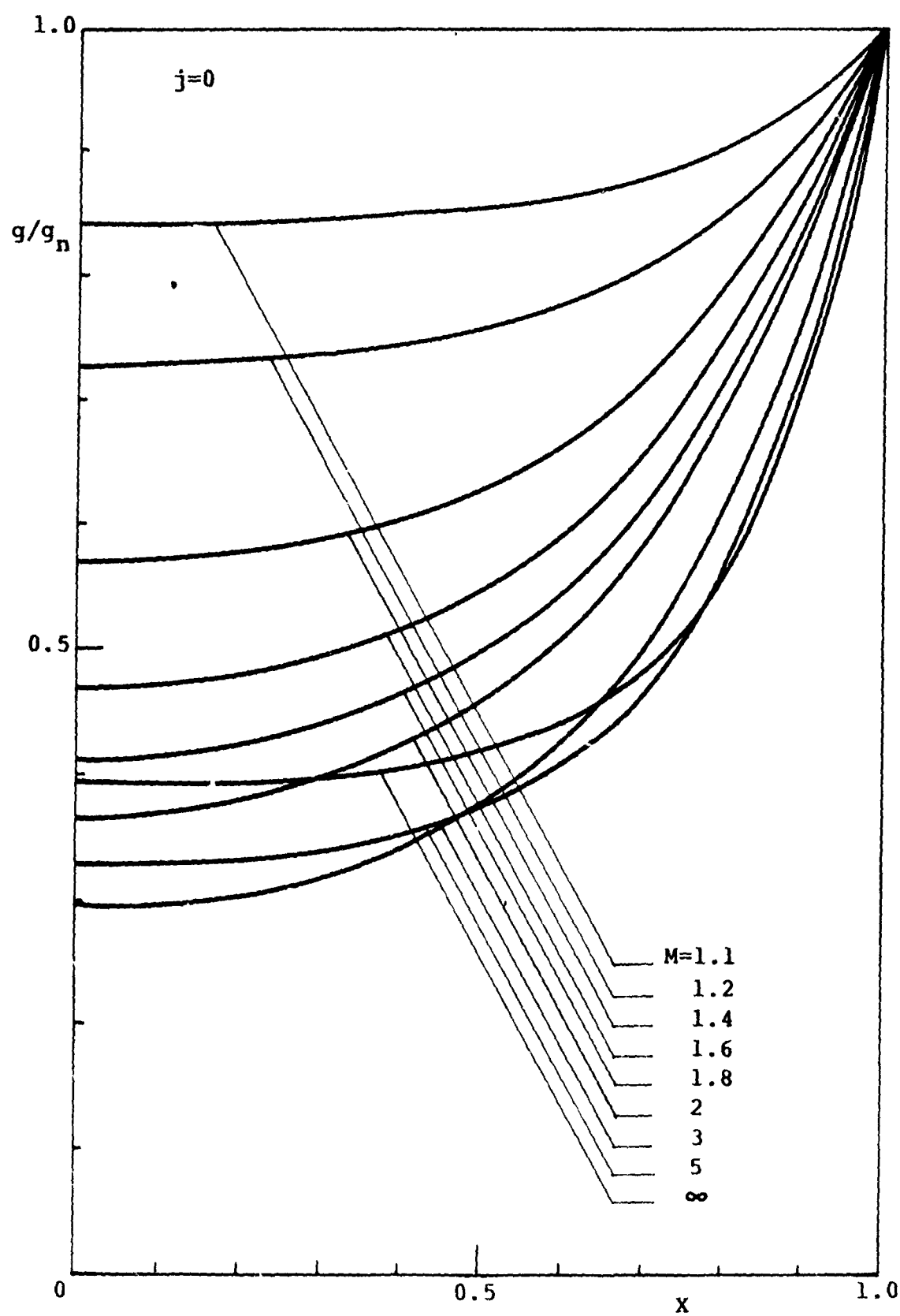
Fig. IV.1.13
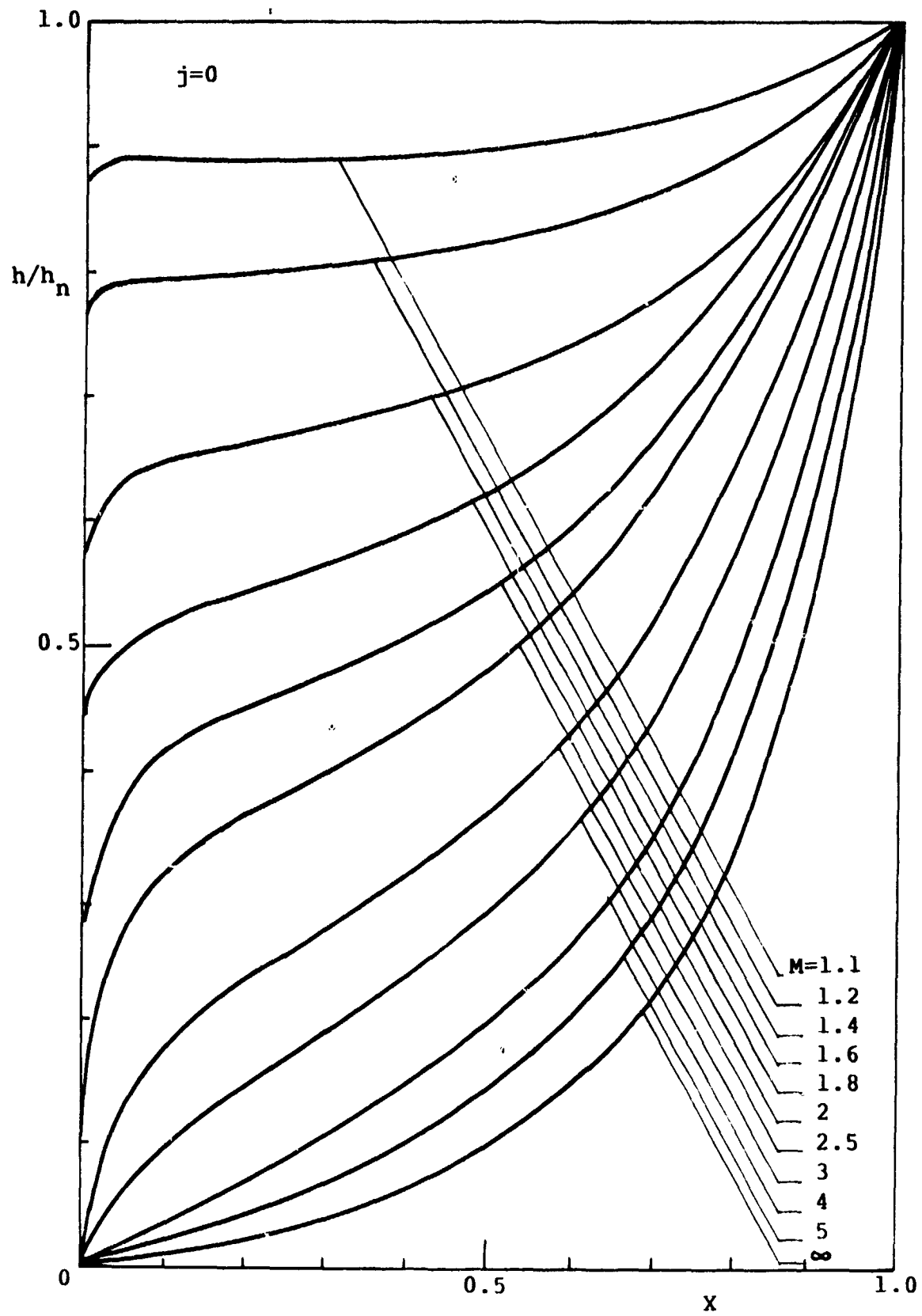
Fig. IV.1.14
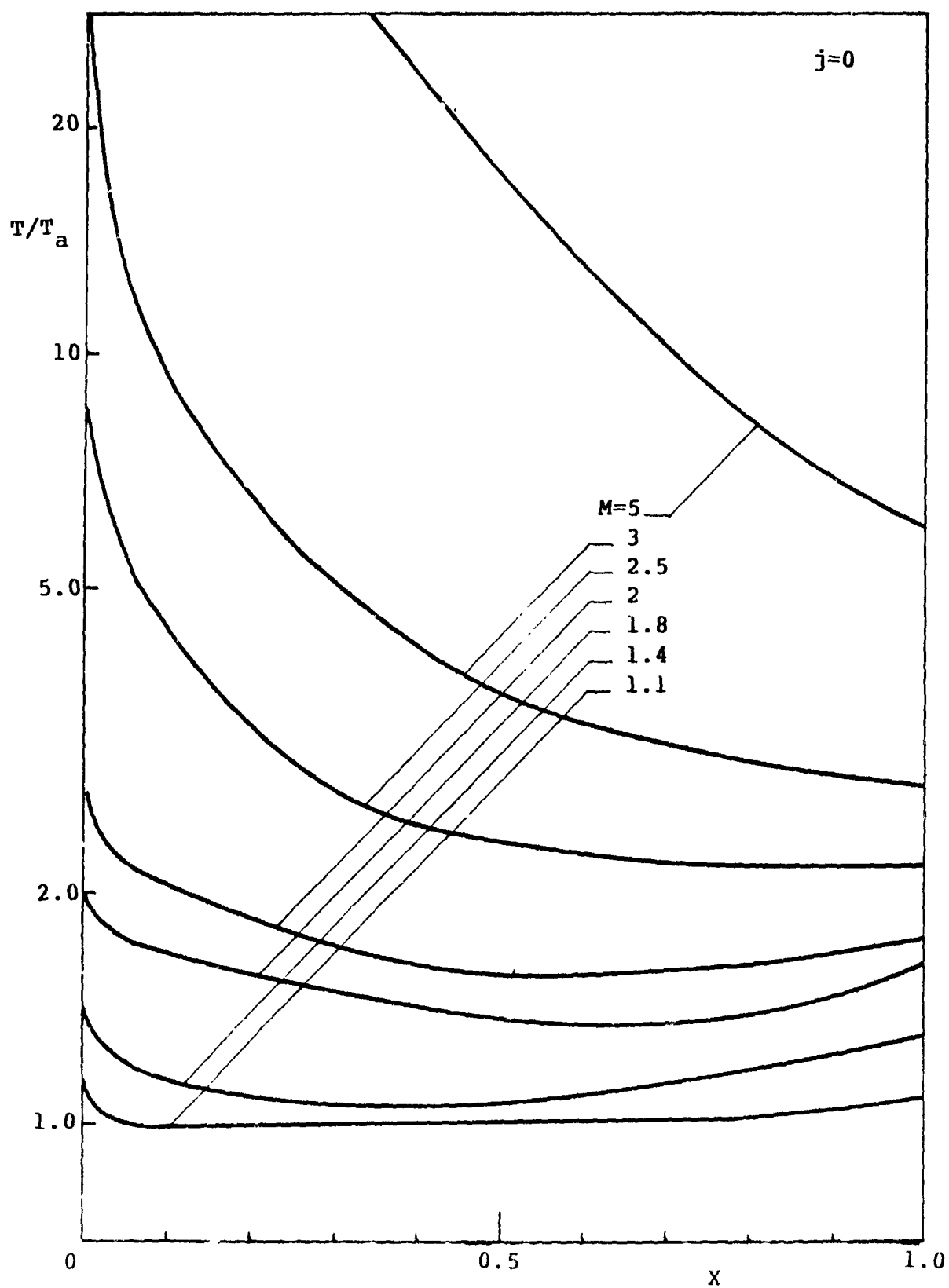
Fig. IV.1.15
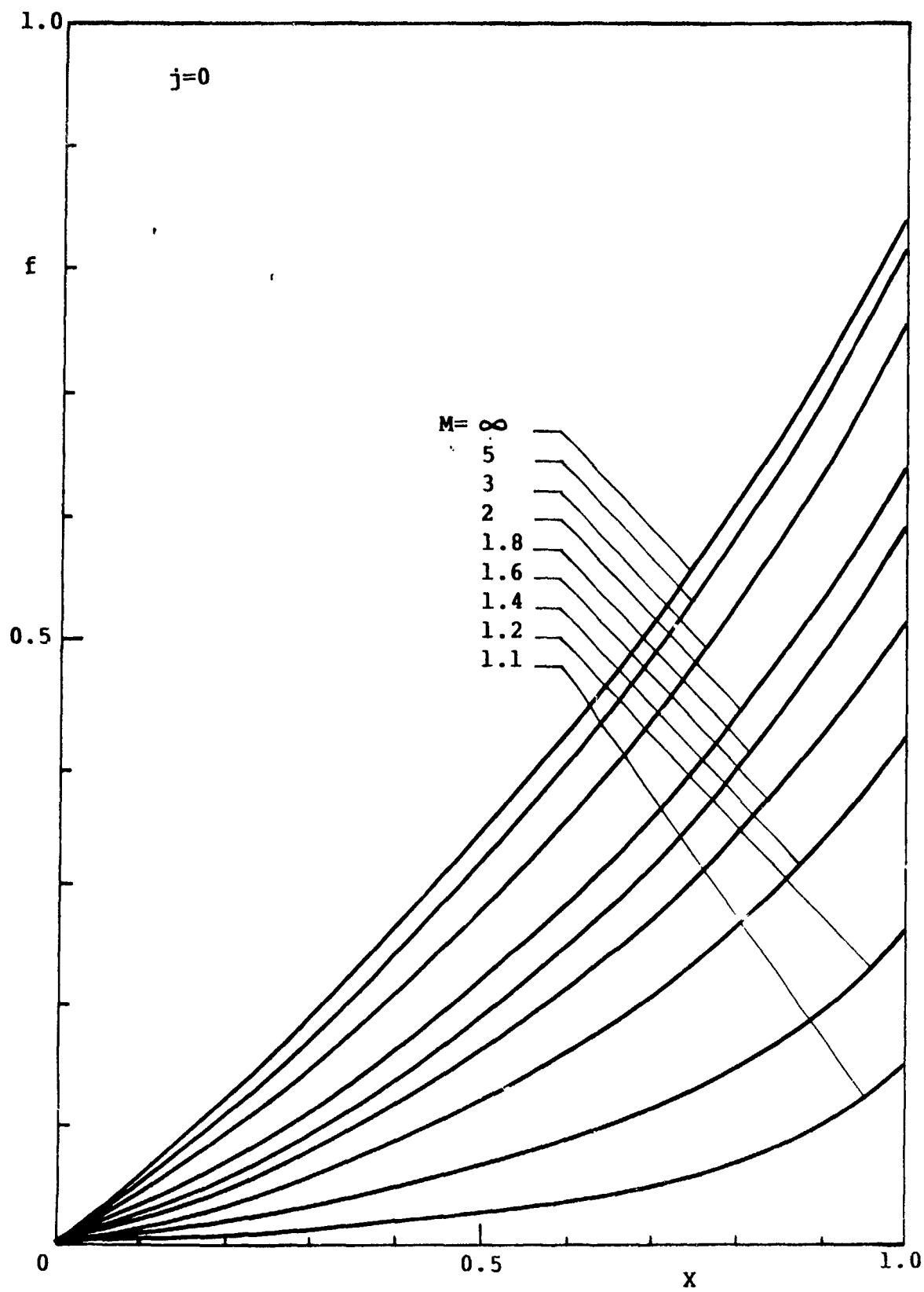
Fig. IV.1.16
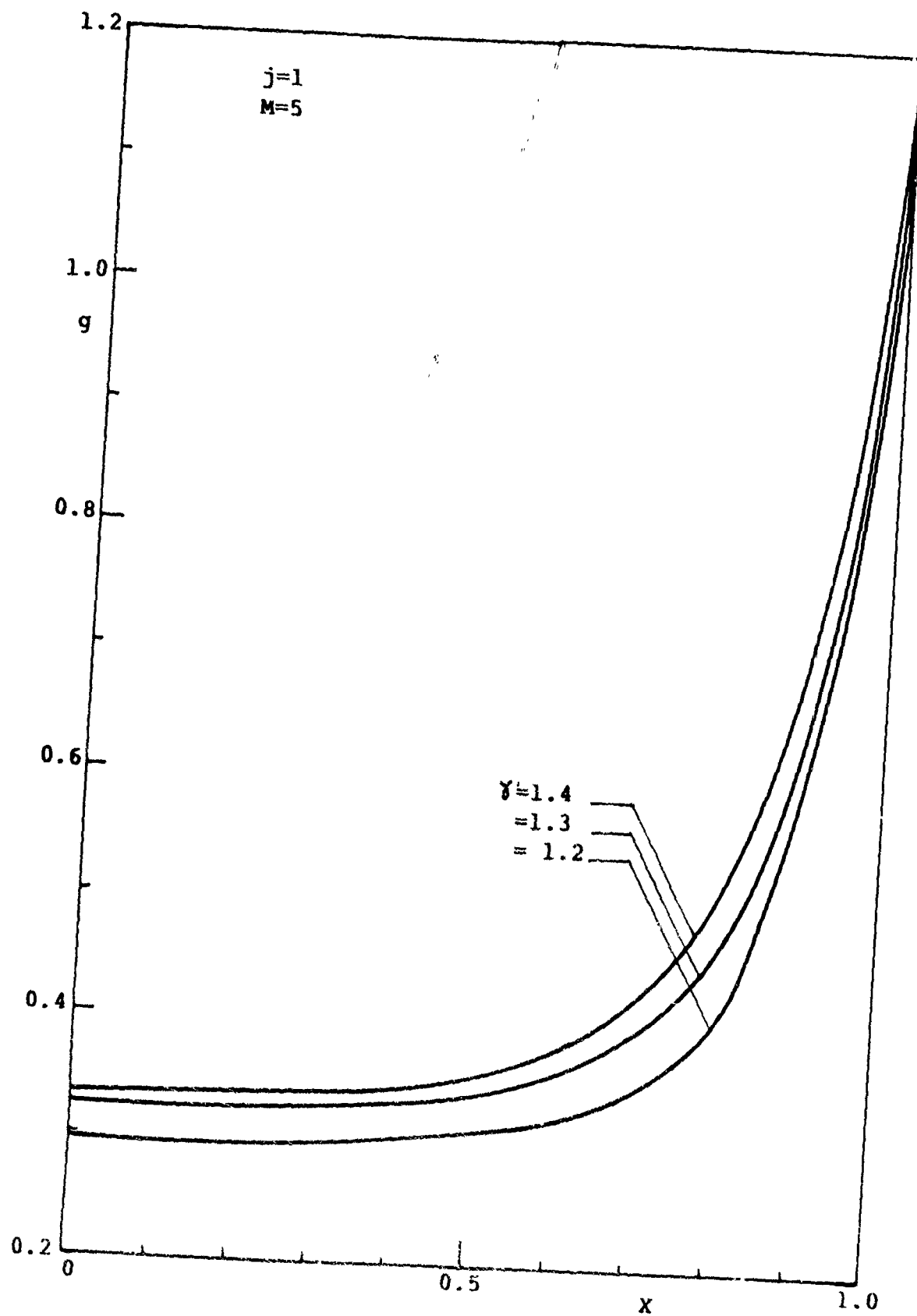
Fig. IV.1.17
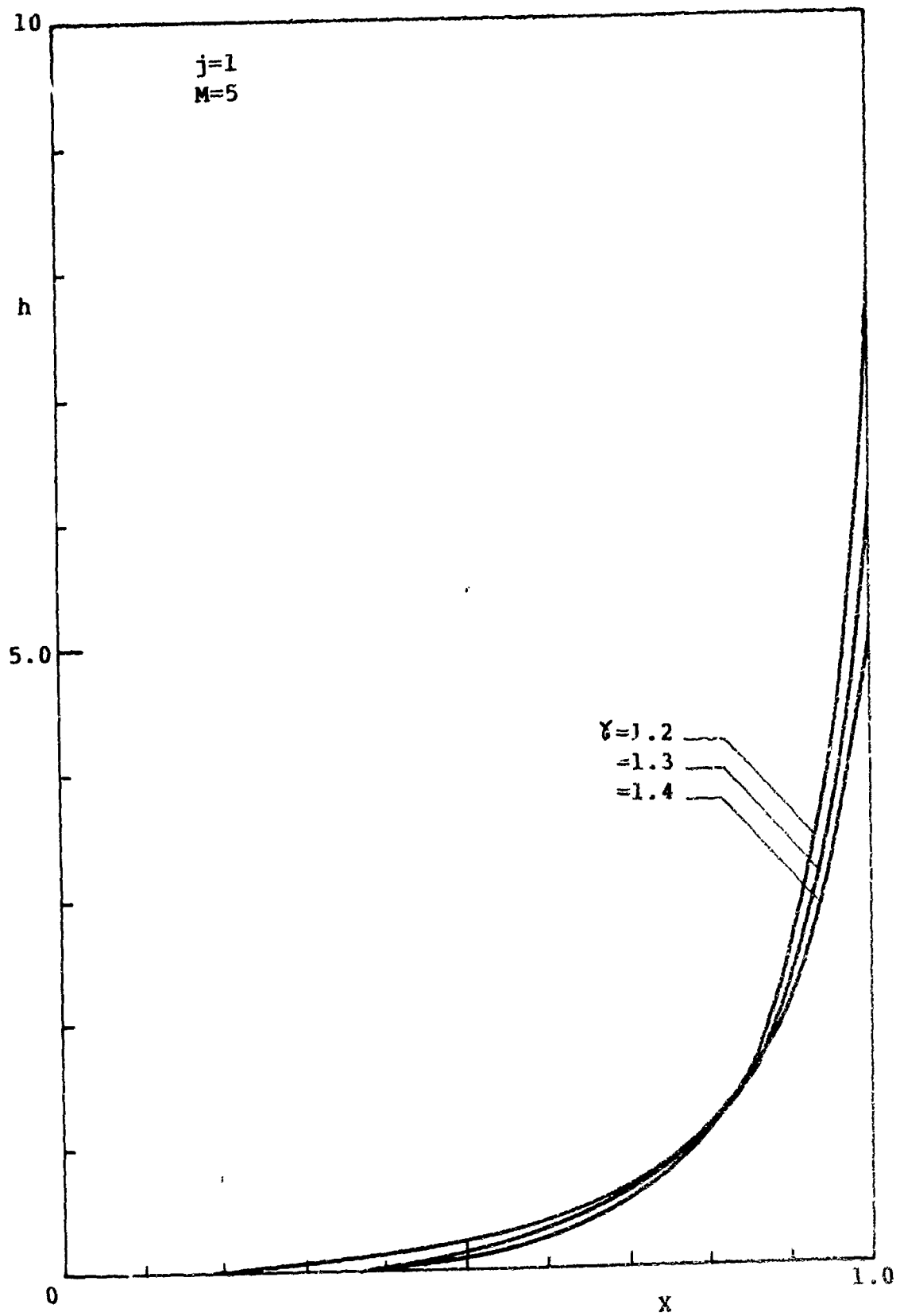
Fig. IV.1.18
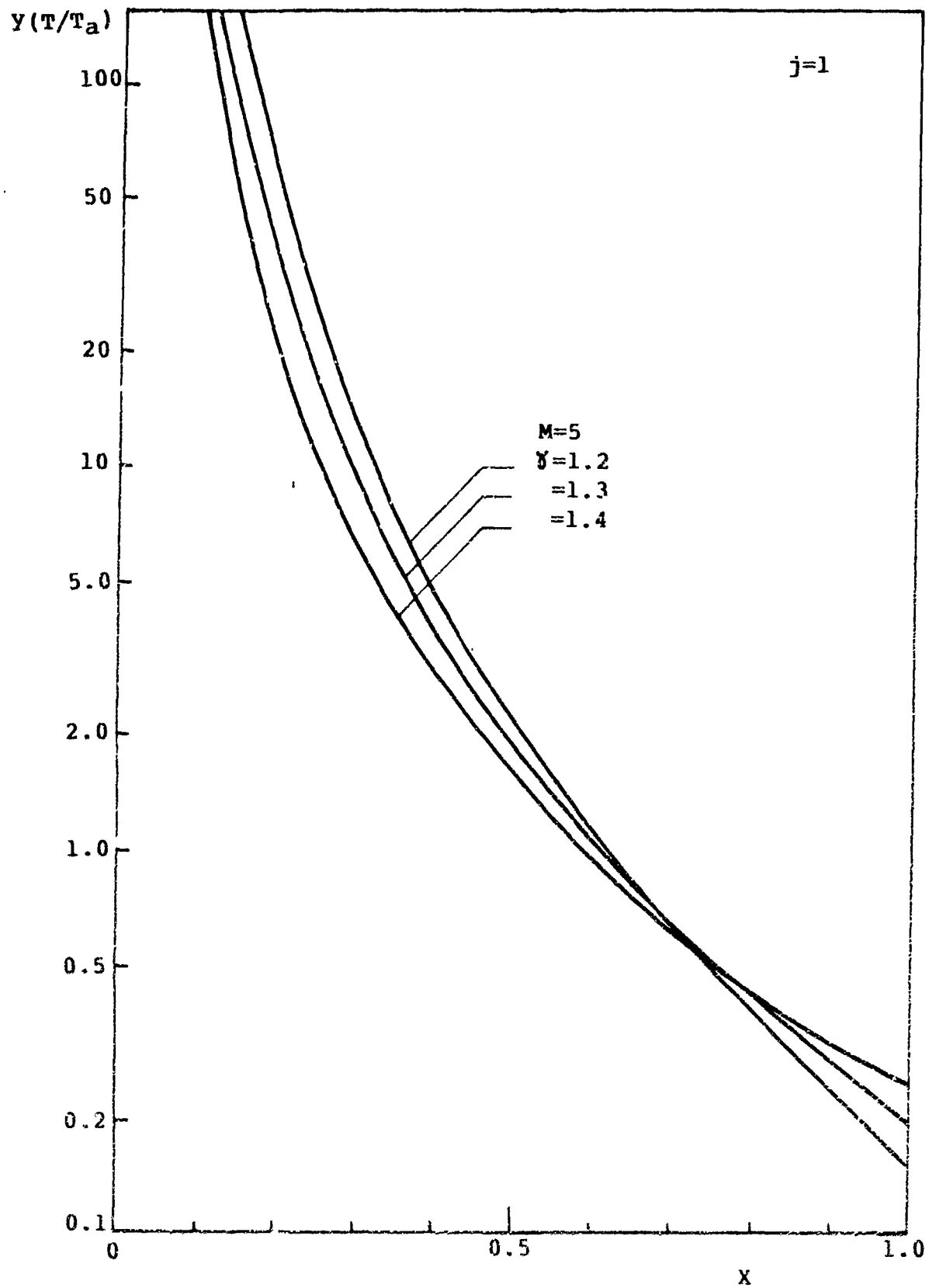
Fig. IV.1.19
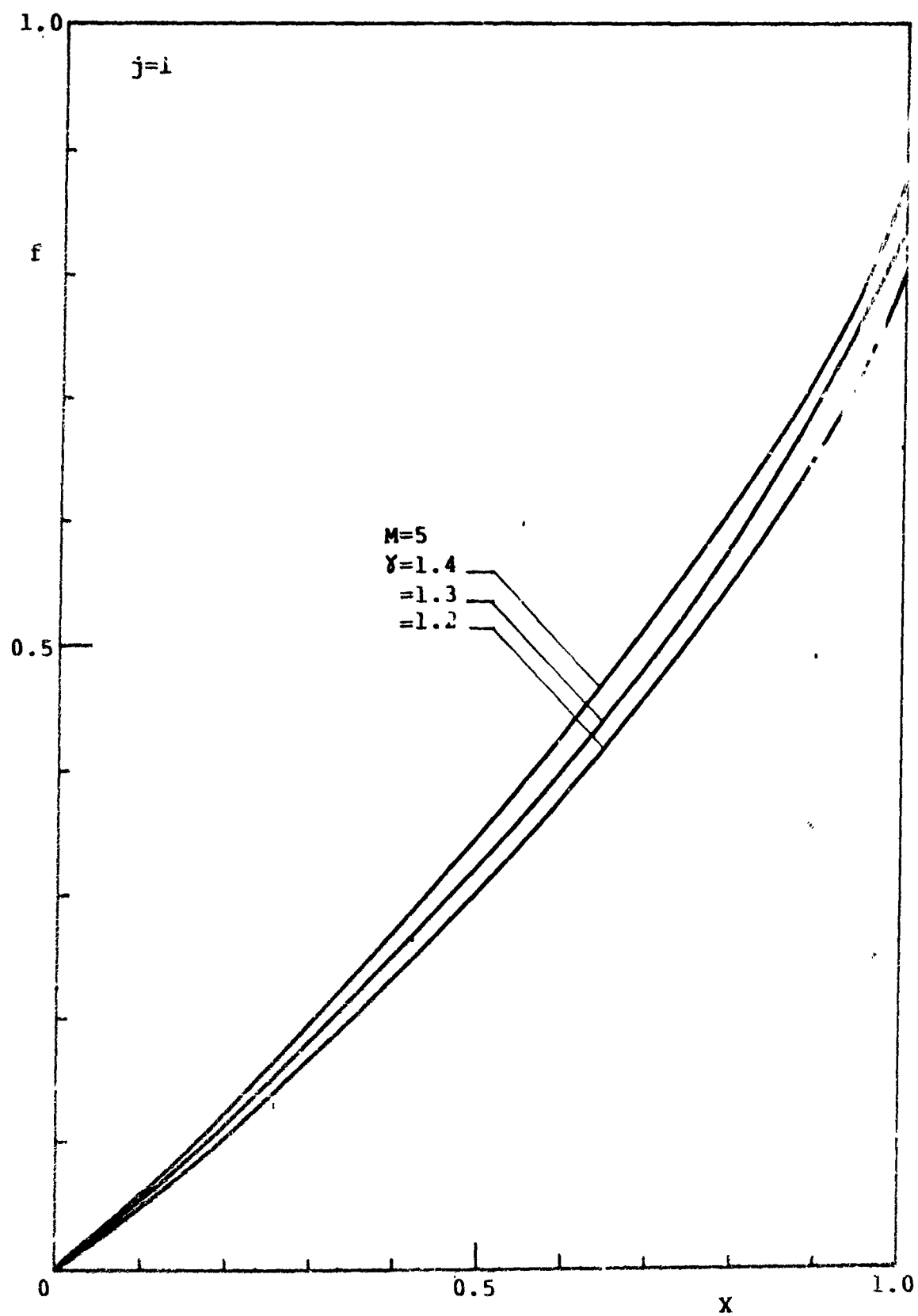
Fig. IV.1.20
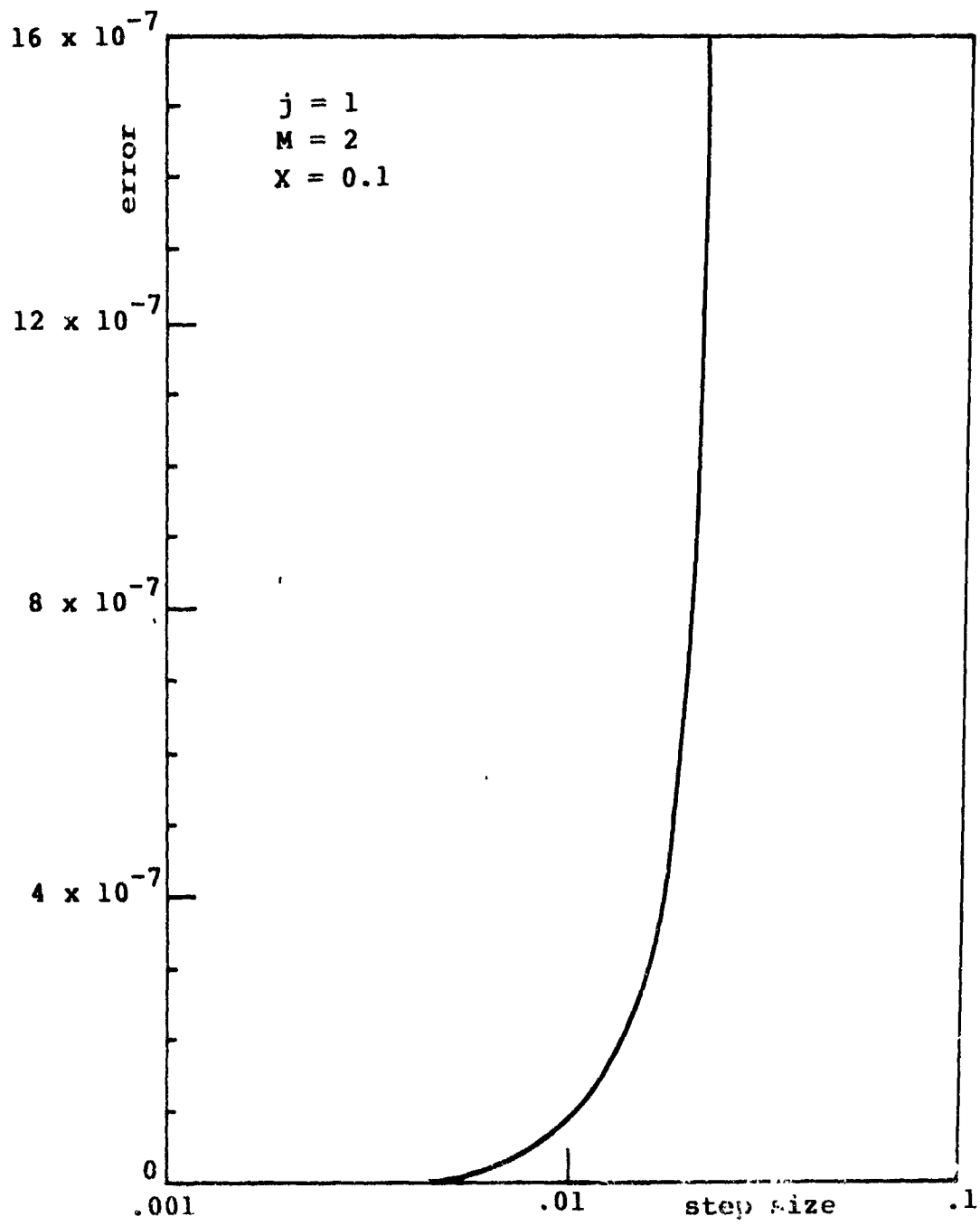
Fig. IV.1.21
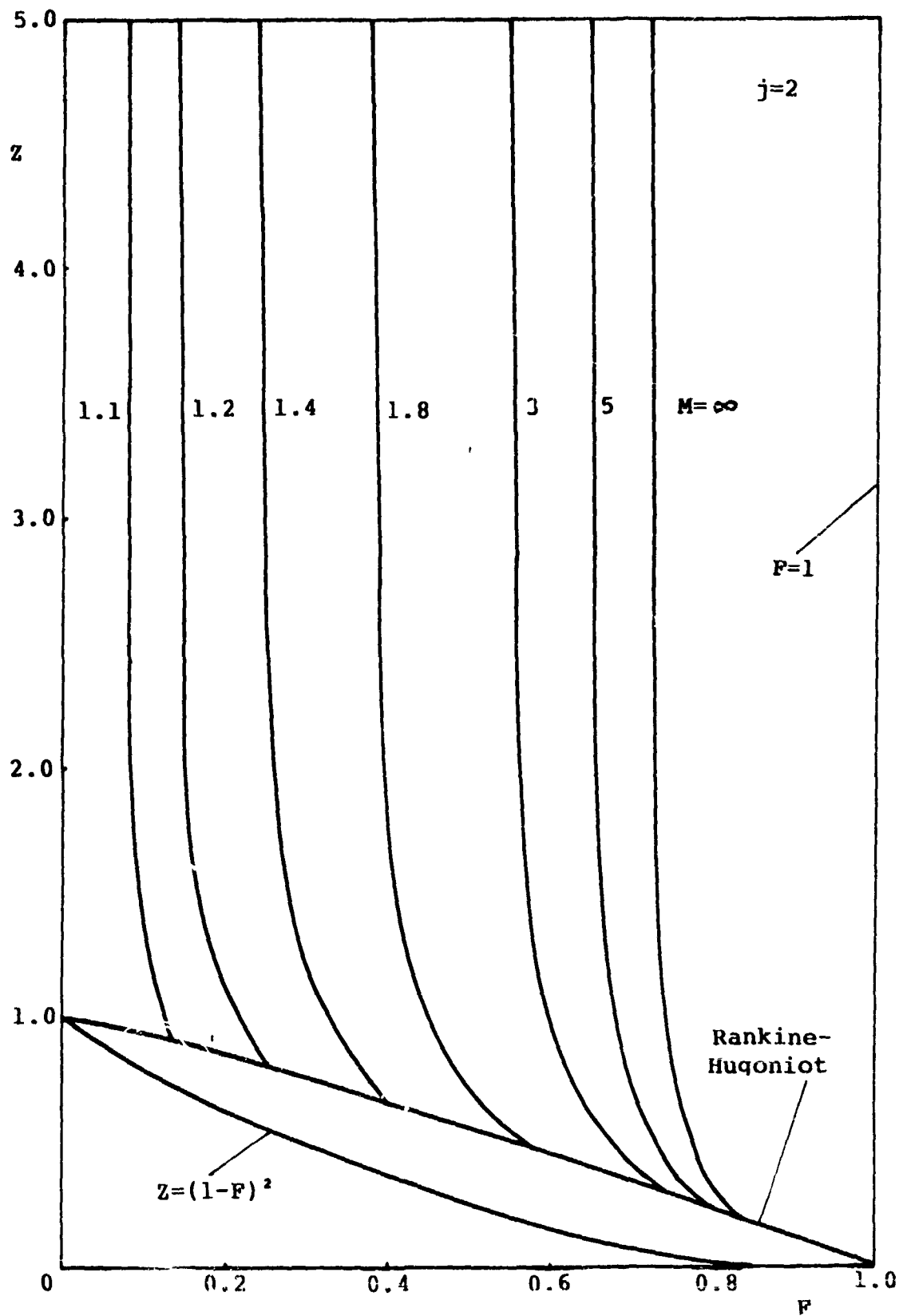
Fig. IV.1.22
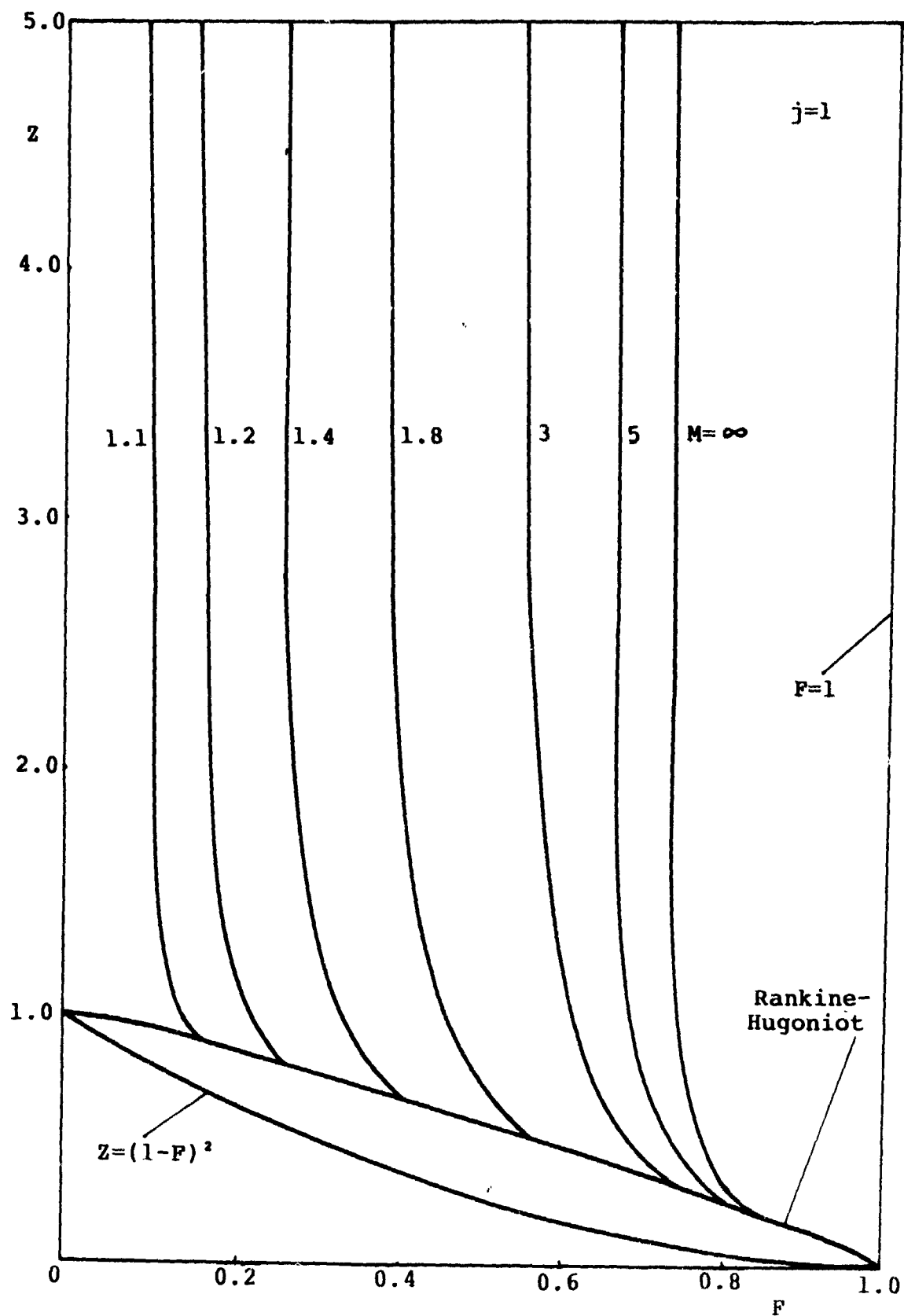
Fig. IV.1.23
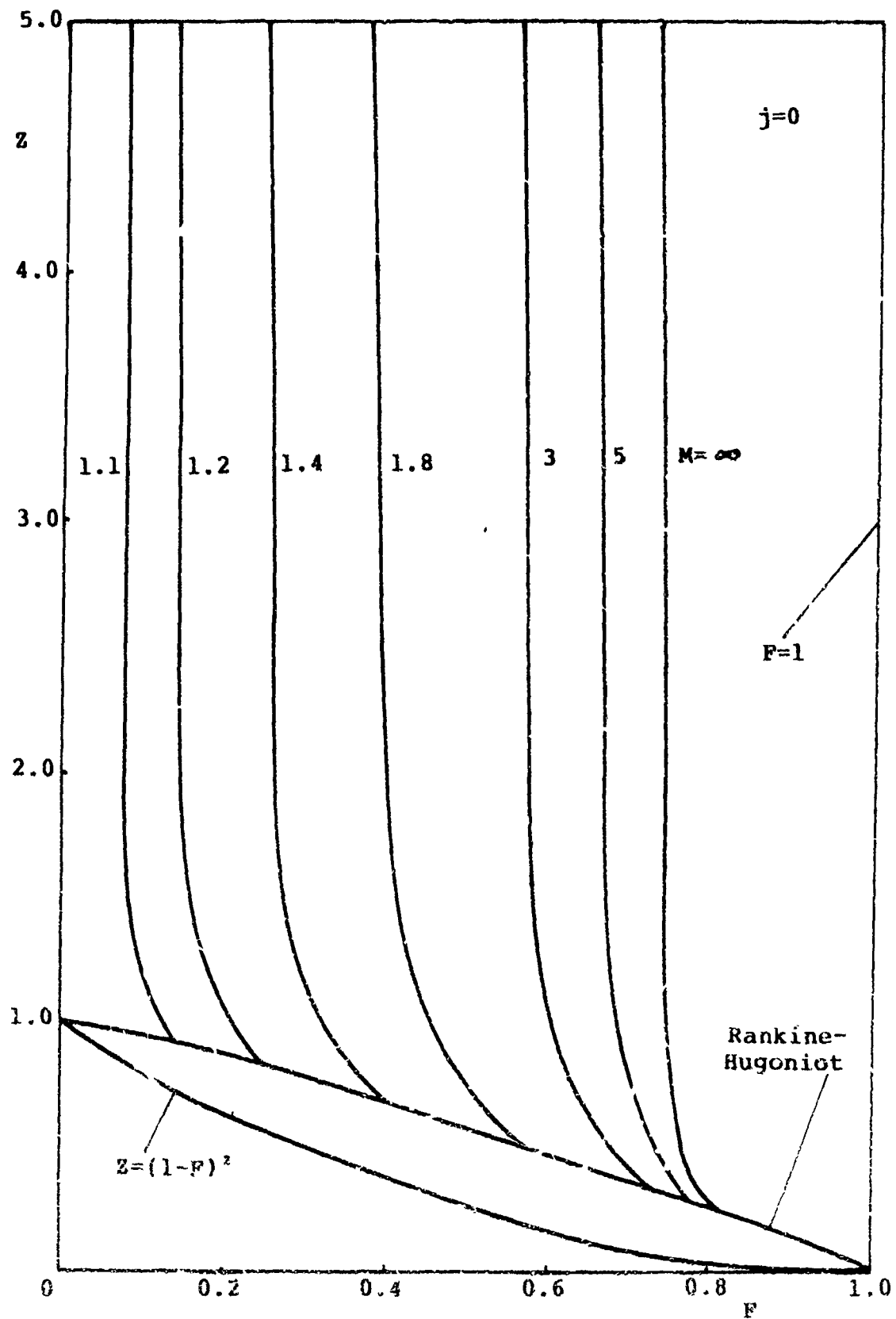
Fig. IV.1.24

Fig. IV.1.25

$(j+1)\int_0^1 hx^j dx$

Fig. IV.1.26

102
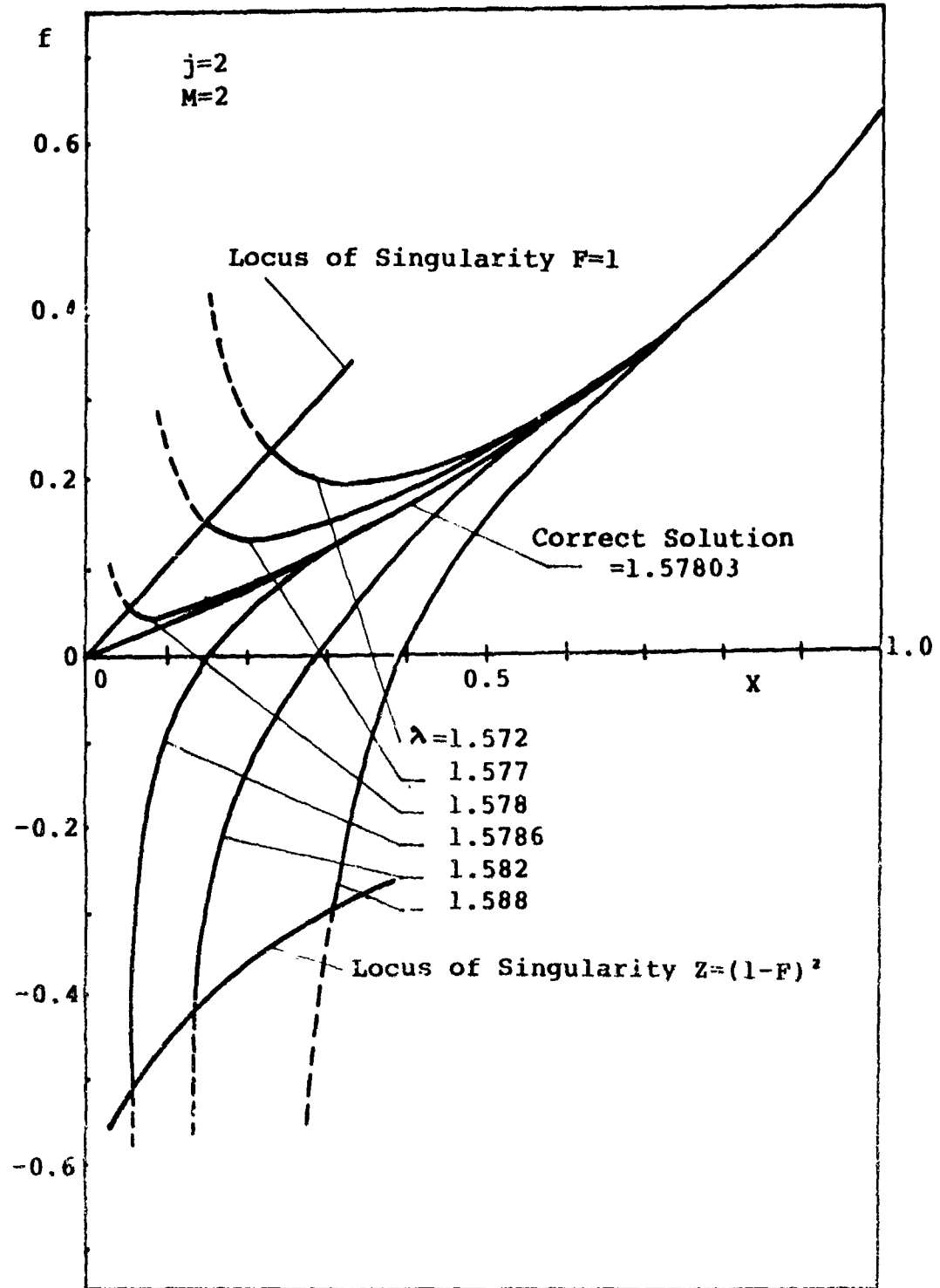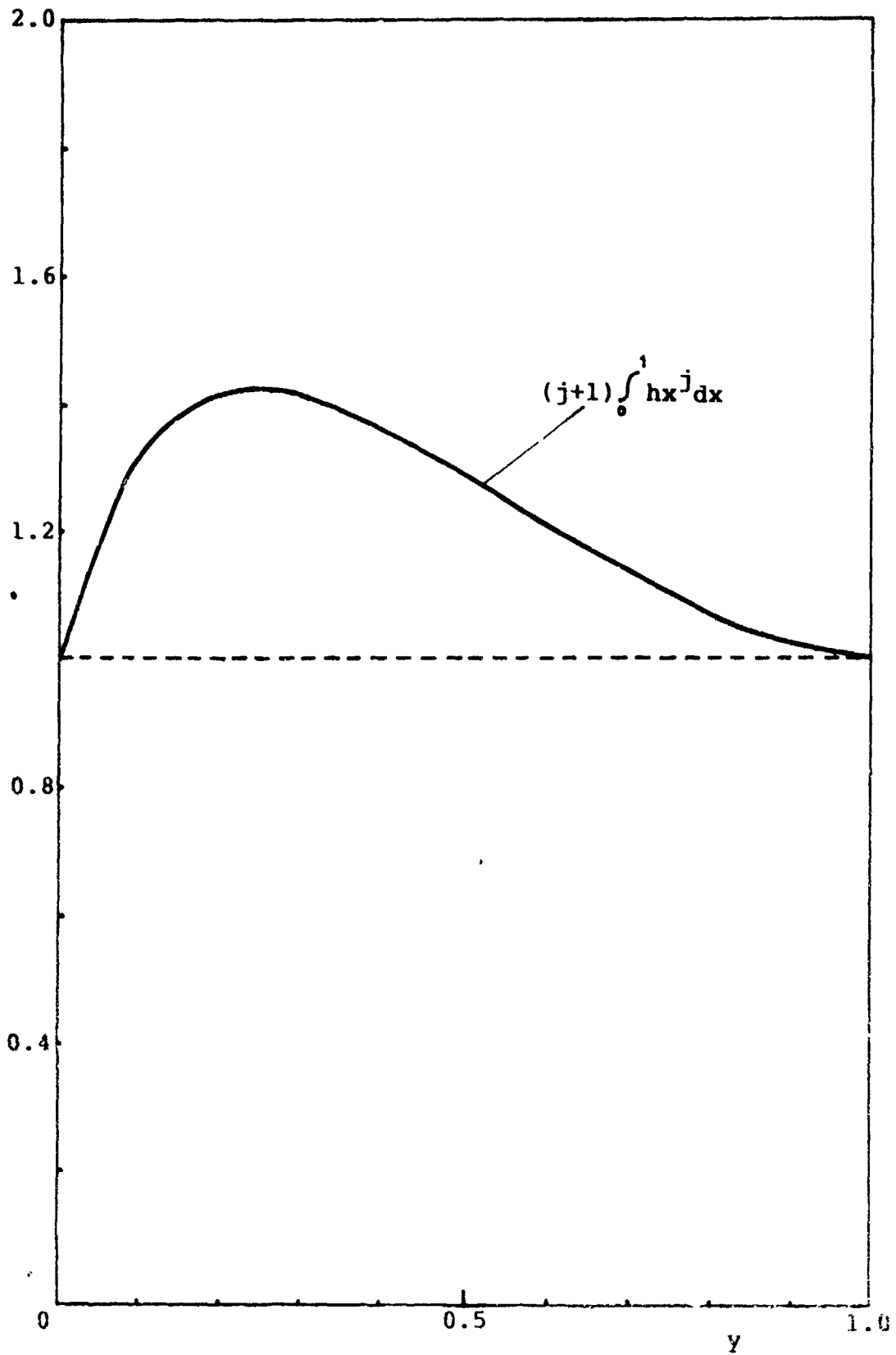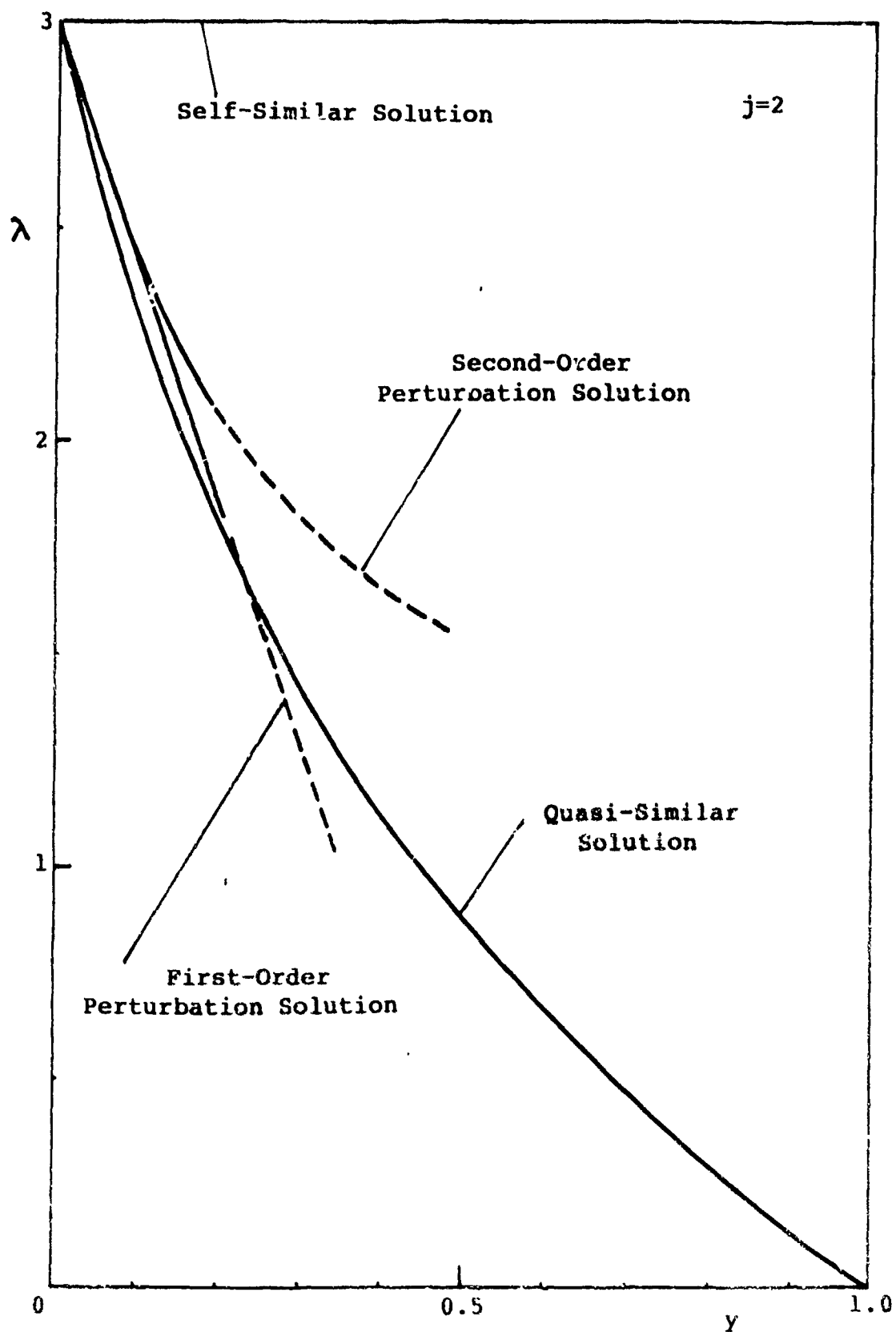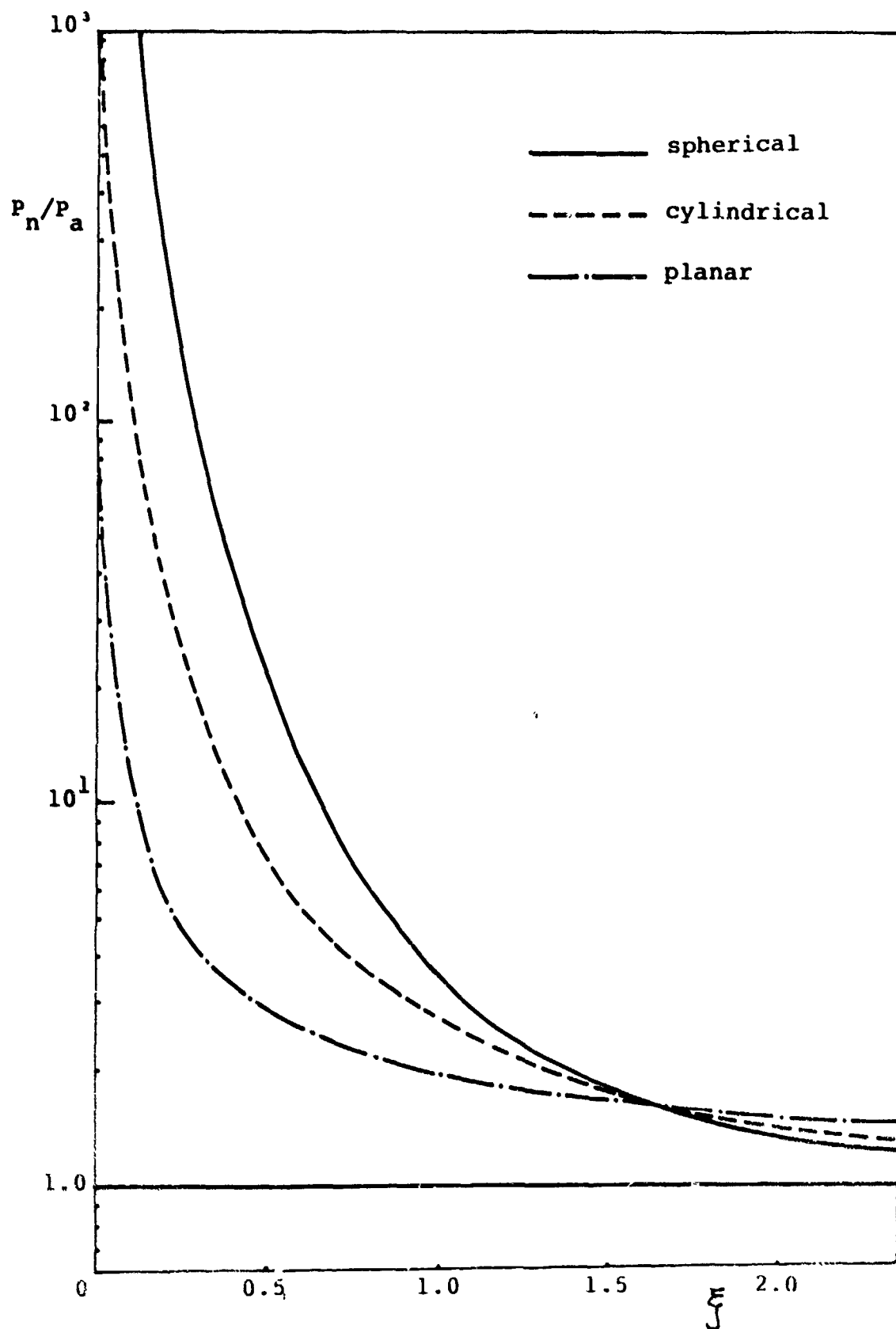
Fig. IV.1.27

Fig. IV.1.28
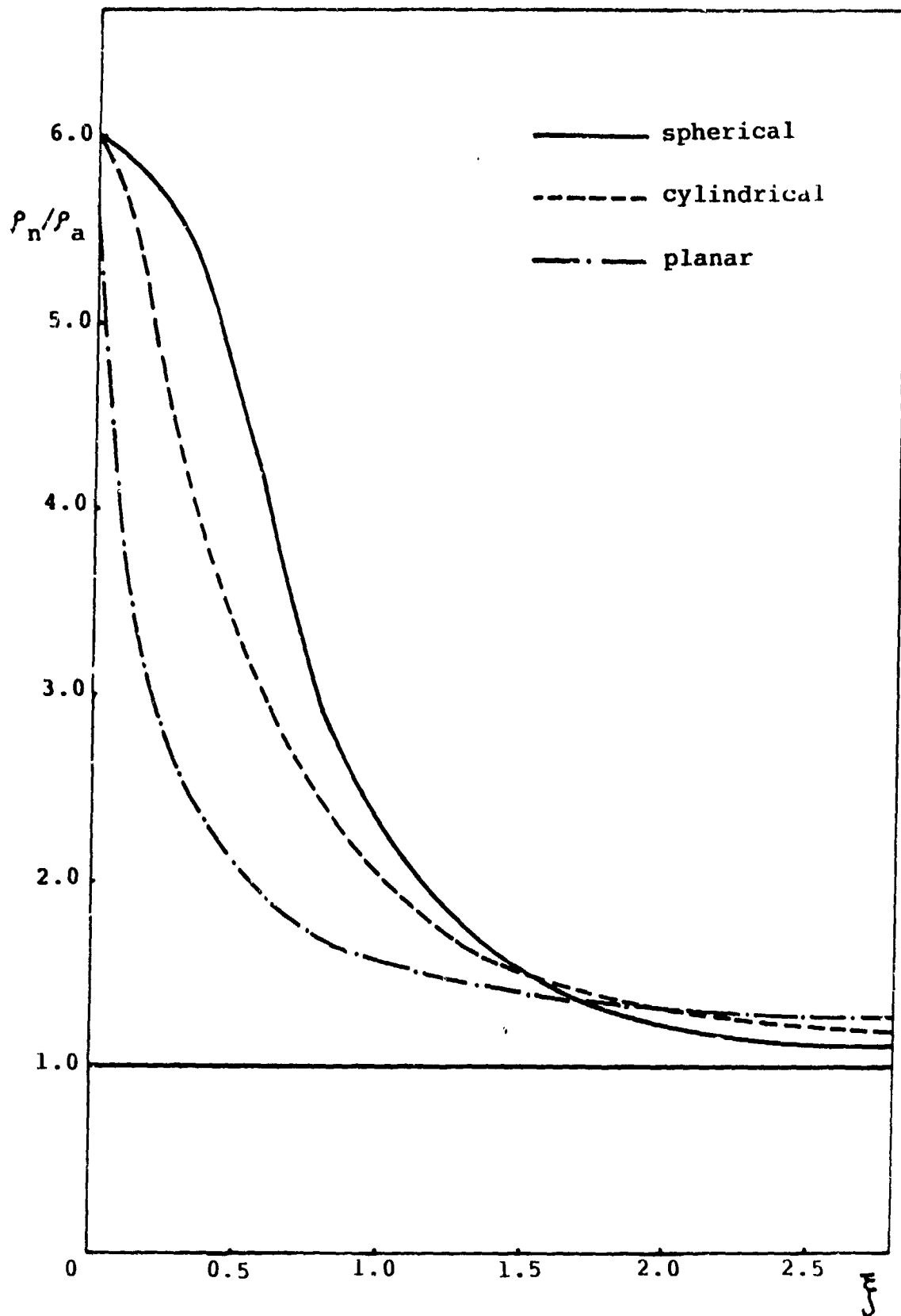
Fig. IV.1.29
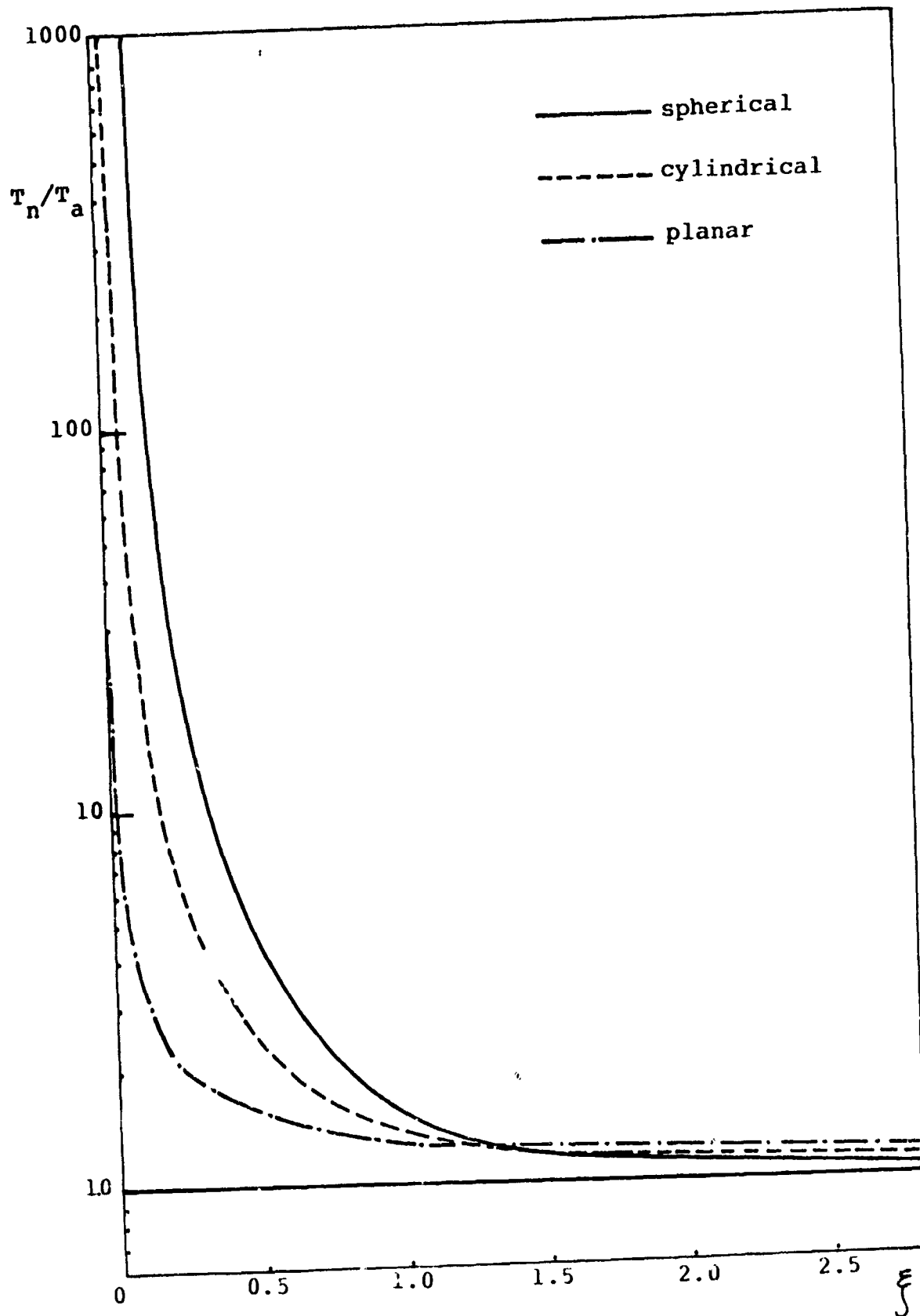
Fig. IV.1.30
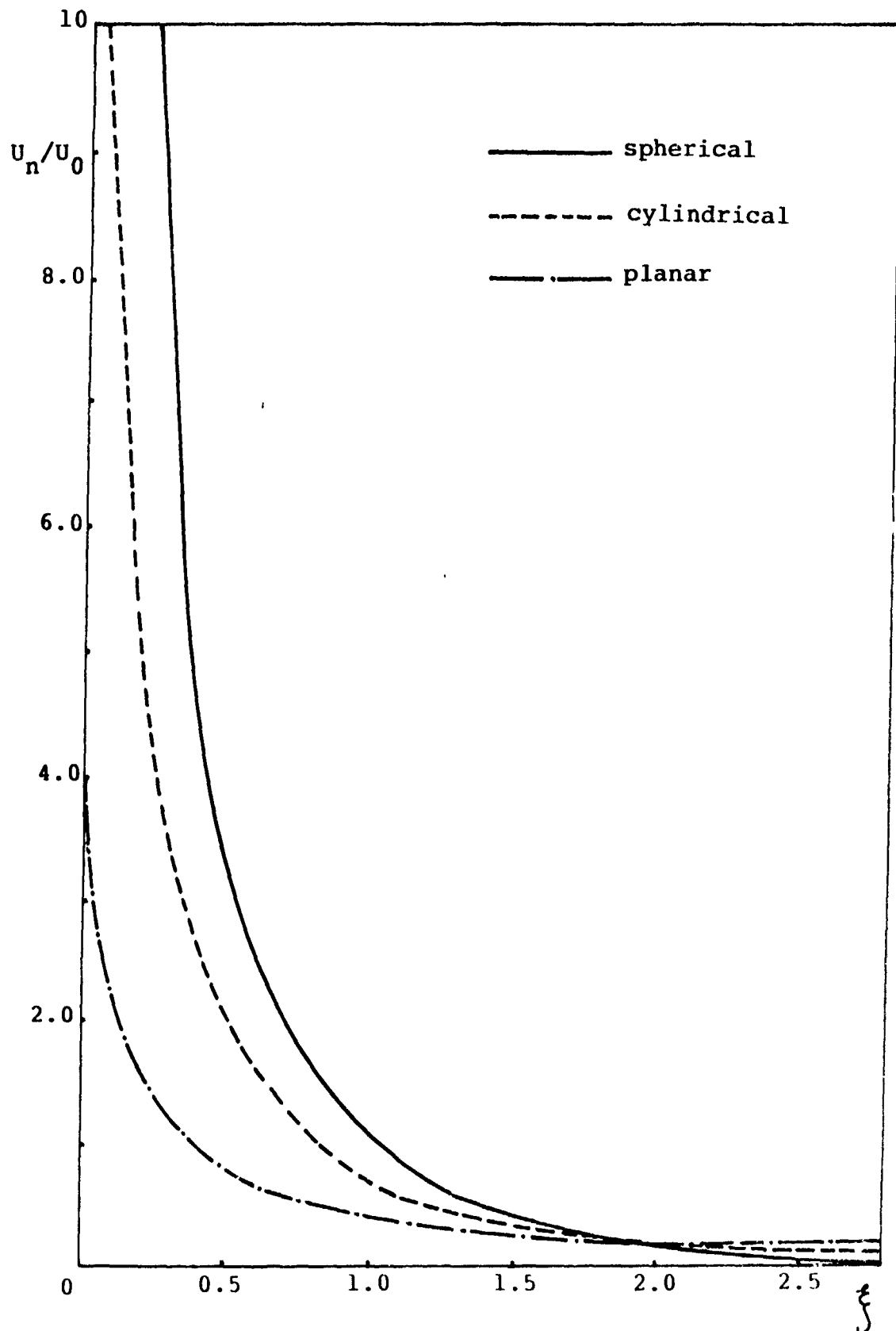
Fig. IV.1.31
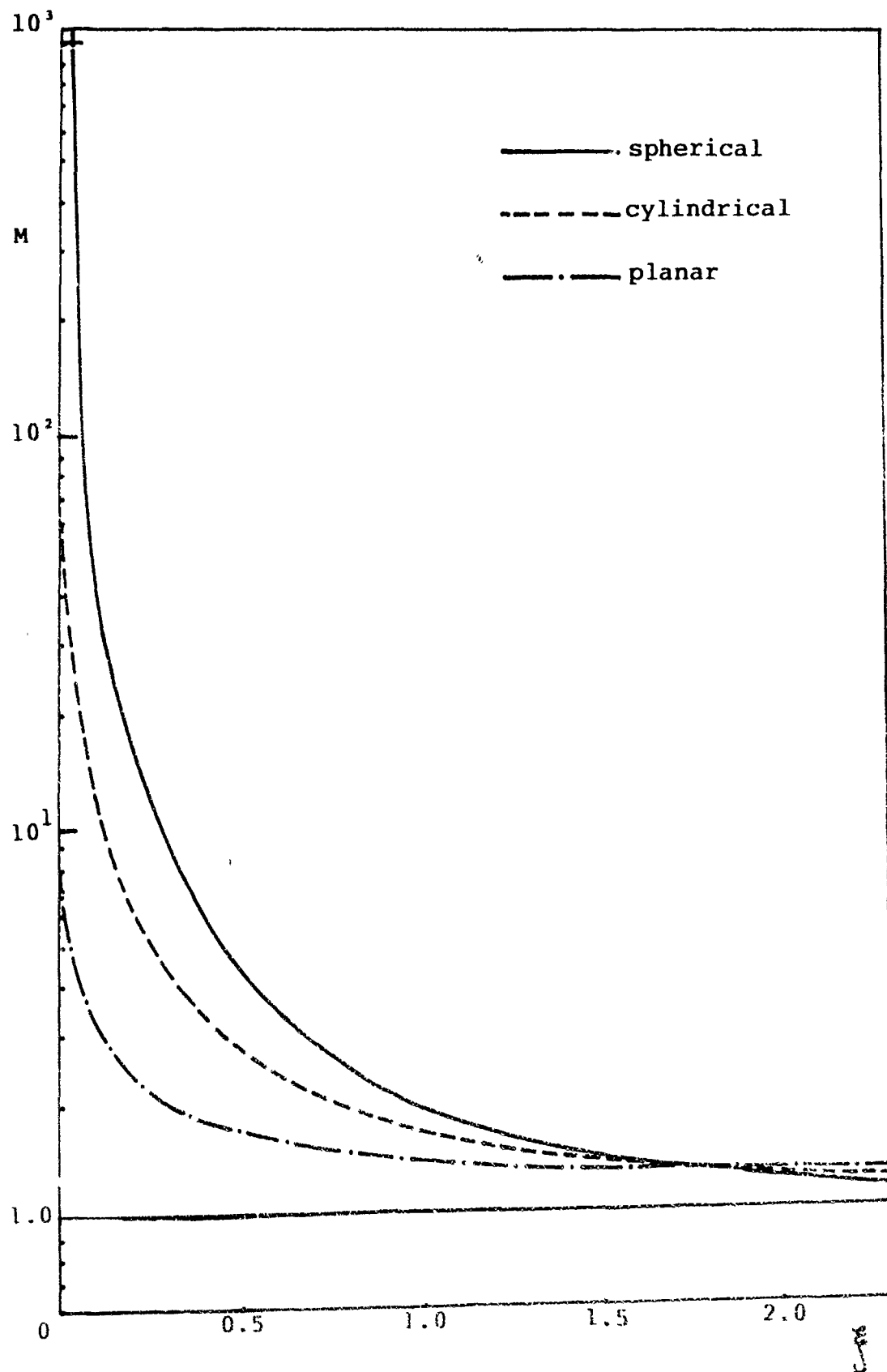
Fig. IV.1.32
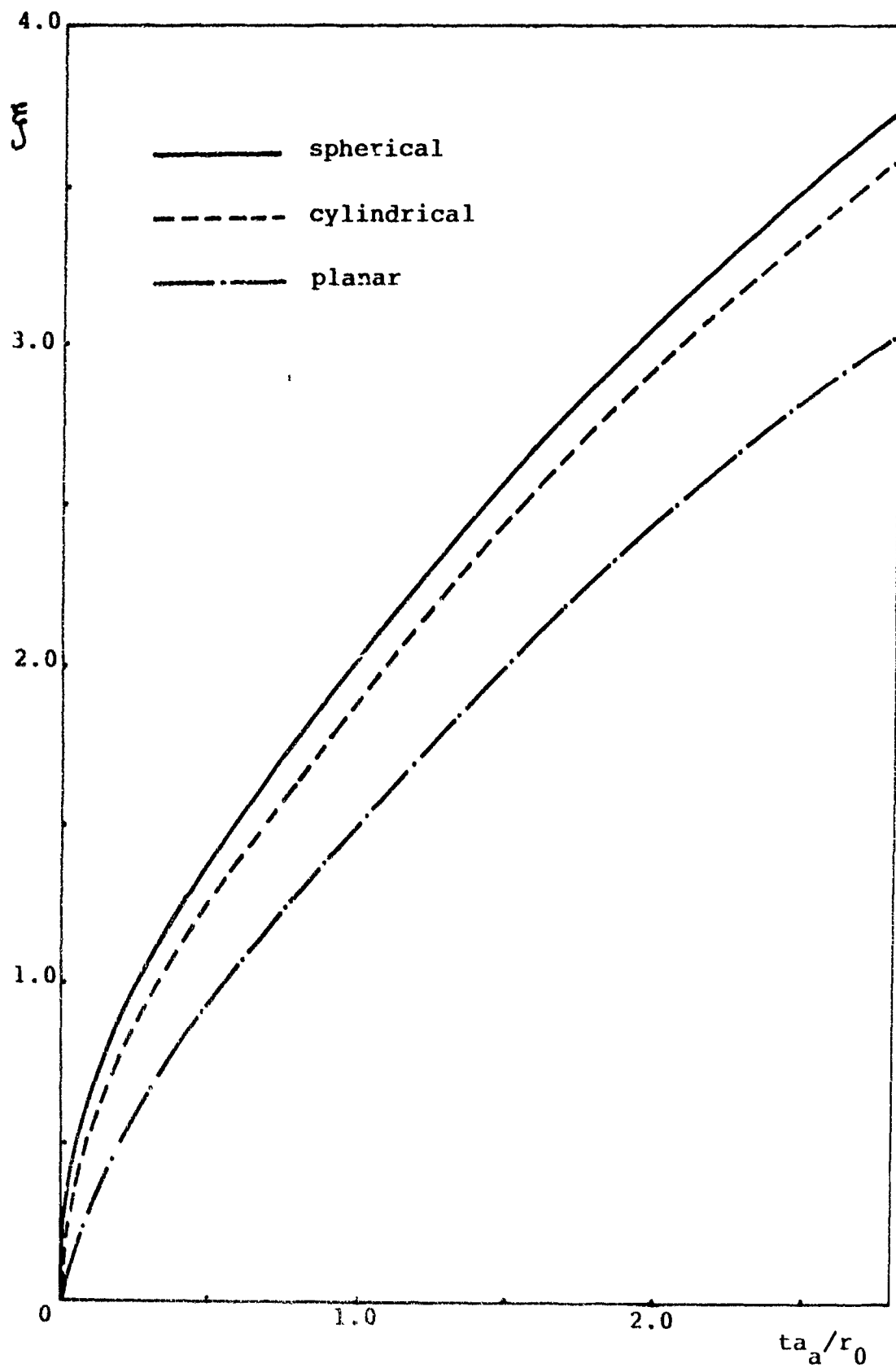
Fig. IV.1.33
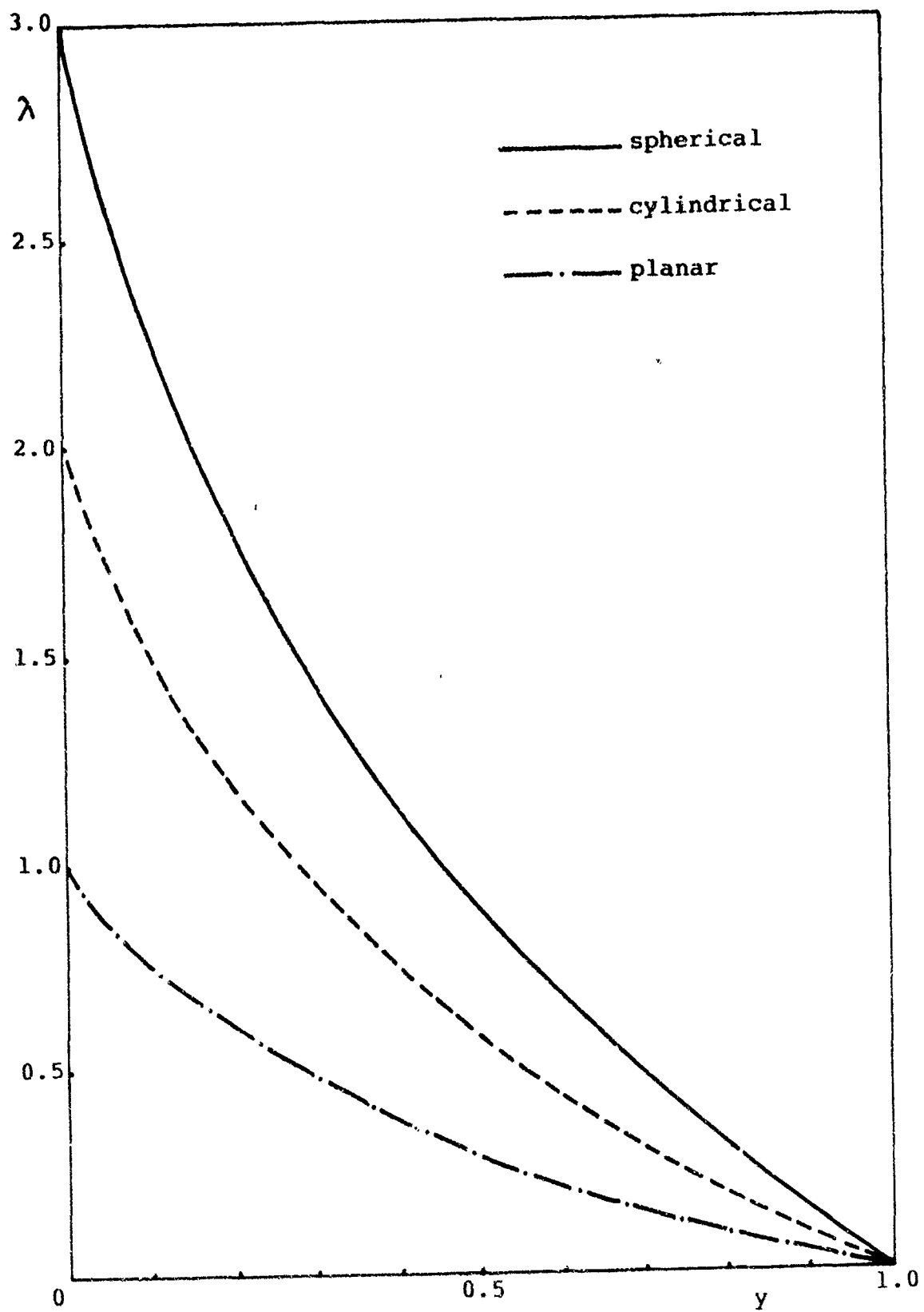
Fig. IV.1.34
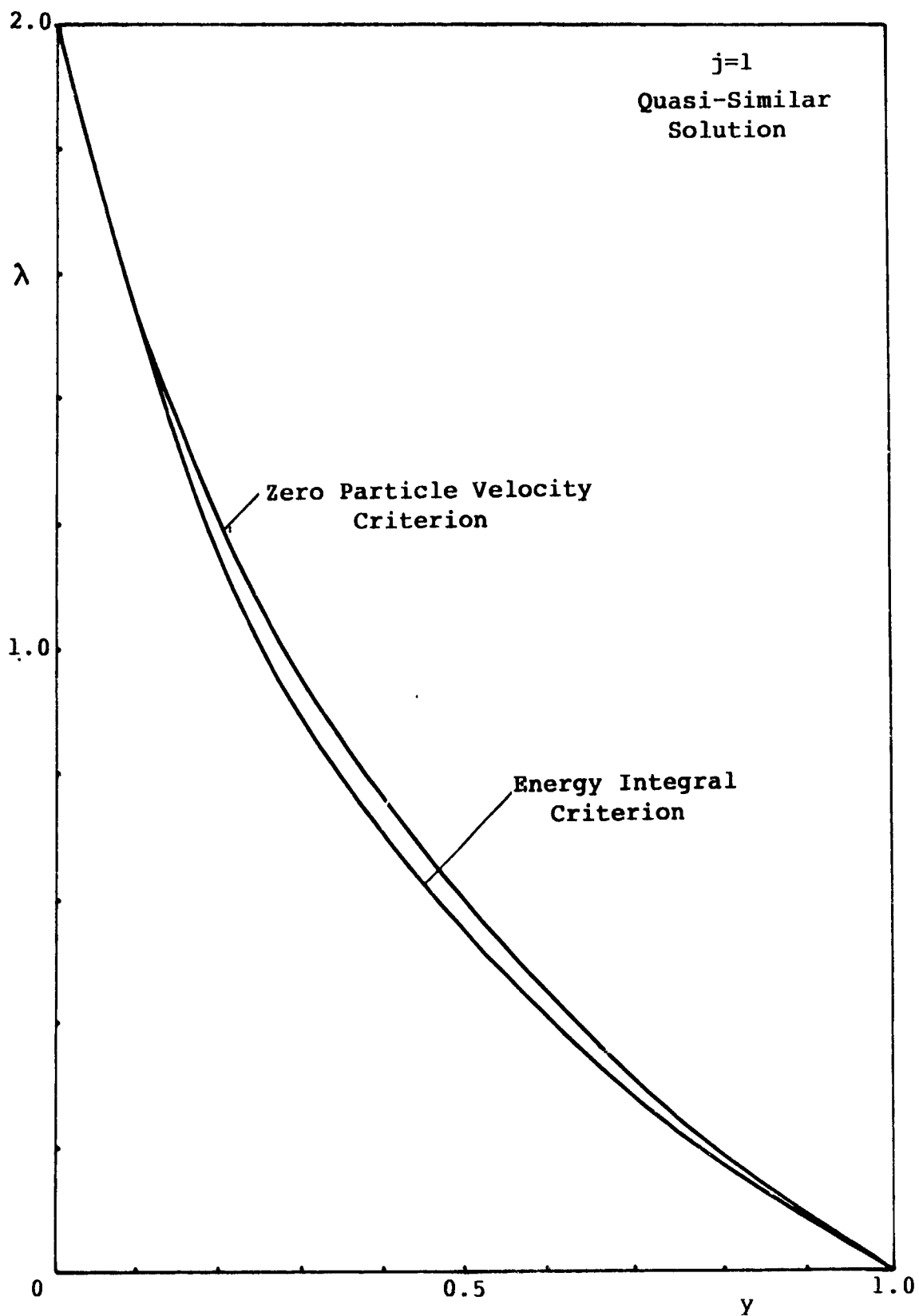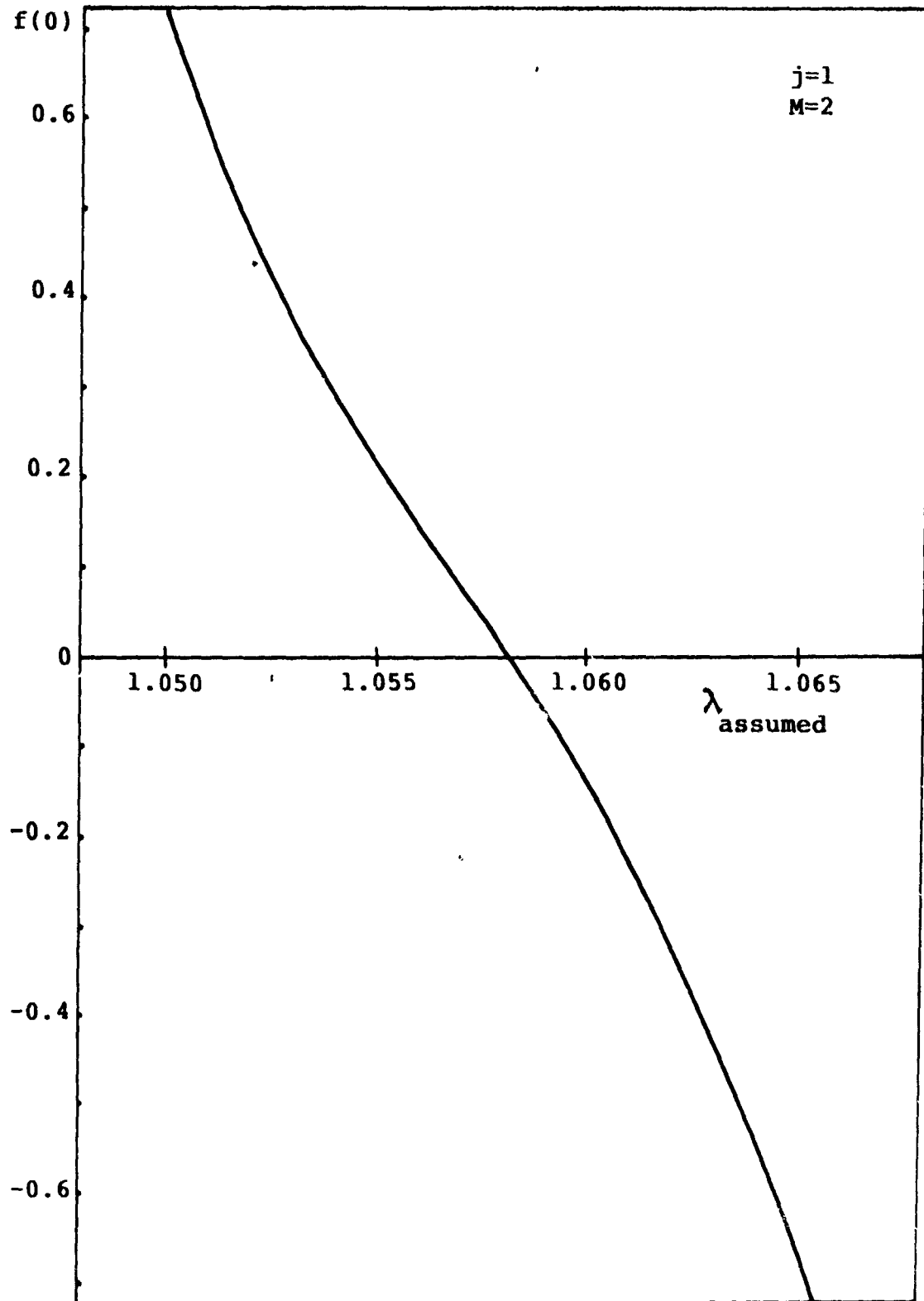
Fig. IV.1.35

Fig. IV.1.36

IV.2. QUASI-SIMILAR SOLUTIONS OF ADIABATIC POINT EXPLOSIONS--
AN ANALYTICAL SOLUTION*

i) Introduction

In this section, the quasi-similarity is introduced to study the flow field structure of adiabatic blast waves. The formulation of the problem is made applicable for the three geometrical symmetries: spherical, cylindrical and planar waves. The flow field is assumed to be inviscid and the flowing medium is treated as a perfect gas with a mean specific heat ratio γ. An approximate analytical solution is obtained and the results are compared with other existing solutions. Finally, depending on these results, the validity of the quasi-similar theory is discussed.

ii) Problem Formulation:

The conservation equations in their general form are given by Eqs. (II.20), (II.22) and (II.24). For inviscid and sourceless flow field, all ϕ's in these equations vanish. Moreover, when the flowing medium is treated as a perfect gas with a mean specific heat ratio, γ, and when ρ_a is constant, these equations are simply reduced to

$$\mathcal{J} \frac{\partial h}{\partial \mathcal{J}} + (f-x) \frac{\partial h}{\partial x} + h\left(\frac{\partial f}{\partial x} + j\frac{f}{x}\right) = 0$$

$$\mathcal{J} \frac{\partial f}{\partial \mathcal{J}} + (f-x) \frac{\partial f}{\partial x} - \frac{\lambda}{2} f + \frac{1}{h} \frac{\partial g}{\partial x} = 0 \qquad \right\} \qquad (IV.2.1)$$

$$\mathcal{J} \frac{\partial g}{\partial \mathcal{J}} + (f-x) \frac{\partial g}{\partial x} - \lambda g + \gamma g\left(\frac{\partial f}{\partial x} + j\frac{f}{x}\right) = 0$$

---

*This application is based on Oshima (1964).

The governing equations, Eqs. (IV.2.1), are subject to the boundary conditions given by the Rankine-Hugoniot relations, Eqs. (II.88) - (II.90), which may be rewritten as follows

$$
\left.
\begin{aligned}
f_n &= f(1, \zeta) = \frac{2}{\gamma+1}(1-y) \\[2ex]
g_n &= g(1, \zeta) = \frac{2\gamma-(\gamma-1)y}{\gamma(\gamma+1)} \\[2ex]
h_n &= h(1, \zeta) = \frac{\gamma+1}{\gamma-1+2y}
\end{aligned}
\right\}
\qquad \text{(IV.2.2)}
$$

For adiabatic point explosions and sourceless flow fields, the energy integral, Eq. (II.95), reduces to

$$
J_3 = \frac{y}{\gamma}\left[\zeta^{-(j+1)} + \frac{1}{(j+1)(\gamma-1)}\right]
\qquad \text{(IV.2.3)}
$$

Utilizing the concept of quasi-similarity, the governing equations reduce to a system of ordinary differential ones, given by Eqs. (III.23) - (III.25) in which all the ϕ 's equal to zero for a sourceless flow field. Therefore, one may rewrite the governing equations of the quasi-similar solutions as follows:

$$
\left.
\begin{aligned}
(f-x)\frac{dh}{dx} + h\left(\frac{df}{dx} + j\frac{f}{x}\right) + \lambda A h &= 0 \\[2ex]
(f-x)\frac{df}{dx} + \frac{1}{h}\frac{dg}{dx} + \lambda B f &= 0 \\[2ex]
(f-x)\frac{dg}{dx} + \gamma g\left(\frac{df}{dx} + j\frac{f}{x}\right) + \lambda g C &= 0
\end{aligned}
\right\}
\qquad \text{(IV.2.4)}
$$

where

$$A \equiv - \frac{2y}{\gamma - 1 + 2y}$$

$$B \equiv - \frac{y + 1}{2(1 - y)}$$

and

$$C \equiv - \frac{2\gamma}{2\gamma - (\gamma - 1)y}$$

The adiabatic integral, Eq. (III.3S), may be rewritten directly as

$$h^{\gamma} \left[h\,(x - f)\,x^{j} \right]^{\frac{2\gamma\lambda\,[y/(\gamma-1+2y) - 1/(2\gamma+y-\gamma y)]}{j+1 - 2\lambda y/(\gamma-1+2y)}}$$

$$= \frac{\gamma(\gamma+1)\left[(\gamma+1)/(\gamma-1+2y)\right]^{\gamma}}{2\gamma - \gamma y + y} \qquad (IV.2.5)$$

In order to use this integral as a check through the numerical integration, one may introduce the following new variables

$$I = x - f \qquad \text{and} \qquad K = 1 - \frac{(x-f)^{2}h}{\gamma g} \qquad (IV.2.6)$$

then, the basic equations, Eqs. (IV.2.4), in terms of I and K, will take the form

$$\frac{dI}{dx} = 1 - \frac{df}{dx} = A' + \left(B' - j\frac{I}{x}\right)\frac{1}{K} + C'\frac{x}{I}\left(1 - \frac{1}{K}\right) \left.\begin{array}{l} \\ \\ \\ \\ \\ \\ \\ \end{array}\right\}$$

$$\frac{dK}{dx} = \frac{1-K}{I}\left[\frac{x-f}{g}\cdot\frac{dg}{dx} - 2\left(1 - \frac{df}{dx}\right) - \frac{x-f}{h}\frac{dh}{dx}\right] \qquad \text{(IV.2.7)}$$

$$= \frac{1-K}{I}\left[D' - (\gamma+1)\frac{dI}{dx} - j(\gamma-1)\frac{I}{x}\right]$$

where

$$A' = 1 - \frac{(1+y)}{2(1-y)}\cdot\lambda$$

$$B' = \left[\frac{1+y}{2(1-y)} - \frac{2}{2\gamma+y-\gamma y}\right]\lambda + j$$

$$C' = \frac{(1+y)}{2(1-y)}\lambda$$

and

$$D' = (\gamma-1)(j+1) + \frac{2\lambda y}{\gamma-1+2y} - \frac{2\gamma\lambda}{2\gamma-(\gamma-1)y}$$

and the boundary conditions are transformed to

$$I_n = I(1,y) = 1 - f_n = \frac{\gamma-1+2y}{\gamma+1} \left.\begin{array}{l} \\ \\ \\ \\ \\ \\ \end{array}\right\}$$

$$\qquad \text{(IV.2.8)}$$

$$K_n = K(1,y) = 1 - \frac{(1-f_n)^2 h_n}{\gamma g_n} = \frac{(\gamma+1)(1-y)}{2\gamma-(\gamma-1)y}$$

Thus, the problem is transformed to a boundary value one in which λ is an un-known factor for each value of y . An iteration procedure is performed until the correct λ is obtained, which must satisfy the adiabatic integral, Eq.

(IV.2.5), to a sufficient accuracy. The values of λ determined are presented
in Table IV.2.1

iii) Approximate Relations

It is found from the calculated results that the solution may be represented
approximately in the form

$$I = \alpha x + \beta x^n \tag{IV.2.9}$$

where α, β and n are determined by the boundary conditions and the asymptotic behaviour of I and K to $x = 0$. From Eq. (IV.2.7), one has

$$\frac{dI}{dx}\Big|_{x=0} = \lim_{x \to 0} \left(\frac{dI}{dx}\right)$$

$$= \lim_{x \to 0} \left[A' + (B' - j\frac{I}{x})\frac{1}{K} + C'\frac{x}{I}(1 - \frac{1}{K}) \right]$$

$$= A' + B' - j\frac{dI}{dx}\Big|_{x=0}$$

thus

$$\frac{dI}{dx}\Big|_{x=0} = \frac{A' + B'}{j + 1}$$

while from Eq. (IV.2.9)

$$\frac{dI}{dx}\Big|_{x=0} = \alpha$$

Thus

$$\alpha = \frac{A' + B'}{j + 1} = 1 - \left(\frac{2}{j+1}\right)\left(\frac{\lambda}{2\gamma + y - \gamma y}\right) \tag{IV.2.10}$$

Also, from Eq. (IV.2.9), one has

$$I_n = \alpha + \beta$$

Thus

$$\beta = I_n - \alpha = \frac{\gamma - 1 + 2y}{\gamma + 1} + \frac{2\lambda}{(j+1)(2\gamma + y - \gamma y)} - 1 \qquad \text{(IV.2.11)}$$

while

$$n = \frac{(\frac{dI}{dx})_n - \alpha}{I_n - \alpha} = \frac{(\frac{dI}{dx})_n - \alpha}{\beta} \qquad \text{(IV.2.12)}$$

where

$$\left(\frac{dI}{dx}\right)_n = \frac{dI}{dx}(1, y) = A' + \frac{B' - jI_n}{K_n} + \frac{C'}{I_1}\left(1 - \frac{1}{K_n}\right)$$

By using the values of λ determined previously, the values of α, β and n can be obtained from the above relations. These values as well as $\mathcal{J}_3$ and $\mathcal{J}$ are tabulated in Table IV.2.2.

For integrating the second of Eqs. (IV.2.7), it follows that

$$\frac{dK}{1-K} = \frac{D'}{I}\, dx - \frac{(\gamma + 1)\frac{dI}{dx}}{I}\, dx - \frac{j(\gamma - 1)}{x}\, dx$$

integration of the above equation yields

$$-\ln(1-K) = D' \int \frac{dx}{\alpha x + \beta x^n} - \ln I^{\gamma + 1} - \ln x^{j(\gamma - 1)}$$

$$= \frac{D'}{\alpha} \int \left[\frac{1}{x} - \frac{\beta x^{n-2}}{(n-1)(\alpha + \beta x^{n-1})}\right] dx - \ln\left[I^{\gamma + 1}\, x^{j(\gamma - 1)}\right]$$

$$= \ln x^{\frac{D'}{\alpha}} - \ln (\alpha + \beta x^{n-1})^{\frac{D'}{\alpha(n-1)}} - \ln \left[I^{\gamma+1} x^{j(\gamma-1)} \right] - \ln (const._1)$$

Thus

$$1 - K = const._1 \, I^{\gamma + 1 + \frac{D'}{\alpha(n-1)}} \cdot x^{j(\gamma-1) - \frac{n D'}{\alpha(n-1)}}$$

The constant of integration is determined by using the boundary conditions at $x = 1$ to yield finally

$$K = 1 - (1 - K_n) \left(\frac{I}{I_n} \right)^{\gamma + 1 + \frac{D'}{\alpha(n-1)}} x^{j(\gamma-1) - \frac{n D'}{\alpha(n-1)}} \qquad (IV.2.13)$$

From Eqs. (IV.2.4), one has

$$\frac{dh}{h} = - \left[\frac{j}{x} + \frac{\frac{dI}{dx}}{I} + \frac{\frac{2\lambda y}{\gamma - 1 + 2y} - (j+1)}{I} \right] dx$$

which yields upon integration

$$h = Const._2 \, \left(\frac{1}{I} \right)^{\frac{j+1 - \frac{2\lambda y}{\gamma - 1 + 2y}}{\alpha(n-1)} + 1} \cdot x^{\frac{n \left(j+1 - \frac{2\lambda y}{\gamma - 1 + 2y} \right) - j}{}}$$

Applying the boundary conditions yields

$$h = h_n \left(\frac{I_n}{I} \right)^{\frac{j+1 - \frac{2\lambda y}{\gamma - 1 + 2y}}{\alpha(n-1)} + 1} x^{\frac{n \left(j+1 - \frac{2\lambda y}{\gamma - 1 + 2y} \right)}{n(n-1)} - j} \qquad (IV.2.14)$$

It follows also from Eqs. (IV.2.4) that

$$\frac{dg}{g} = \left[\frac{-j\gamma f}{x(f-x)} + \frac{2\gamma\lambda}{2\gamma - \delta y + y} \cdot \frac{1}{(f-x)} + \frac{\gamma \frac{df}{dx}}{x-f} \right] dx$$

$$= \left[\frac{-j\gamma}{x} + \frac{j\gamma + \gamma - \frac{2\sigma\lambda}{2\gamma - \delta y + y}}{I} - \frac{\gamma \frac{dI}{dx}}{I} \right] dx$$

$$= \left[\frac{-j\gamma}{x} + \frac{\alpha \gamma (j+1)}{I} - \gamma \frac{\frac{dI}{dx}}{I} \right] dx$$

Integration yields

$$g = Const._3 \left(\frac{x}{I} \right)^{\frac{\gamma(n+j)}{n-1}}$$

Determining the value of the constant from the boundary conditions yields

$$g = g_n \left(\frac{x I_n}{I} \right)^{\frac{\gamma(n+j)}{n-1}} \tag{IV.2.15}$$

Equations (IV.2.9), (IV.2.14) and (IV.2.15) are the approximate relations for determining the non-dimensional gasdynamic parameters f, h and g, respectively.

In order to determine a relation between λ and γ, one may differentiate the relation of Eq. (IV.2.9) twice and eliminate β to obtain at $x = 1$:

$$\left(\frac{d^2 I}{dx^2} \right)_n (I_n - \alpha) = \left[\left(\frac{dI}{dx} \right)_n - \alpha \right] \left[\left(\frac{dI}{dx} \right)_n - I_n \right] \tag{IV.2.16}$$

With the aid of Eqs. (IV.2.8) and (IV.2.9), one has

$$I_n = \frac{\gamma - 1 + 2y}{\gamma + 1} \quad , \quad K_n = \frac{(\gamma + 1)(1 - y)}{2\gamma - (\gamma - 1)y}$$

$$\left(\frac{dI}{dx}\right)_n = A' + \frac{B' - jI_n}{K_n} + \frac{G'}{I_n}\left(1 - \frac{1}{K_n}\right)$$

$$\left(\frac{d^2I}{dx^2}\right)_n = \frac{(jI_n - B')}{K_n^2}\left(\frac{dK}{dx}\right)_n + \frac{G'}{I_n K_n}\left\{\frac{1}{K_n}\cdot\left(\frac{dK}{dx}\right)_n\right.$$

$$+ (K_n - 1)\left[1 - \frac{1}{I_n}\cdot\left(\frac{dI}{dx}\right)_n\right]\Big\}$$

$$+ \frac{j}{K_n}\left[I_n - \left(\frac{dI}{dx}\right)_n\right]$$

$$\left(\frac{dK}{dx}\right)_n = \frac{(1 - K_n)}{I_n}\left[D' - (\gamma + 1)\left(\frac{dI}{dx}\right)_n - j(\gamma - 1)I_n\right]$$

Substituting the values of $\left(\frac{d^2I}{dx^2}\right)_n$, $\left(\frac{dI}{dx}\right)_n$, I_n and α into Eq. (IV. .16), a third order algebraic equation in λ is obtained. In the case of p anar waves, this equation is reduced to a second order algebraic equation and its proper root is given by

$$\lambda = \frac{-\psi - \sqrt{\psi^2 - 4\varphi\theta}}{2\varphi} \tag{IV.2.17}$$

where

$$\varphi = D''F'' \quad ; \quad \psi = C''F'' + D''E'' + B'' \quad ; \quad \theta = C''E'' - A''$$

$$A'' = 4 \left[4\gamma - 2 + (\gamma + 5)\, y - (\gamma - 1)\, y^2 \right] (1 - y)^2 (\gamma - 1 + 2y)$$

$$B'' = 2 (3 + y) \left[4\gamma - 2 + (\gamma + 5)\, y - (\gamma - 1)\, y^2 \right] (\gamma - 1 + 2y)$$

$$C'' = 2 (1 - y) \left[2\gamma - (\gamma - 1)\, y \right]$$

$$D'' = - 2 (\gamma + 1)$$

$$E'' = -4 \left[4\gamma - 2 + (\gamma + 5)\, y - (\gamma - 1)\, y^2 \right] + 2 (\gamma + 1)(1 - y)^2$$

$$F'' = 2 \left[4\gamma - 2 + (\gamma + 5)\, y - (\gamma - 1)\, y^2 \right] \left\{ \frac{4y}{\gamma - 1 + 2y} - \frac{2\gamma}{2\gamma - (\gamma - 1)\, y} + \frac{3 + y}{1 - y} \right\} - (\gamma + 1)(3 + y)$$

iv) Results and Conclusions:

The distributions of the gasdynamic parameters f, g and h are presented in Figs. IV.2.1 to IV.2.6 to show the applicability of the approximate formulae, given by Eqs. (IV.2.9), (IV.2.14) and (IV.2.15), which are compared with numerical and Sakurai's second approximation perturbation solutions. These are for the case of cylindrical waves, as an example, with two different values of Mach number, $M = 2$ and $M = 3$, while $\gamma = 1.4$. This comparison proves the usefulness of these formulae. Especially, in the neighborhood of $x = 0$, where the original equations show a singularity at the center

of symmetry, $\mathcal{X}$ = 0, these formulae yield good insight into the problem under study.

The pressure and temperature distributions are also shown in Figs. IV.2.7 to IV.2.14, for the three geometrical symmetries. These figures show that the pressure is approximately uniform near the center of symmetry while the temperature has a steep increase near the center of symmetry to infinity as a result of neglecting the heat transfer effects.

Figure IV.2.15 shows the variation of λ with y for different values of δ , in the case of planar waves, by using the approximate analytical formula given by Eq. (IV.2.17).

It is observed from the experimental data (Oshima, 1960) that the quasi-similarity assumptions fail for the strong blast waves. It is also clear that the central region in the quasi-similar solution has an infinitely high temperature core which is never realized in the actual flow. This last phenomena is due to the fact that transport processes have been neglected in the governing Eqs. (IV.2.1) and not due to quasi-similarity assumptions. Later in this chapter we shall deal with this issue.

Therefore, the region in which the quasi-similar solution is applicable is limited to the flow fields of blast waves with moderate strength excluding the central region.

Figure IV.2.16 shows a comparison of the values of λ obtained by the quasi-similar technique with that calculated previously by Sakurai (1954), Sedov (1957) and Brode (1955, 1959), all for the spherical waves with j = 2.

Sedov (1957) expressed the velocity, pressure and density as functions of $\mathcal{X}$ and y . These variables were expanded in a power series of y , and f was assumed to take the form,

$$ f^{3} = \frac{1}{J_{3}} \cdot y \; e^{Ay} $$

then neglecting the higher order terms, the basic equations were reduced to a system of linear differential equations containing the unknown constant A .

This value of A was determined so that the boundary conditions at $x = 1$ and $x = 0$ were satisfied. It was close to 1.92 in the case of $j = 2$. Finally, the results obtained were expressed by

$$\lambda = \frac{3}{1 + 1.92\,y}$$

and

$$\mathcal{J}^3 = 1.667\ y\ e^{1.92\,y}$$

Brode (1955, 1959) calculated numerically the adiabatic point explosion problem using artificial viscosity technique, and presented an approximate formula well in agreement with the calculated results using the quasi-similar technique, which is given by

$$\lambda = \frac{3(1-y)}{(1+y)}$$

and

$$\mathcal{J}^3 = (1.629)\,\frac{y}{(1-y)^2}$$

Finally, Sakurai (1954) obtained the following results

$$\lambda = 3\,(1 - 1.918\,y)$$

and

$$\mathcal{J}^3 = (1.678)\,\frac{y}{(1 - 1.918\,y)}$$

which is also compatible with previous ones.

- 124 -

Figure Captions

Fig. IV.2.1   The distribution of the non-dimensional particle velocity
f based on the present approximate formulae as compared
with those of numerical and Sakurai's second order pertur-
bation solutions for the case of j = 1 at M = 3.

Fig. IV.2.2   The distribution of the non-dimensional pressure g based
on the present approximate formulae as compared with
those of numerical and Sakurai's second order perturba-
tion solutions for the case of j = 1 at M = 3.

Fig. IV.2.3   The distribution of the non-dimensional density h based
on the present approximate formulae as compared with
those of numerical and Sakurai's second order perturba-
tion solutions for the case of j = 1 at M = 3.

Fig. IV.2.4   The distribution of the non-dimensional particle velocity
f based on the present approximate formulae as compared
with those of numerical and Sakurai's second order pertur-
bation solutions for the case of j = 1 at M = 2.

Fig. IV.2.5   The distribution of the non-dimensional pressure g based
on the present approximate formulae as compared with
those of numerical and Sakurai's second order perturba-
tion solutions for the case of j = 1 at M = 2.

Fig. IV.2.6   The distribution of the non-dimensional density h based
on the present approximate formulae as compared ith
those of numerical and Sakurai's second order per urba-
tion solutions for the case of j = 1 at M = 2.

Fig. IV.2.7   Pressure distribution at different values of the shock
Mach number M for planar waves with γ = 1.4.

| M | y | $\gamma = 1.4$ | $\gamma = 1.667$ | $\gamma = 1.4$ | |
		$j = 0$	$j = 0$	$j = 1$	$j = 2$
1.1	0.8264	0.076	0.078	0.152	0.24
1.2	0.6944	0.150	0.156	0.304	0.474
1.4	0.5102	0.284	0.284	0.568	0.870
1.6	0.3906	0.390	0.410	0.772	1.156
2.0	0.25	0.530	0.550	1.058	1.58
3.0	0.1111	0.74	0.78	1.458	2.16
	0	1.0	1.0	2.0	3.0

TABLE IV.2.1 - Values of λ

	M	y	α	β	n	$\mathcal{J}_3$	$\mathcal{F}$
$j=0$ $\gamma=1.4$	1.1	0.8264	0.9385	-0.0832	7.6490	2.2604	4.254
	1.2	0.6944	0.8811	-0.1356	5.2478	2.1356	1.738
	1.4	0.5102	0.7812	-0.1923	3.2262	1.8690	0.860
	1.6	0.3906	0.7049	-0.2126	2.8645	1.7505	0.505
	2.0	0.25	0.6074	-0.2323	2.4249	1.5949	0.258
$j=0$ $\gamma=1.667$	1.1	0.8264	0.9439	-0.0741	7.9433	1.3229	9.8619
	1.2	0.6944	0.8913	-0.1205	4.9668	1.1377	3.5336
	1.4	0.5102	0.8103	-0.1776	3.3412	1.1235	1.4229
	1.6	0.3906	0.7332	-0.1902	3.0941	1.0938	0.7688
	2.0	0.25	0.6527	-0.2151	2.5397	1.0346	0.3789
$j=1$ $\gamma=1.4$	1.1	0.8264	0.9385	-0.0830	5.7470	1.320	2.890
	1.2	0.6944	0.8795	-0.1340	3.9918	1.0523	1.9414
	1.4	0.5102	0.7814	-0.1894	3.0412	0.9533	1.2716
	1.6	0.3906	0.7080	-0.2157	2.6871	0.9161	0.9556
	2.0	0.25	0.6082	-0.2331	2.4921	0.8263	0.6976
$j=2$ $\gamma=1.4$	1.1	0.8264	0.9353	-0.0798	5.3195	0.7592	2.271
	1.2	0.6944	0.8747	-0.1292	3.9520	0.7093	1.745
	1.4	0.5102	0.7766	-0.1846	3.0970	0.6469	1.320
	1.6	0.3906	0.7085	-0.2162	2.5550	0.6026	1.121
	2.0	0.25	0.6099	-0.2348	2.5021	0.5710	0.883

TABLE IV.2.2 - Values of α, β, n, $\mathcal{J}_3$ and $\mathcal{F}$
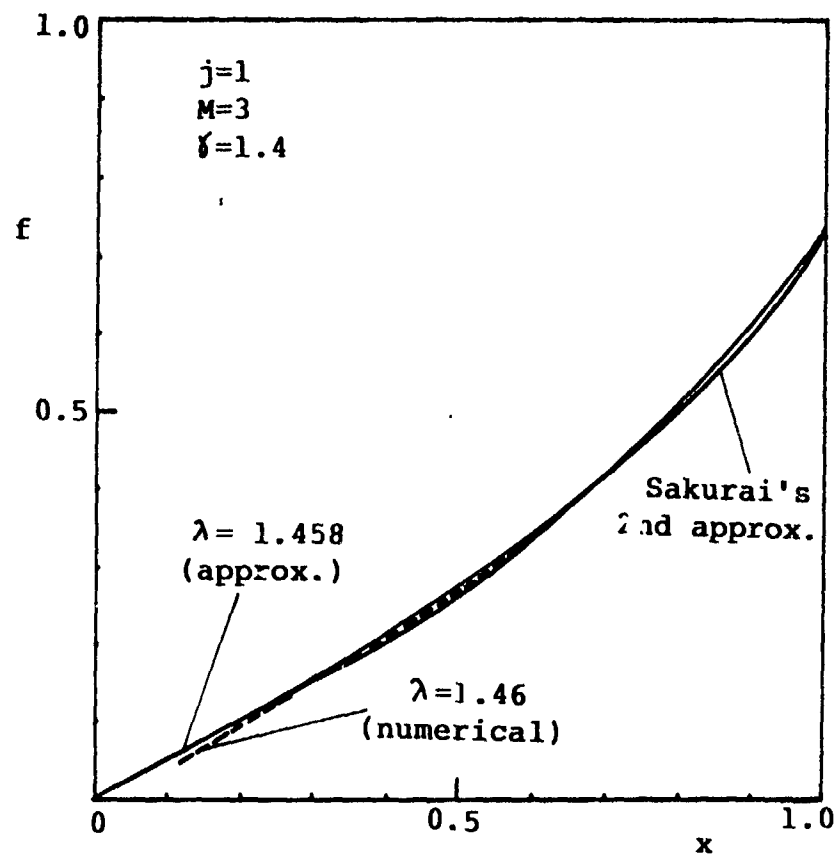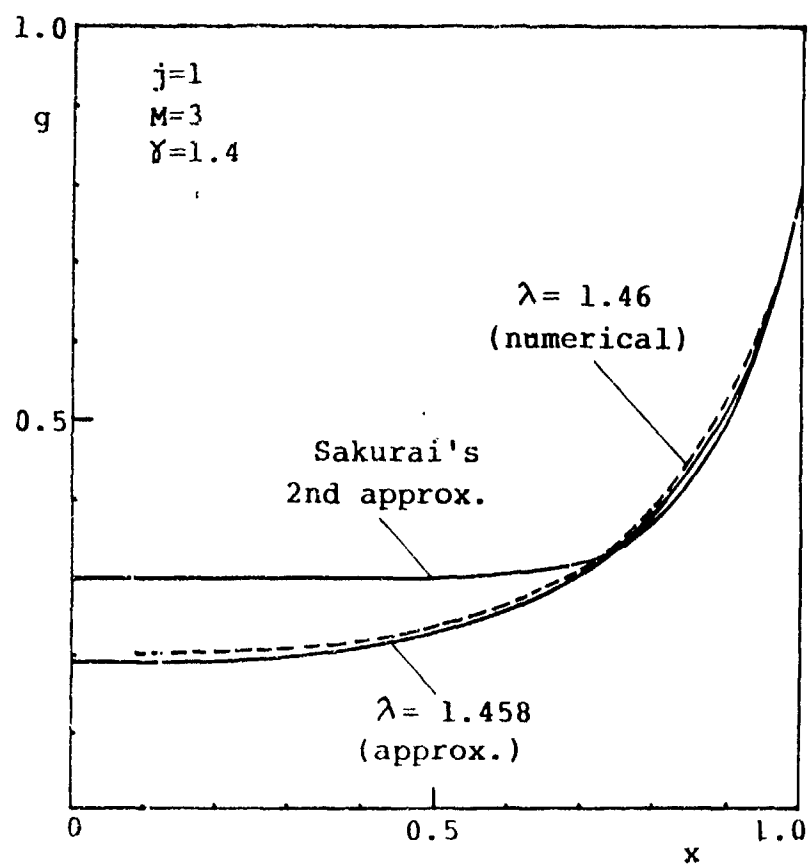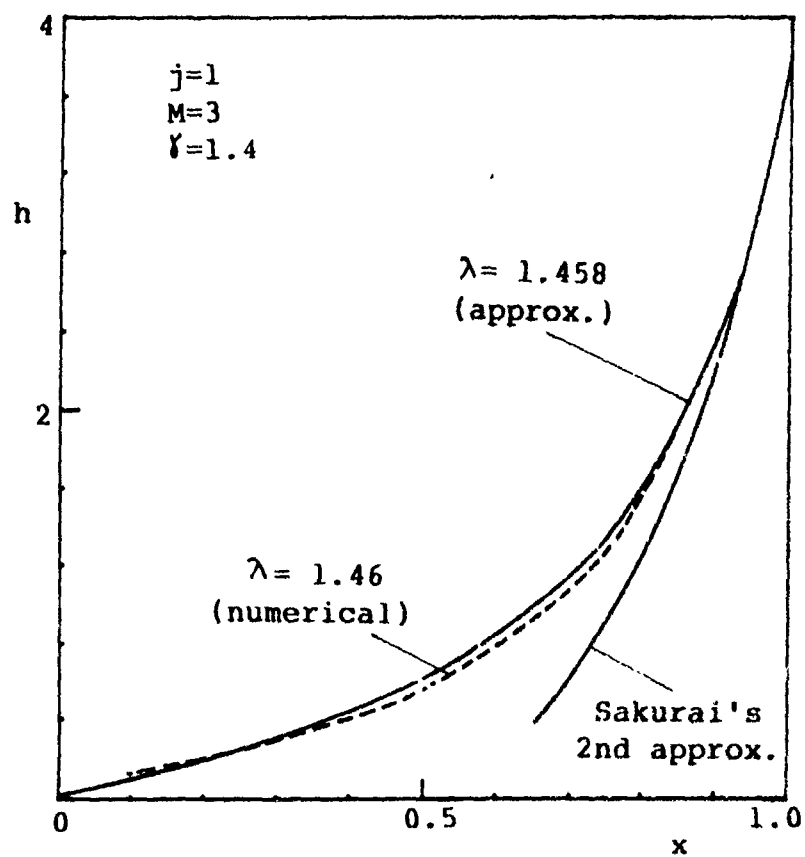
Fig. IV.2.1

Fig. IV.2.2

Fig. IV.2.3
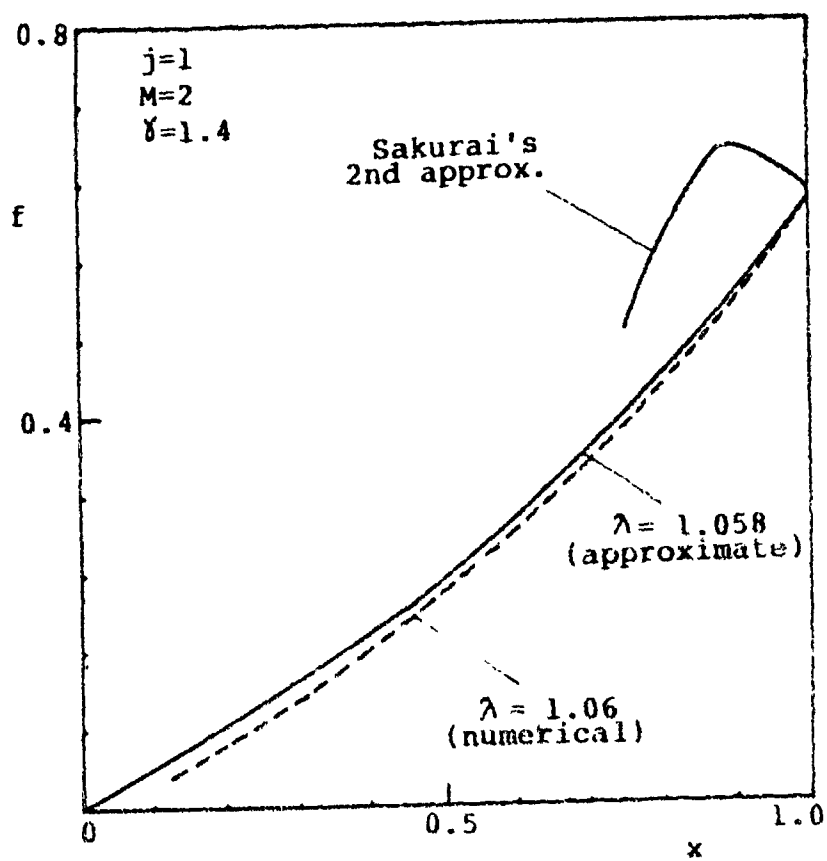
Fig. IV.2.4
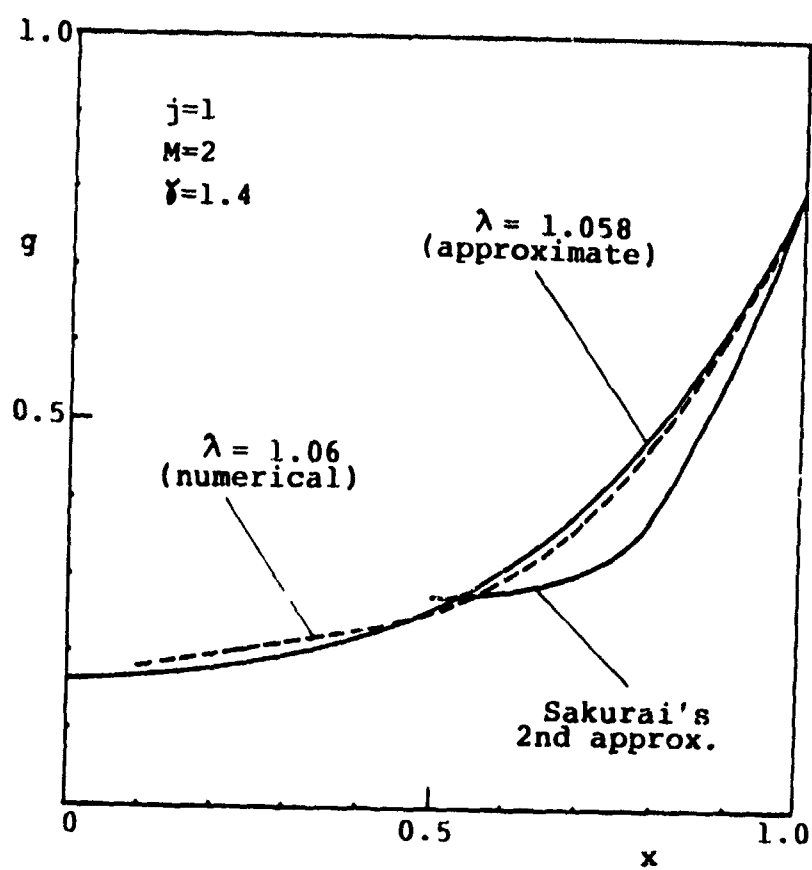
Fig. IV.2.5
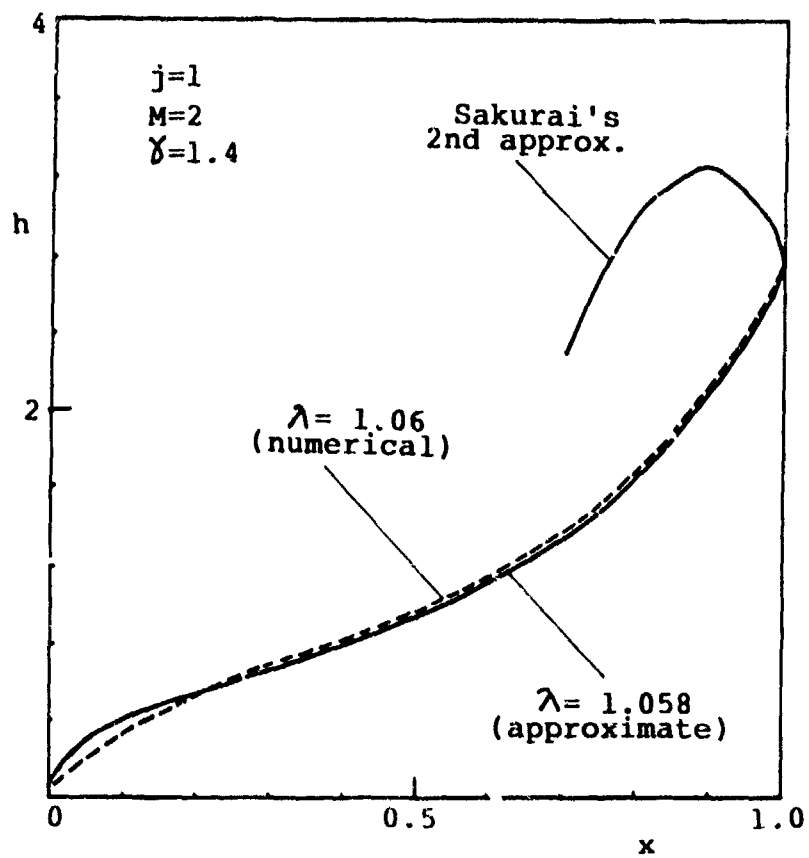
Fig. IV.2.6
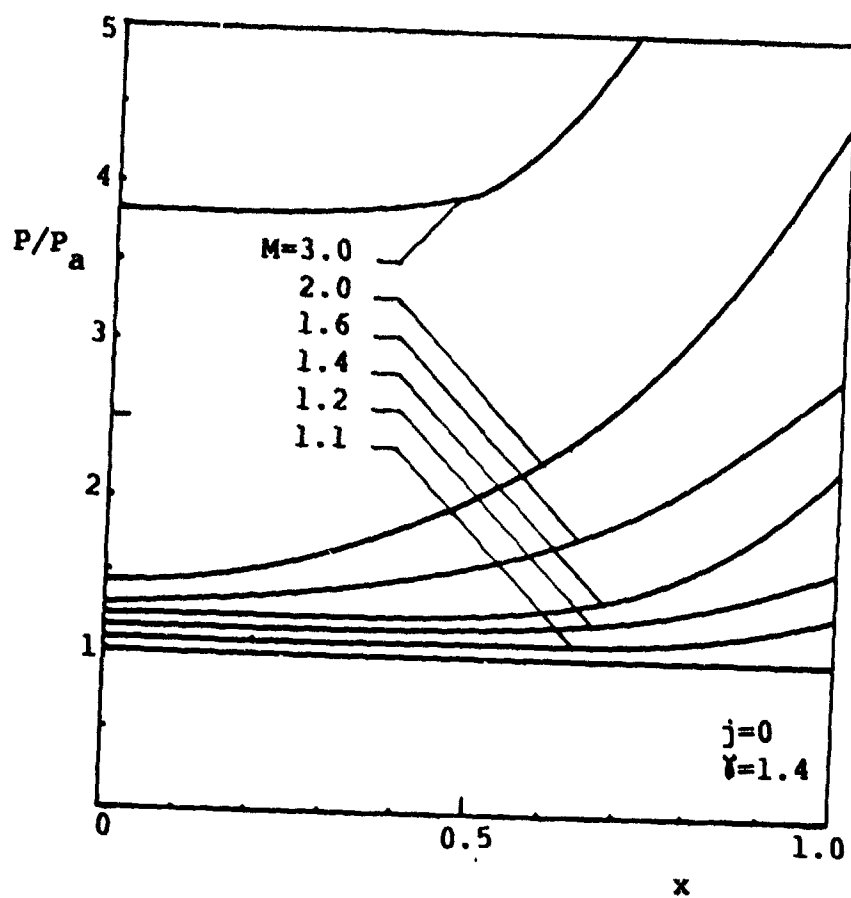
Fig. IV.2.7
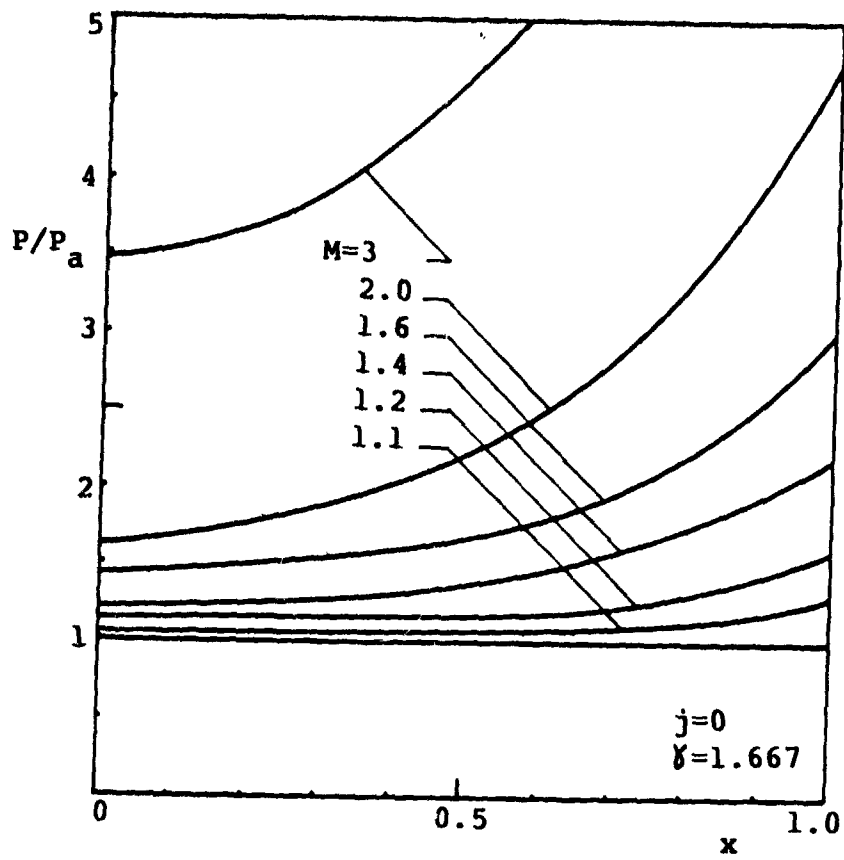
Fig. IV.2.8
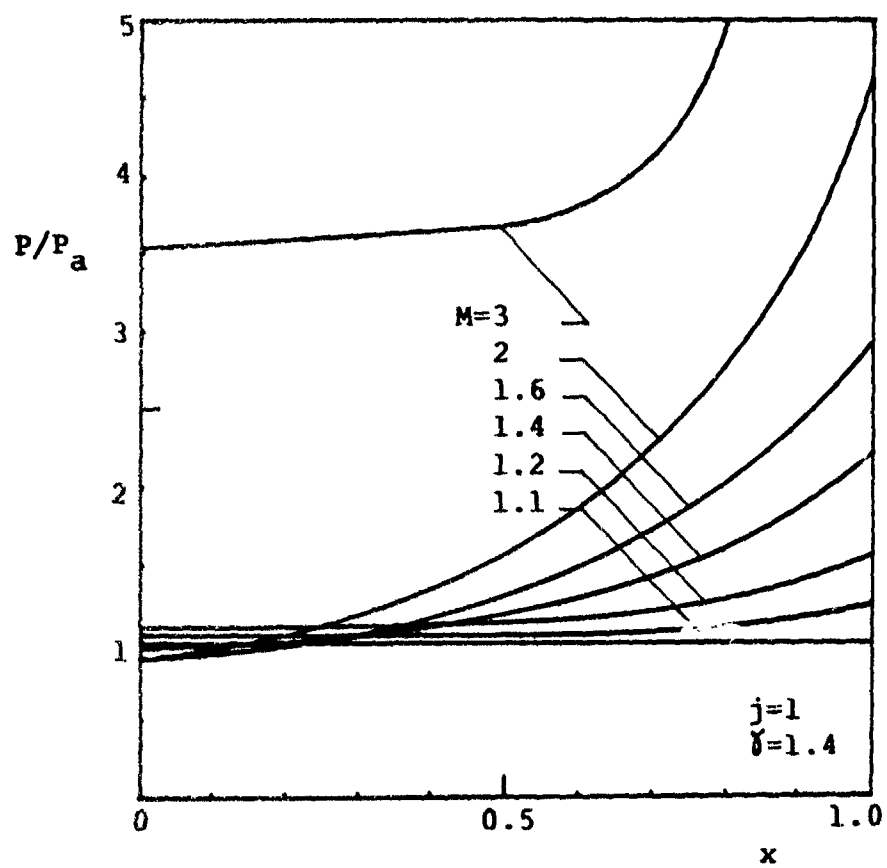
Fig. IV.2.9
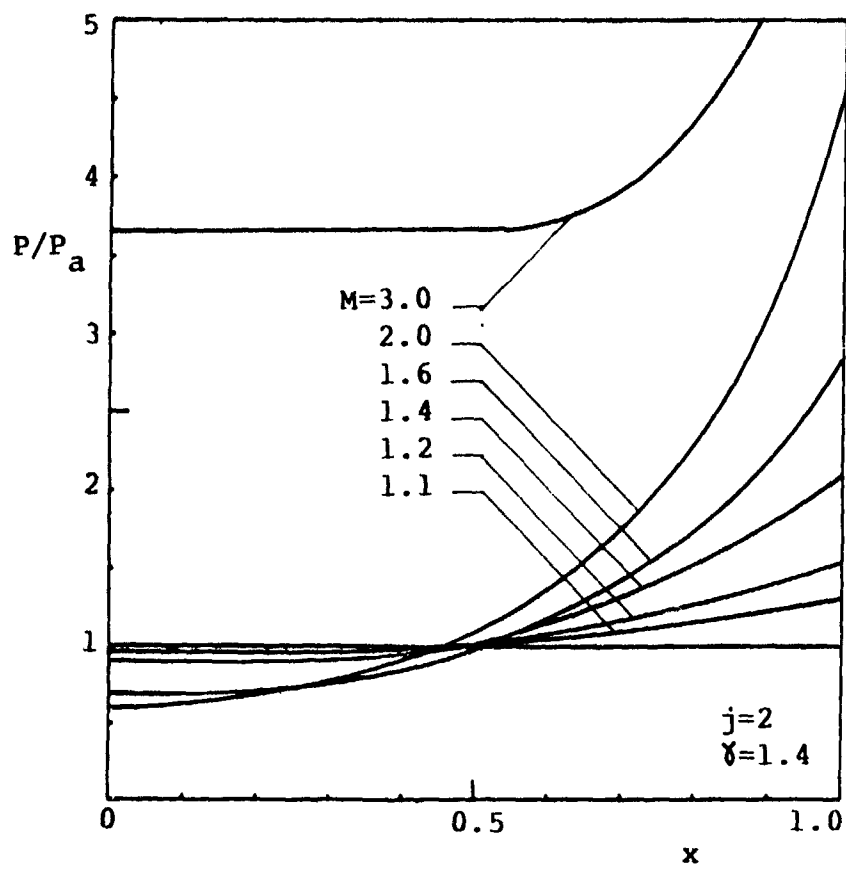
Fig. IV.2.10
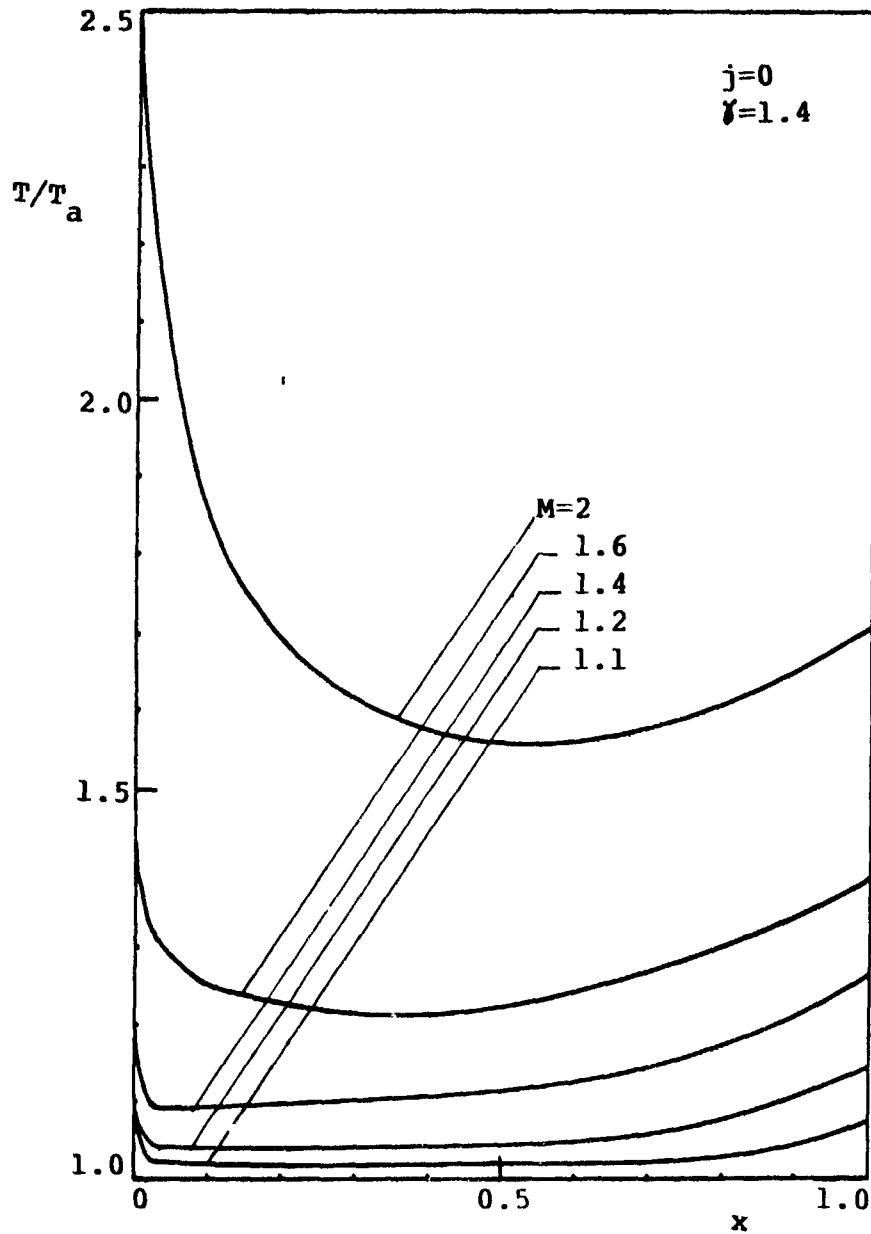
Fig. IV.2.11
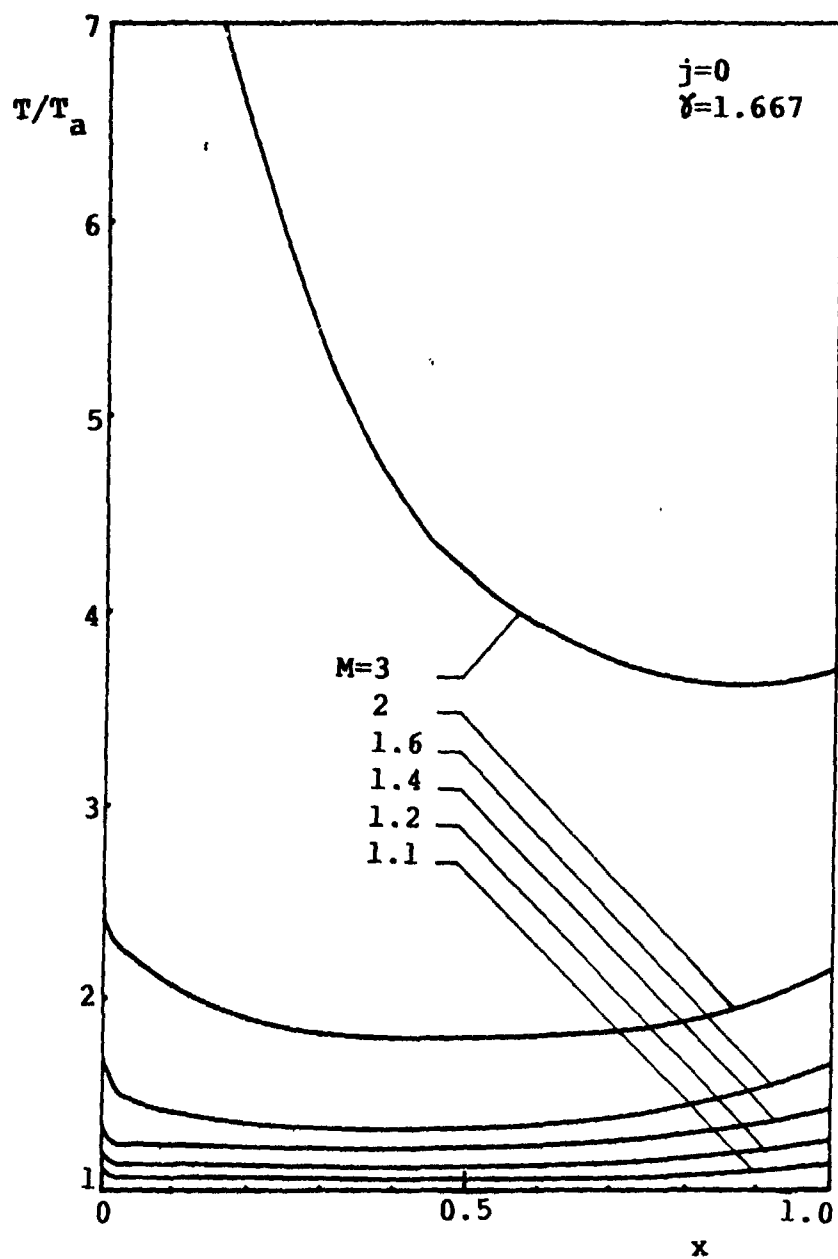
Fig. IV.2.12
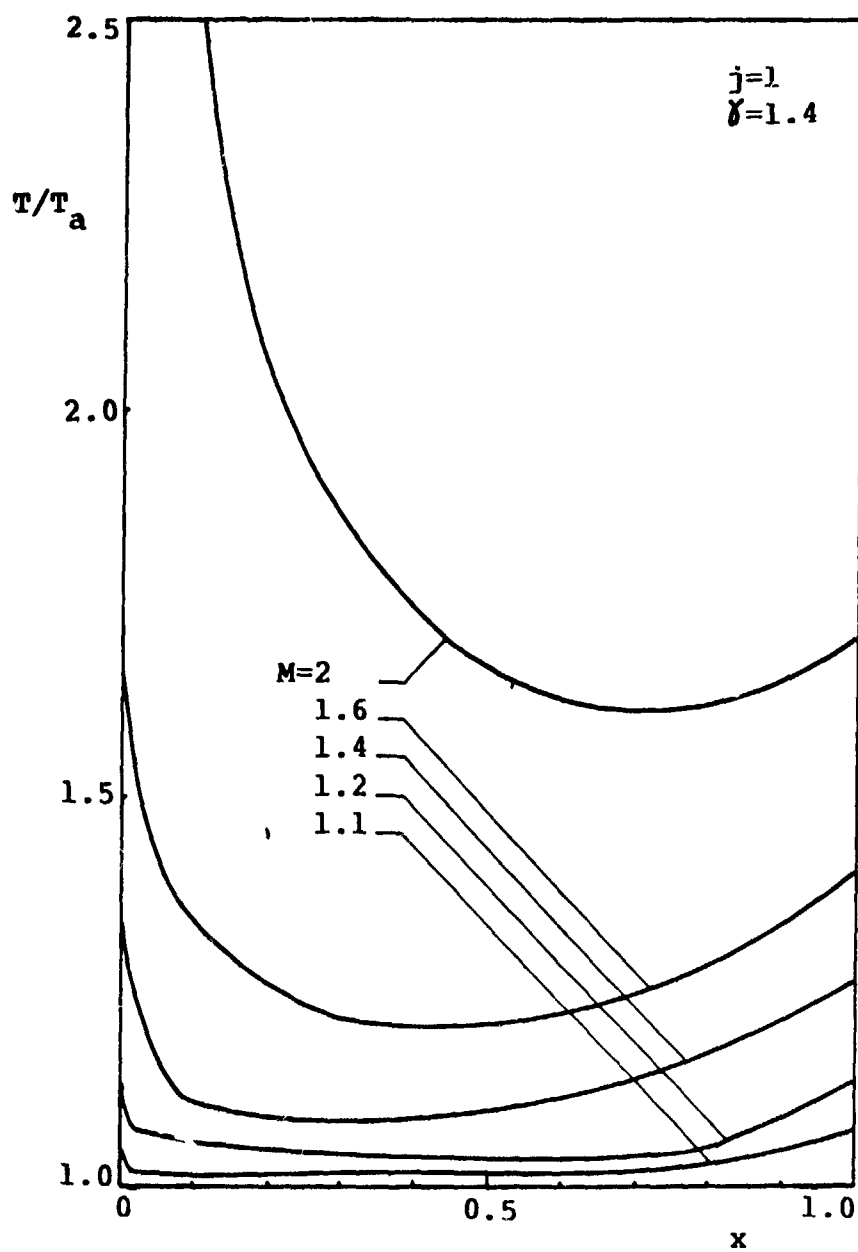
Fig. IV.2.13
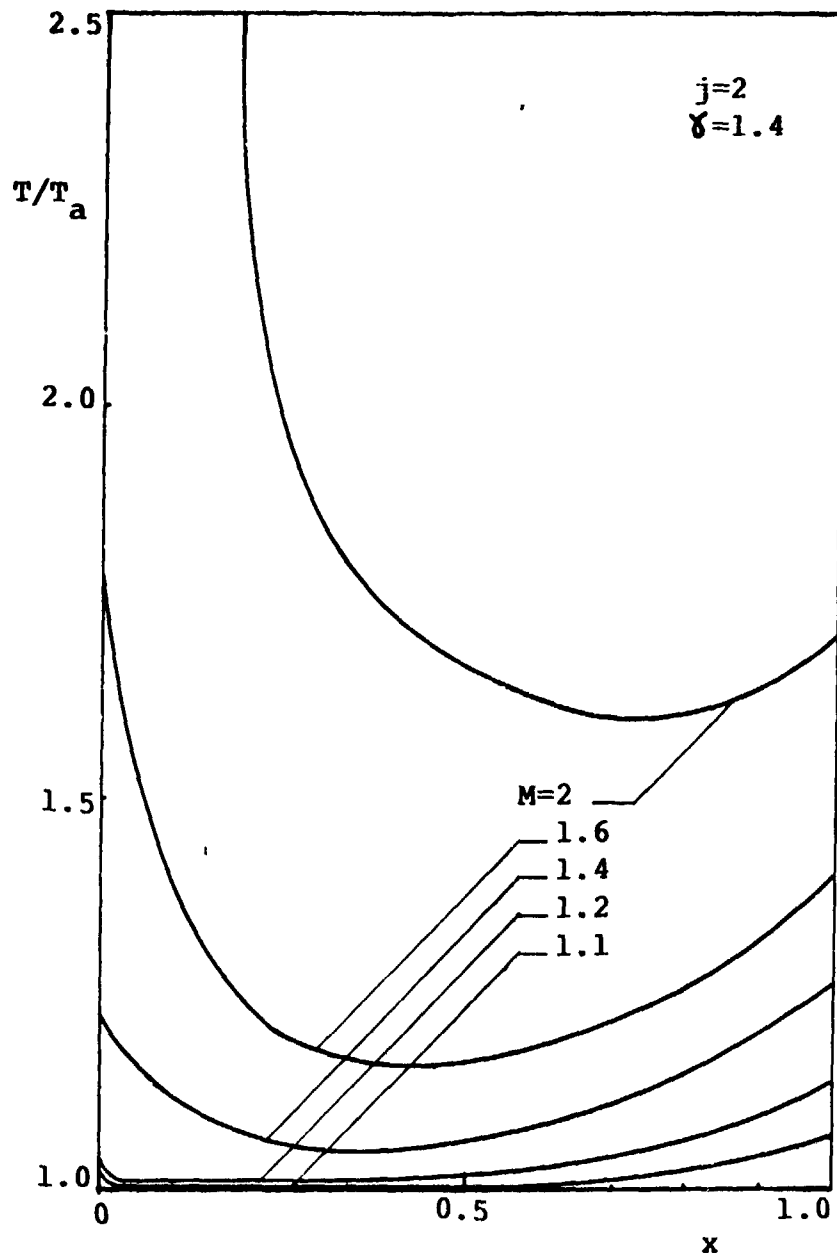
Fig. IV.2.14
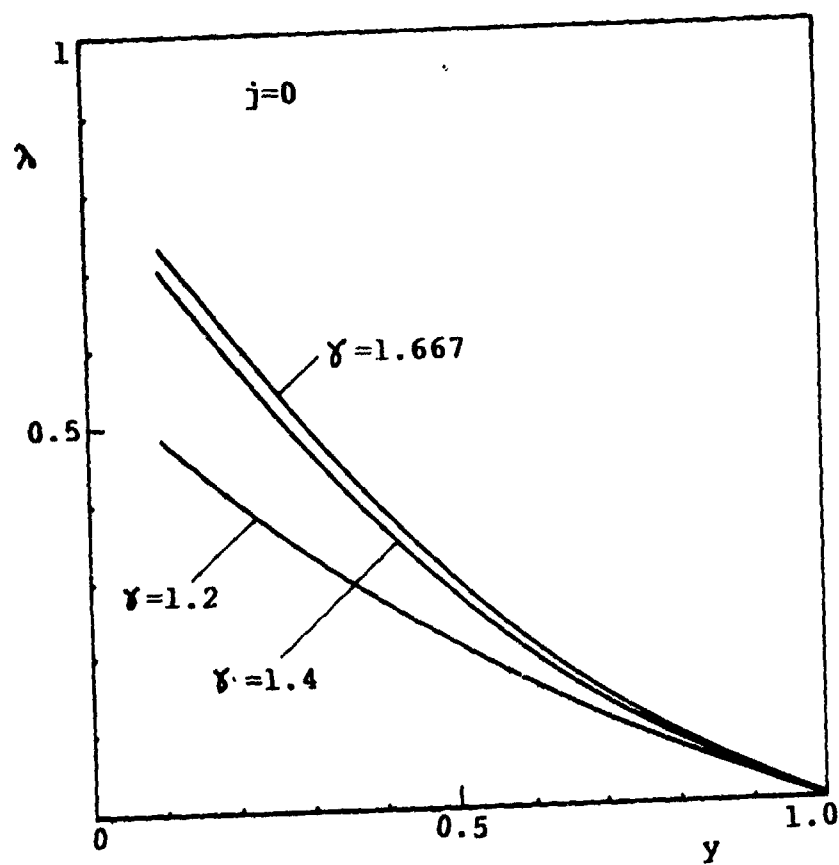
Fig   IV.2.15
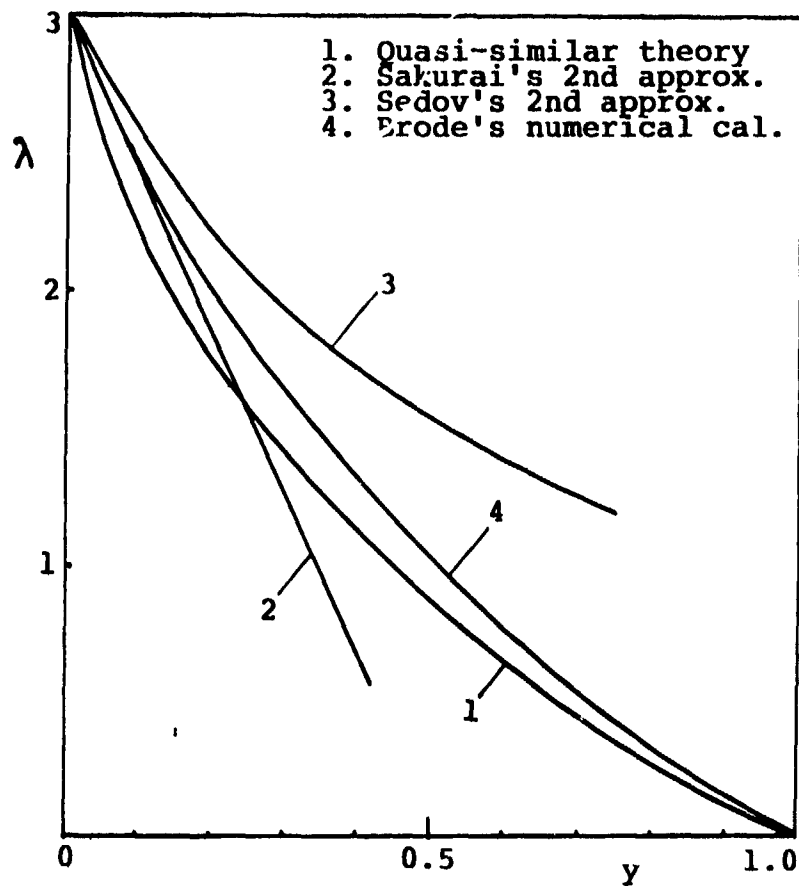
Fig. IV.2.16

IV.3 **BLAST WAVES IN REAL GASES***

i) Introduction

In the prevailing number of cases, with very few exceptions, despite the high
temperatures involved, the gaseous medium affected by blast waves has been
treated in the literature as a perfect gas with constant specific heats. How-
ever, due to the extremely high temperatures prevailing close to the centers
of blast waves, one should expect the excitation of all possible degrees of
freedom of the internal energy of the gas. One, therefore, should take into
account such phenomena as vibrational excitation, dissociation, electronic
exitation and ionization, as well as the influence of compressibility at high
pressures.

In this section, the real gas effects in adiabatic point explosions are taken
into account. For this purpose, an equilibrium thermodynamic analysis is car-
ried out in different ranges of pressures and temperatures. At high pressures,
the compressibility effect is considered using empirical formulae, such as the
Beattie-Bridgeman equation, as well as the concept of residual properties. At
high temperatures, on the other hand, quantum statistical thermodynamic con-
cepts are used to determine the degree of excitation leading to dissociation
and ionization of the gas. As formulated previously in Chapter II, the real
gas characteristics are expressed in terms of two thermodynamic properties.
These are a non-dimensional speed of sound factor, Γ , and the dimensionless
internal energy, σ . The geometry of the generated field, whether it is a
plane, cylindrical or spherical, is considered. The flow field is assumed to
be sourceless, inviscid, non-conducting and non-radiating.

ii) Problem Formulation

The general form of the governing equations, including real gas effects, are
given by Eqs. (II.20), (II.22) and (II.27). In the absence of all source
terms and when ρ_a is constant, these equations become

---

* This application is based on Ghonier (1975).

$$\frac{\partial \ln h}{\partial \ln \zeta} + \left(\frac{f}{x} - 1\right) \frac{\partial \ln h}{\partial \ln x} + \frac{f}{x}\left(\frac{\partial \ln f}{\partial \ln x} + j\right) = 0$$

$$-\frac{\lambda}{2} + \frac{\partial \ln f}{\partial \ln \zeta} + \left(\frac{f}{x} - 1\right)\frac{\partial \ln f}{\partial \ln x} + \frac{g}{hxf}\frac{\partial \ln g}{\partial \ln x} = 0 \qquad \text{(IV.3.1)}$$

and

$$-\lambda + \frac{\partial \ln g}{\partial \ln \zeta} + \left(\frac{f}{x} - 1\right)\frac{\partial \ln g}{\partial \ln x} - \Gamma\left[\frac{\partial \ln h}{\partial \ln \zeta} + \left(\frac{f}{x} - 1\right)\frac{\partial \ln h}{\partial \ln x}\right] = 0$$

where Γ is defined by Eq. (II.6) as

$$\Gamma \equiv \left(\frac{\partial \ln P}{\partial \ln \rho}\right)_s = \frac{\rho}{P} a^2 \qquad \text{(IV.3.2)}$$

The boundary conditions of the problem are given by Eqs. (II.54) - (II.56) which may be rewritten as follows

$$h_n = \frac{1}{1 - f_n}$$

$$g_n = f_n + \frac{y}{\Gamma_a} \qquad \text{(IV.3.3)}$$

and

$$\sigma_n = \sigma_a + \frac{y}{\Gamma_a} f_n + \frac{1}{2} f_n^2$$

where σ is defined in Eq. (II.15) as

$$\sigma \equiv \frac{e}{w_n^2} \qquad\qquad (IV.3.4)$$

The mass and energy integrals, Eqs. (II.65) and (II.73), in this case, are given by

$$J_1 = \int_0^1 h\, x^j\, dx = \frac{1}{j+1} \qquad\qquad (IV.3.5)$$

and

$$J_3 = \int_0^1 \left(\sigma + \frac{f^2}{2}\right) h\, x^j\, dx = \frac{\sigma}{j+1} + \frac{y}{\Gamma_a} \cdot \mathcal{J}^{-(j+1)} \qquad\qquad (IV.3.6)$$

while the decay coefficient λ has the form given by Eq. (II.76) as

$$\lambda = \frac{(j+1)\, J_3 - \sigma_a}{J_3 - y\, \dfrac{dJ_3}{dy}} \qquad\qquad (IV.3.7)$$

iii) Real Gas Analysis

As discussed previously, the real gas behaviour is expressed in terms of two thermodynamic properties, namely the internal energy σ and the speed of sound factor Γ . Thus, before attempting to solve the governing equations, these two quantities must be related to other thermodynamic variables in such a manner as to take into account the effects of compressibility and high temperature. To this end. the thermal equation of state may be expressed in the form of a perfect gas law that incorporates a compressibility deviation factor, Z_c , as well as a high temperature deviation factor, Z_r . Hence, one

may write an equation of state in the form

$$g = z_c \, z_r \, h \, \theta \qquad\qquad (IV.3.8)$$

where

$$\theta = \frac{RT}{W_n'} \qquad\qquad (IV.3.9)$$

with R being the gas constant.

One may then think of determining appropriate forms for the deviation factors z_c and z_r .

The compressibility deviation in the thermal equation of a perfect gas is often taken into consideration by means of semi-empirical relations. The other properties, like internal energy and specific heats, are then calculated using the concept of residual properties (Saad, 1960). These are the deviations in the real gas properties from those of the perfect gas due to the effect of specific volume or pressure on specific heats. For example, the internal energy may be expressed as $e = e^* + e_r$ where e^* is the internal energy of the perfect gas and it is a function of temperature only, e_r is the residual internal energy and it is a function of both temperature and specific volume, it is given by Rozhdestrenskii (1961) as

$$e_r = \int_{\infty}^{v} \left[T \left(\frac{\partial P}{\partial T} \right)_v - P \right] dv \qquad\qquad (IV.3.10)$$

where v is the specific volume. However, the thermal equation of state can be put in the form

$$P = T \, f_1(v) \left[1 - \frac{C}{v \, T^3} \right] + f_2(v) \qquad\qquad (IV.3.11)$$

where the functions f_1 and f_2 can be chosen to satisfy equations such as the Van der Waals' equation or the Beattie-Bridgeman equation and C is a constant. The above equation is found to fit the experimental data of many gases to within 0.5% accuracy over a wide range of pressures and temperatures.

The residual internal energy may now be calculated by differentiating Eq. (IV. 3.11) with respect to temperature and then carrying out the integration in Eq. (IV.3.10). This yields

$$e_r = \frac{3C}{T^2} \int_\infty^V \frac{f_1}{V} \, dV - \int_\infty^V f_2 \, dV \qquad (IV.3.12)$$

The residual specific heat C_{V_r} , difference in specific heats, $C_p - C_v$ and Γ may be obtained using similar relations as Eq. (IV.3.10), given by Saad (1969). With a similar procedure, one obtains the following expressions:

$$C_{V_r} = -\frac{6C}{T^3} \int_\infty^V \frac{f_1}{V} \, dV \qquad (IV.3.13)$$

$$C_p - C_v = \frac{-T\left(1 + \frac{2C}{VT^3}\right) f_1}{T f_1' \left(1 - \frac{C}{VT^3}\right) + f_2' + \frac{C}{VT^3} f_1} \qquad (IV.3.14)$$

and

$$\Gamma = -\gamma \left\{ \frac{VT}{P} \left[\left(1 - \frac{C}{VT^3}\right) f_1' + \frac{C}{V^2 T^3} f_1 \right] + \frac{V}{P} f_2' \right\} \qquad (IV.3.15)$$

where primes indicate differentiation with respect to V .

For the Beattie-Bridgeman equation, which is considered here, the expressions for f_1 and f_2 and their derivatives and integrations are

$$f_1 = \frac{R}{V^2}\left[V - B_0\left(1 - \frac{b}{V}\right)\right] \quad ; \quad f_2 = -\frac{A_0}{V^2}\left(1 - \frac{\bar{a}}{V}\right)$$

$$f_1' = \frac{-R}{V^2}\left[1 + \frac{B_0}{V}\left(1 - \frac{3b}{V}\right)\right] \quad ; \quad f_2' = \frac{A_0}{V^3}\left(2 - \frac{3\bar{a}}{V}\right)$$

and

$$\int \frac{f_1}{V}\, dV = \frac{-R}{V}\left[1 + \frac{B_0}{V^2}\left(\frac{1}{2} - \frac{b}{3V}\right)\right] \quad ; \quad \int f_2\, dV = \frac{A_0}{V}\left(1 - \frac{\bar{a}}{2V}\right)$$

(IV.3.16)

where A_0, $\bar{a}$, B_0, b and C are constants which may be determined experimentally for each gas.

To define the caloric equation ($e = e^+ + e_r$) completely, an expression for the perfect gas internal energy e^* should be given. De Broglie suggested that particles on the atomic scale behave in a wave-like manner, i.e. associated with each particle there is a wave with a certain frequency. The Schroedinger equation, using the above postulate, describes the motion of the particle in terms of its kinetic energy ϵ_{kin} and its potential energy ϵ_{pot} as follows:

$$\nabla^2 \Psi + \frac{8\pi^2 m}{h^2}\left(\epsilon - \epsilon_{pot}\right)\Psi = 0$$

(IV.3.17)

where Ψ and m are the displacement and the mass of the particle, respectively, while h is Planck's constant, and

$$\epsilon = \epsilon_{kin} + \epsilon_{pot}$$

Since the internal energy of the perfect gas molecule may be considered to be associated with translational, rotational and vibrational motion, in addition to that resulting from electronic excitation, the Schroedinger equation, Eq.

(IV.3.17), may be solved for each mode of motion independently to obtain the various available energy levels. These are given as

$$
\left.
\begin{aligned}
\epsilon_{trans} &= \frac{h^2}{8m}\left[(\frac{n_x}{a})^2 + (\frac{n_y}{b})^2 + (\frac{n_z}{c})^2\right] \\[2mm]
\epsilon_{rot} &= \frac{h^2}{8\pi^2 I}J(J+1) \\[2mm]
\epsilon_{vib} &= (n+\frac{1}{2})\, h\, \nu
\end{aligned}
\right\}
\qquad\text{(IV.3.18)}
$$

and

where n_x, n_y, n_z, J and n are the corresponding quantum numbers, I is the moment of inertia of the dumbell-shaped molecule and ν is the frequency of vibration of the harmonic oscillator. However, for a system of N particles, each single molecule can exist in any one of these energy levels, i.e. there is a certain distribution of molecules among available energy levels. This distribution is governed by the thermodynamic probability factor W. According to the Boltzmann distribution function (Saad, 1969), the distribution of particles in the most probable case, which is defined by $\delta W = 0$, is given by

$$
N_i = \frac{N}{Z}\, g_i\, e^{-\beta \epsilon_i} \qquad\text{(IV.3.19)}
$$

where Z is the partition function and is defined as

$$
Z \equiv \sum_i g_i\, e^{-\beta \epsilon_i} \qquad\text{(IV.3.20)}
$$

g_i is the degeneracy (multiplicity) of energy levels with the same value of energy

and $\beta \equiv \dfrac{1}{kT}$ with k being the Boltzmann constant.

The internal energy for N molecules is $e^* = \sum_i N_i \epsilon_i$ and since N_i is given by Eq. (IV.3.19), the caloric equation is put in the form

$$e^* = \frac{N}{Z} \sum_i g_i \epsilon_i e^{-\beta \epsilon_i} = N k T^2 \left(\frac{\partial \ln Z}{\partial T}\right)_V \qquad (\text{IV}.3.21)$$

which is evident since $\frac{\partial Z}{\partial T}\Big)_V = \frac{1}{kT^2} \sum_i g_i \epsilon_i e^{-\beta \epsilon_i}$.

The value of the partition function may be evaluated using Eqs. (IV.3.18) and (IV.3.20), after the summation sign is approximated by an integration sign, since the separation between successive energy levels is small (Lee et al., 1963). The integration yields:

$$Z_{trans} = V \left(\frac{2\pi m k T}{h^2}\right)^{3/2}$$

$$Z_{rot} = \begin{cases} 1 + 3 e^{-2\frac{\theta_r}{T}} + 5 e^{-6\frac{\theta_r}{T}} + \cdots & T < \theta_r \\ \\ \frac{T}{\theta_r}\left(1 + \frac{1}{3}\frac{\theta_r}{T} + \frac{1}{15}\left(\frac{\theta_r}{T}\right)^2 + \cdots\right) & T > \theta_r \end{cases} \qquad (\text{IV}.3.22)$$

and

$$Z_{vib} = \frac{e^{-\frac{T_v}{2T}}}{1 - e^{-T_v/T}}$$

where θ_r is the characteristic temperature of rotation

$$\theta_r \equiv \frac{h^2}{8\pi^2 I k}$$

T_V is the characteristic temperature of vibration

$$T_V \equiv \frac{h^2 \nu}{k}$$

Now, according to the type of the molecules, the partition function and the internal energy of the perfect gas may be evaluated.

For a monatomic gas, the molecules have only translational motion, accordingly

$$Z_{mon} = V \left(\frac{2 \pi m k T}{h^2} \right)^{3/2}$$

and

$$e_{mon} = \frac{3}{2} k N T$$

(IV.3.23)

On the other hand, for a diatomic gas, the molecules have translational, rotational and vibrational motion. From Eqs. (IV.3.20) and (IV.3.21) one obtains

$$Z_{dia} = V \left(\frac{2 \pi m k T}{h^2} \right)^{3/2} \frac{T}{\theta_r} \left(\frac{e^{-\frac{T_V}{2T}}}{1 - e^{-\frac{T_V}{T}}} \right)$$

and

$$e_{dia} = \frac{5}{2} k N T + N k T_V \left[\frac{1}{2} + \frac{1}{(e^{T_V/T} - 1)} \right]$$

(IV.3.24)

It is to be noted that Eq. (IV.3.24) is valid for $T > \theta_r$, which is the case of most gases at $T > 100°K$.

The deviation factor Z_c is thus obtained from Eq. (IV.3.11) and Eqs. (IV.3.16) in the following form

$$
Z_c = \left[1 - B_o^* h (1 - b^* h) \right] \left[1 - c^* h \left(\frac{y}{\theta} \right)^3 \right]
$$
$$
- A_o^* h \frac{y}{\theta} (1 - \bar{a}^* h)
$$

where

$$
A_o^* \equiv \frac{A_o \, \rho_a}{\Gamma_a R T_a} \qquad ; \qquad B_o^* \equiv B_o \, \rho_a
$$

$$
\bar{a}_o^* \equiv \bar{a} \, \rho_a \qquad ; \qquad b^* \equiv b \, \rho_a
$$

and

$$
c^* \equiv \frac{c \, \rho_a}{(\Gamma_a T_a)^3}
$$

(IV.3.25)

The high temperature deviation factor, Z_r, includes, of course, the effects of both dissociation and ionization of gases.

During the process of dissociation, the composition of a diatomic gas A_2 is given by

$$
A_2 = (1 - \alpha_d) \, A_2 + 2 \, \alpha_d \, A
$$

(IV.3.26)

where α_d is the degree of dissociation. It is defined as the ratio of the number of dissociated molecules to the initial number of molecules A_2. The total number of molecules at any instant is given from Eq. (IV.3.26) as $(1 + \alpha_d)$ per molecule of A_2. Considering each constituent as a perfect gas, the thermal equation of the dissociating gas may be written in the form

$$P = (1 + \alpha_d) \, \wp R_2 T \tag{IV.3.27}$$

where R_2 is the gas constant of A_2 .

To predict the equilibrium composition of the gas, or the value of α_d as a function of pressure and temperature, the law of mass action, Van't Hoff's equation, is applied. In its classical form it is given as

$$\frac{d \ln K_P}{dT} = \frac{Q_P}{RT^2} \tag{IV.3.28}$$

where K_P is the equilibrium constant, and Q_P is the heat of reaction at constant pressure. These are given by

$$Q_P = \sum \left[(\nu \, i_i)_p - (\nu \, i_i)_r \right] \quad \text{and} \quad K_P = \frac{\prod_p p^\nu}{\prod_r p^\nu}$$

where ν is the number of molecules and i_i is the enthalpy. Subscripts P and r denote products and reactants, respectively.

The partial pressure of each constituent in Eq. (IV.3.26) is given as

$$P_A = \frac{2 \alpha_d}{1 + \alpha_d} \cdot P$$

and

$$P_{A_2} = \frac{1 - \alpha_d}{1 + \alpha_d} \, P$$

$$\tag{IV.3.29}$$

Then the equilibrium constant may be calculated from Eqs. (IV.3.28) and

(IV.3.29) as

$$K_p = \frac{4 \, \alpha_d^2}{1 - \alpha_d^2} \, P \qquad\qquad (IV.3.30)$$

When the condition of statistical equilibrium is applied to a reacting system, the statistical form of the law of mass action is obtained in the form

$$K_p = \frac{N}{P} \, \frac{\pi \, Z_P}{\pi \, Z_r} \, exp \left(\frac{-e_{rec}}{kT} \right) \qquad\qquad (IV.3.31)$$

where e_{rec} is the change in the ground state energy during the reaction. Equations (IV.3.23) and (IV.3.24) represent the partition functions of the reactant and the product of dissociation, respectively. Hence, substituting in Eq. (IV.3.31), one obtains the equilibrium constant in the form (Grossman, 1969),

$$K_{p_d} = 2 \, k \, \theta_r \left(\frac{\pi \, m_A \, k}{h^2} \right)^{3/2} T^{3/2} \left[1 - exp \left(- \frac{T_v}{T} \right) \right] exp \left(\frac{-e_d}{kT} \right)$$
$$(IV.3.32)$$

where e_d is the dissociation energy.

The caloric equation of a dissociating gas is given as

$$e = (1 - \alpha_d) \, e_{A_2} + 2 \, \alpha_d \, e_A + \alpha_d \, e_d \qquad\qquad (IV.3.33)$$

Differentiating the above equation with respect to T , one obtains the specific heat at constant volume, C_v , as

$$C_V = (1 - \alpha_d) \, C_{V_{A_2}} + 2 \, \alpha_d \, C_{V_A} + (2 \, e_A - e_{A_2} + e_d)(\frac{\partial \alpha_d}{\partial T})_V \qquad \text{(IV.3.34)}$$

The value of $(\frac{\partial \alpha_d}{\partial T})_V$ is obtained by differentiating Eq. (IV.3.30) with respect to temperature and using Eq. (IV.3.27) to substitute for P. After some algebraic manipulations, one obtains

$$(\frac{\partial \alpha_d}{\partial T})_V = \frac{\alpha_d}{T} (\frac{1 - \alpha_d}{2 - \alpha_d}) \left[\frac{3}{2} + \frac{T_d}{T} - \frac{T_V}{T} \frac{1}{(e^{-T_V/T} - 1)} \right] \qquad \text{(IV.3.35)}$$

where

$$T_d = \frac{e_d}{k}$$

Using the same procedure, the specific heat at constant pressure, C_P, is obtained as

$$\left. \begin{array}{l} C_P = (1 - \alpha_d) \, C_{P_{A_2}} + 2 \, \alpha_d \, C_{P_A} + (2 \, i_A' - i_{A_2}' + e_d)(\frac{\partial \alpha_d}{\partial T})_P \\ \\ \text{with} \\ \\ (\frac{\partial \alpha_d}{\partial T})_P = \frac{\alpha_d}{2T} (1 - \alpha_d^2) \left[\frac{5}{2} + \frac{T_d}{T} - \frac{T_V}{T} \frac{1}{(e^{-T_V/T} - 1)} \right] \end{array} \right\} \qquad \text{(IV.3.36)}$$

Finally, the isentropic compressibility, or the speed of sound factor, Γ, is obtained by differentiating Eq. (IV.3.27) with respect to P and substituting in Eq. (IV.3.2). It is found to equal

$$\Gamma = \frac{C_P}{C_V} \cdot \frac{2}{2 + \alpha_d - \alpha_d^2} \qquad \text{(IV.3.37)}$$

Thus, Eq. (IV.3.30) and (IV.3.31) define the value of α_d , and Eqs. (IV.3.34), (IV.3.36) and (IV.3.37) determine the value of Γ .

Ionization is treated very similar to dissociation from the point of view of thermodynamics. The composition of the ionized gas A at any temperature is given by

$$A = (1 - \alpha_i) A + \alpha_i A^+ + \alpha_i e^- \qquad \text{(IV.3.38)}$$

where α_i is the degree of ionization (subscript i = 1,2 for the first and second ionizations, respectively) and e^- denotes a free electron. It is defined as the ratio of the number of ionized atoms A^+ to the original number of atoms A . The thermal equation can be written in the form

$$P = (1 + \alpha_i) \, \rho R T \qquad \text{(IV.3.39)}$$

where R is the gas constant of A .

The equilibrium constant of ionization is determined by substituting from Eq. (IV.3.23) for Z into Eq. (IV.3.31), realizing that all plasma constituents, in this case, can be treated as monatomic gases. Thus, one obtains

$$K_{P_i} = k \left(\frac{2 \pi m_e \, k}{h} \right)^{3/2} T^{5/2} \frac{z_{e_{A^+}} \, z_{e_{e^-}}}{z_{e_A}} \exp \left(- \frac{e_i}{kT} \right) \qquad \text{(IV.3.40)}$$

where e_i is the ionization energy

m_e is the electronic mass

$z_{e_{e^-}}$ is the electronic partition function of free electrons = 2

z_{e_A} and $z_{e_{A^+}}$ are the partition functions of electronic excitation of
$\qquad A$ and A^+ respectively.

The partial pressure of each constituent is evaluated in terms of α_i using Eq. (IV.3.38), as previously done for dissociation. Substituting in Eq. (IV.3.28), one obtains

$$K_{p_i} = \frac{\alpha_i^2}{1 - \alpha_i^2} \, P \tag{IV.3.41}$$

Equations (IV.3.40) and (IV.3.41) give the equilibrium composition of the ionized gas in terms of its pressure and temperature. The resulting equation is the Saha Equation (Benson, 1967).

The internal energy of the ionized gas is given by

$$e = (1 - \alpha_i) \, e_A + \alpha_i \, e_{A^+} + \alpha_i \, e_{e^-} + e_{elec}$$

and, since all constituents are treated as monatomic gases

$$e = (1 + \alpha_i)(\tfrac{3}{2}) \, R_A T + \alpha_i \, e_i + e_{elec} \tag{IV.3.42}$$

The value of C_v, C_p and Γ are obtained in a similar manner as in dissociation, thus one gets

$$\left. \begin{array}{l} C_v = \tfrac{3}{2} R_A (1 + \alpha_i) + (\tfrac{3}{2} R_A T + e_i)\left(\dfrac{\partial \alpha_i}{\partial T}\right)_v \\[4mm] \text{and} \\[4mm] C_p = \tfrac{5}{2} R_A (1 + \alpha_i) + (\tfrac{5}{2} R_A T + e_i)\left(\dfrac{\partial \alpha_i}{\partial T}\right)_p \end{array} \right\} \tag{IV.3.43}$$

where

$$\frac{\partial \alpha_i}{\partial T}\bigg)_v = \frac{\alpha_i (1-\alpha_i)}{T (2-\alpha_i)}\left(\frac{3}{2} + \frac{T_i}{T}\right)$$

and

$$\left(\frac{\partial \alpha_i}{\partial T}\right)_p = \frac{\alpha_i}{2T}(1-\alpha_i^2)\left(\frac{5}{2} + \frac{T_i}{T}\right)$$

(IV.3.44)

with

$$T_i = \frac{e_i}{k}$$

while

$$\Gamma = \frac{c_p}{c_v} \cdot \frac{2}{2+\alpha_i - \alpha_i^2}$$

(IV.3.45)

The case of multiple ionization is obtained directly by modifying the set of equations of single ionization. For example, the Saha Equation may be extended (Camble, 1963) for the nth electron to yield

$$\frac{\alpha_n^2}{1-\alpha_n^2} = 2k\left(\frac{2\pi m_e k}{h^2}\right)^{3/2} \cdot \frac{z_{e_n}}{z_{e_{n-1}}} \cdot \frac{T^{5/2}}{P} \cdot exp\left(-\frac{e_{in}}{kT}\right)$$

(IV.46)

Similarly, Eqs. (IV.3.42) - (IV.3.45) may also be extended by substituting α_n to replace α_i .

Since the electron motion around the nucleus is very complicated, the Schroe-

dinger equation is not solved to obtain electronic energy levels. However,
since the separation between successive energy levels is high, Z may be
expanded in the form

$$Z_e = g_0 + g_1 e^{-\frac{\epsilon_1}{kT}} + g_2 e^{-\frac{\epsilon_2}{kT}} + \cdots \cdots \qquad (IV.3.47)$$

where both the degeneracies g_i and the energies ϵ_i are determined experimen-
tally from spectroscopic data (Rozhdestvenskii et al., 1961).

To determine the electronic internal energy and specific heat, Eq. (IV.3.47)
is differentiated twice. It yields

$$Z_e' = \sum_m g_m \frac{T_m}{T^2} e^{-\frac{\epsilon_m}{kT}}$$

and

$$Z_e'' = \sum_m (\frac{T_m}{T} - 2) g_m \frac{T_m}{T^3} e^{-\frac{\epsilon_m}{kT}}$$

$$(IV.3.48)$$

where primes denote differentiation with respect to T.

Substituting from Eq. (IV.3.48) in Eq. (IV.3.21), the internal energy is ob-
tained. However, by differentiating Eq. (IV.3.21), C_v is obtained in terms
of Z_e, Z_e' and Z_e'' in the form

$$C_{v_e} = RT^2 \left(\frac{Z_e Z_e'' - Z_e'^2}{Z_e^2} \right) + 2RT \frac{Z_e'}{Z_e} \qquad (IV.3.49)$$

The main difficulty in obtaining solutions with the series expressed in Eq.
(IV.3.47) is that it is not a finite sum. The terms approach infinity as the

energy level ϵ_i approaches a constant value, namely the ionization energy. However, a two-term approximation is used here to evaluate the thermodynamic properties.

The temperature deviation factor, Z_r, is then obtained from Eq. (IV.3.27) and (IV.3.39) for a double ionized gas as

$$Z_r = 1 + \alpha_d \left[1 + 2\alpha_1 \left(1 + 2\alpha_2 \right) \right] \tag{IV.3.50}$$

where

$$\alpha \equiv \sqrt{\frac{K_P^*}{1 + K_P^*}}$$

The non-dimensional equilibrium constant K_P^* is obtained from Eqs. (IV.3.32) and (IV.3.46), after substituting for the dimensionless variables. They are given as

$$K_{P_d}^* = \frac{K_{P_d}}{4P} = C_d \frac{\theta^{1.5}}{g \, y^{0.5}} \left[1 - exp\left(-\frac{\theta_v y}{\theta} \right) \right] exp\left(-\frac{\theta_d y}{\theta} \right)$$

and

$$K_{P_i}^* = \frac{K_{P_i}}{P} = C_i \frac{\theta^{2.5}}{g \, y^{1.5}} \frac{Z_{e_{A^+}}}{Z_{e_A}} \, exp\left(-\frac{\theta_i y}{\theta} \right)$$

where

$$C_d = 2 \, k \, \theta_r \left(\frac{\pi \, m_A \, k}{h^2} \right)^{1.5} \frac{T_a \sqrt{T_a \, T_a}}{4 P_a}$$

and

$$C_i = 2 \left(\frac{2 \pi m_e k}{\hbar^2} \right)^{1.5} k \quad \frac{T_a \sqrt{T_a \, T_a}}{P_a} = 6.5 \times 10^{-7} \frac{T_a \sqrt{T_a \, T_a}}{P_a}$$

The pressure P_a is in atm. and the temperature T is in °K.

The total internal energy of a gas may be expressed as the summation of the contribution of various effects, i.e.

$$e = e^* + e_{comp} + e_{diss} + e_{ion} + e_{elec}$$

that is a sum of the ideal gas internal energy and those due to compressibility, dissociation, ionization and electronic excitation, respectively.

Therefore, the internal energy may take the following non-dimensional form

$$\sigma = (1 - \alpha_d)(\sigma_2 + \sigma_{comp} + \sigma_{e_2}) + \alpha_d \theta_d y$$

$$+ 2 \alpha_d \left[\sigma_1 + (1 - \alpha_1) \sigma_{e_1} + \alpha_1 \theta_1 y \right.$$

$$\left. + \alpha_1 \left\{ (1 + \alpha_2) \sigma_1 + (1 - \alpha_2) \sigma_{e^+} + \alpha_2 (\theta_2 y + \sigma_{e^{++}}) \right\} \right]$$

$$(IV.3.51)$$

where σ 's are obtained from Eqs. (IV.3.10), (IV.3.23), (IV.3.24), (IV.3.33) and (IV.3.42) as

$$\sigma_1 = 1.5\,\theta$$

$$\sigma_2 = 2.5\,\theta + \theta_v \left\{ 0.5 + \frac{1}{[\exp(\frac{\theta_v y}{\theta}) - 1]} \right\}$$

and

$$\left. \begin{array}{l} \sigma_{comp} = -6\,c^* h \left(\frac{y}{\theta}\right)^3 \theta \left\{ 1 + B_o^* h \left(0.5 - \frac{b^*}{3} h\right) \right\} \\[2mm] \qquad\quad - A_o^* h\, y \left(1 - \frac{\bar{a}^*}{2} h\right) \end{array} \right\} \qquad \text{(IV.3.52)}$$

where

$$\theta_v \equiv \frac{T_v}{\Gamma_a T_a} \quad ; \quad \theta_d \equiv \frac{T_d}{\Gamma_a T_a} \quad ; \quad \theta_i \equiv \frac{T_i}{\Gamma_a T_a}$$

and

$$\sigma_e = \theta^2 \frac{Z_e'}{Z_e}$$

while both Z_e and Z_e' are given in Eqs. (IV.3.47) and (IV.3.48).

The non-dimensional speed of sound factor Γ, which is defined in Eq. (IV.3.2), can be put in the form

$$\Gamma \equiv \frac{\partial \ln P}{\partial \ln \rho}\Big)_s = \gamma \left(\frac{\partial \ln P}{\partial \ln \rho}\right)_T \qquad \text{(IV.3.53)}$$

The value of γ is given by C_p / C_v, which are obtained from Eqs. (IV.3.34),

(IV.3.36) and (IV.3.43). The composition of the gas A_2 is given at any instant by Eqs. (IV.3.26) and (IV.3.38) in the following form

$$A_2 = (1-\alpha_d) A_2 + 2\alpha_d \Big\{ (1-\alpha_1) A + \alpha_1 e^- + \alpha_1 \big[(1-\alpha_2) A^+$$

$$+ \alpha_2 A^{++} + \alpha_2 e^- \big] \Big\} \qquad (IV.3.54)$$

For such a gas, C_V is given by

$$C_V = (1-\alpha_d) C_{V_2} + 2\alpha_d \Big\{ C_{V_1} + (1-\alpha_1) C_{V_{e^+}} + \alpha_1 \big[(1+\alpha_2) C_{V_1}$$

$$+ (1-\alpha_2) C_{V_{e^+}} + \alpha_2 C_{V_{e^{++}}} \big] \Big\} + \left(\frac{\partial \alpha_d}{\partial T} \right)_V \big[-\sigma_2 + \theta_d y$$

$$+ 2 \big\{ \sigma_1 + (1-\alpha_1) \sigma_{e^+} + \alpha_1 \theta_1 y + \alpha_1 \big((1+\alpha_2) \sigma_1$$

$$+ (1-\alpha_2) \sigma_{e^+} + \alpha_2 (\sigma_{e^{++}} + \theta_2 y) \big) \big\} \big] + 2\alpha_d \Big\{ \left(\frac{\partial \alpha_1}{\partial T} \right)_V \big[-\sigma_1$$

$$+ \theta_1 y + (1+\alpha_2) \sigma_1 + (1-\alpha_2) \sigma_{e^+} + \alpha_2 (\sigma_{e^{++}} + \theta_2 y) \big] \Big\}$$

$$+ \alpha_1 \Big\{ \left(\frac{\partial \alpha_2}{\partial T} \right)_V \big[\sigma_1 - \sigma_{e^+} + \sigma_{e^{++}} + \theta_2 y \big] \Big\} \qquad (IV.3.55)$$

The electronic specific heats C_{V_e} are given in Eq. (IV.3.49), while $\left(\frac{\partial \alpha}{\partial T} \right)_V$

are expressed in Eqs. (IV.3.35) and (IV.3.44).

Since various energy modes are excited subsequently, their contribution on

$(\frac{\partial \ln P}{\partial \ln \rho})_T$ may be expressed as

$$\left(\frac{\partial \ln P}{\partial \ln \rho}\right)_T = \left(\frac{\partial \ln P}{\partial \ln \rho}\right)_{comp} \prod_m \frac{2}{2 + \alpha_m + \alpha_m^2} \tag{IV.3.56}$$

where $m \leqq d$, 1 and 2.

The term $(\frac{\partial \ln P}{\partial \ln \rho})_{comp}$ may be obtained with the aid of Eqs. (IV.3.9) and (IV.3.25) which yields

$$\left(\frac{\partial \ln P}{\partial \ln \rho}\right)_{comp} = -\frac{\theta}{gh}\left[1 - C^* h \left(\frac{y}{\theta}\right)^3\right]\left[1 - B_o^*(1 - b^* h)\right]$$

$$+ A_o^* h^2 \frac{y}{g}\left(1 - \frac{\bar{a}^* h}{2}\right) \tag{IV.3.57}$$

iv) Solution

a) The Self-Similar Solution

Since self-similarity reduces appreciably the mathematical complications of the solution, it has always been the first step in seeking a solution for blast wave problems. The utilized equation of state of the flowing gas should also satisfy the conditions of self-similarity, i.e. it should not contain any dimensional constant whose dimensions are dependent on pressure. As previously suggested by Korobeinikov et.al. (1961) and Sedov (1957), its general form is

$$e = P \phi(\rho) \tag{IV.3.58}$$

where ϕ is a function of density only. The corresponding thermal equation may be derived as follows: from the first law of thermodynamics

$$T\,ds = de + P\,dv$$

thus

$$ds = \frac{1}{T}\left[\left(\frac{\partial e}{\partial \rho}\right)_P d\rho + \left(\frac{\partial e}{\partial P}\right)_\rho dP\right] - \frac{1}{T} \cdot \frac{P}{\rho^2}\,d\rho$$

and since $s = s(P, \rho)$, then

$$ds = \left(\frac{\partial s}{\partial P}\right)_\rho dP + \left(\frac{\partial s}{\partial \rho}\right)_P d\rho$$

Comparing the above two expressions and using Eq. (IV.3.57) to express the differentials of the internal energy in terms of ϕ and some thermodynamic identities (Thompson, 1972), one obtains

$$\frac{1}{\rho^2}\left(\frac{\partial \rho}{\partial T}\right)_s = \frac{1}{T}\,\phi$$

and

$$-\frac{1}{\rho^2}\left(\frac{\partial P}{\partial T}\right)_s = \frac{P}{T}\left(\phi' - \frac{1}{\rho^2}\right)$$

(IV.3.59)

where

$$\phi' = \frac{d\phi}{d\rho}$$

The above two equations are transformed into two ordinary differential equations in an isentropic process. The above two isentropic relations of the

gas obeying Eq. (IV.3.58) are obtained by integrating them as

$$T \exp\left(-\int \frac{d\rho}{\rho^2 \phi}\right) = C_1(S)$$

and

$$P\phi \exp\left(-\int \frac{d\rho}{\rho^2 \phi}\right) = C_2(S)$$

(IV.3.60)

Since one can put $C_1 = \Psi(C_2)$, the general thermal equation for a gas obeying the self-similarity restrictions is obtained as

$$T = \exp\left(\int \frac{d\rho}{\rho^2 \phi}\right) \cdot \Psi\left(P\phi \exp\left(\int -\frac{d\rho}{\rho^2 \phi}\right)\right)$$

(IV.3.61)

A special, but important, form of Eq. (IV.3.61) may be obtained if Ψ is expressed as a linear function of its arguments, yielding

$$T = B P \phi(\rho)$$

(IV.3.62)

where B is a constant.

The Clausius equation of state is suggested to represent the gas behavior at high pressures and temperatures (Thompson, 1972), since it takes into account the effect of the volume occupied by the molecules. As it satisfies the self-similar conditions, it may be used here. This equation may be written in the form

$$P = RT\left(\frac{\rho}{1 - \beta\rho}\right)$$

(IV.3.63)

where β is a constant.

For fluids described by Eq. (IV.3.63), one has $e = e(T)$ only, just as the ideal gas, and that $R = C_v(\gamma-1)$. Thus

$$e = \frac{R}{\gamma - 1} \cdot T \qquad \text{(IV.3.64)}$$

with γ being a mean value for the specific heat ratio.

Comparing Eqs. (IV.3.63) and (IV.3.64) with Eq. (IV.3.58), the function ϕ is found to be

$$\phi = \frac{1}{\rho_a(\gamma-1)} \cdot \frac{1 - \beta^* h}{h} \qquad \text{(IV.3.65)}$$

where

$$\beta^* \equiv \rho_a \beta$$

The non-dimensional speed of sound factor, Γ, is found by substituting in Eq. (IV.3.2) from Eq. (IV.3.58) and knowing that

$$\left(\frac{\partial P}{\partial \rho}\right)_s = -\frac{\frac{\partial e}{\partial \rho}\big)_P - P/\rho^2}{\left(\frac{\partial e}{\partial P}\right)_\rho}$$

then

$$\Gamma = -\frac{\rho}{P}\left(\frac{P\phi' - P/\rho^2}{\phi}\right) = \frac{1 - \rho^2\phi'}{\rho\phi} \qquad \text{(IV.3.66)}$$

which means that Γ is a function of density only.

Substituting from Eq. (IV.3.65) into Eq. (IV.3.66), one gets

$$\Gamma = \frac{\gamma}{1 - \beta^* h} \tag{IV.3.67}$$

which reduces to $\Gamma = \gamma$ for a perfect gas ($\beta^* = 0$).

The governing equations, Eqs. (IV.3.1), in the case of strong explosion condition, $y = 0$, are reduced to

$$(f-x)\frac{dh}{dx} + h\left(\frac{df}{dx} + j\frac{f}{x}\right) = 0$$

$$(f-x)\frac{df}{dx} + \frac{1}{h}\cdot\frac{dg}{dx} - \frac{\lambda}{2}f = 0$$

and

$$(f-x)\frac{dg}{dx} + \Gamma\left(\frac{df}{dx} + j\frac{f}{x}\right)g - \lambda g = 0 \tag{IV.3.68}$$

The decay coefficient, Eq. (IV.3.7), will take the simple form

$$\lambda = j + 1 \tag{IV.3.69}$$

Equations (IV.3.68) may be rewritten in their autonomous form as

$$\frac{df}{dx} = \frac{\frac{j\gamma g f}{x(1-\beta^* h)} + f(f-x)h\frac{(j+1)}{2} - (j+1)g}{h(f-x)^2 - \frac{\gamma g}{(1-\beta^* h)}}$$

$$\frac{dh}{dx} = -\frac{h}{(f-x)}\left(\frac{df}{dx} + j\frac{f}{x}\right) \tag{IV.3.70}$$

and

$$\frac{dg}{dx} = -h\left[(f-x)\frac{df}{dx} - \frac{(j+1)}{2}f\right]$$

The boundary conditions of the self-similar flow are deduced directly from Eqs. (IV.3.3), when applying the condition of $y = 0$ and consequently $\sigma_a = 0$, one obtains

$$f_n = 1 - \frac{1}{h_n}$$

$$g_n = f_n = 1 - \frac{1}{h_n}$$

and

$$\sigma_n = \frac{1}{2} f_n^2 = \frac{1}{2}\left(\frac{h_n - 1}{h_n}\right)^2$$

(IV.3.71)

The value of h_n is evaluated from the last of Eqs. (IV.3.71) when σ_n is substituted by $\rho_a g_n \phi_n$, then after some algebraic manipulations, one gets

$$h_n = \frac{\gamma + 1}{\gamma - 1 + 2\beta^*}$$

and

$$f_n = g_n = 2\left(\frac{1 - \beta^*}{\gamma + 1}\right)$$

(IV.3.72)

Since the boundary conditions depend on β^*, they depend on the initial conditions represented by ρ_a and hence, the whole solution is expected to depend on the initial conditions. However, it should be noted here that the value of β^* for most gases (Saad, 1969) is in the order of 0.002 at the standard atmospheric conditions. Thus, its effect on the deviation of the gas, and consequently on the whole solution, is expected to be negligible. On the other hand, for moderate values of initial density ρ_a, the problem is greatly affected by the deviation factor β^* since it increases with ρ_a.

The governing equations for the self-similar solution, Eqs. (IV.3.70) which are subject to the boundary conditions, Eqs. (IV.3.72), are then integrated numerically.

b) The Quasi-Self-Similar Solution

Once the self-similar solution is established, one can then proceed to obtain the non-self-similar solution. Before attempting to solve the governing equations, Eqs. (IV.3.1), in order to obtain the flow field structure, the jump conditions across the shock have to be determined. The Rankine-Hugoniot equation is found by substituting for σ from Eq. (IV.3.51) into the last of Eqs. (IV.3.3) as

$$\sigma(g_n, h_n) - \sigma_a = \frac{y}{\Gamma_a^2}\left(1 - \frac{1}{h_n}\right) + \frac{1}{2}\left(1 - \frac{1}{h_n}\right)^2 \qquad \text{(IV.3.73)}$$

The solution procedure may be outlined as follows

a) A trial value of h_n is assumed. The corresponding value of the perfect gas, Eq. (II.89), at the same front Mach number may be used.

b) The value of g_n is calculated from Eq. (IV.3.3) as

$$g_n = \frac{y}{\Gamma_a} + \left(1 - \frac{1}{h_n}\right)$$

where Γ_a may be taken as γ, since the undisturbed medium is considered as

a perfect gas.

c) Equation (IV.3.8), the thermal equation, is solved numerically with the aid of Eqs. (IV.3.25) and (IV.3.50), for the temperature θ_n. The false position method is used to minimize the number of trials needed to satisfy Eq. (IV.3.8).

d) The values of g_n, h_n and θ_n are substituted back in the Rankine-Hugoniot equation, Eq. (IV.3.73). If it is satisfied to a certain permissible error ϵ, the assumed value of h_n is taken as the correct one. If not, another trial value is assumed in the direction which reduces the error and the whole precedure is repeated. Here, also, the false position method may be used to speed up the convergence of the solution.

This method is straight-forward and it gives for any values of σ_a and Γ_a the properties behind the shock wave up to any desired degree of accuracy. In general, the equations are convergent and the number of trials do not exceed 5.

Obtaining the boundary conditions, one may then numerically calculate the derivatives of the gasdynamic variables with respect to ζ, which are equal to their values at the front as stated by the quasi-similar technique. The Newton finite difference for differentiation is used with six points of M around the value of M at which the field is calculated.

The computational procedure may be put in a step-wise manner as follows:

a) For a specified shock Mach number and initial condition, the boundary conditions and their derivatives are calculated numerically.

b) A trial value of λ is assumed and the integration of Eqs. (IV.3.1) is carried out numerically with a constant step size $\Delta x = 0.01$. The temperature θ is calculated at every step in the integration using a subroutine which applies the false position method to solve Eq. (IV.3.8) for any values of g and h.

c) The integration is stopped when either of the singularities $x = f$ or $x = f \pm \sqrt{\frac{\Gamma g}{h}}$ is encountered. According to the type of singularity, λ is decreased or increased.

d) When the value of λ is sufficient to carry out the integration to a

point near the center of symmetry, $\overline{x} \cong 0.03$, the velocity profile is extra-polated to check the value of f at the center, f_o , i.e. $f(o,y)$. The correct solution is obtained when $f(o,y) = 0$, Eq. (II.112); however, if $f_o < \mathcal{E}$ where $\mathcal{E}$ is a small error, the corresponding value of λ is accepted. If f_o $> \mathcal{E}$, the integration is repeated for values of λ around this value and a curve between λ and f_o is drawn, the correct value of λ is that correspon-ding to $f_o = 0$ on the curve.

It is to be noted that the quasi-similarity approximation does not conserve global mass, see Sec. (IV.1), i.e. the density profiles calculated using this method do not satisfy the mass integral, Eq. (IV.3.5). On the other hand, the velocity profiles at moderate Mach numbers are not accurate around the center of symmetry since in this region the particle velocity should be negative as the particles at the stage of expansion return back to their original position. However, the degree of accuracy is sufficient for a good qualitative compari-son between solution for perfect gases and real gases using the same method.

v) Results and Conclusions

Since blast waves are high temperature phenomena, real gas effects at high tem-peratures, including vibrational excitation, molecular dissociation, electronic excitation and ionization, are analyzed to determine the thermodynamic proper-ties of gases under these conditions. The condition of statistical equilibrium between various species in a chemical reaction is used to evaluate the equili-brium degree of excitation of the reaction processes and then, the thermodyna-mic properties are calculated considering the gas to be a mixture of perfect gases. The analysis of thermodynamic properties for real gases is suitable for any monatomic or diatomic gas, or mixture of such gases as in the case of air. However, in order to simplify the computations, the data of nitrogen are used in this application.

The effect of the potential energies of the molecules, which may be divided in-to the vibrational energy, energy of dissociation and energy of ionization, on the internal energy of the gas are represented in Fig. IV.3.1. The effect of the reacting properties on the deviation factor Z_r , on the other hand, is gi-ven in Fig. IV.3.2 as a function of pressure and temperature. The first stage

represents the increase in the number of particles due to dissociation, thus indicating the degree of dissociation. Similarly, the second stage shows twice the degree of ionization, since each diatomic molecule splits into two monatomic ones. The maximum values of C_v and the corresponding minimum values of Γ, Figs. IV.3.3 and IV.3.4, occur as a result of the rapid increase in the internal energy at the beginning of dissociation and every successive ionization.

From the physical point of view, the function of density, ϕ, in the self-similar solution should be selected to satisfy one of the well-known equations of state suitable to be applied in the range of conditions of self-similar flow. Thus, the Clausius equation of state is used to represent the non-perfect gas deviation due to compressibility at high pressures, in terms of β^* which depends on ρ_a. However, since both ϕ and the boundary conditions depend on ρ_a, contrary to the case of perfect gases, the whole solution should be carried out for specified values of ρ_a. The results represented in Figs. IV.3.5 - IV.3.8 are obtained for values of $\beta^* = 0.0$, 0.016 and 0.032. These values are corresponding to high values of ρ_a at which the compressibility effect due to high pressures overcomes the effect of high temperatures that reduces such effect. Of course, at these high temperatures, the effect of compressibility is neglected at normal densities. The results are calculated for $j = 2$ and $\gamma = 1.4$.

Due to the complicated form of the equation of state in the case of real gases, the variation of the gasdynamic properties across the shock wave, which represent the boundary conditions of the problem, are evaluated numerically by solving the Rankine-Hugoniot equation with the caloric equation of state using the false position method to solve a system of algebraic equations.

The density ratio h_n increases with the excitation of successive energy modes, Fig. IV.3.9. From Eq. (IV.3.3) for strong shock waves, $\sigma_n = \frac{1}{2}(1 - \frac{1}{h_n})^2$. Thus, as σ_n increases due to the effect of the potential energy, h_n also increases. On the other hand, the perfect gas density ratio for strong shock waves, which is given by $h_n = \frac{\gamma+1}{\gamma-1}$, may help in explaining the sequence of events of Fig. IV.3.9. Since γ decreases due to vibrational excitation and reaches a minimum at the beginning of dissociation, h_n increases to reach

a maximum at the same point. Also, the decrease of h_n with Mach number during ionization is related to the increase in γ , since at this region c_v increases due to the increase in the number of particles which overcomes the effect of the potential energy (Zel'dovich et al., 1966).

The temperature ratios decrease with respect to those of perfect gases due to the expenditure of energy as potential energy, as well as the increase in the number of particles. The high values of potential energy as compared to the translational energy and the increase in c_v decrease the rate at which the temperature ratio increases with Mach number as detected from Fig. IV.3.10.

Figure IV.3.11 shows that the pressure ratio is not affected appreciably by the real gas properties. This can be qualitatively seen from Eqs. (IV.3.3) which indicate that the pressure ratio varies as γ / Γ_a , which is not affected by the real gas properties inside the blast wave. However, since h_n increases for real gases, the pressure ratio also increases.

Actually, the density ratio curve has a number of maxima which occur at the beginning of the successive ionizations like that occurring at the beginning of dissociation. After the occurrence of total ionization the gas transforms into a mixture of monatomic particles which have a constant value of $\gamma = 1.667$. Thus, h_n asymptotically approaches the value of four.

The effect of initial pressure on density ratio and temperature ratio across the shock wave is shown in Figs. IV.3.12 and IV.3.13, respectively. At a certain Mach number, as the ambient pressure increases, the temperature ratio increases while the density ratio decreases.

The flow fields generated by blast waves at various values of front Mach numbers are evaluated by integrating the system of equations, Eqs. (IV.3.1), with Γ expressed by Eq. (IV.3.53). Using the quasi-similarity approximation, the derivatives, with respect to f , are substituted for by their corresponding values at the front. The integration is carried out numerically using the Runge-Kutta fourth order method with a step size $\Delta x = 0.01$. The computations are performed for the spherical wave only, $j = 2$.

The decay coefficient λ , which is calculated using an iterative procedure to satisfy the compatability condition at the center of symmetry, decreases with

the excitation of the successive energy modes, Fig. IV.3.14. Although this decrease seems to be slight, its effect is rather important since the field is very sensitive to the value of λ and any change in its third decimal value affects the field appreciably. This weak dependence of the decay coefficient on the field was previously observed by Kamel (1973b). However, the slight decrease in value of λ may be due to the expenditure of energy in the excitation processes which can be represented as an energy sink. The deviation in λ from its corresponding value of the perfect gas decreases, approaching zero at M = 2.5 where temperature inside the field is not sufficiently high to excite any additional energy modes.

It is logical that temperature distributions inside the field are greatly affected by real gas behaviour since a great amount of the blast energy is used as a potential energy, beside the translational energy. It is to be noted that when comparing the temperature distribution of the perfect gas field with that of the real gas, other effects beside the energy of excitation should be taken into consideration. For example, when the vibrational motion of the molecules are excited, an amount of energy is expended which would decrease the temperature. But, on the other hand, the excitation of vibrational motion of the atoms relative to each other increases the volume occupied by the molecules and, consequently, increases the temperature. The predominant factor of these two effects depends on the degree of excitation of the vibrational motion. The resultant effect may be observed in the field of M = 3 and 5 in Figs. IV.3.15 and IV.3.16. Figure IV.3.17 shows a comparison between the temperature profiles for the perfect gas, with different γ , and for the real gas, while Fig. IV.3.18 shows the effect of initial pressure on the temperature profiles.

However, in the process of dissociation and ionization, the heat of reaction is very high and, thus, the decrease in temperature is always appreciable and the portions of lower gradients in the temperature curves, Figs. IV.3.15 through IV.3.18 represent the successive reacting processes.

The density profiles, Figs. IV.3.19 through IV.3.22, are related directly to the temperature profiles. These figures indicate that the density increases behind the shock front and in the vicinity of the center of symmetry.

- 177 -

In contrast to the large deviations in temperature and density profiles from those for perfect gases, the pressure and particle velocity profiles are found to be less sensitive, Figs. IV.3.23 through IV.3.25. This is a direct conse-quence of the fact that both pressure and particle velocity are related to the particle translational energy. Although the direct proportionality between the particle translational energy and the temperature would suggest that the former should decrease sharply, according to the behaviour of the latter given by Figs. IV.3.15 through IV.3.18, the large increase in t.ie number of partic-les due to dissociation and ionization, tend to offset this effect, hence the insensitivity depicted in Figs. IV.3.23 through IV.3.25.

Finally, the changes in Γ and C_v within the flow field are illustrated in Figs. IV.3.26 through IV.3.29, where their behaviour, as in the case of tempe-rature, manifests the different modes of excitation within the blast wave struc-ture.

Figure Captions

Fig. IV.3.1   Real gas effect on internal energy at different values of the ambient pressure for $j = 2$.

Fig. IV.3.2   Real gas deviation factor z_r as a function of temperature at different values of the ambient pressure for $j = 2$.

Fig. IV.3.3   Effect of vibrational exitation, dissociation and ionization on Γ at different values of the ambient pressure for $j = 2$.

Fig. IV.3.4   Effect of dissociation and ionization on C_v at different values of the ambient pressure for $j = 2$.

Fig. IV.3.5   Self-similar density profiles at different values of the parameter β^* with $\gamma = 1.4$ while $j = 2$.

Fig. IV.3.6   Self-similar pressure profiles at different values of the parameter β^* with $\gamma = 1.4$ while $j = 2$.

Fig. IV.3.7   Self-similar velocity profiles at different values of the parameter β^* with $\gamma = 1.4$ while $j = 2$.

Fig. IV.3.8   Self-similar temperature profiles at different values of the parameter β^* with $\gamma = 1.4$ while $j = 2$.

Fig. IV.3.9   Real gas effects on density ratio across a shock wave.

Fig. IV.3.10   Real gas effects on temperature ratio across a shock wave.

Fig. IV.3.11   Comparison between real and perfect gas pressure ratios across a shock wave.

Fig. IV.3.12   Effect of initial pressure on the density ratio across a shock wave.

Fig. IV.3.1

Fig. IV.3.2

Fig. IV.3.3

Fig. IV.3.4

Fig. IV.3.5
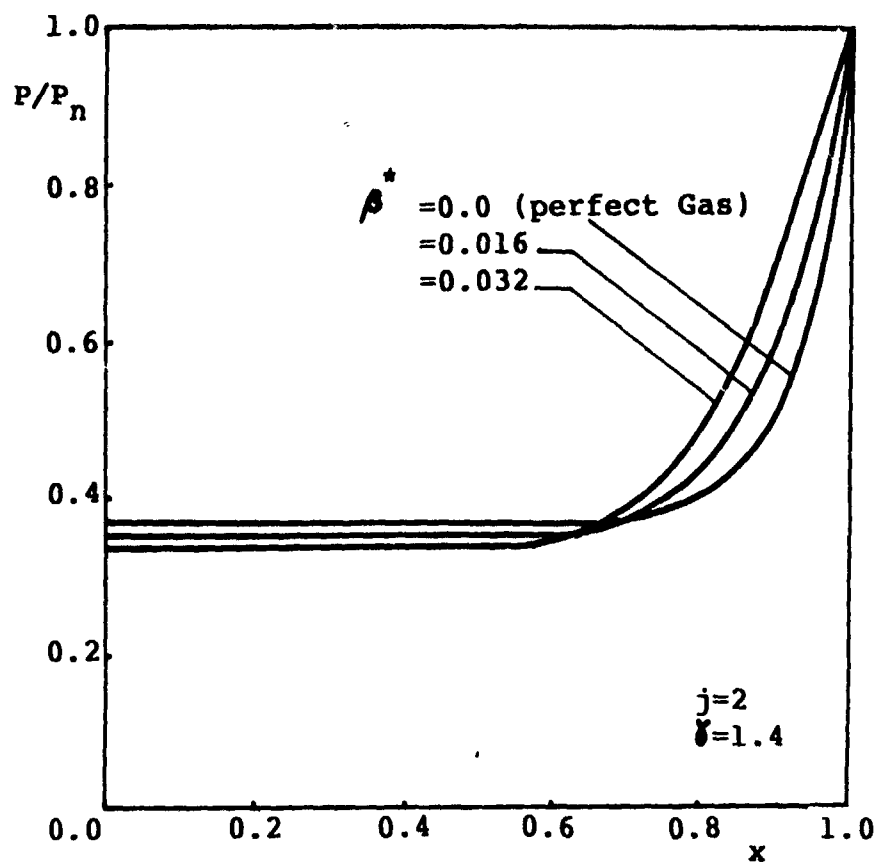
Fig. IV.3.6
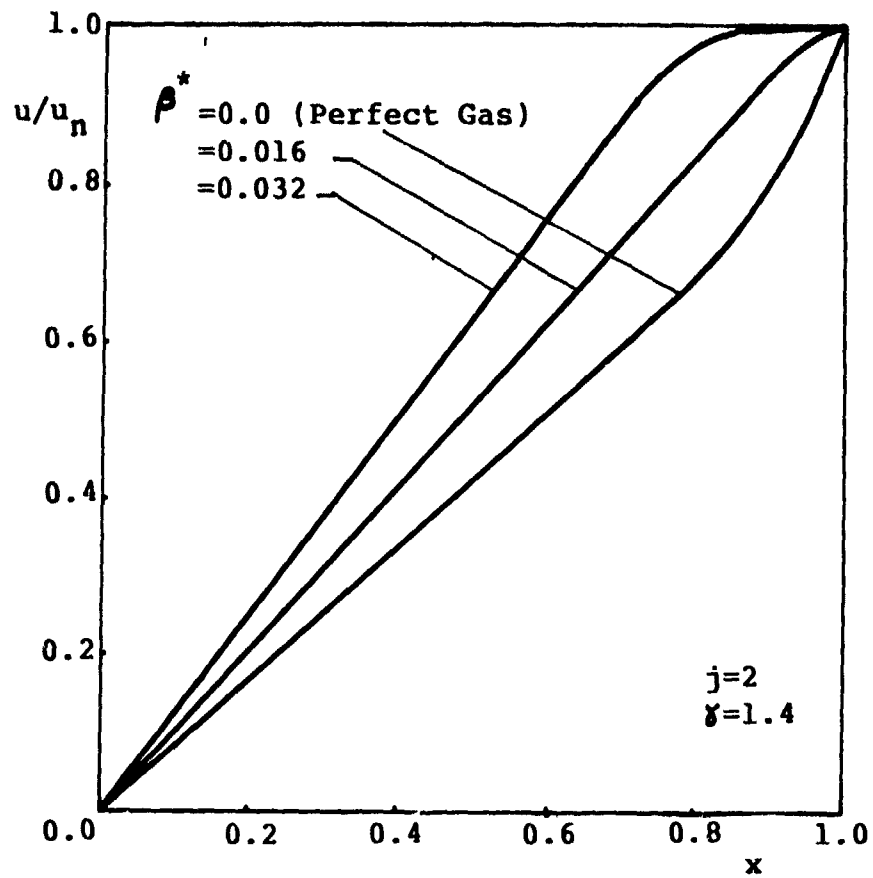
Fig. IV.3.7
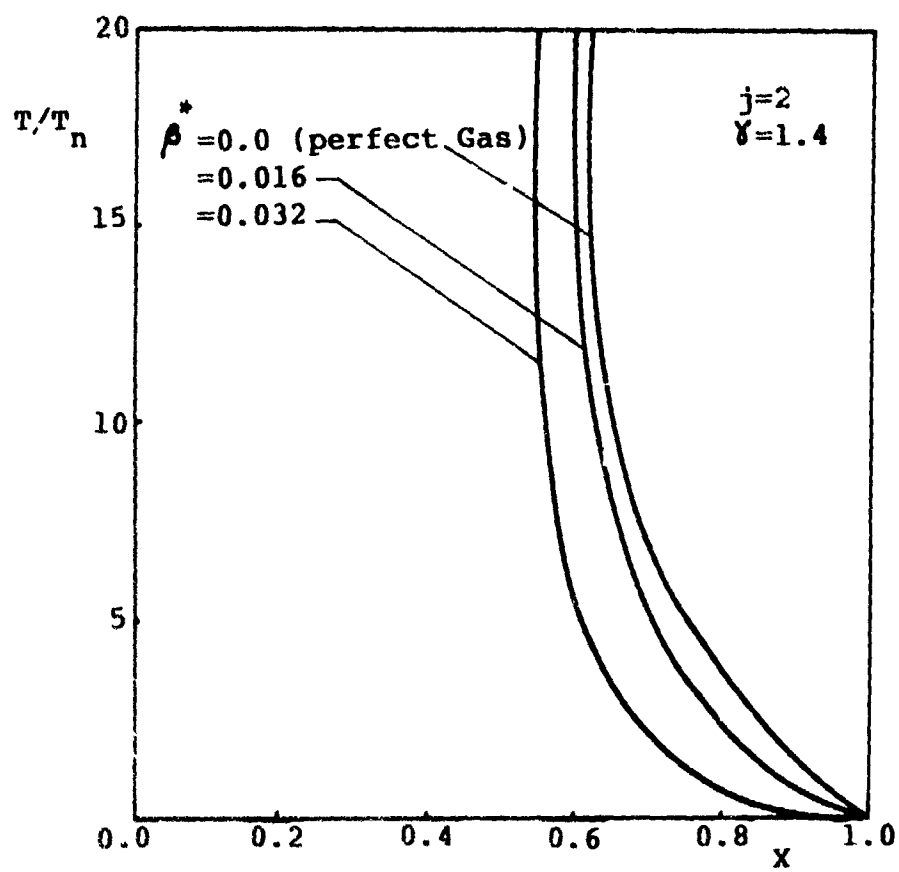
Fig. IV.3.8
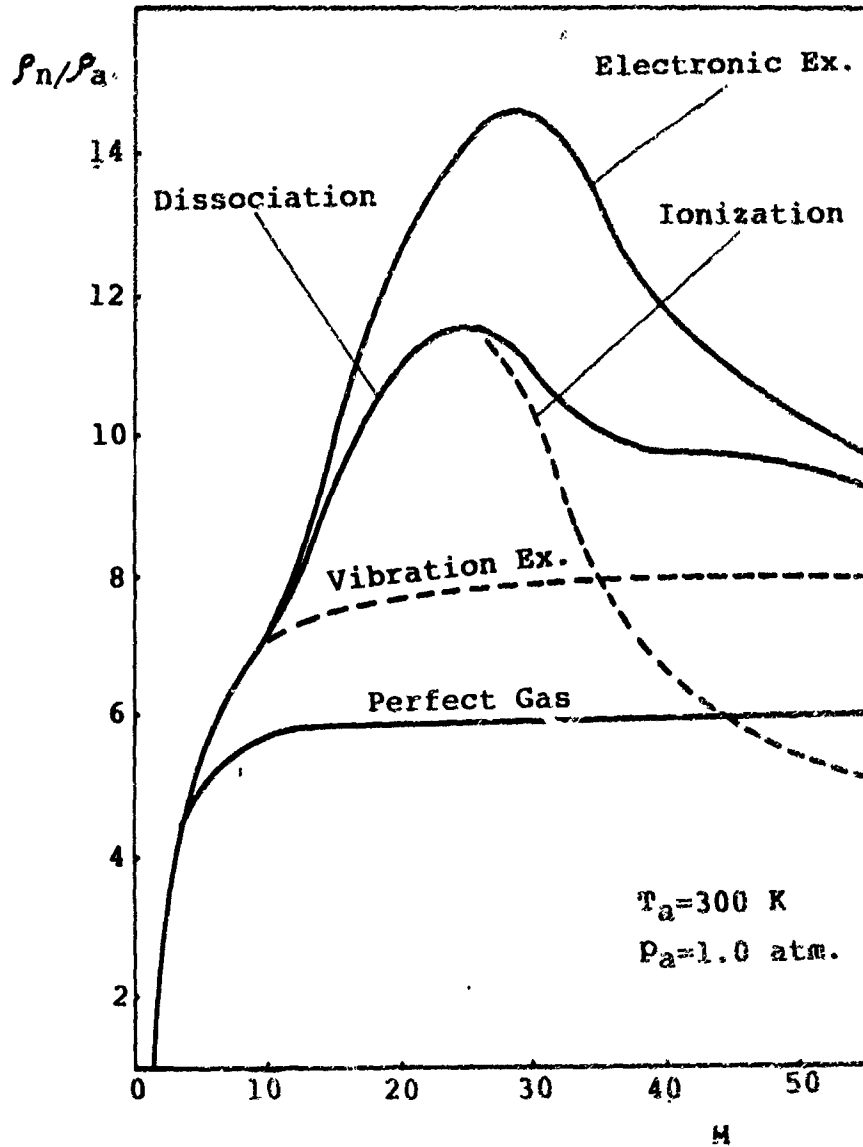
Fig. IV.3.9
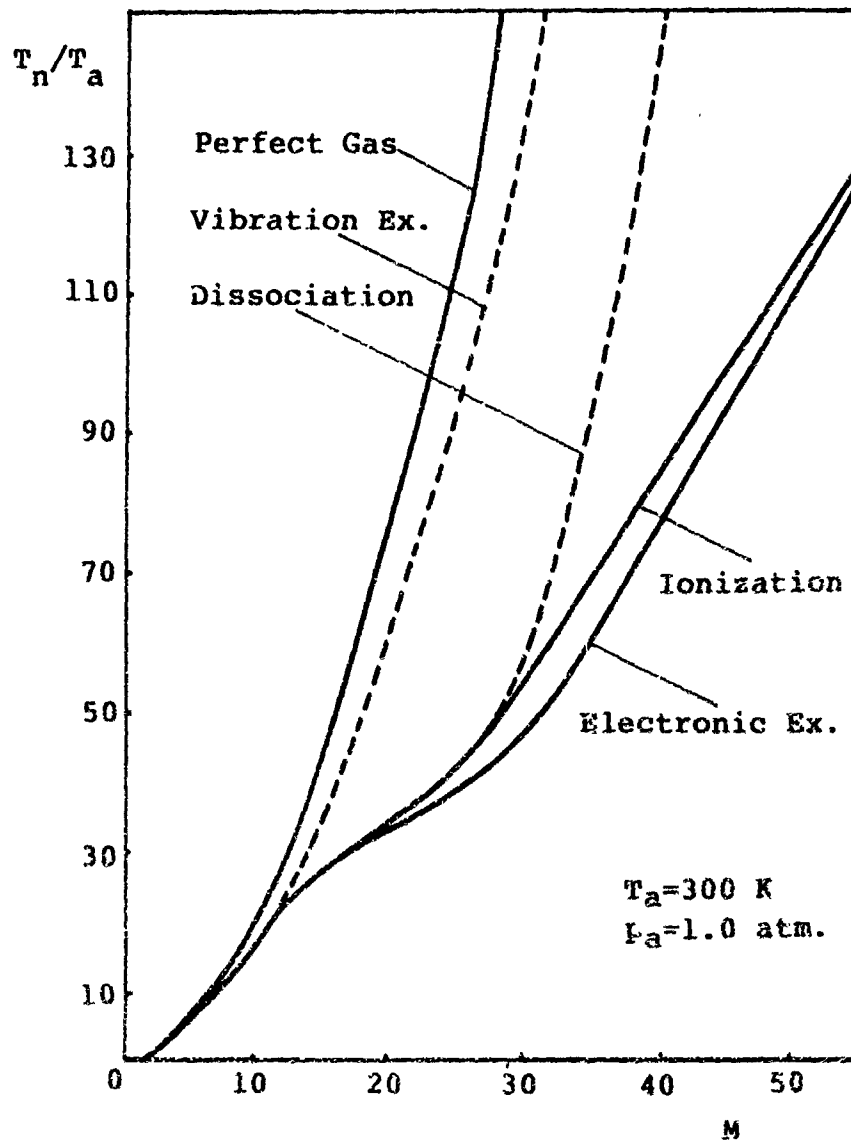
Fig. IV.3.10
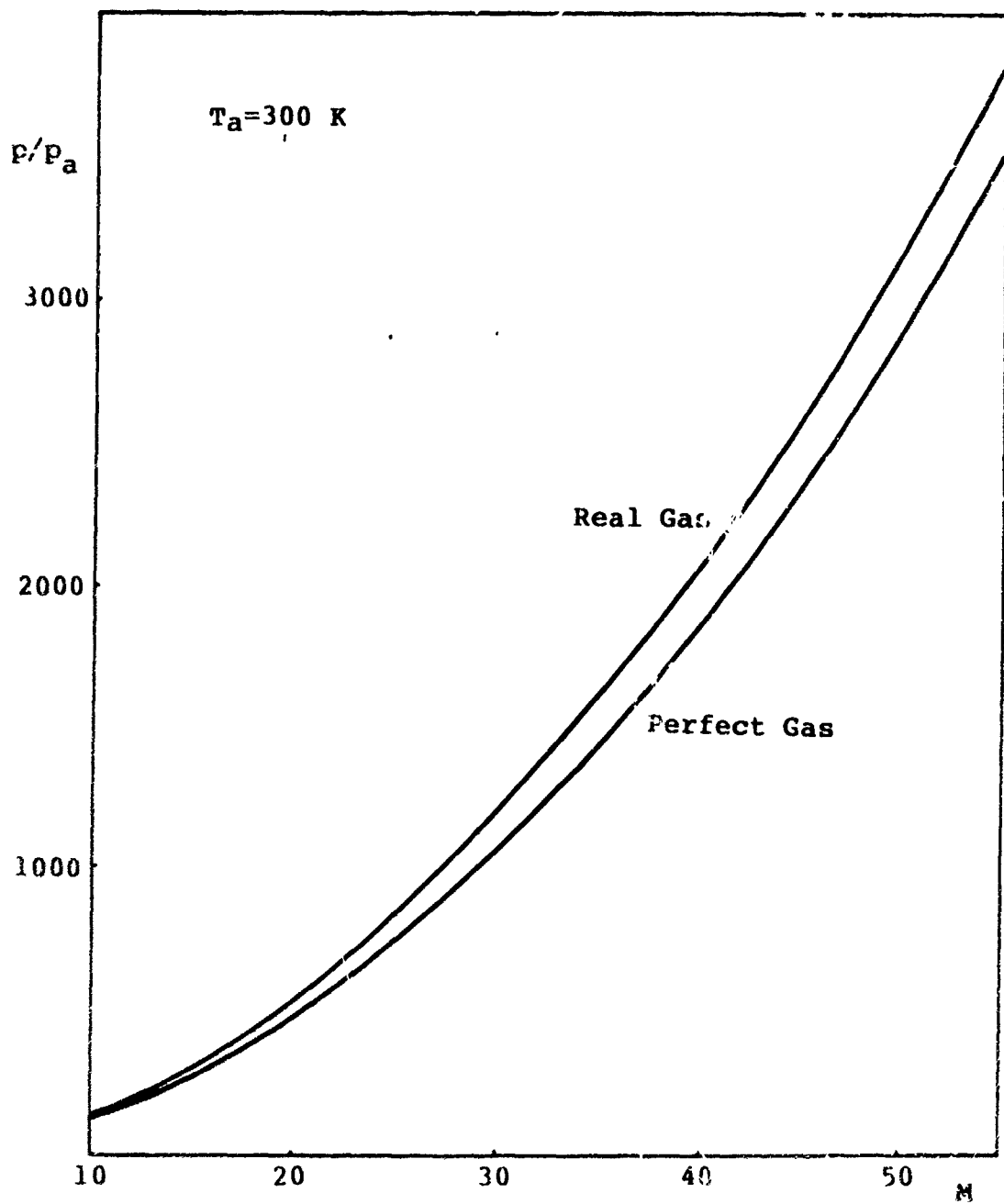
Fig. IV.3.11
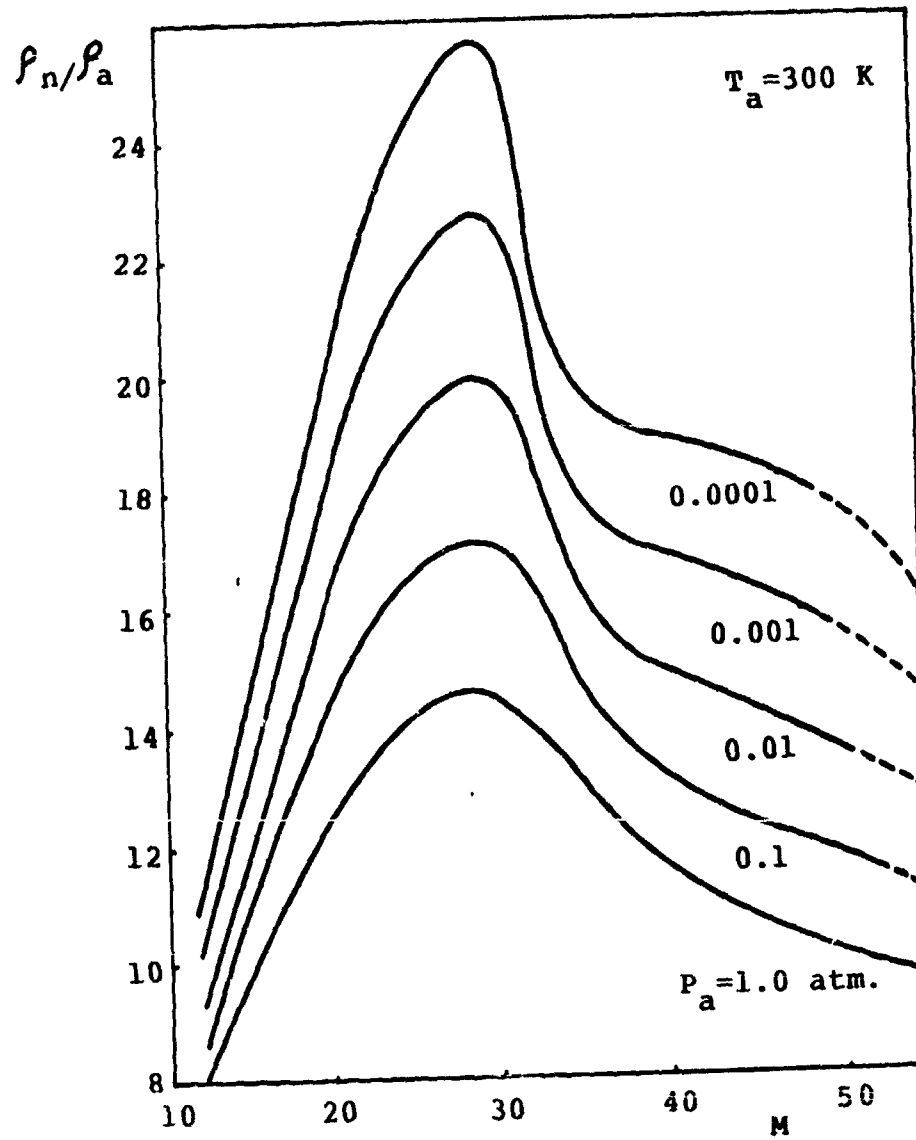
Fig. IV.3.12
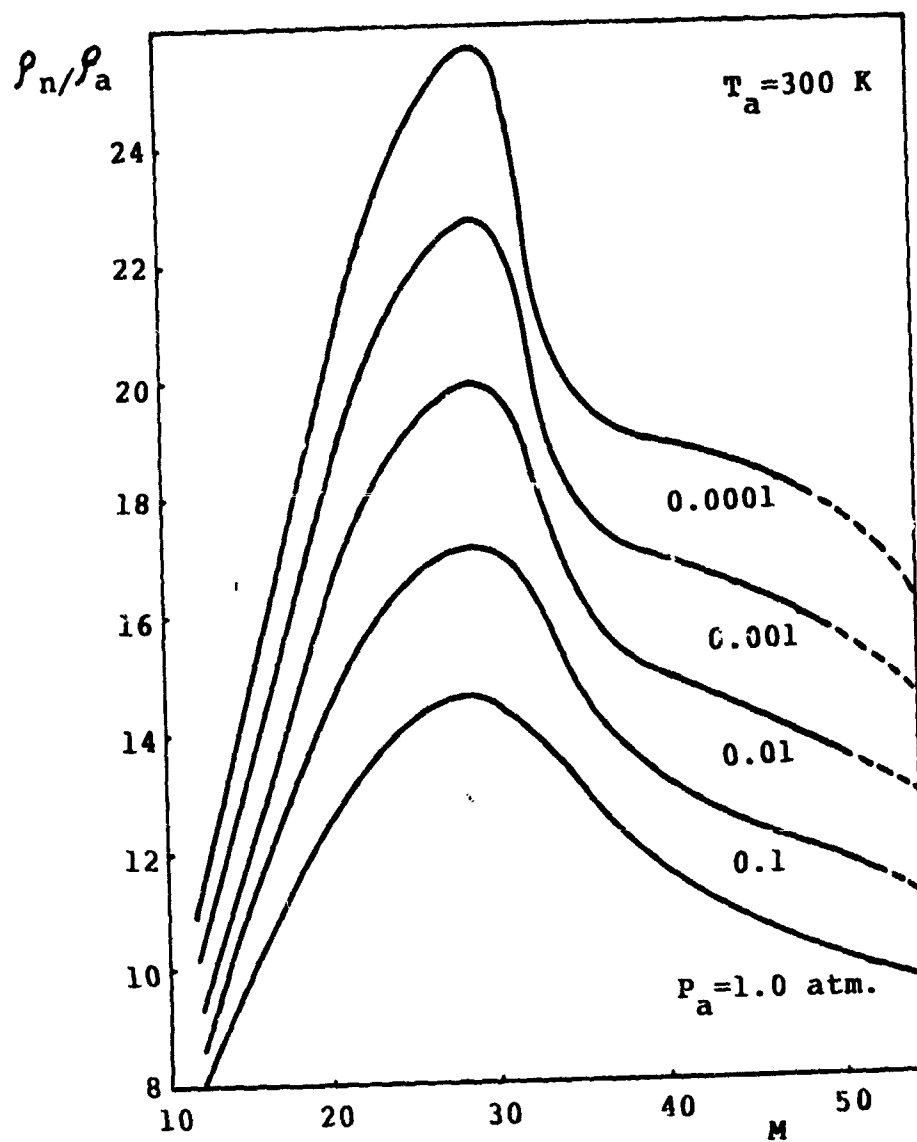
Fig. IV.3.12
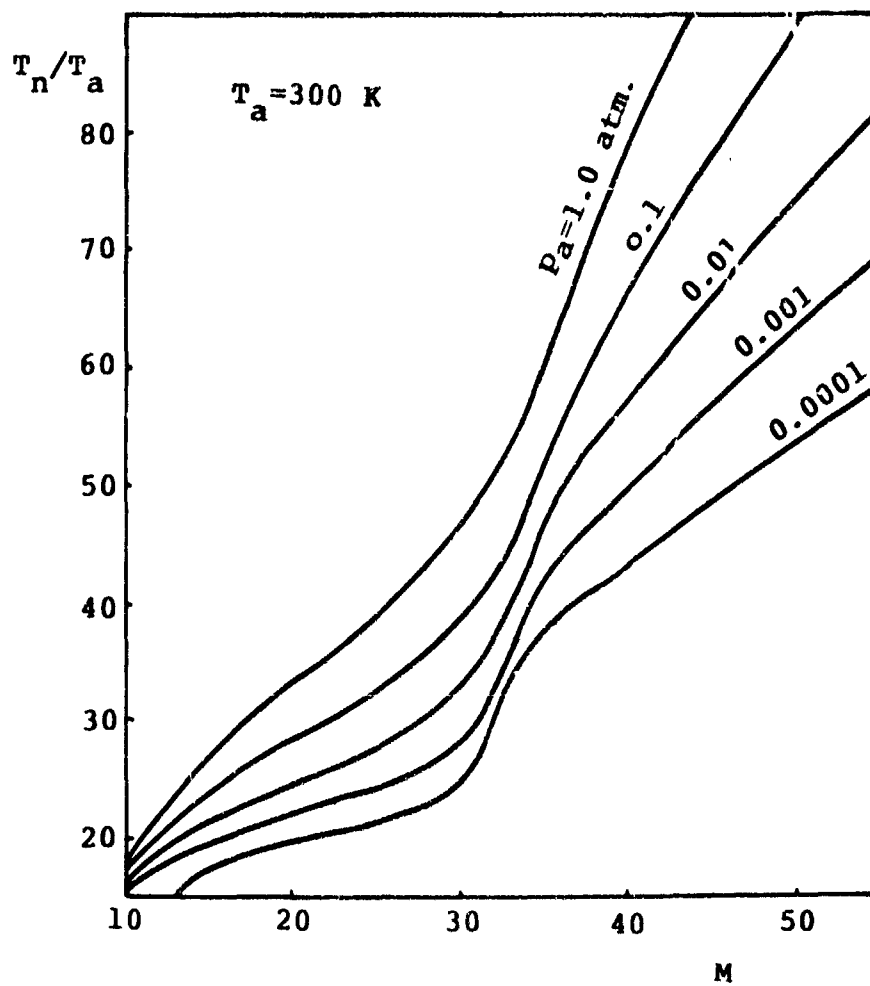
Fig. IV.3.13
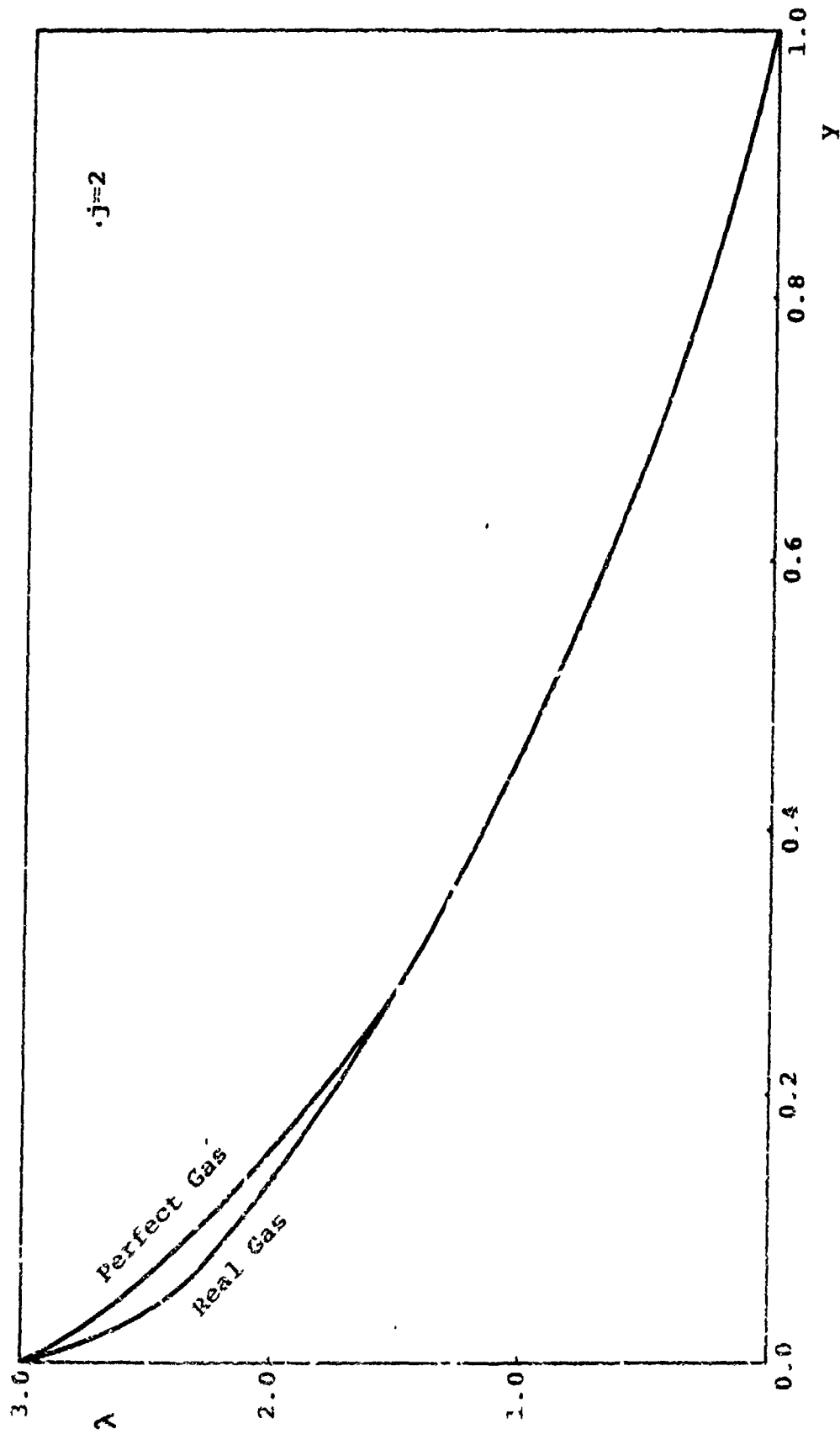
Fig. IV.3.14
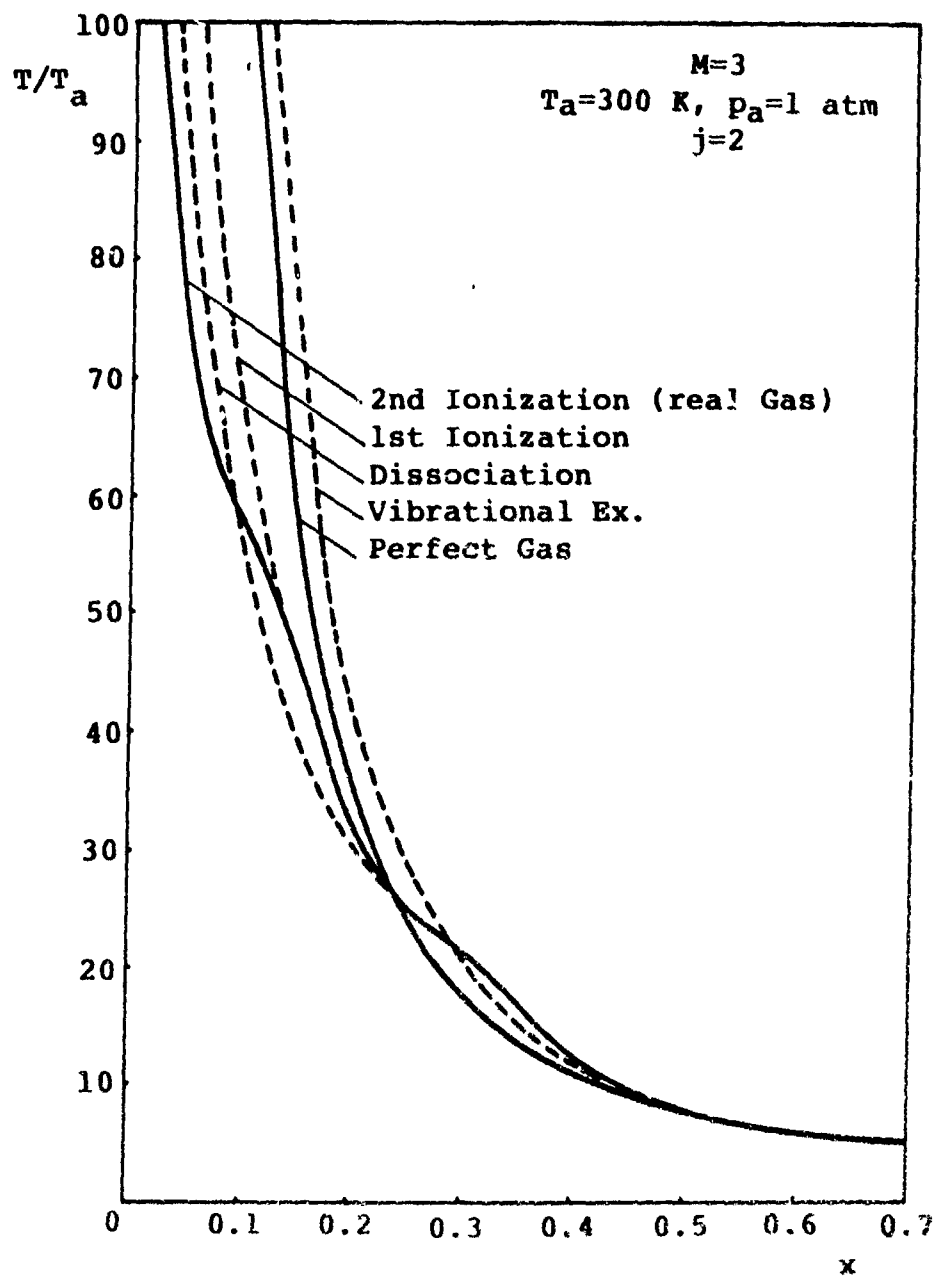
Fig. IV.3.15
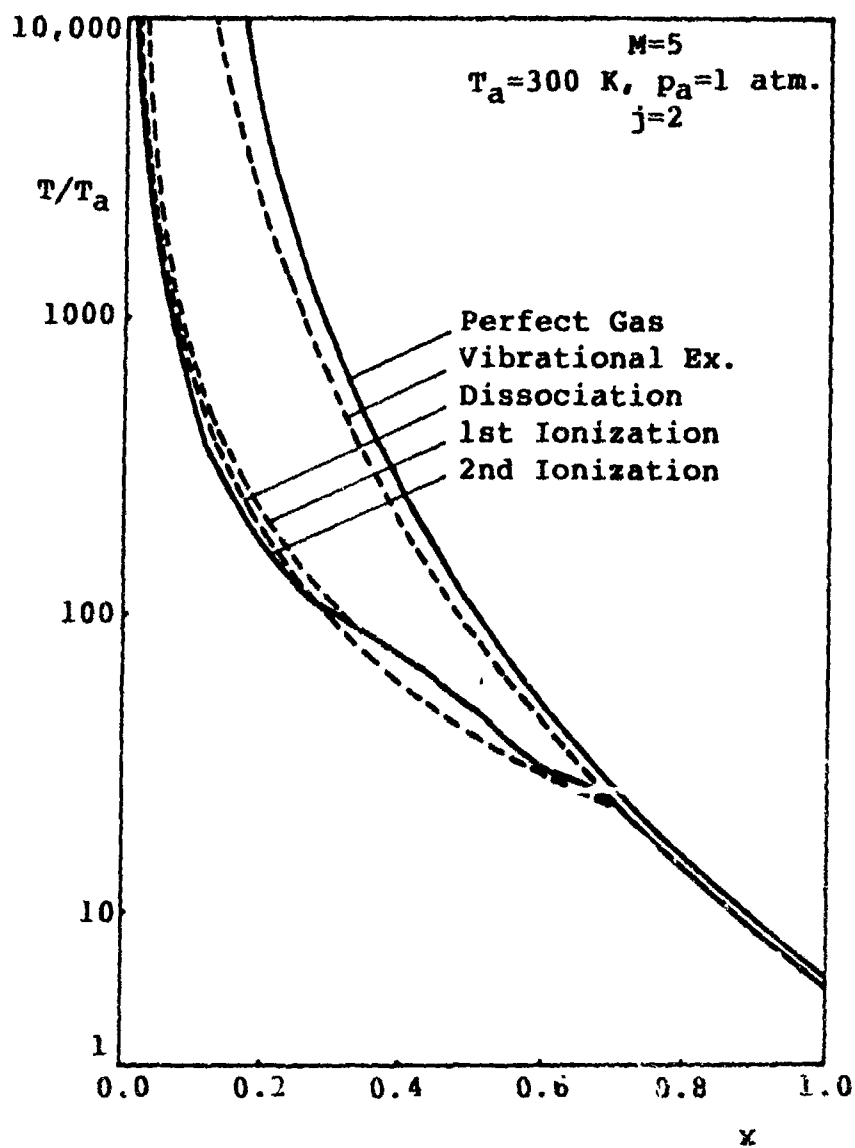
Fig. IV.3.16
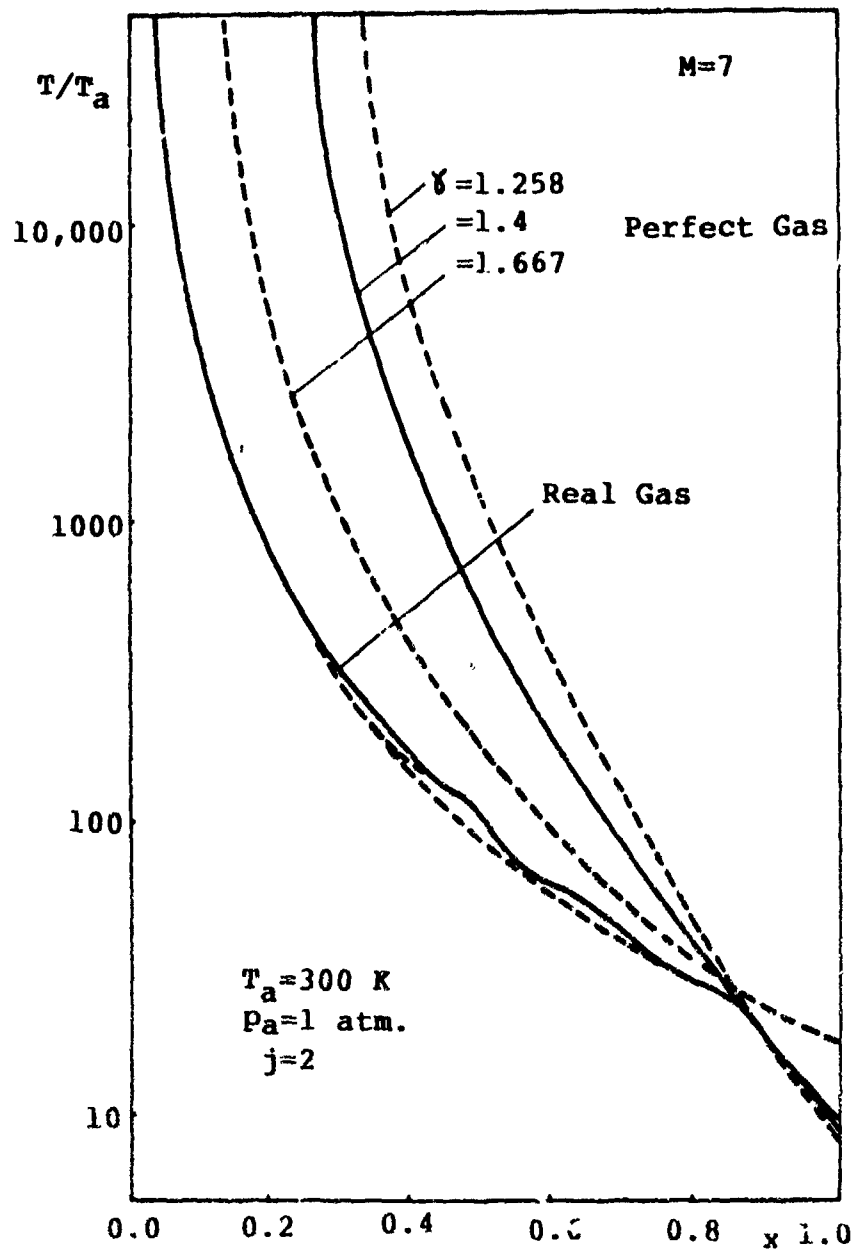
Fig. IV.3.17
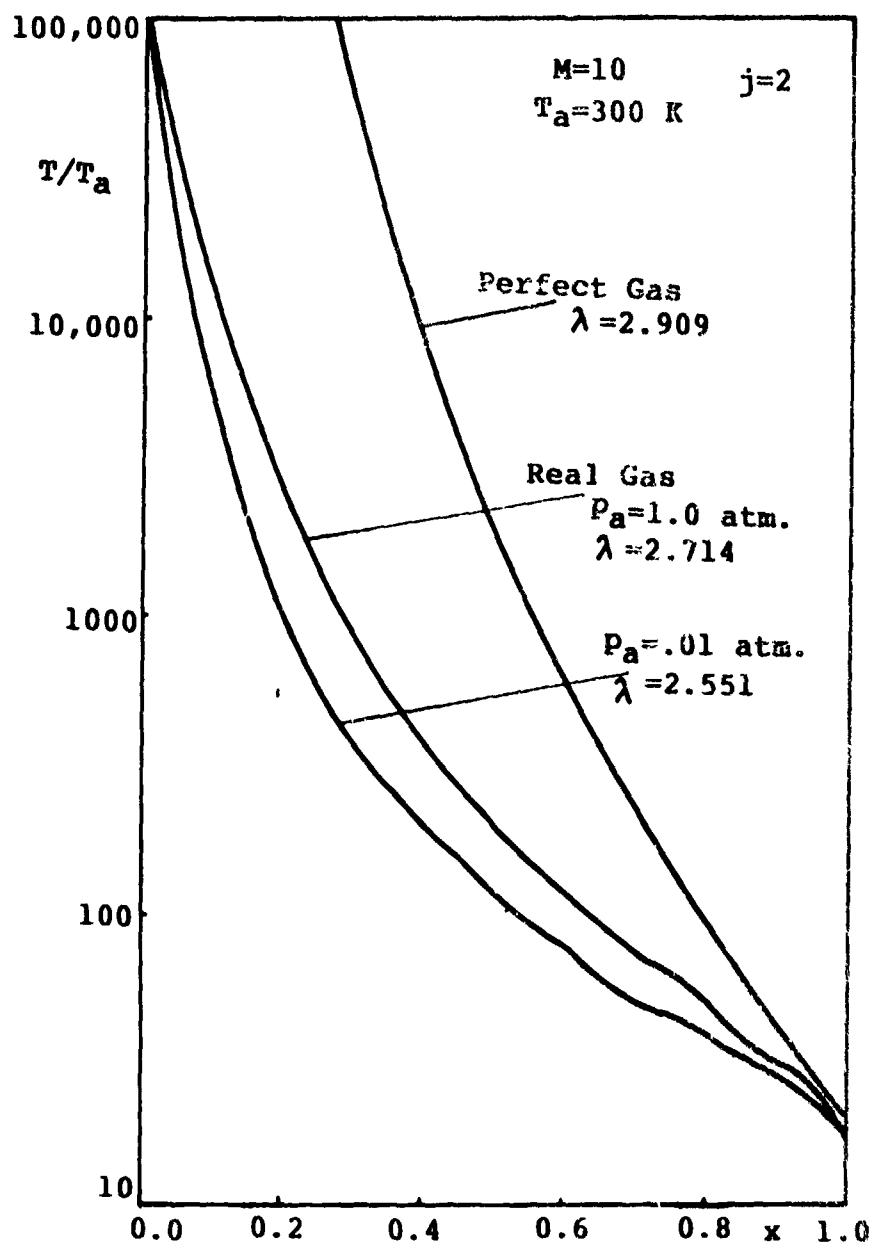
Fig. IV.3.18
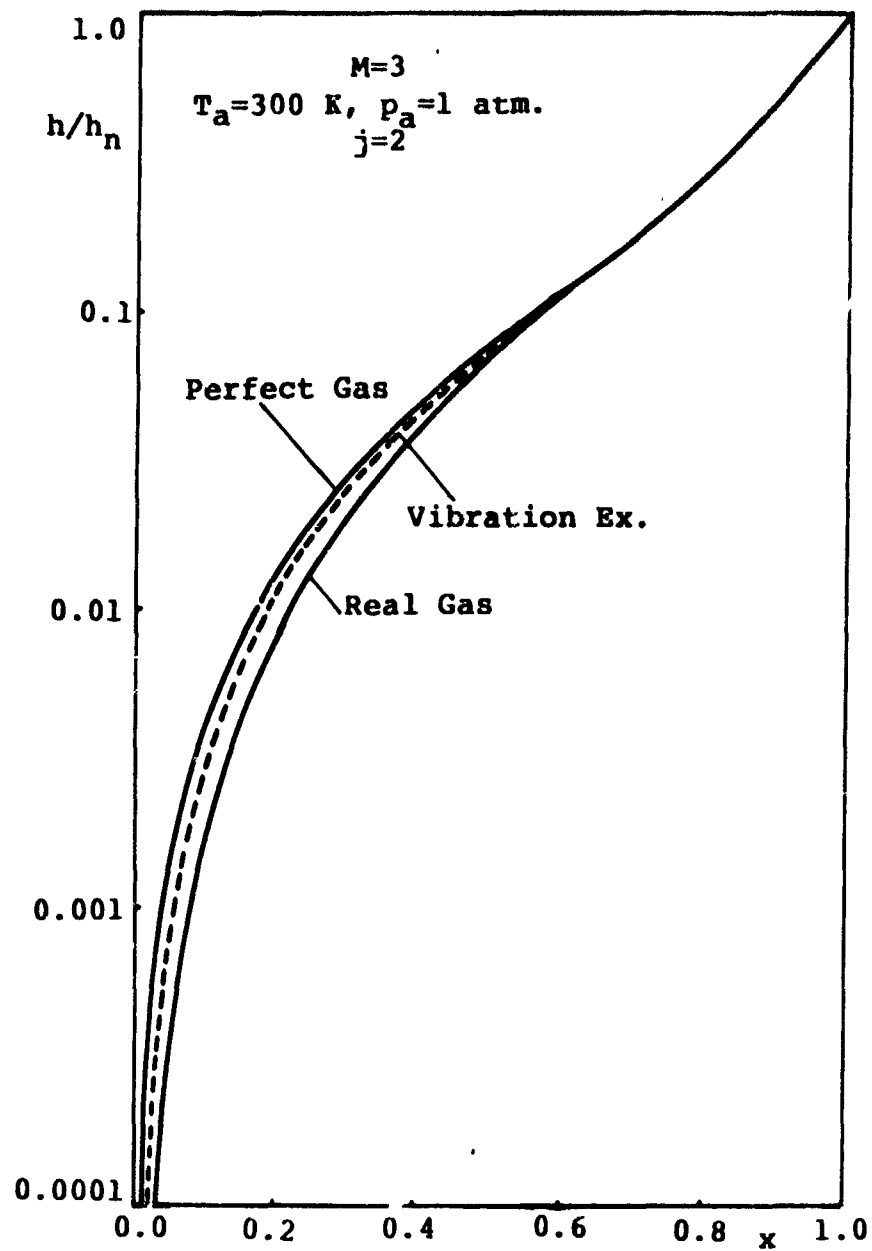
Fig. IV.3.19
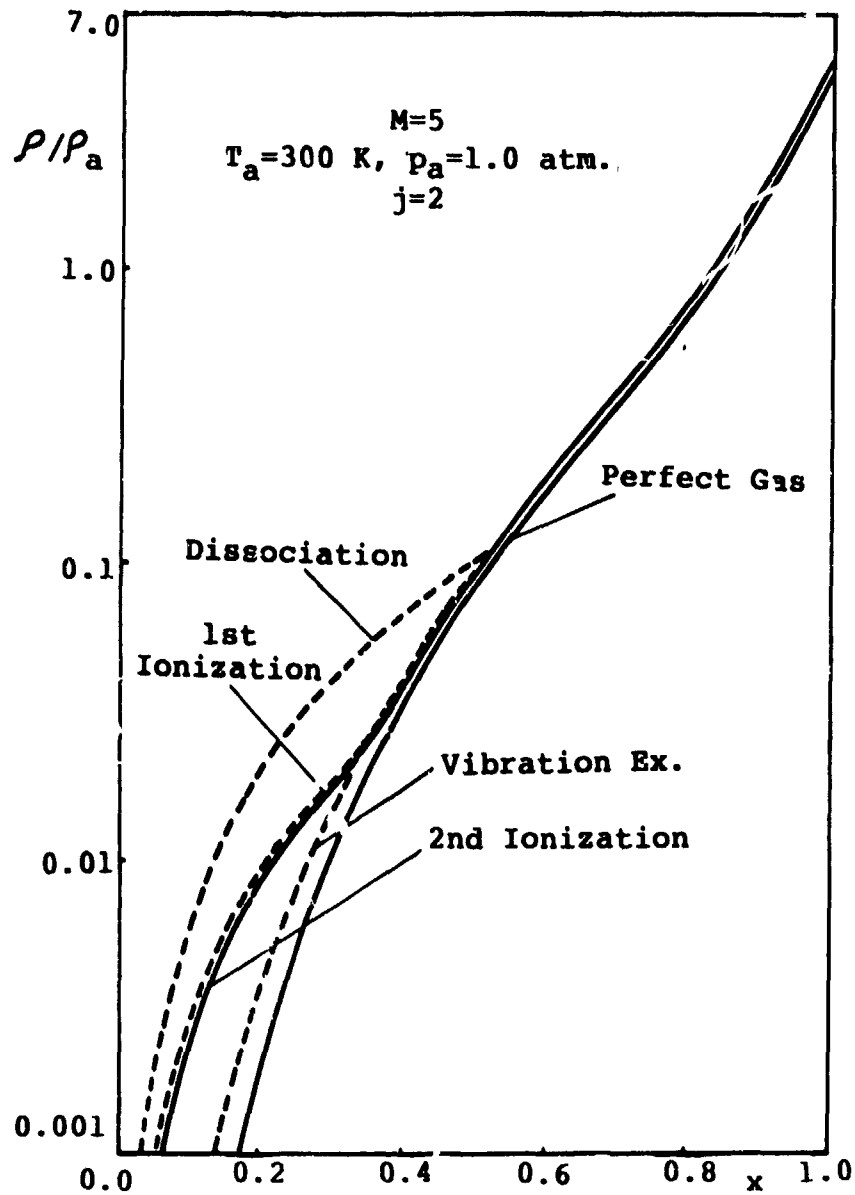
Fig. IV.3.20
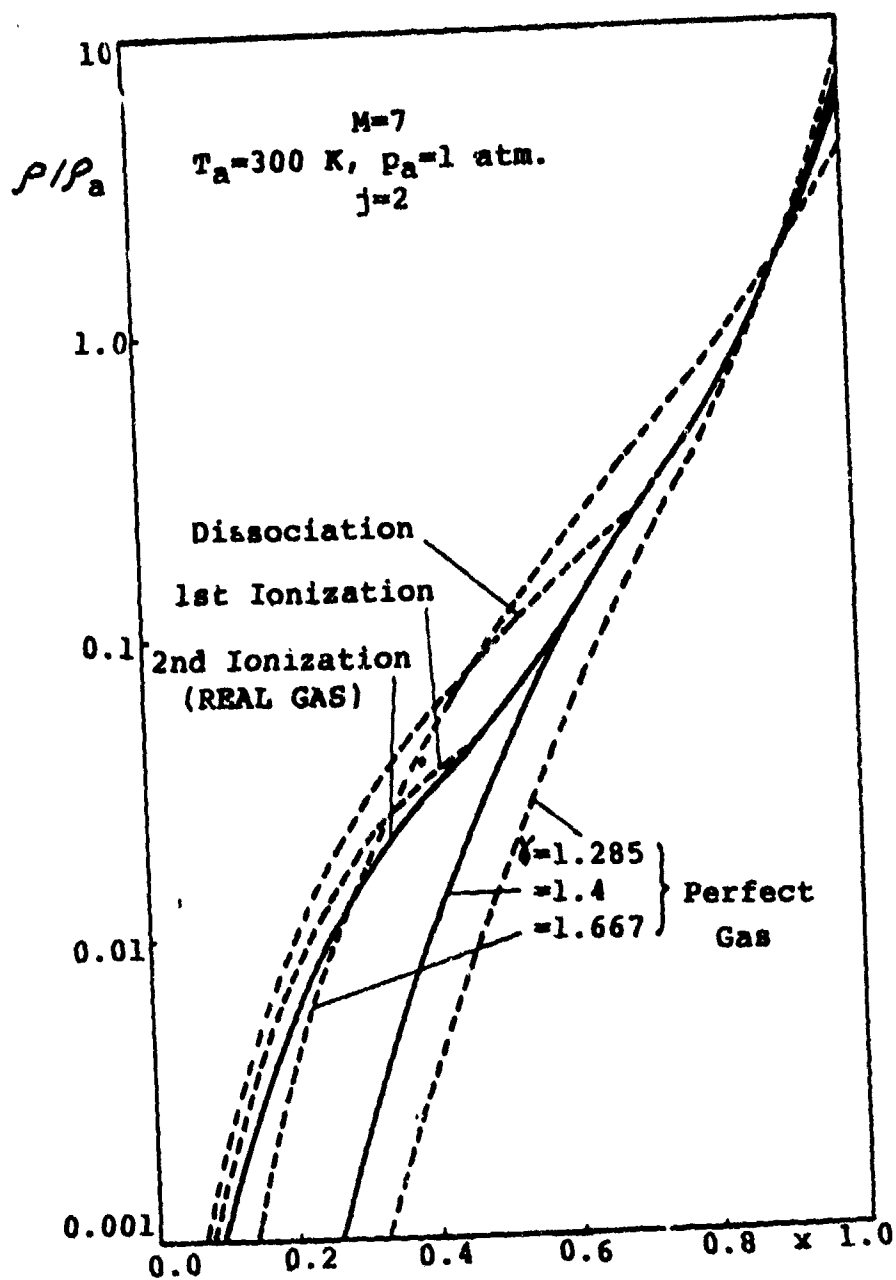
Fig. IV.3.21
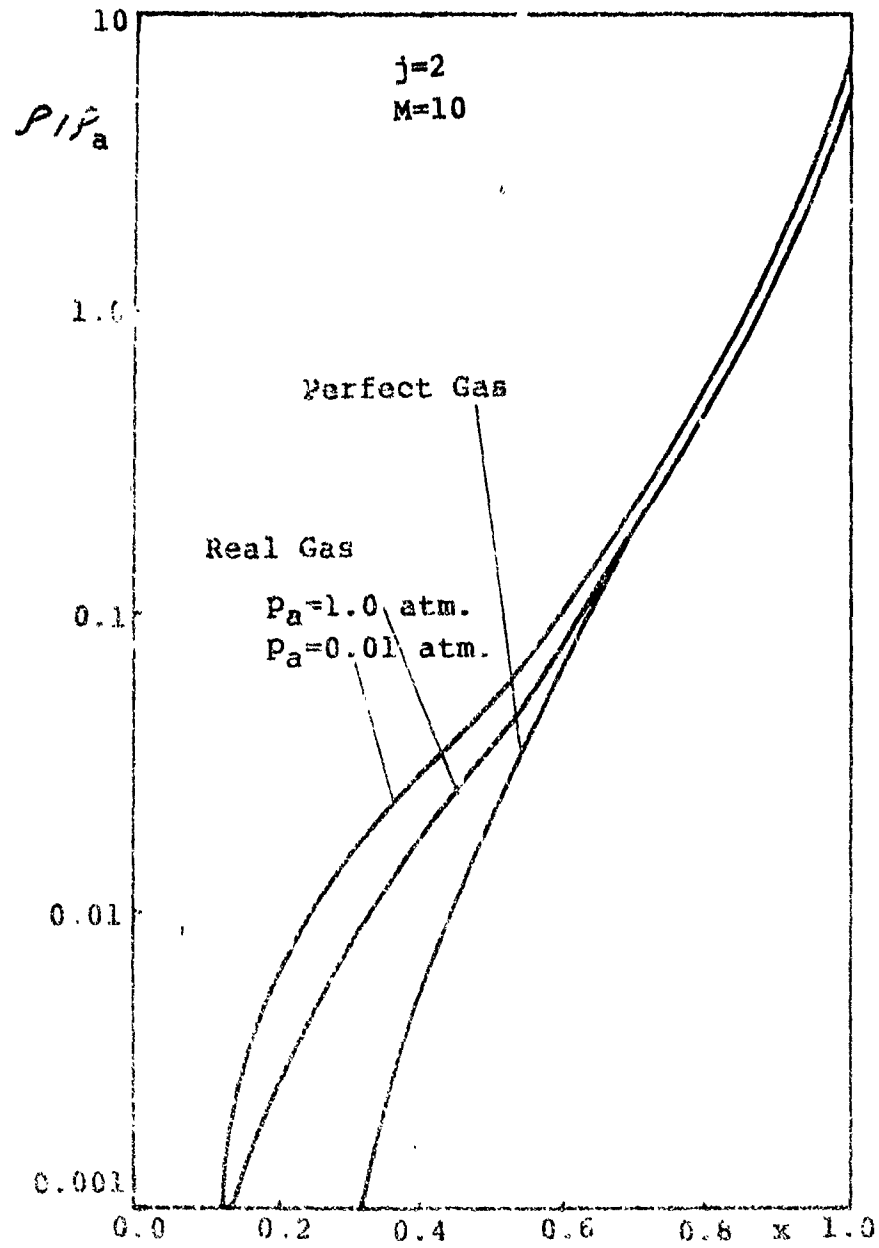
Fig. IV.3.22
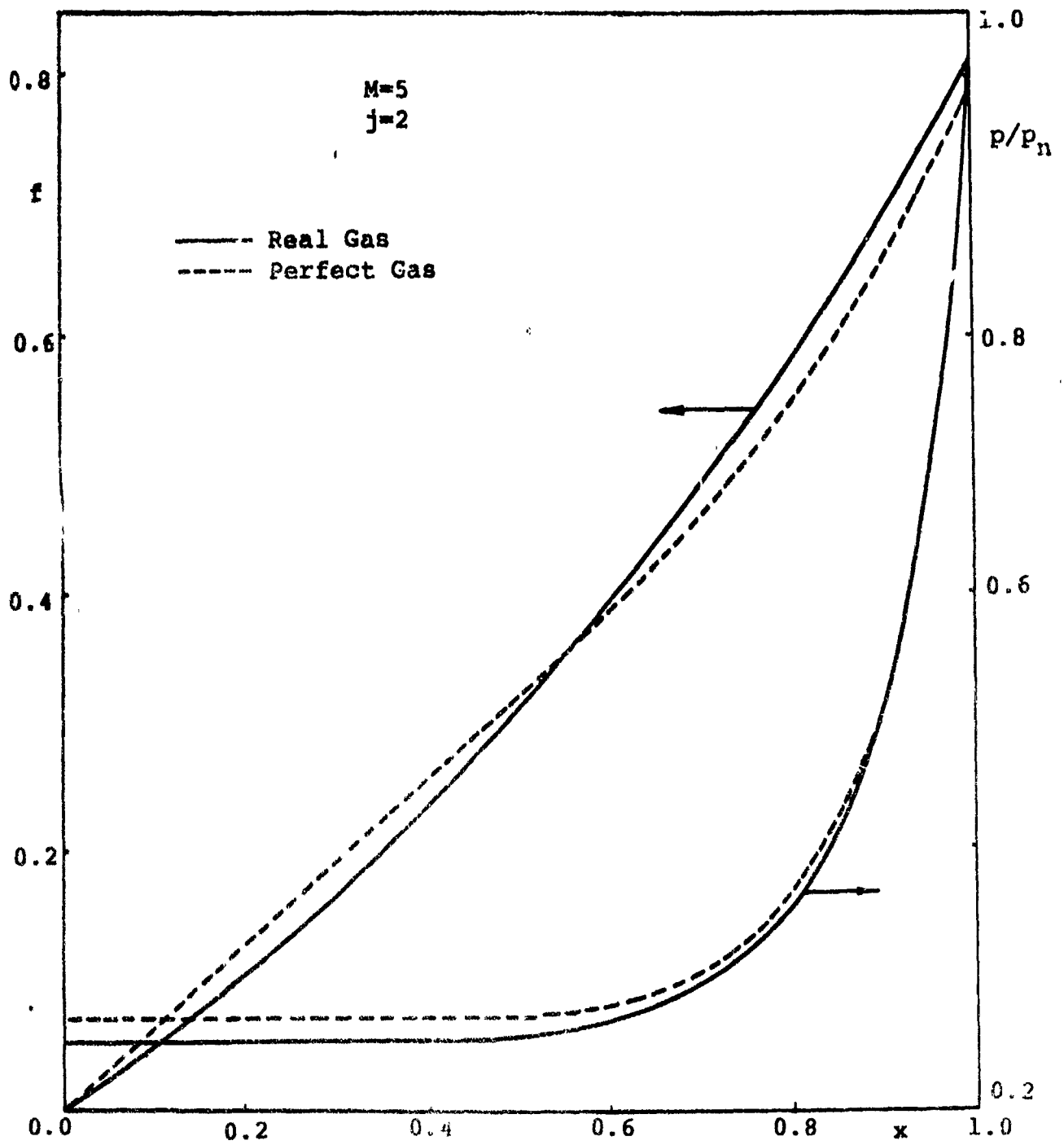
Fig. IV.3.23
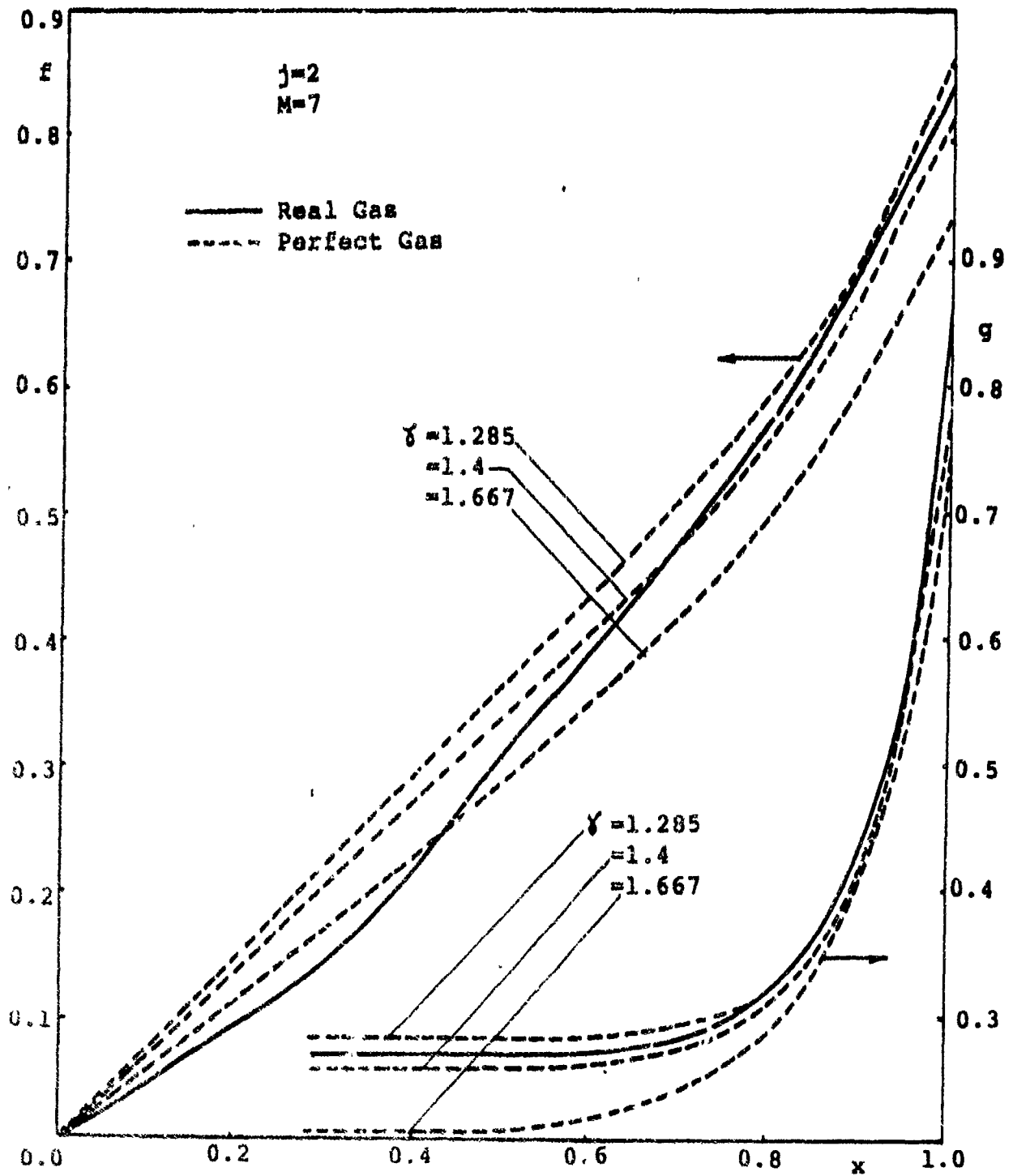
Fig. IV.3.24
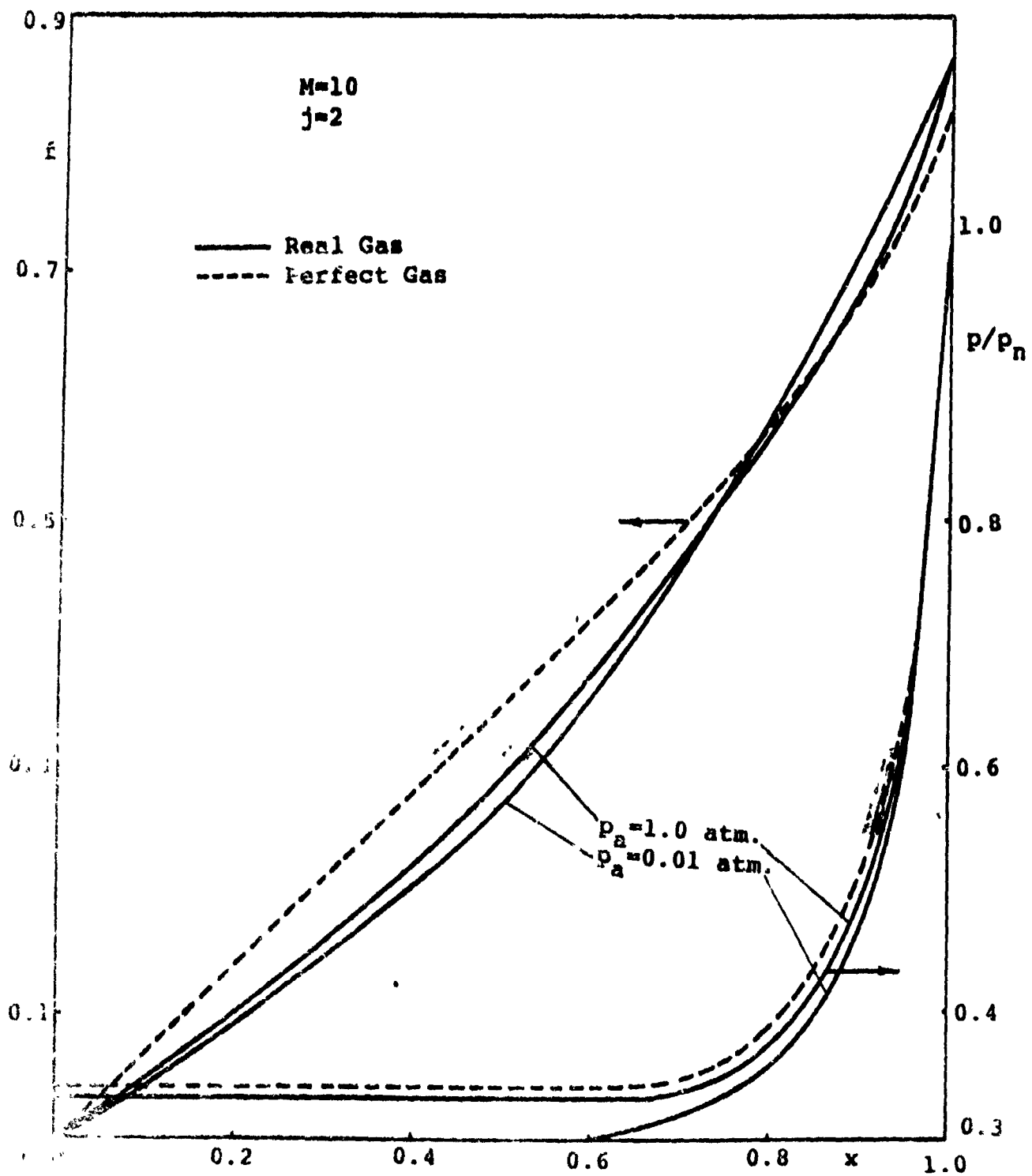
Fig. IV.3.25
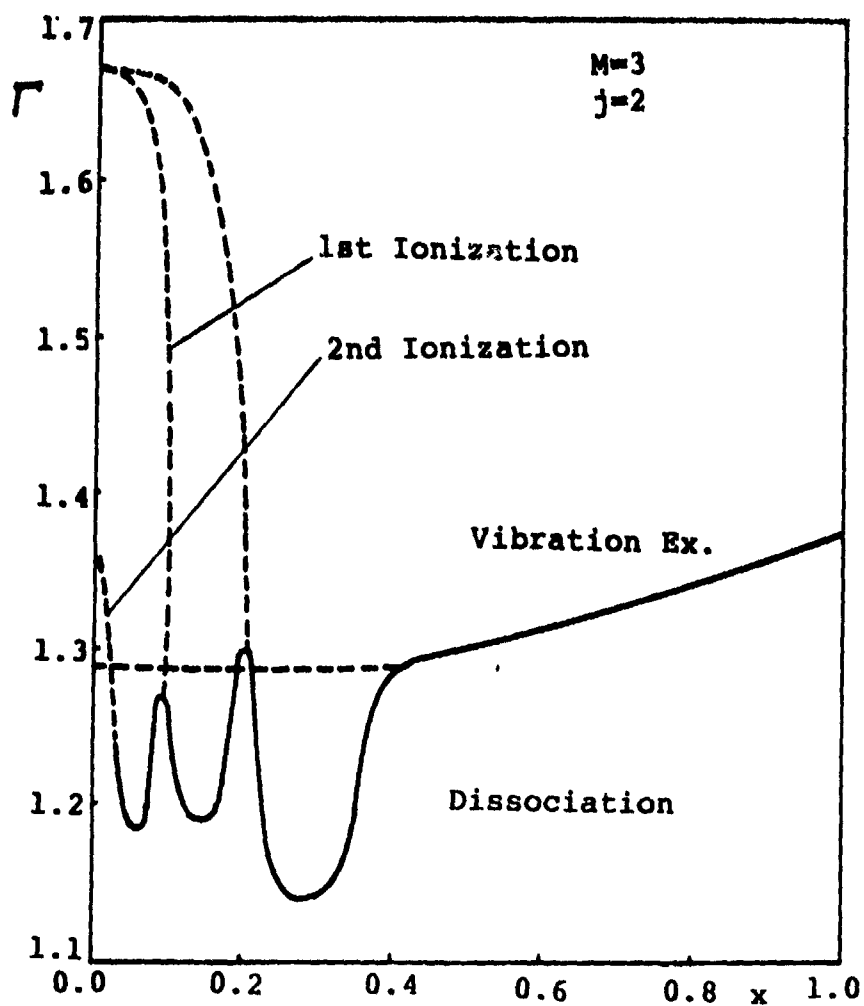
Fig. IV.3.26
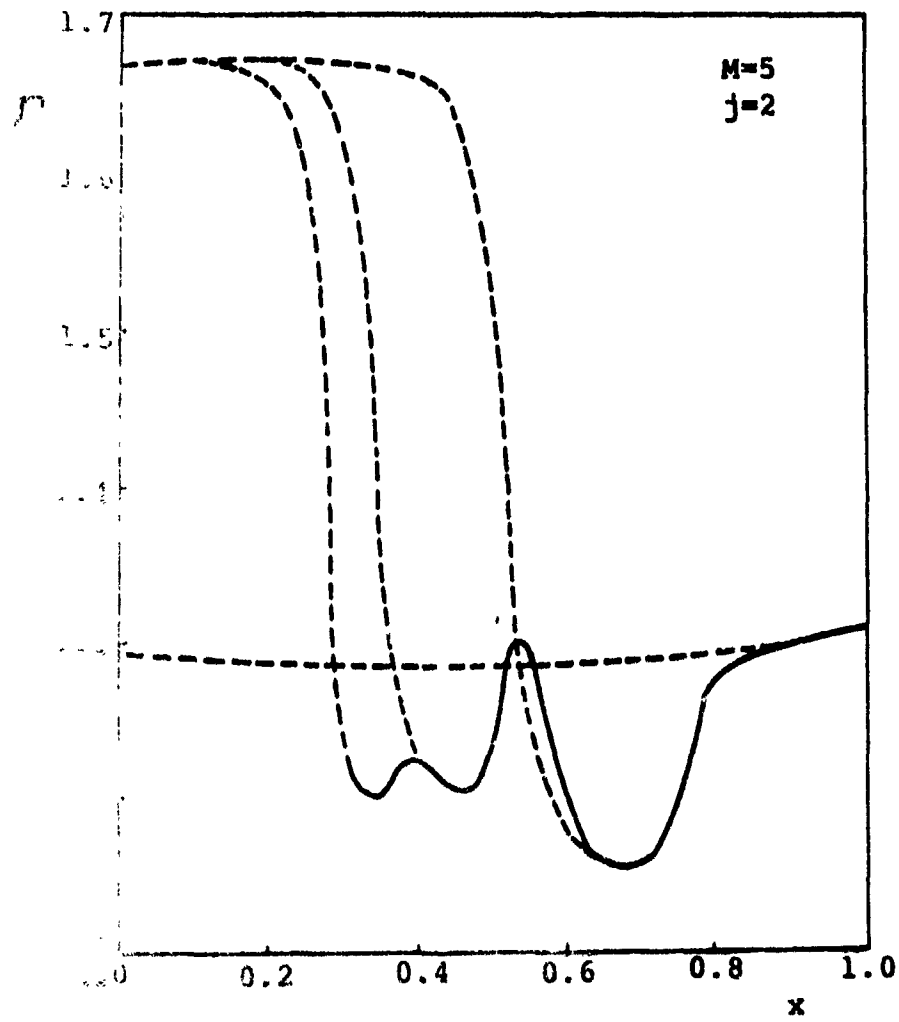
Fig. IV.3.27
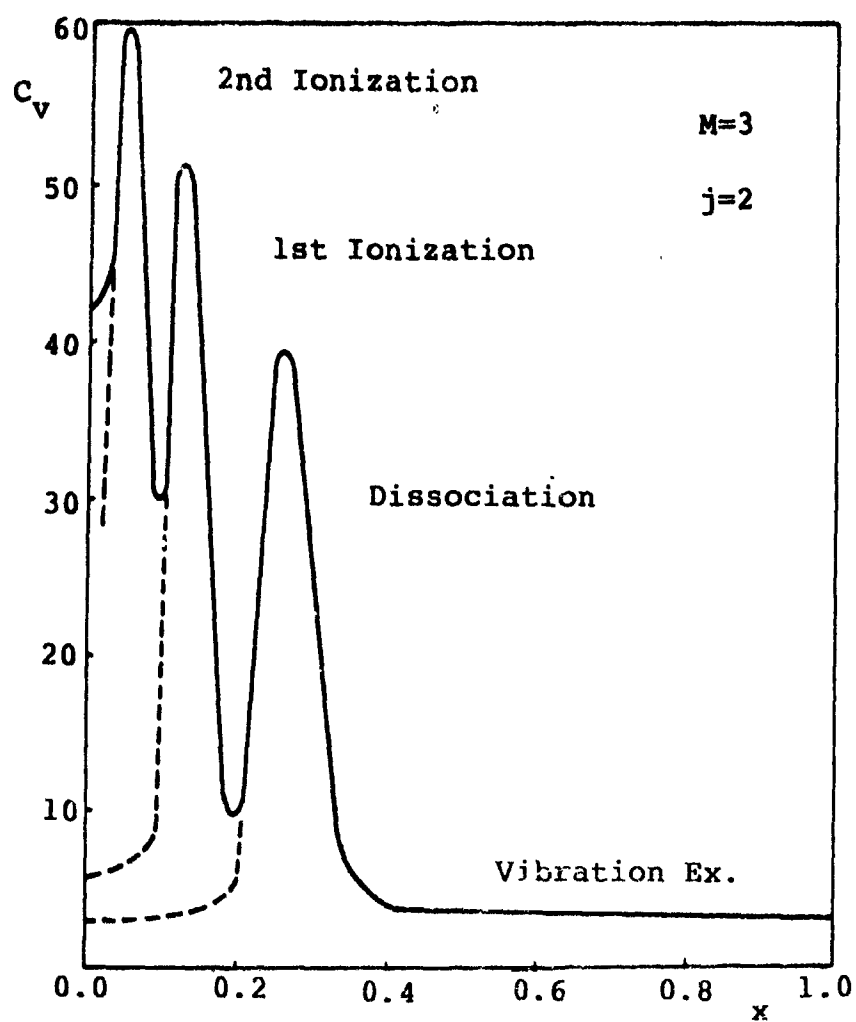
Fig. IV.3.28
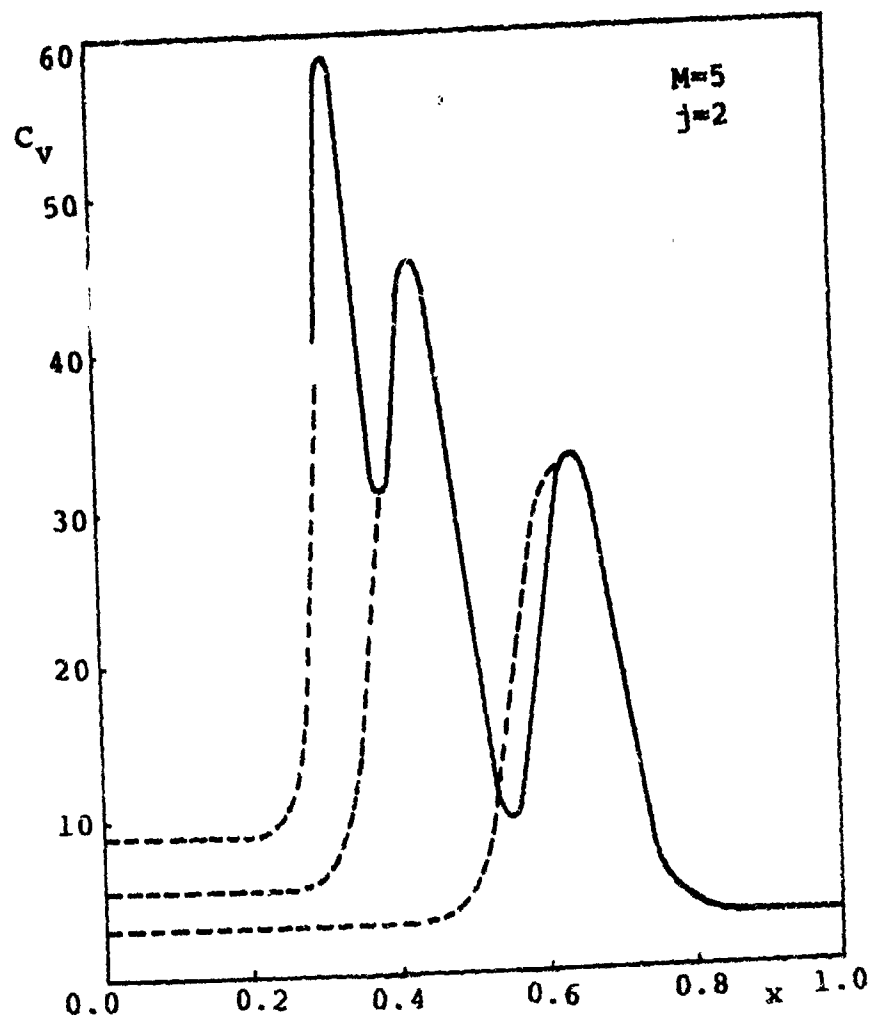
Fig. IV.3.29

IV.4. BLAST WAVES IN A DETONATING MEDIUM*

i) Introduction

In this section, a study of the gasdynamic aspects accompanying the propagation of a detonation wave in a uniform combustible medium is presented.

According to the Chapman-Jouguet theory (Oppenheim, 1966), a detonation wave, once formed, will propagate at a constant velocity independent of the details of its initiation processes, and dependent only on the properties of the explosive medium in the front of the wave.

The simplest model to use as a basis for an initiation theory would be the instantaneous formation of a reactive blast wave front.

Since methane is the major constituent of natural gas, the most predominantly used explosive gas mixture, the detonating medium in this application is assumed to be a stoichiometric methane-air mixture. The detonation medium itself is taken as a perfect gas with a mean specific heat ratio, γ , that is capable of producing an amount of exothermic energy, q , per unit mass of the mixture.

The solution obtained here is for the non-self-similar flow fields that result from instantaneous deposition of energy at a point, along a line or at a plane in an inviscid medium. It traces the decay of the detonation front from its initial self-similar limit, corresponding to the adiabatic point explosion to its Chapman-Jouguet condition.

ii) Problem Formulation

The basic equations governing the problem can be specified directly from Eqs. (II.20), (II.22) and (II.24) by equating all ϕ 's as well as ρ'_α 's to zero, since we have a sourceless flow field and a uniform ambient medium. These equations are

---

*This application is based on Abdel-Raouf (1962).

$$\lambda y \frac{\partial h}{\partial y} + (f - x) \frac{\partial h}{\partial x} + h\left(\frac{\partial f}{\partial x} + j\frac{f}{x}\right) = 0$$

$$\lambda y \frac{\partial f}{\partial y} - \frac{\lambda}{2} f + (f - x) \frac{\partial f}{\partial x} + \frac{1}{h} \frac{\partial g}{\partial x} = 0$$

and

$$\lambda y \frac{\partial g}{\partial y} - \lambda g + (f - x) \frac{\partial g}{\partial x} + \gamma g\left(\frac{\partial f}{\partial x} + j\frac{f}{x}\right) = 0$$

(IV.4.1)

The boundary conditions of the problem are given by the Hugoniot relations, Eqs. (II.93), (II.54) and (II.85), which may be rewritten as

$$f_n = \frac{1-y}{\gamma+1} + \left[\left(\frac{1-y}{\gamma+1}\right)^2 - 2\left(\frac{\gamma-1}{\gamma+1}\right) y\bar{q}\right]^{1/2}$$

$$h_n = \frac{1}{1 - f_n}$$

(IV.4.2)

and

$$g_n = f_n + \frac{y}{\gamma}$$

The shock strength at the Chapman-Jouguet condition of overdriven detonation is given by Eq. (II.94) as

$$y_{CJ} = \left[(\gamma^2 - 1)\bar{q} + 1\right] - \sqrt{\left[(\gamma^2 - 1)\bar{q} + 1\right]^2 - 1}$$

(IV.4.3)

The mass and energy integrals for the present problem, Eqs. (II.64) and (II.96), respectively, are given by

$$\sigma_1 = \int_0^1 h x^j \, dx = \frac{1}{j+1}$$

(IV.4.4)

and

$$\mathcal{J}_3 = \int_o^1 \left[\frac{g}{(\gamma-1)h} + \frac{f^2}{2} \right] h \, x^j \, dx$$

$$= \frac{y}{\gamma} \left[\mathcal{J}^{-(j+1)} + \frac{1}{(j+1)(\gamma-1)} + \frac{\gamma \bar{q}}{(j+1)} \right] \tag{IV.4.5}$$

The mass integral, Eq. (IV.4.4), is used here as a check on the density profiles, while the energy integral, Eq. (IV.4.5), is used for determining the non-dimensional radius, $\mathcal{J}$.

The decay coefficient, λ , takes its form given by Eq. (II.97)

$$\lambda = \frac{(j+1) \mathcal{J}_3 - \frac{y}{\gamma(\gamma-1)} - \bar{q} y}{\mathcal{J}_3 - y \frac{d\mathcal{J}_3}{dy}} \tag{IV.4.6}$$

which for the strong self-similar blast wave (y = 0), reduces to

$$\lambda = (j+1) \tag{IV.4.7}$$

Finally, the compatability condition which must be satisfied at the center of symmetry by the correct solution is given by Eq. (II.112), namely

$$f(o,y) = o \tag{IV.4.8}$$

Applying the concept of the quasi similar technique on the governing equations, they reduce to the following ordinary differential equations, given previously

by Eqs. (I.I.23) - (III.25), when all Φ 's vanish

$$(f-x)\frac{dh}{dx} + h(\frac{df}{dx} + j\frac{f}{x}) + \lambda h \cdot A = 0$$

$$(f-x)\frac{df}{dx} + \frac{1}{h}\frac{dg}{dx} + \lambda f B = 0 \qquad (IV.4.9)$$

and

$$(f-x)\frac{dg}{dx} + \delta g(\frac{df}{dx} + j\frac{f}{x}) + \lambda g G = 0$$

where

$$A = \frac{\varphi}{1 - f_n}$$

$$B = \frac{\varphi}{f_n} - 0.5$$

and

$$G = \frac{\delta\varphi + y}{\delta f_n + y} - 1$$

with

$$\varphi = y \frac{df_n}{dy} = (\frac{-y}{\delta+1})\left[1 - \frac{(1-y) + (\delta^2 - 1)\bar{q}}{(1-y) - (\delta+1)f_n}\right]$$

Equations (IV.4.9) thus yield

$$\frac{df}{dx} = \frac{\frac{j \, \forall g f}{x} + \lambda g G - \lambda h \, f(f-x) B}{h \, (f-x)^2 - \forall g}$$

$$\frac{dh}{dx} = \frac{-h}{(f-x)} \left(\frac{df}{dx} + j \frac{f}{x} + \lambda A \right)$$

(IV.4.10)

and

$$\frac{dg}{dx} = -h \left[(f-x) \frac{df}{dx} + \lambda f B \right]$$

As discussed previously in Chapter III, there are two different singularities, in addition to the singularity at the center of explosion, which can be directly observed from Eqs. (IV.4.10) These singularities are located at $f = x$ and $h(f-x)^2 = \forall g$. In terms of the reduced variables, F and Z , these singularities are given by

$$F = 1.0 \qquad \text{and} \qquad Z = (1-F)^2 \qquad \text{(IV.4.11)}$$

iii) Solution

Equations (IV.4.10) can be integrated numerically using Runge-Kutta fourth order method, subject to the boundary conditions given by Eqs. (IV.4.2). An iterative procedure must be used to find the correct value of λ which satisfies Eq. (IV.4.8). Since we cannot proceed with the numerical integration till the center of symmetry, due to the existence of the singularity at the center, the solution is based on matching the numerical solution, from $x = 1$ to $x = \bar{x}$, with an asymptotic formula for the non-dimensional velocity, f . However, it can be assumed that the velocity distribution near the center of symmetry is linear, provided that the value of $\bar{x}$ is very small. The value of $\bar{x}$ must be found a priori for each geometrical symmetry.

The y domain in which we are interested ($0 \leqslant y < y_{CJ}$) is divided into small steps, each step (Δy) equals 0.005. The choice of the values of Δx and Δy is based on the grid-independent solution.

If the solution at $y = y_i$ is known, then the solution at $y = y_{i+1}$ ($y_{i+1} = y_i + \Delta y$) is obtained as follows:

a) At a certain value of $y = y_{i+1}$, the boundary conditions f_n , h_n and g_n (at $x = 1$) can be calculated from Eqs. (IV.4.2).

b) An assumed value of the decay coefficient λ_{i+1} is then used to integrate Eqs. (IV.4.10) numerically. The integration is stopped at $x = \bar{x}$.

c) Applying the linear relation between the non-dimensional velocity f and x from $x = \bar{x}$ to $x = 0$, the velocity at the center of symmetry can be obtained by extrapolation.

d) If the absolute value for the velocity at the center of symmetry, which should identically be equal to zero, is greater than the required accuracy, one may repeat the above procedure by changing the assumed λ_{i+1} by $\Delta \lambda$ until the required accuracy is obtained.

e) With the correct value of λ_{i+1} determined, the flow field parameters will be obtained, and then the values of the mass integral, J_1 , and the energy integral, J_2 , can be calculated using Romberg procedure.

f) The whole procedure is repeated for other values of y until the solution is obtained for the whole range of y .

It should be noted that forcing the solution to proceed to too small a value of $\bar{x}$ will throw the solution into the singularity $x = 0$. Also, during the trials of obtaining the correct λ , caution should be exercised lest the solution throw into one or the other of the singularities given by Eq. (IV.4.11).

IV. Results and Conclusions

In order to obtain a numerical solution, it has been assumed that the detonating medium is a stoichiometric methane-air mixture. Therefore, the value of

$\bar{q}$ for such a mixture is 20.0231 and $\delta = 1.3$ (Kamel et al., 1979). For the specific case presented here, Eq. (IV.4.3) yields $y_{CJ} = 0.033786$.

Figures IV.4.1a, b and c show the pressure profiles for planar, cylindrical and spherical geometries with $\delta = 1.3$. At any specified value of y, the pressure immediately behind the wave front is a maximum and falls off to a nearly constant value near the center of symmetry. The fall-off in pressure is greatest for spherical waves, with its greatest value of the decay coefficient λ, and least for the planar waves. As in the case of adiabatic point explosions (Korobeinikov et al., 1969), the pressure ratio at the center decreases first to a minimum before ascending to its Chapman-Jouguet detonation value.

Figures IV.4.2a, b and c and IV.4.3a, b and c show the density and temperature profiles, respectively. These sets of curves are bound to the right by the self-similar solution for the adiabatic point explosion. It is evident that the density at the center is always zero, corresponding to infinite temperature, a characteristic property of the solution obtained for an inviscid, non-conducting and non-radiating gas. As shown in Figs. IV.4.2, nearly all of the mass of the gas engulfed by the blast is concentrated close to the wave front for the self-similar case and is then distributed gradually in the flow field for $y > 0$, until the Chapman-Jouguet state where the distribution of the mass is more uniform. It is seen also that the fall-off in density is greatest for spherical waves, the same tendency in pressure profiles, and least for planar waves.

The particle velocites, as shown in Figs. IV.4.4a, b and c, have a maximum value immediately behind the wave front and decrease to zero at the center of symmetry. At any given x and y, the spehrical flow velocity is the lowest. With larger values of λ, and for planar waves the velocity increases.

The integral curves for different values of y ranging from $y = 0$ to $y = 0.033$, are projected on the $F - Z$ phase plane, for $j = 0$, 1 and 2 in Figs. IV.4.5a, b and c, respectively. Integral curves for $y = 0$ represent the solution at the initial instance, while the initiation energy, E_i, is still the predominant parameter governing the flow field. They are, of course, identical to

those for the self-similar point explosions in an inert gas (Sedov, 1957). As the front decays and, concomitantly, the role of chemical energy becomes more prominent, the value of y increases until it, finally, asymptotically reaches the steady Chapman-Jouguet value characterizing the explosion. Each integral curve starts from a particular point on the Hugoniot curve, specified by the conditions corresponding to $x = 1$. It can be directly observed from Figs. IV.4.5 that the solutions are free from singularities since the locii of the singularity $Z = (1-F)^2$ and the singularity $F = 1$ do not intersect with any of the integral curves. Since a singularity does exist at the C-J condition, the corresponding integral curve is not included. One, however, may approach that condition sufficiently to get a good indication of the quantitative and qualitative nature of the solution.

The mass integral, J_1, and the energy integral, J_3, are depicted in Figs. IV.4.6 and IV.4.7, respectively, for different values of j. These curves start from their respective values for the inert self-similar point explosions at $y = 0$ and end at $y = 0.033$ which nearly equals y_{CJ}. The mass integral is used to check the accuracy of the solution and its exact value is given by Eq. IV.4.6 that some error is obtained in the mass integral which reflects inaccuracy in the density distribution within the flow field. This error, however, is expected due to the quasi-similar approximation which causes the solution to be accurate near the self-similar range and just behind the wave front. The energy integral may be used to iterate on the decay coefficient, which is another method to obtain the correct λ, but it is used here to obtain the non-dimensional wave radius, $\mathcal{F}$, using Eq. IV.4.5.

The decay coefficients, λ, are shown as functions of y in Fig. IV.4.8. An iterative procedure was performed to obtain the correct value of λ which satisfies the condition of zero particle velocity at the center of symmetry. Any assumed value of λ less or greater than the correct one results in a numerical instability. This occurs due to the two different singular points in the flow field, given by Eq. (IV.4.11), which would pull the integral curve to either of them. It was observed that the numerical instability, due to these singularities, may occur in two different forms. The dependent variables f and h may take negative values or may take values greater than the preceeding ones during

the numerical integration of the governing equations. Therefore, it is recommended to use the conditional "IF" statement inside the integration procedure in the computer program to avoid the singular points and save computational time during seeking the correct λ. It was also found that a deviation in the order of 1×10^{-4} in the correct value of λ may lead to the domain of singularities. Because of the singularity $F = 1.0$, the numerical integration of the governing equations was stopped at $\bar{x} = 0.02$ for planar and cylindrical waves and at $\bar{x} = 0.04$ for spherical waves. A linear extrapolation was then applied to f in order to obtain $f(0, y)$. The solution was considered correct when $|f(0,y)| \leqslant 1 \times 10^{-4}$. In order to achieve this accuracy, the improvement in the value of λ was in the order of 1×10^{-4} for planar waves, 1×10^{-6} for cylindrical waves and 1×10^{-8} for spherical ones.

The non-dimensional radius, $\mathcal{J}$, is plotted as a function of the parameter y in Fig. IV.4.9. It appears from this figure that, for all practical purposes, the Chapman-Jouguet state can be considered as well established by the time $\mathcal{J} = 1$. This means that the Chapman-Jouguet condition is practically achieved when $r_n = r_o$. This radius, according to our definition of r_o, is determined by the value of the initiation energy, E_i, rather than by the exothermic energy of the detonating medium, q. In view of the fact that the amount of overdrivenness of the detonation wave is primarily affected by the initiation energy, this result is not altogether surprising.

The results which are obtained here for the inviscid solution can be compared with those obtained by Kamel et al. (1979). The same problem is solved by two different methods. Kamel used the phase space method of solution, while in this work the quasi-similar technique of Oshima is used. The results in the two cases are qualitatively similar. The quasi-similar technique fails to obtain the values of the gasdynamic parameters at the Chapman-Jouguet state which represents a singular point in the solution domain. Therefore, the solution is stopped at $y = 0.033$ which is approaching the y_{CJ} value of 0.033786. However, the quasi-similar technique is easier to perform and it is faster to yield results in a general qualitative manner.

Figures from IV.4.10a to IV.4.17 show the comparison between the results of the

two methods for the pressure profiles, the density profiles, the temperature profiles, the velocity profiles, the integral curves in the F - Z phase plane, the energy integral, $\mathcal{J}_3$, the decay coefficient, λ , and the non-dimensional radius, $\mathcal{J}$, respectively, for different values of $\mathcal{Y}$. From these figures, the two methods of solution appear close enough to warrant the use of the quasi-similar approximation.

Figure Captions

Fig. IV.4.1 (a), (b) & (c)

> Non-dimensional pressure profiles for planar, cylindrical and spherical waves, respectively, at different values of y with $\bar{q} = 20.0231$ and $\gamma = 1.3$.

Fig. IV.4.2 (a), (b) & (c)

> Non-dimensional density profiles for planar, cylindrical and spherical waves, respectively, at different values of y with $\bar{q} = 20.0231$ and $\gamma = 1.3$.

Fig. IV.4.3 (a), (b) & (c)

> Non-dimensional temperature profiles for planar, cylindrical and spherical waves, respectively, at different values of y with $\bar{q} = 20.0231$ and $\gamma = 1.3$.

Fig. IV.4.4 (a), (b) & (c)

> Non-dimensional velocity profiles for planar, cylindrical and spherical waves, respectively, at different values of y with $\bar{q} = 20.0231$ and $\gamma = 1.3$.

Fig. IV.4.5 (a), (b) & (c)

> Integral curves in the F-Z phase plane for planar, cylindrical and spherical waves, respectively, at different values of y with $\bar{q} = 20.0231$ and $\gamma = 1.3$.

Fig. IV.4.6 Mass integral $\mathcal{J}_1$ as a function of y with $\bar{q} = 20.0231$ and $\gamma = 1.3$ while $j = 0$, 1 and 2.

Fig. IV.4.7 Energy integral $\mathcal{J}_3$ as a function of y with $\bar{q} = 20.0231$ and $\gamma = 1.3$ while $j = 0$, 1 and 2.

223

Fig. IV.4.1a

Fig. IV.4.1b

Fig. IV.4.1c

Fig. IV.4.2a

Fig. IV.4.2b

$$j = 2$$
$$\gamma = 1.3$$

y = 0.0
= 0.005
= 0.01
= 0.015
= 0.02
= 0.025
= 0.03
= 0.033

h/h_n
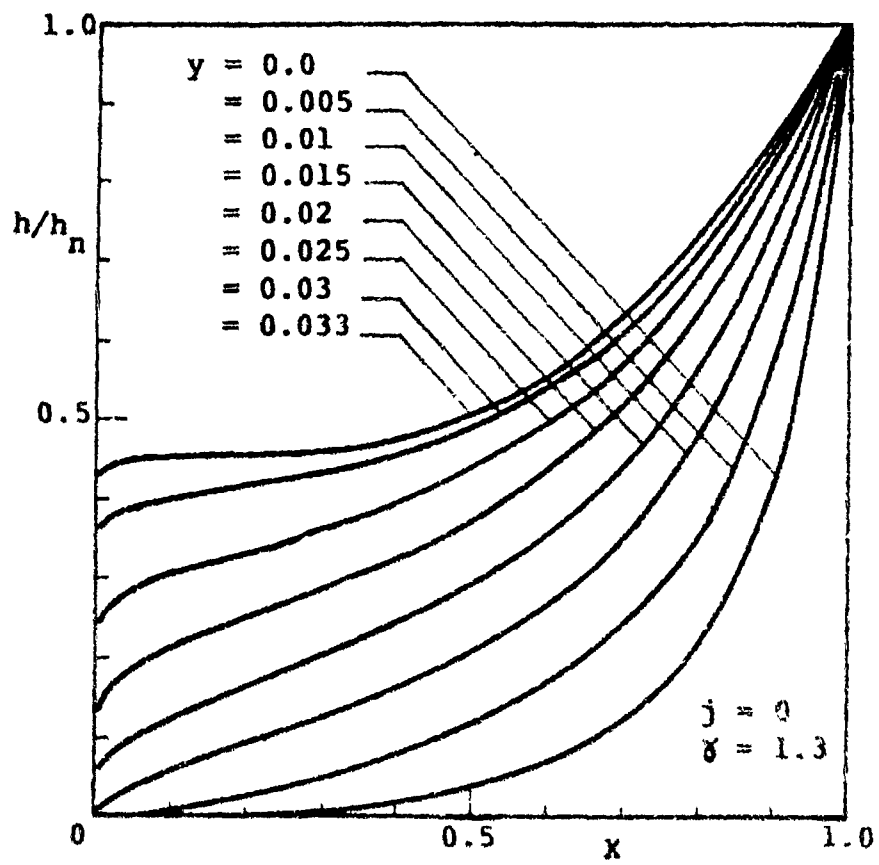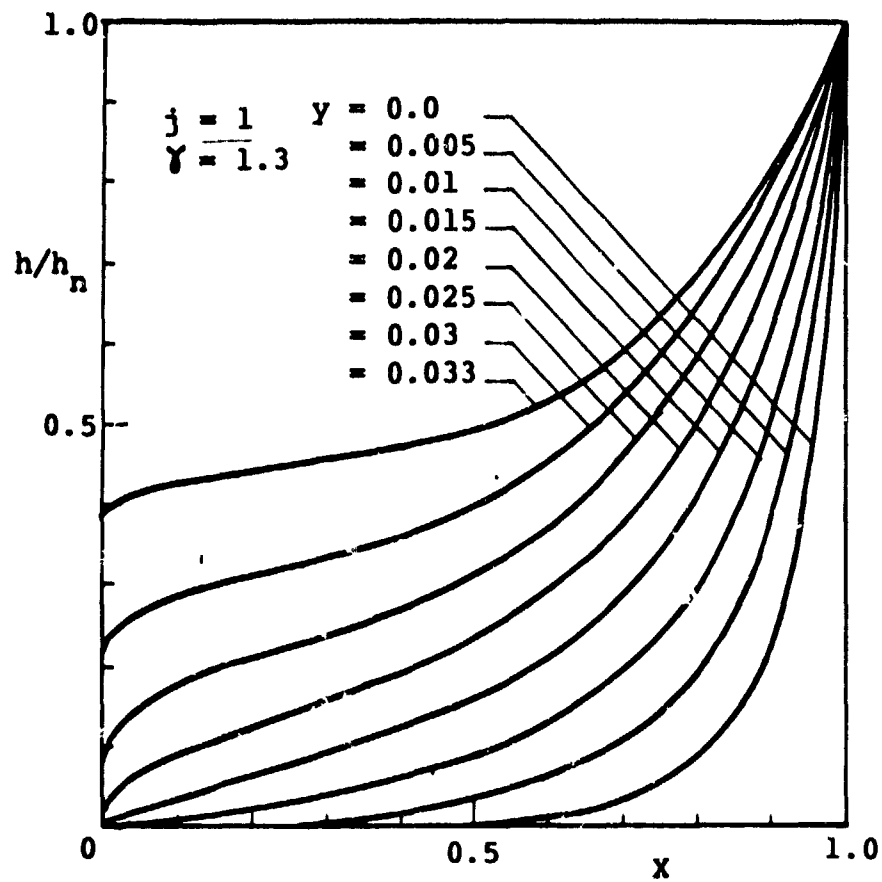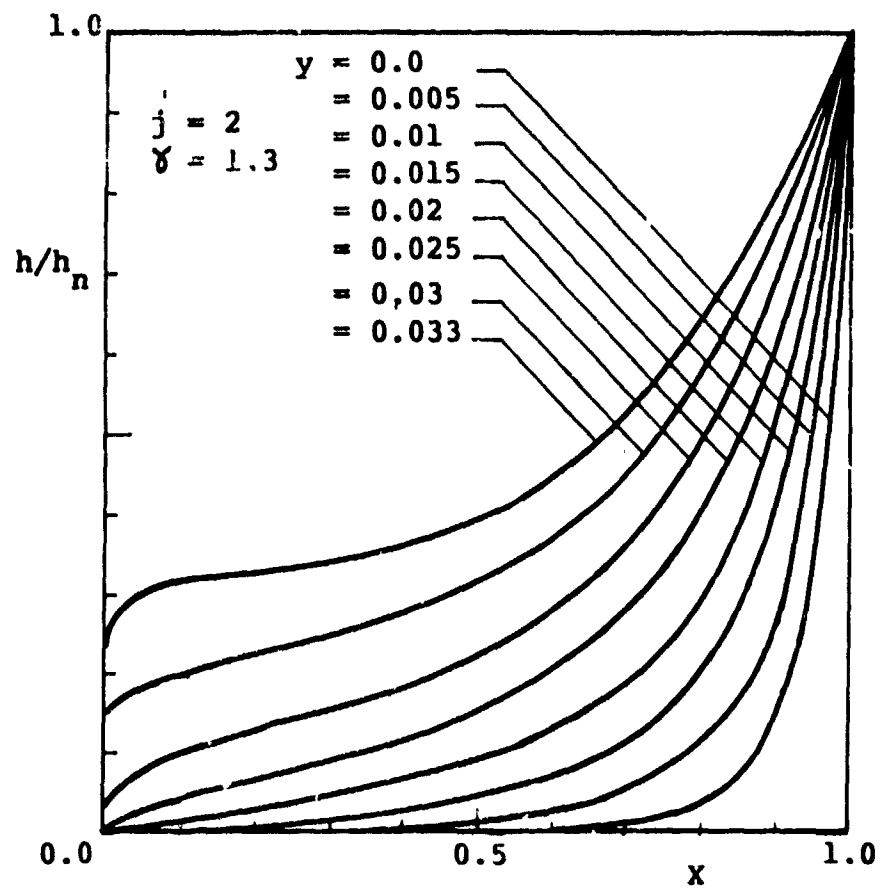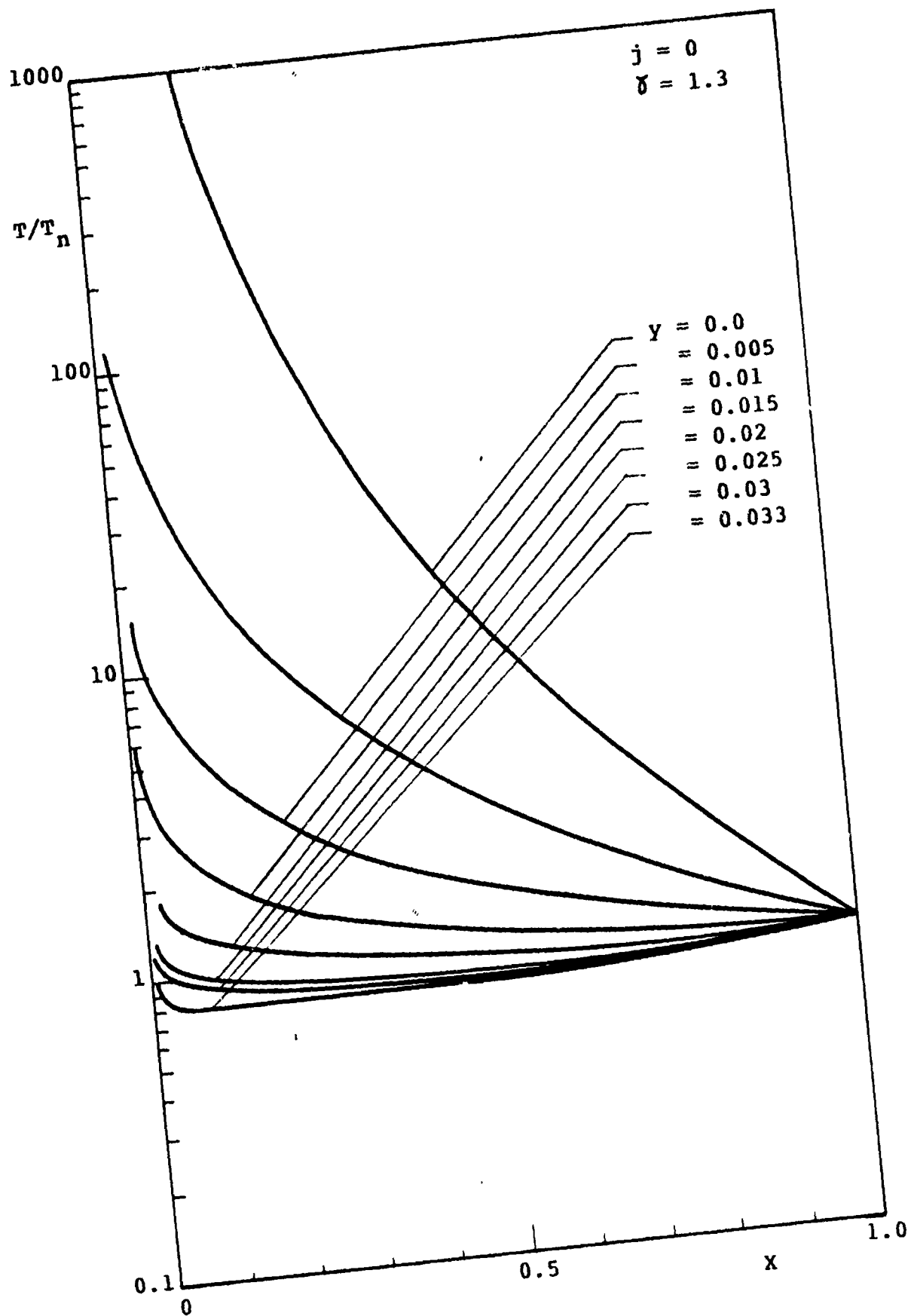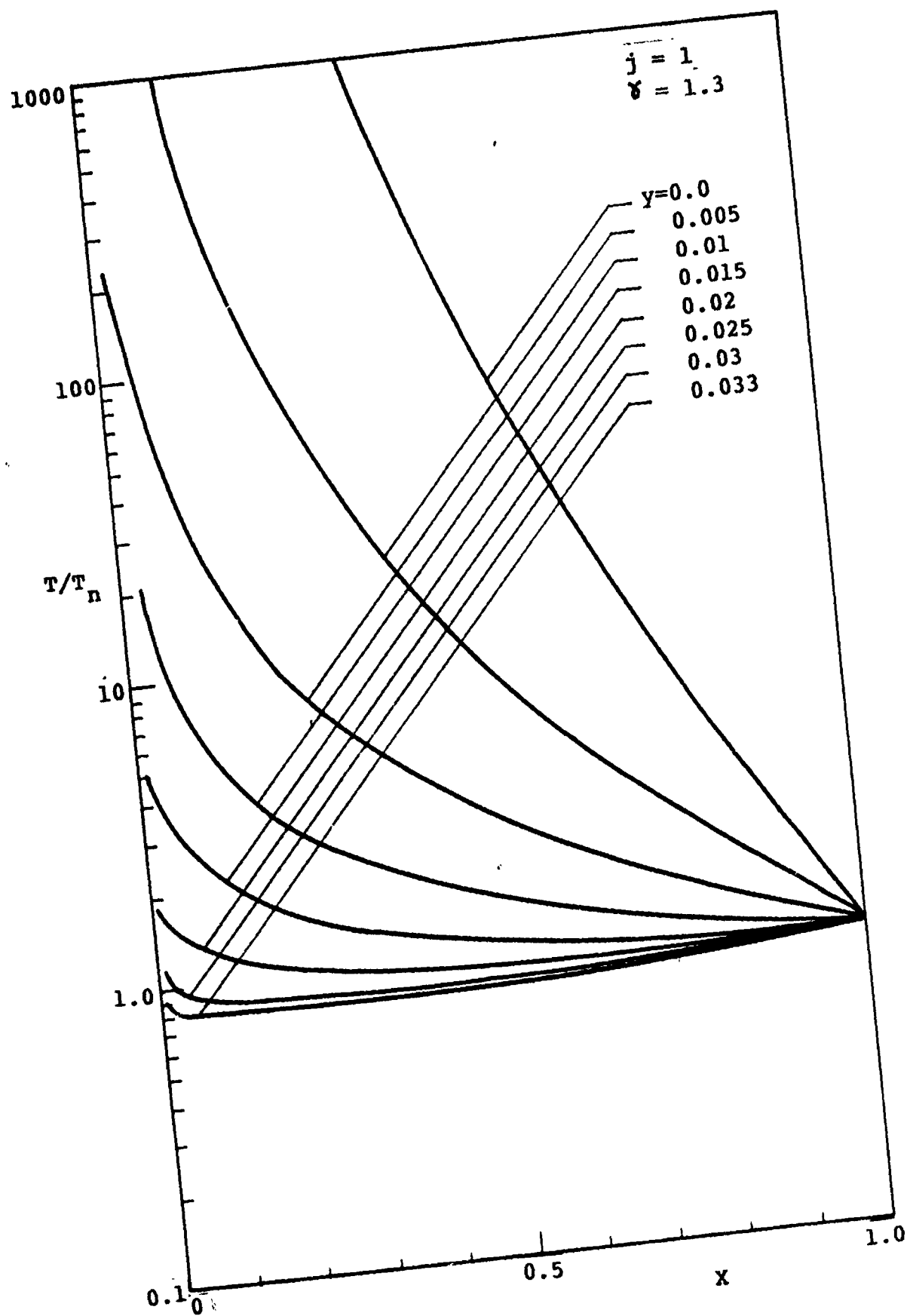
Fig. IV.4.2c

Fig. IV.4.3a

Fig. IV.4.3b
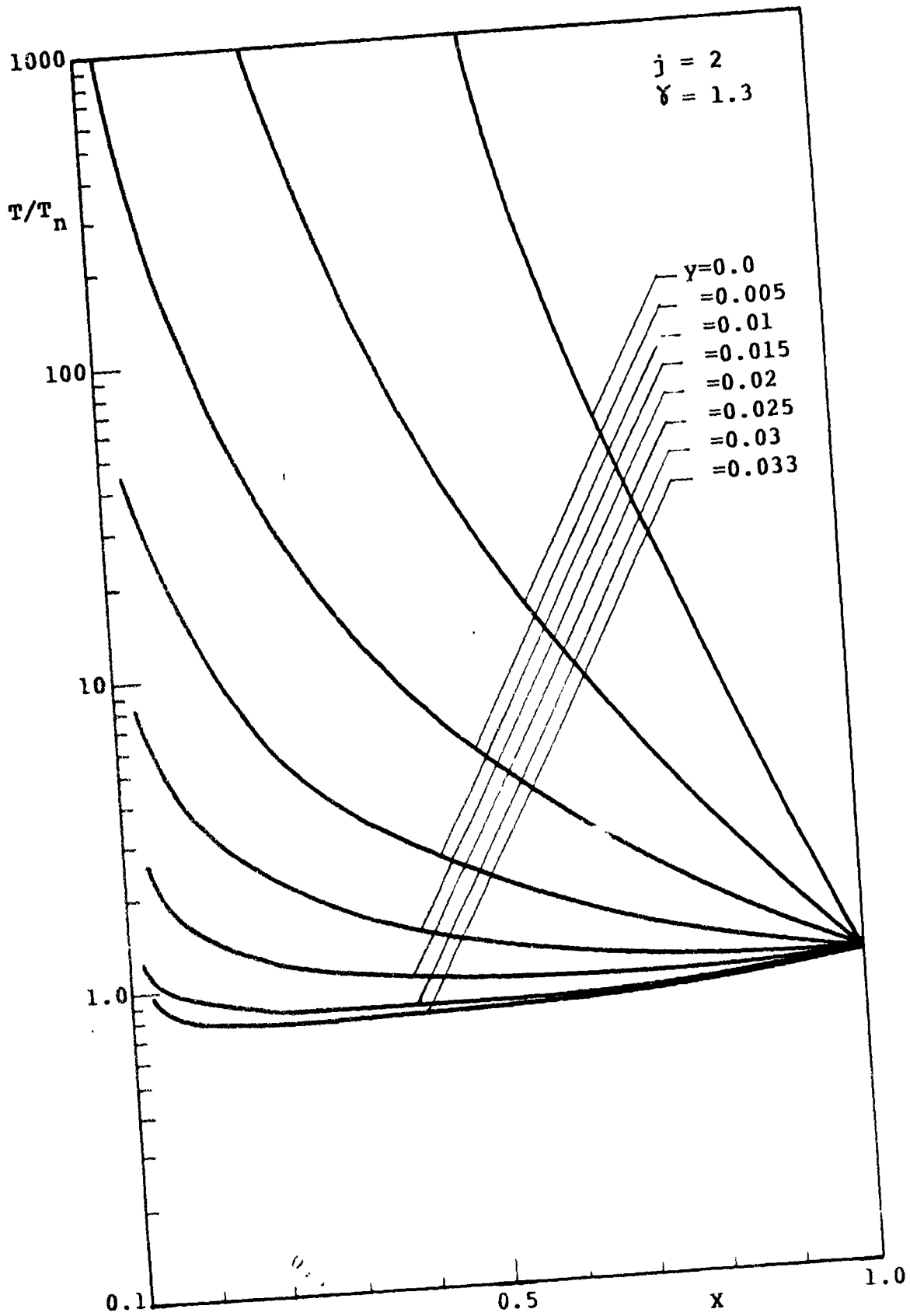
Fig. IV.4.3c
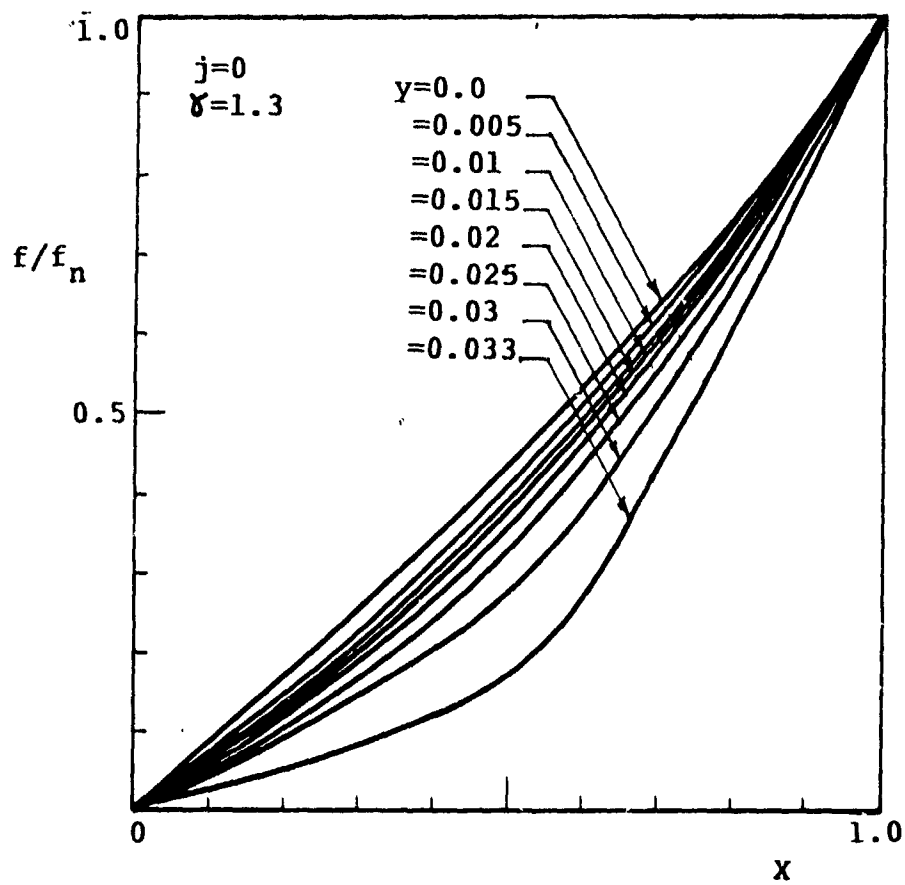
Fig. IV.4.4a

Fig. IV.4.4b
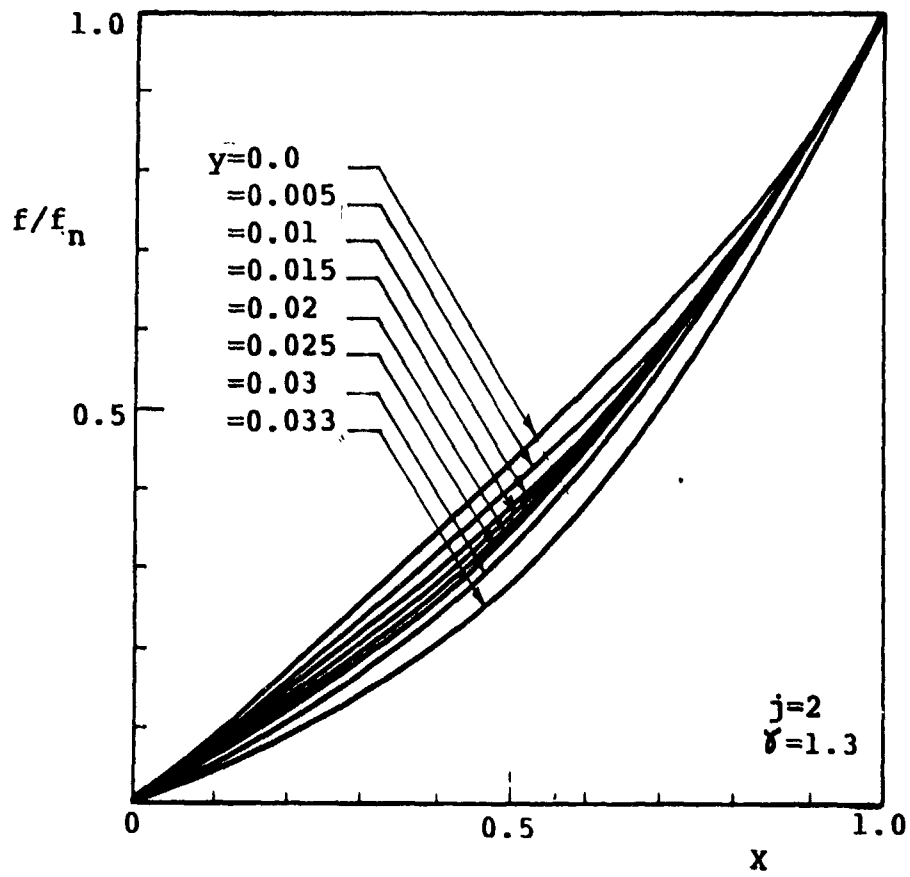
Fig. IV.4.4c
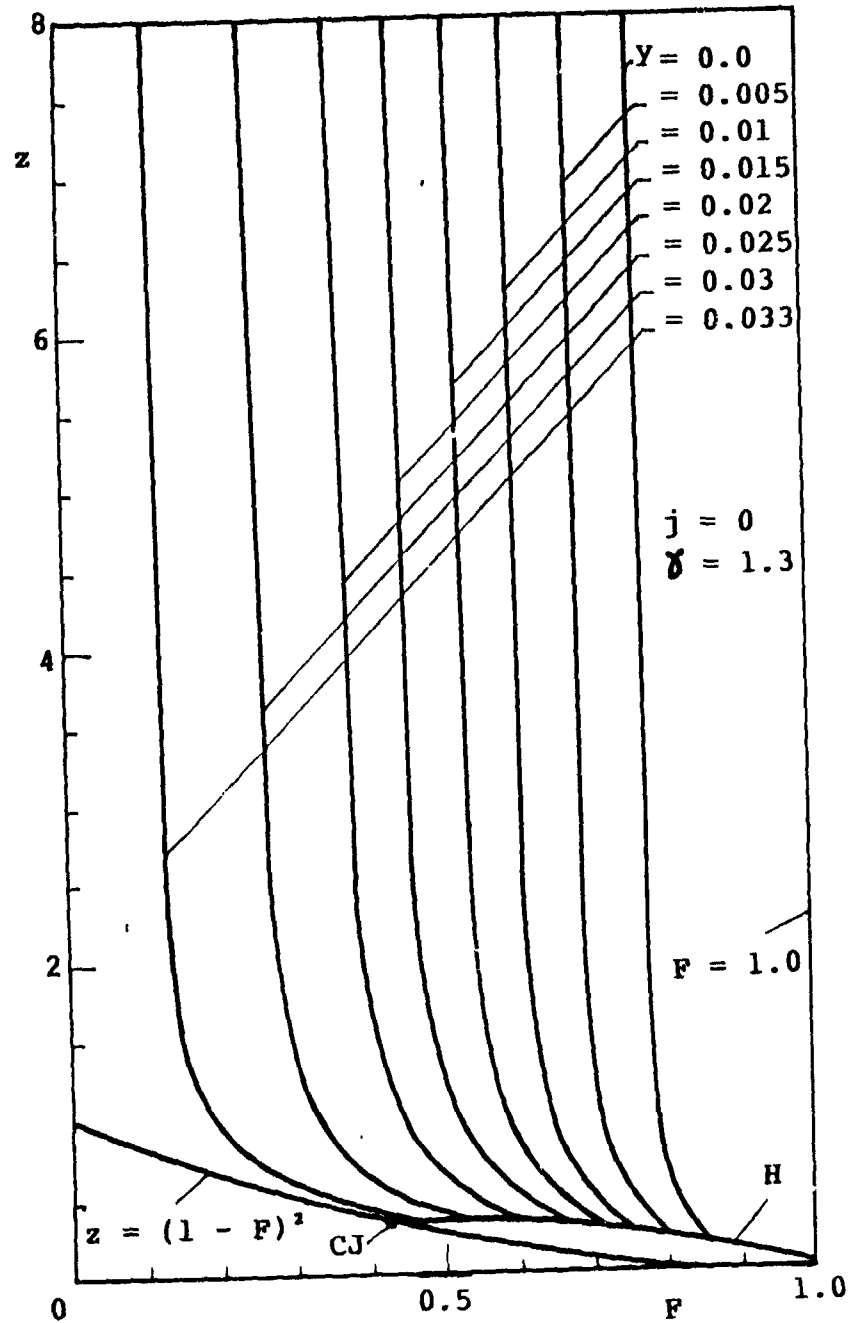
Fig. IV.4.5a
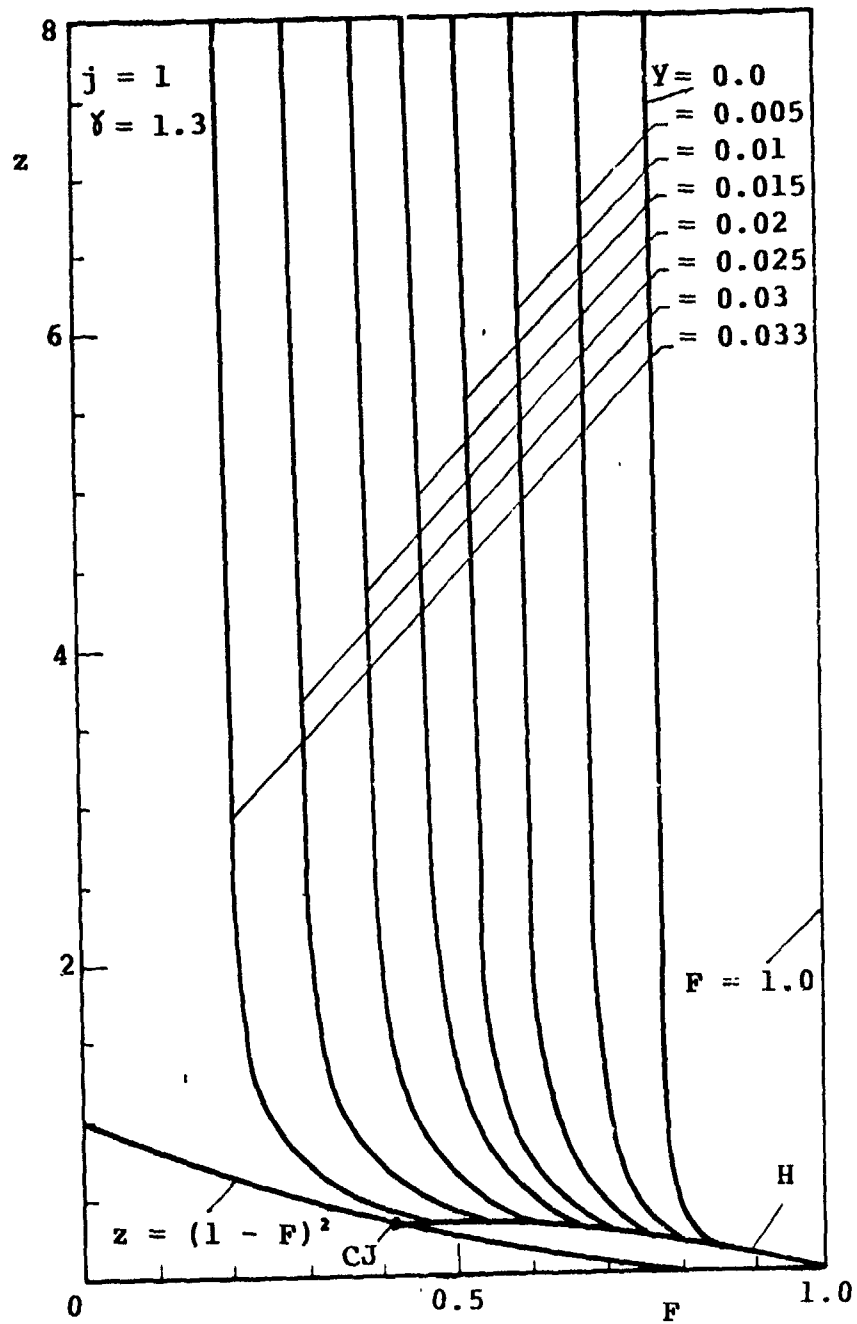
Fig. IV.4.5b
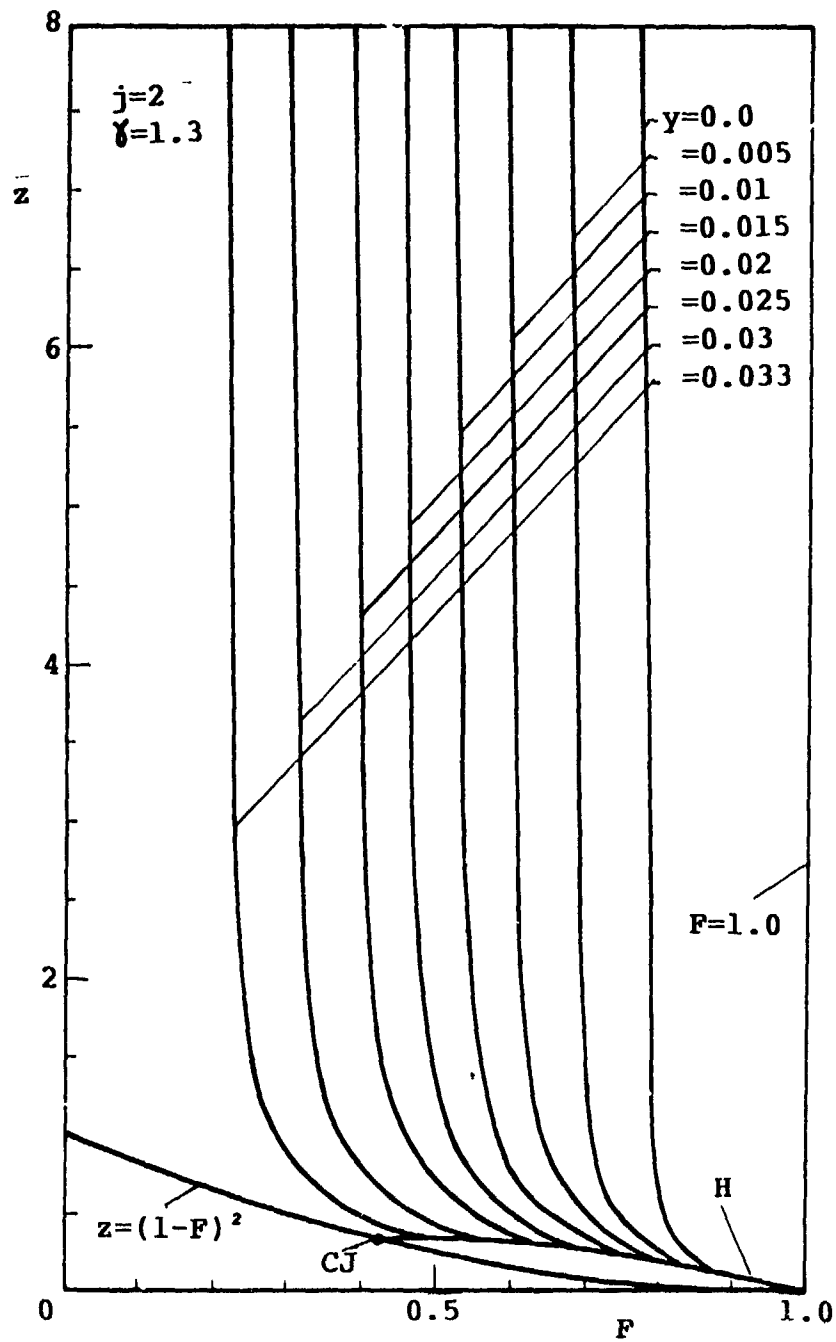
Fig. IV.4.5C
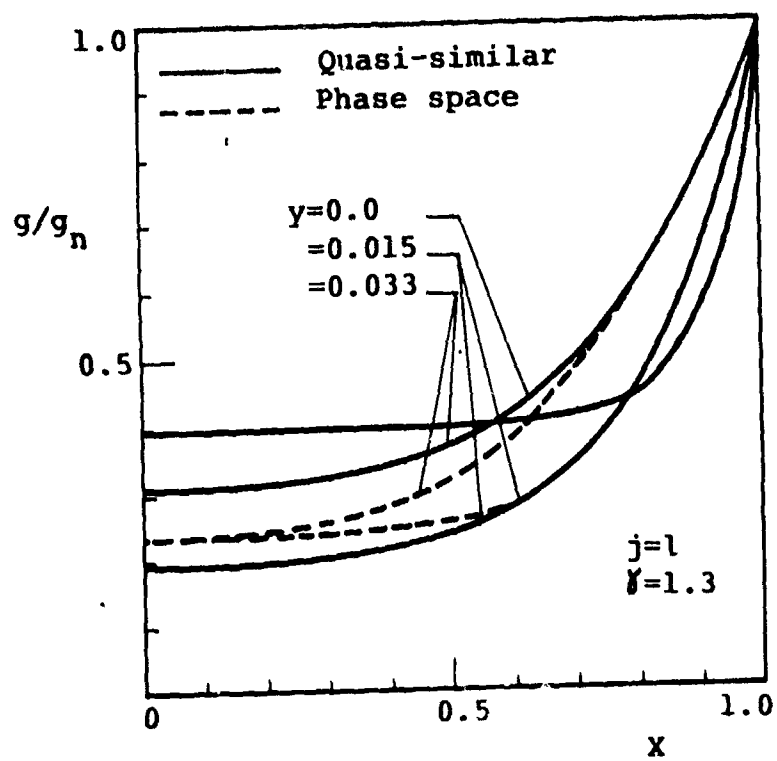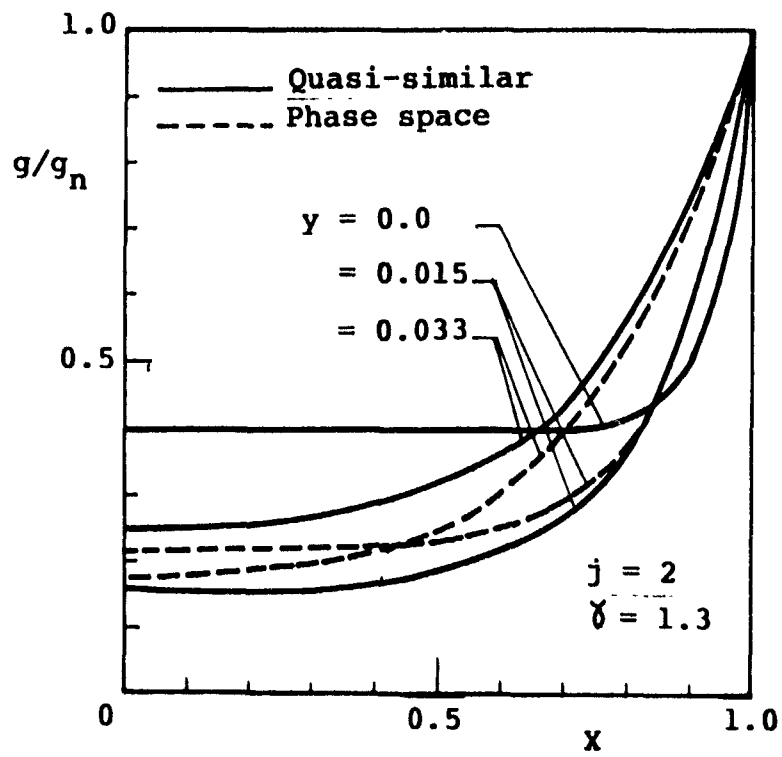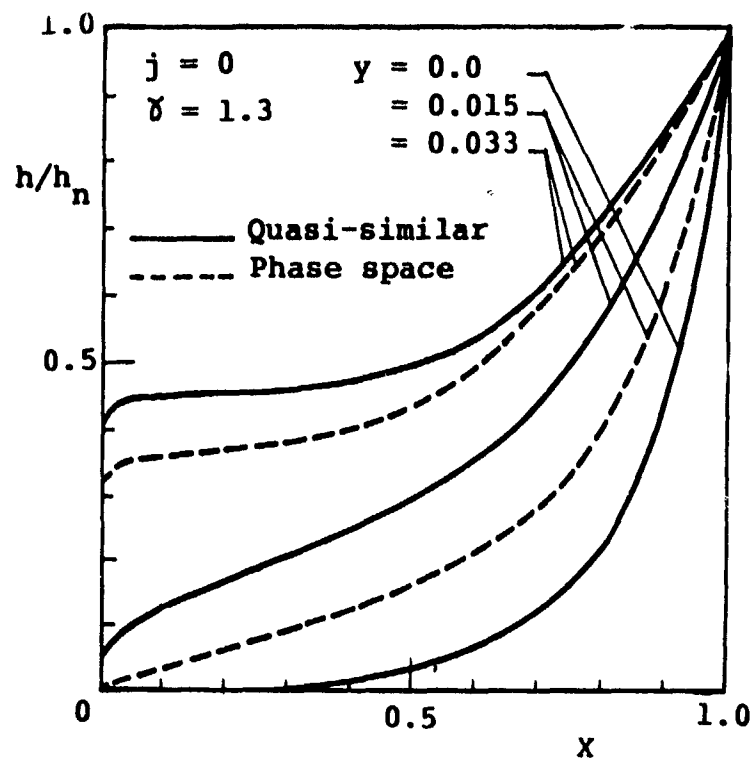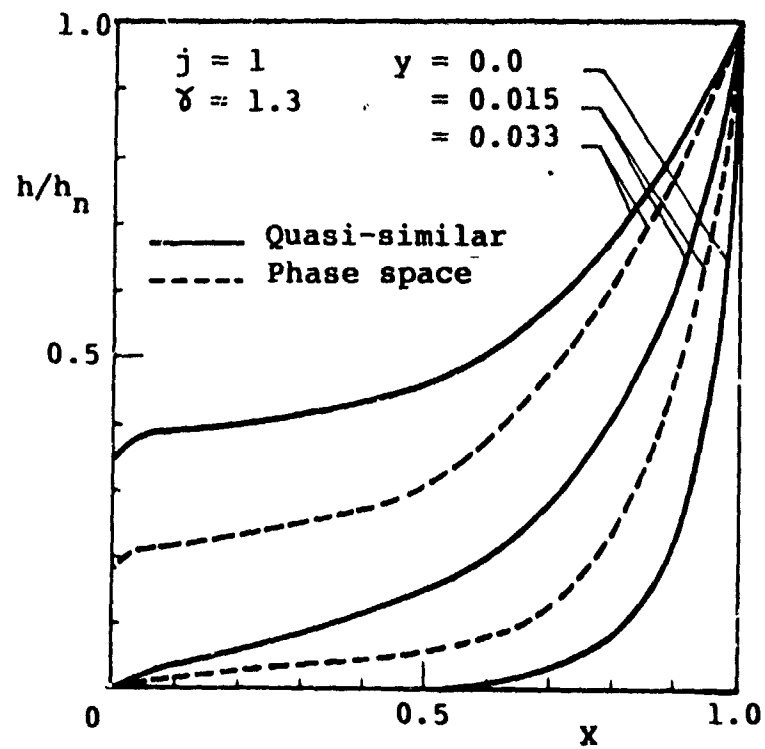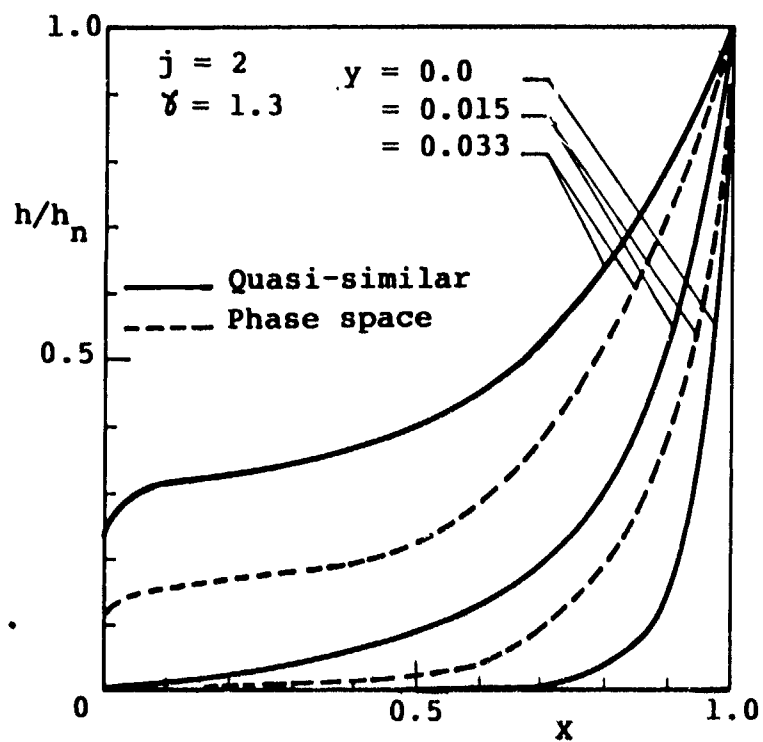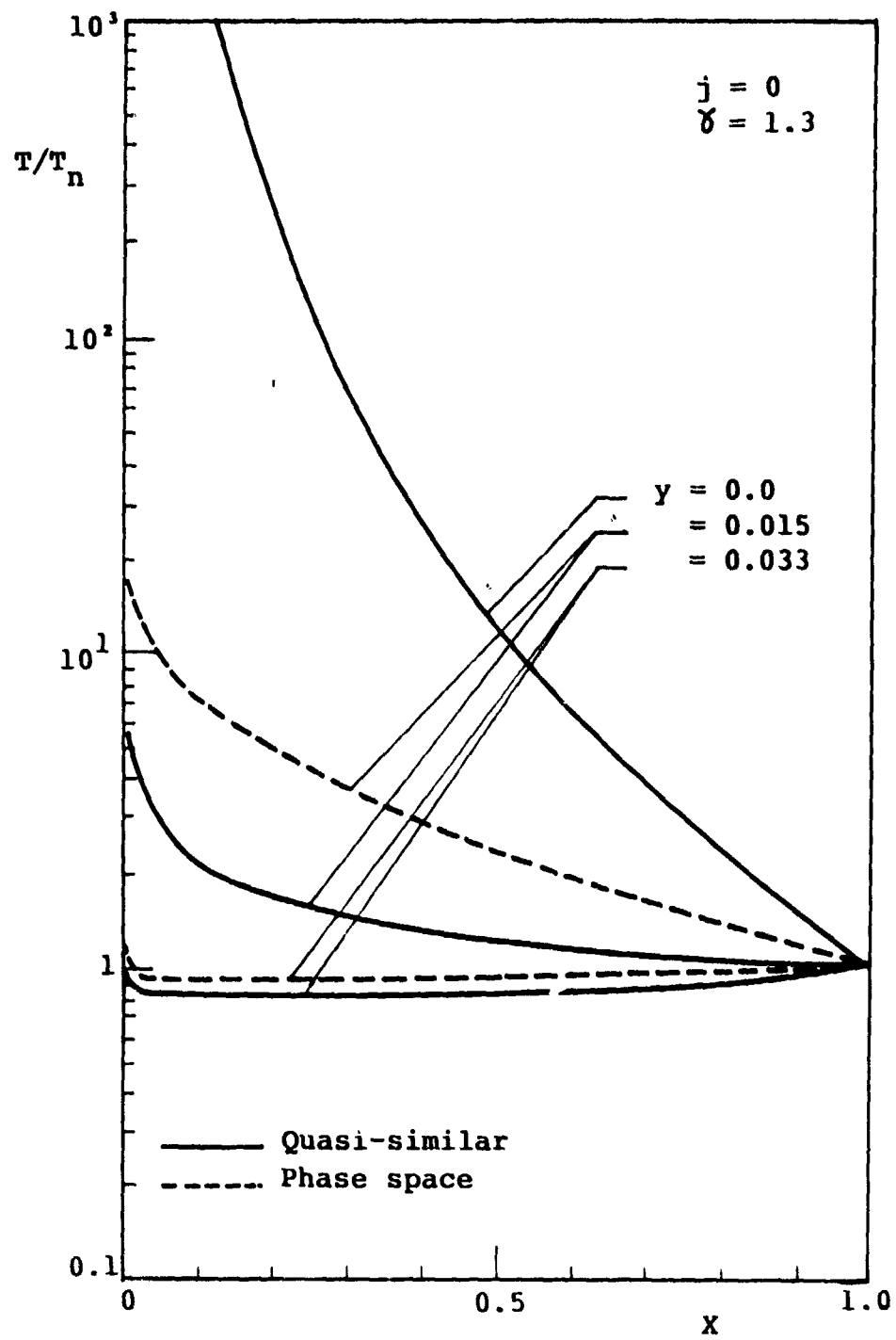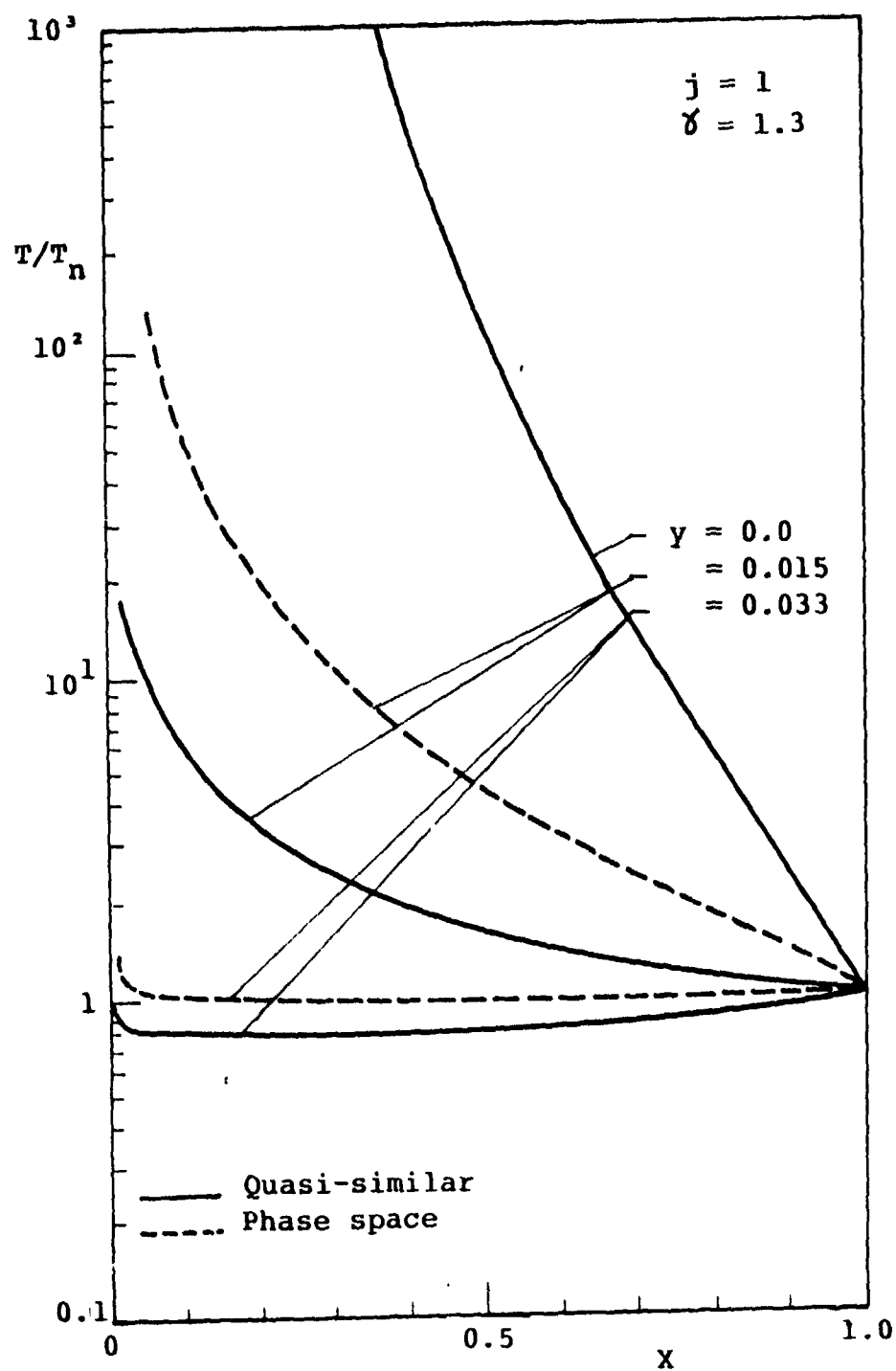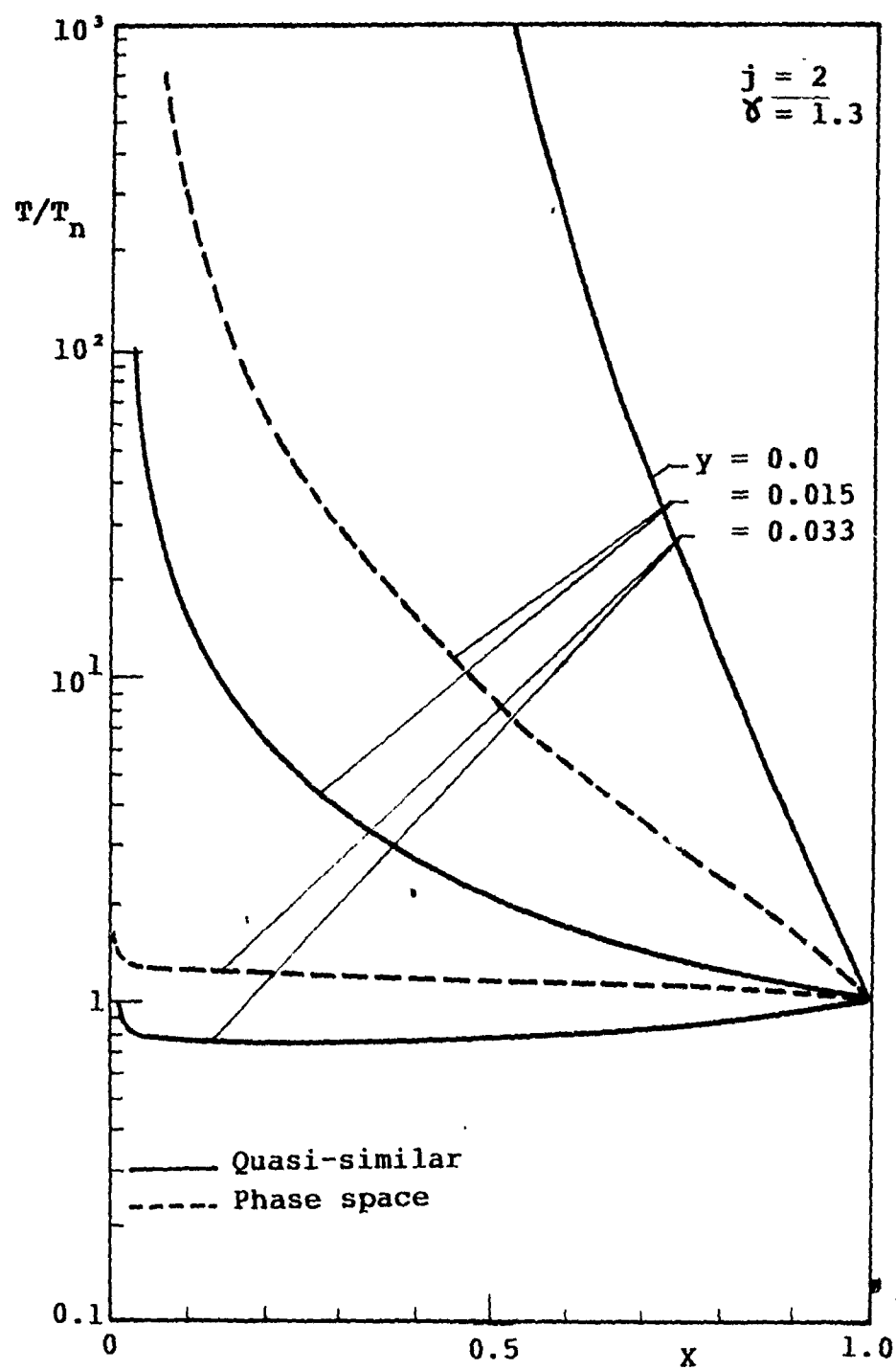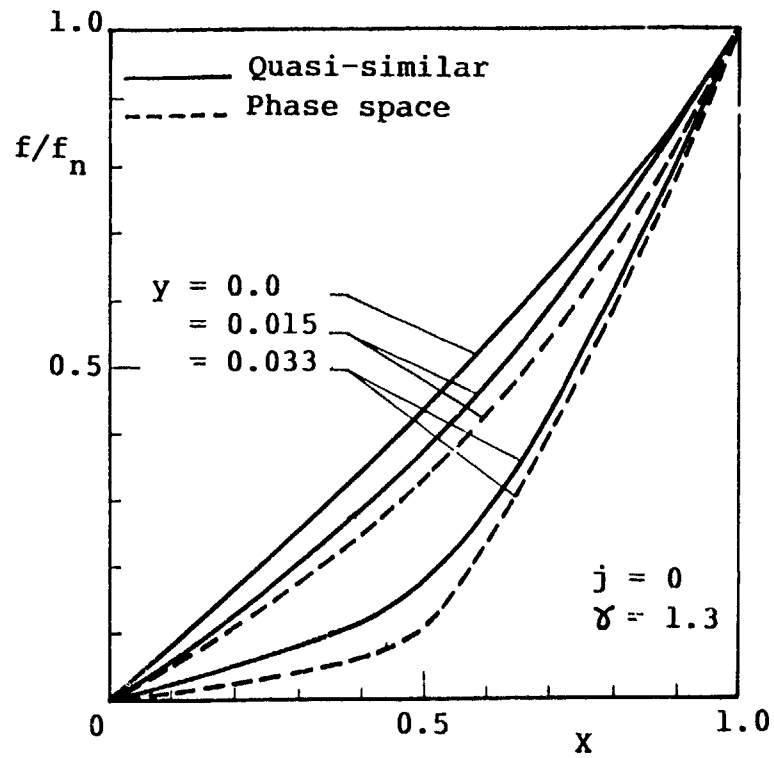
Fig. IV.4.6

Fig. IV.4.7

240
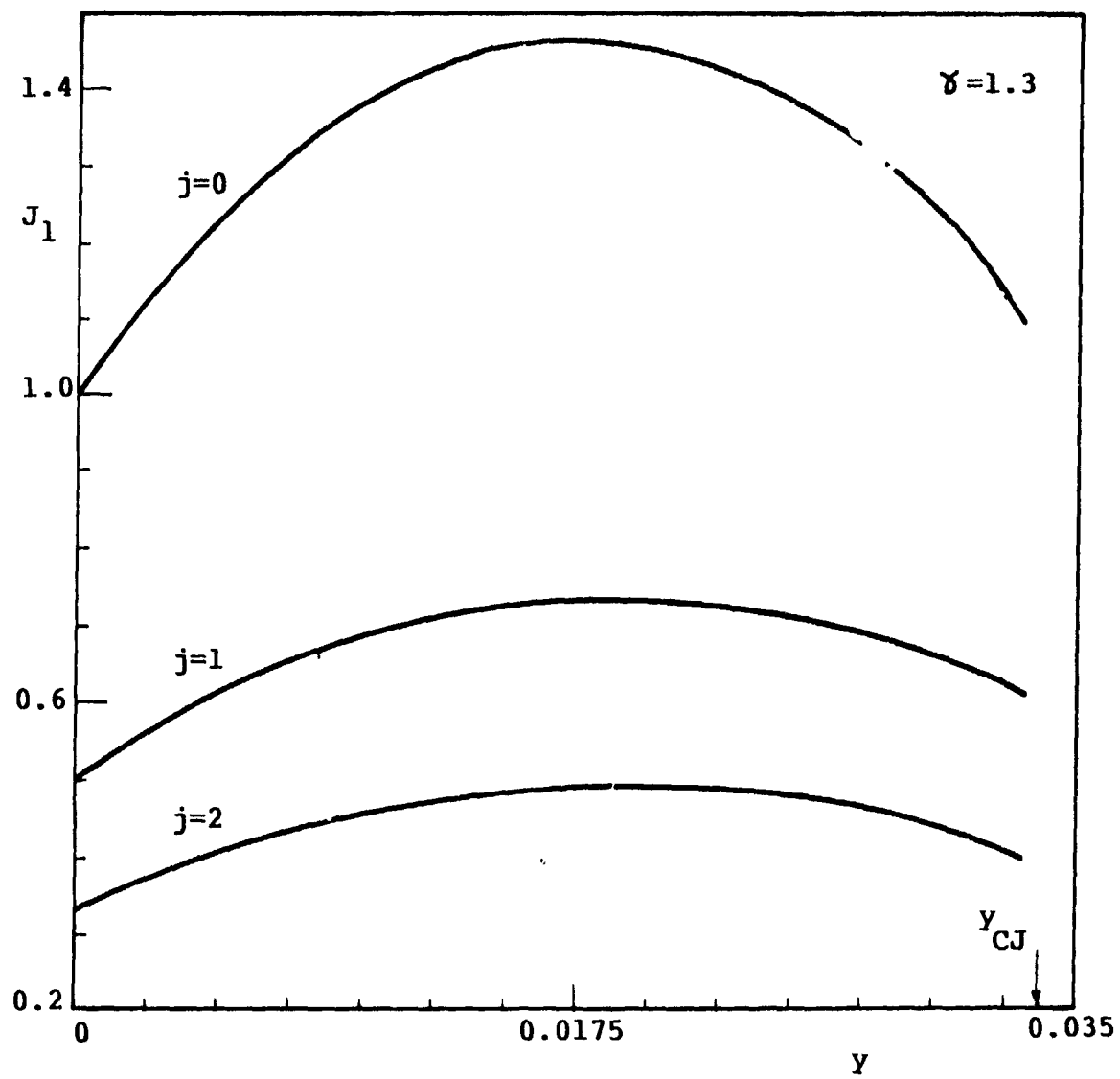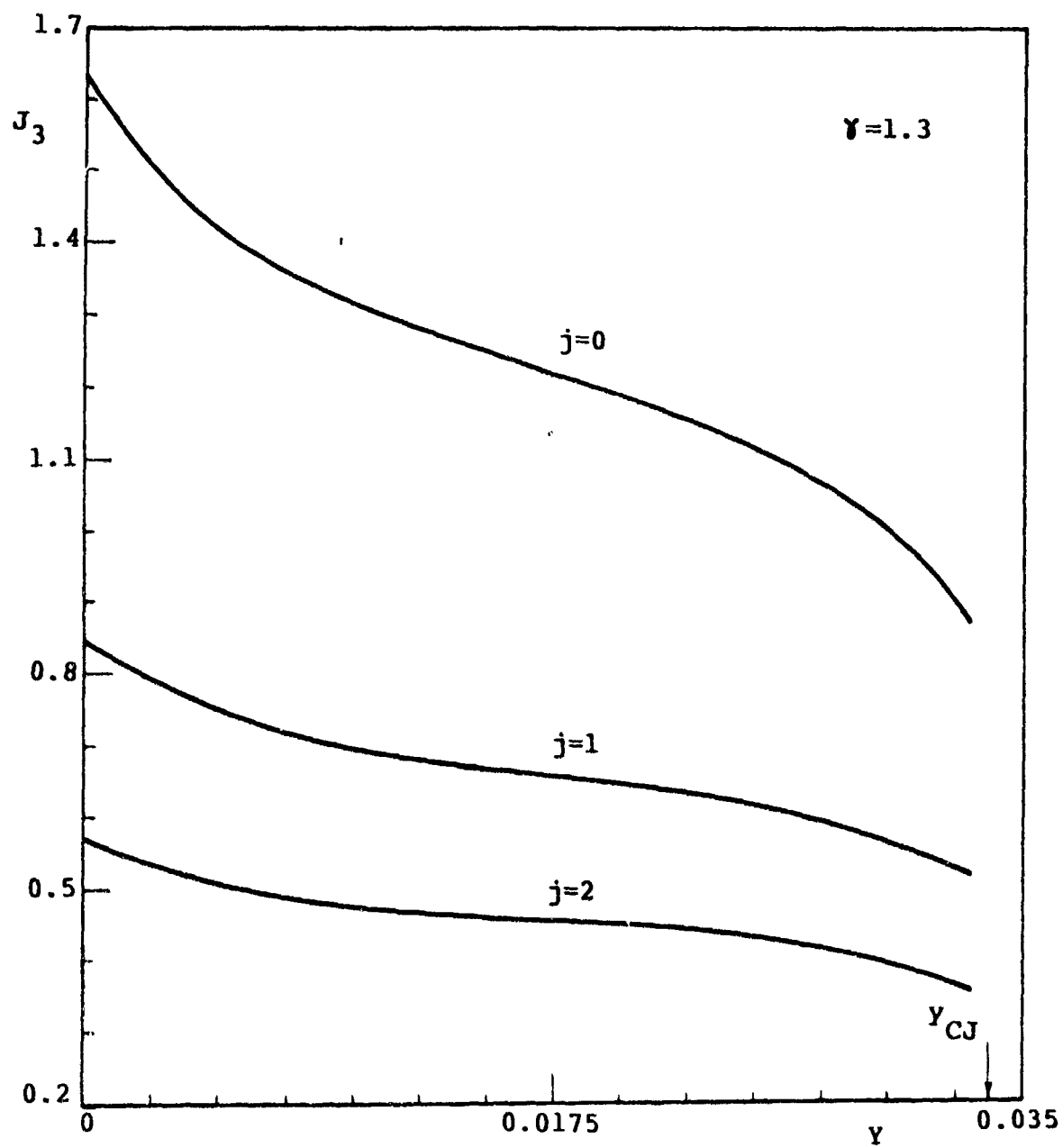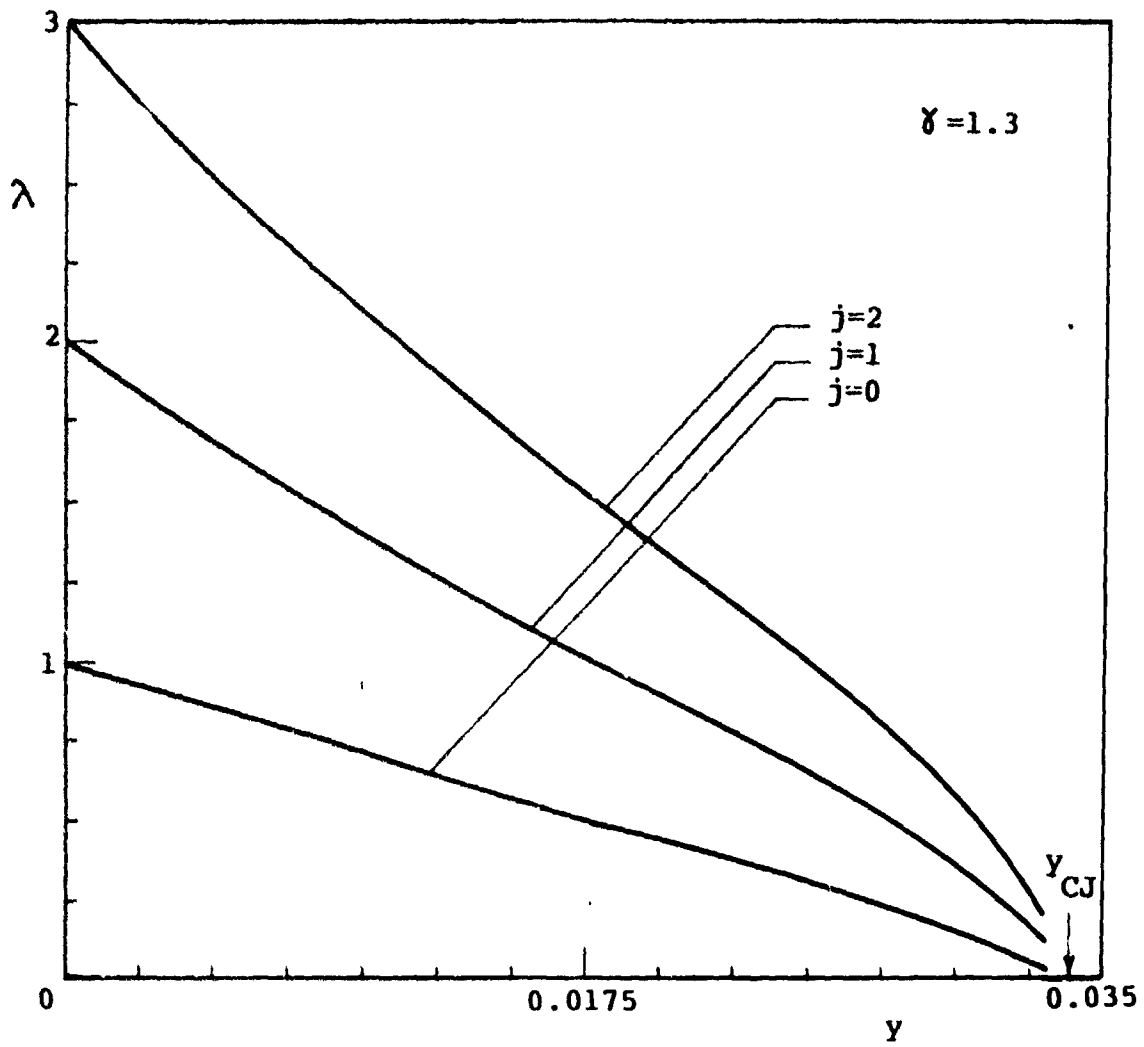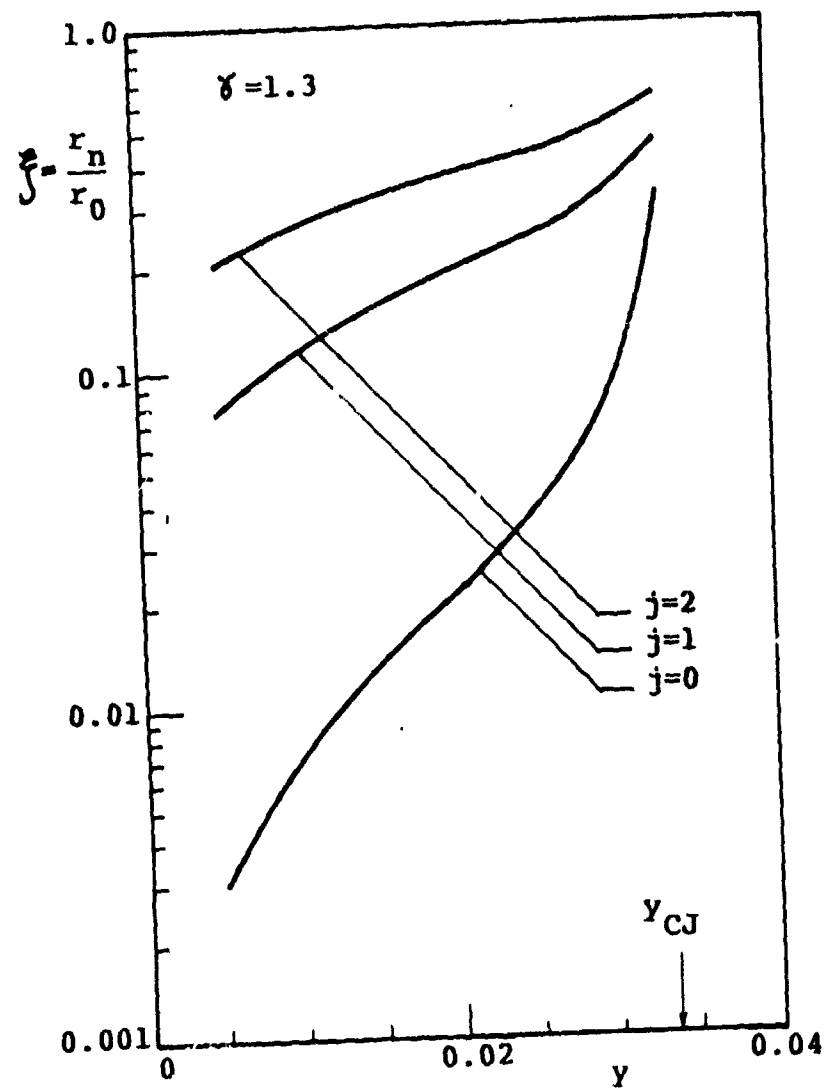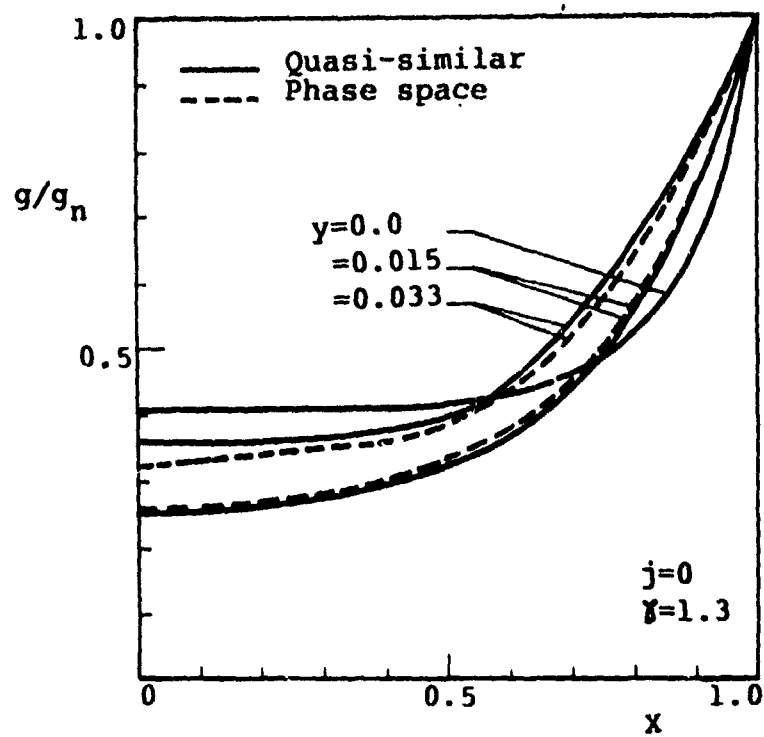
Fig. IV.4.8

Fig. IV.4.9

Fig. IV.4.10a

Fig. IV.4.10b

Fig. IV.4.10c

Fig. IV.4.11a

Fig. IV.4.11b

Fig. IV.4.11c
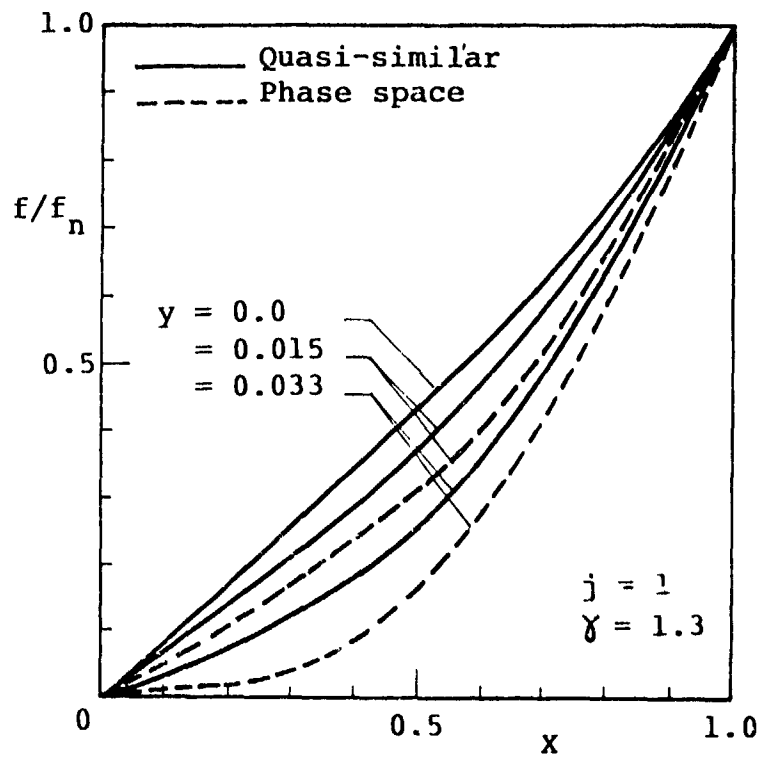
Fig. IV.4.12a
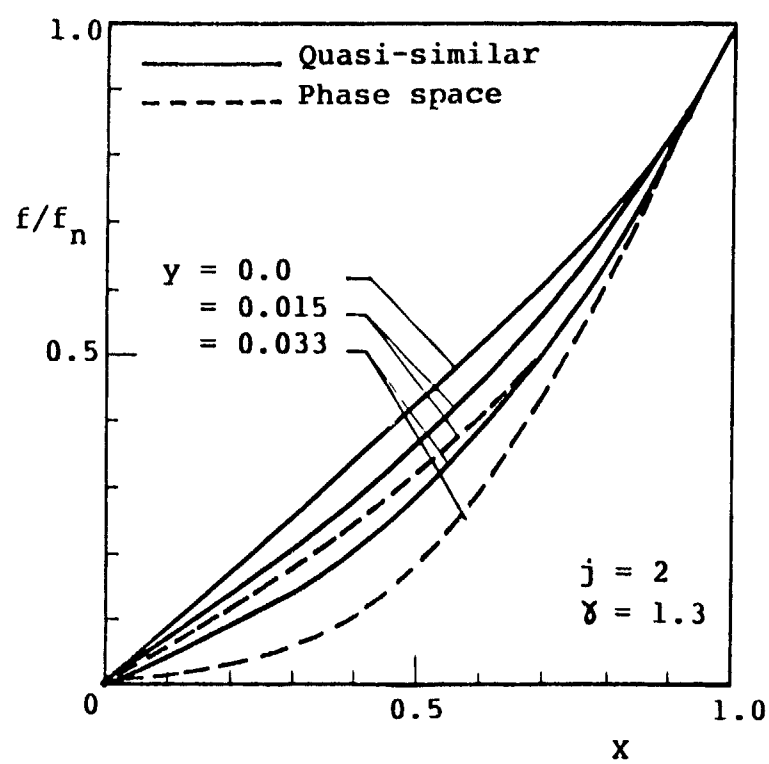
Fig. IV.4.12b

250

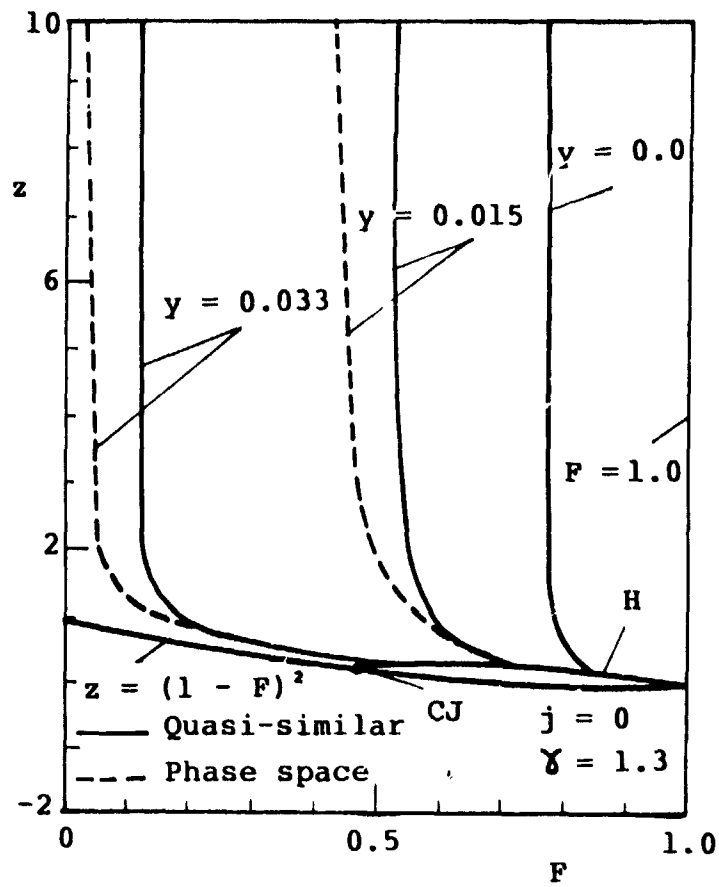
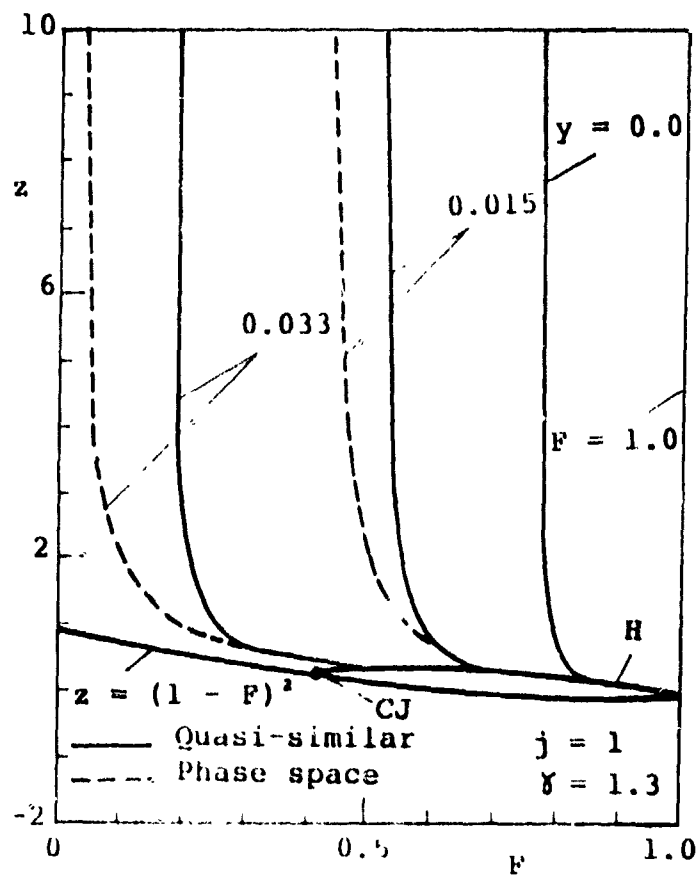Fig. IV.4.12c

Fig. IV.4.13a

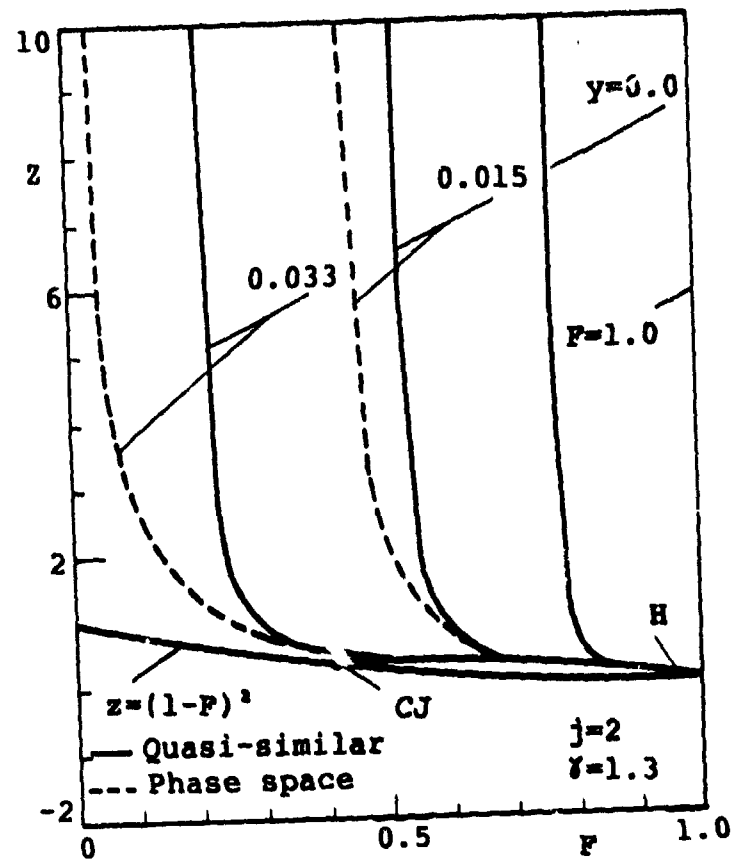Fig. IV.4.13b

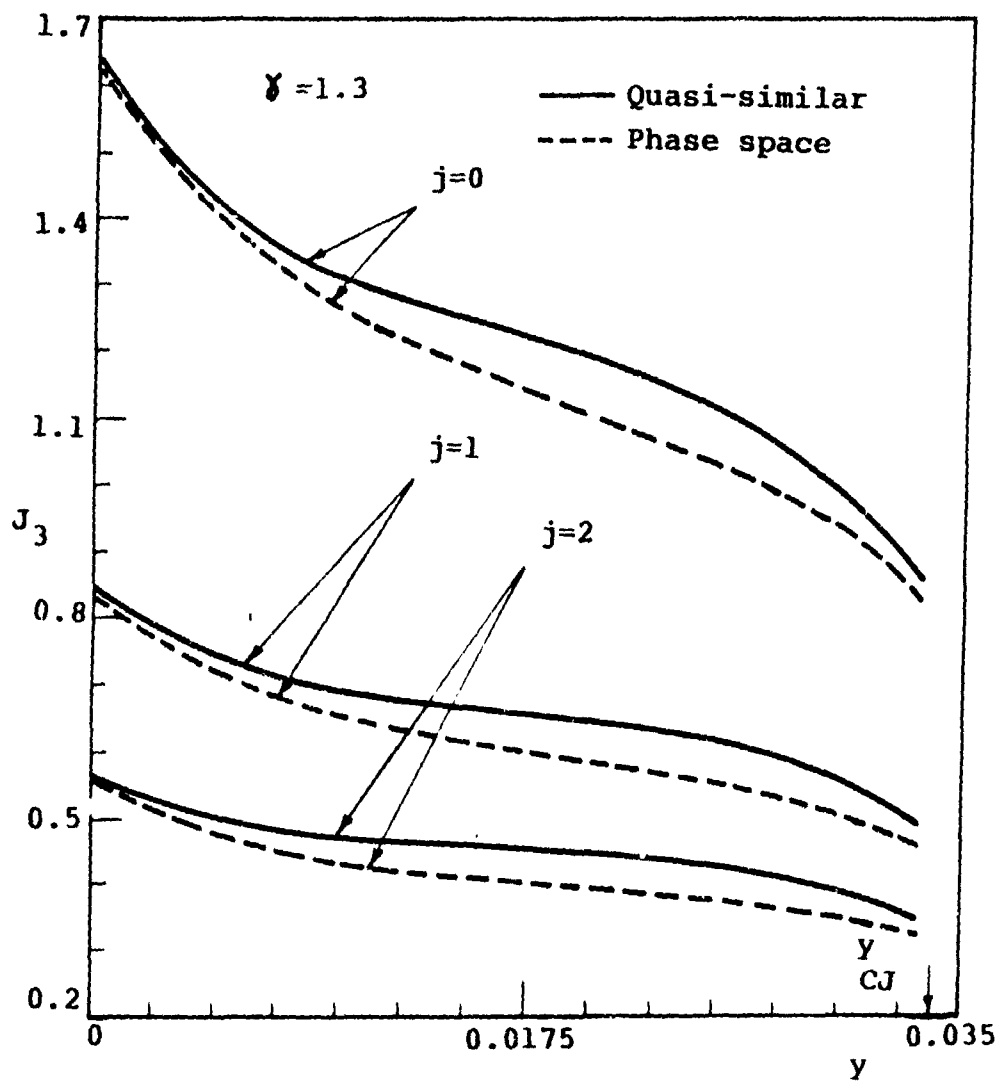Fig. IV.4.13c

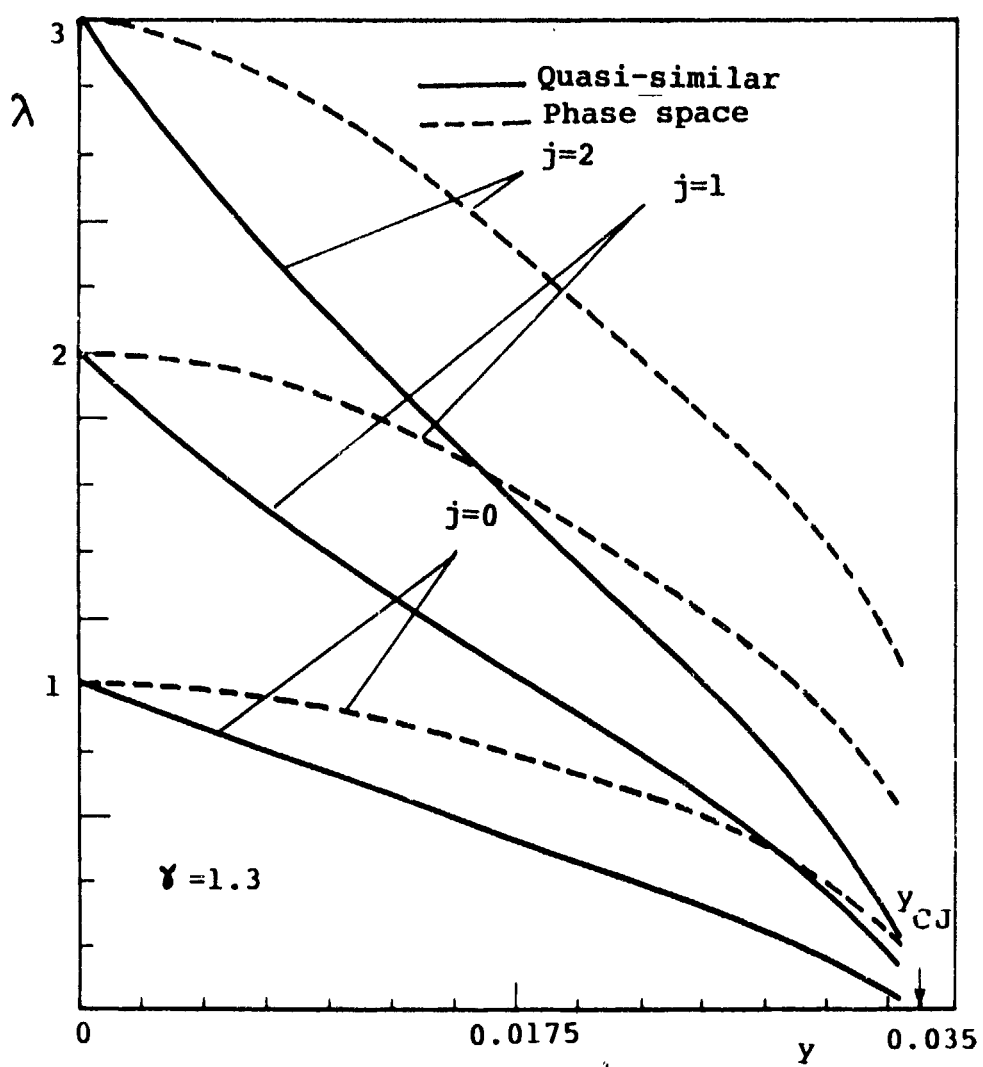Fig. IV.4.14a
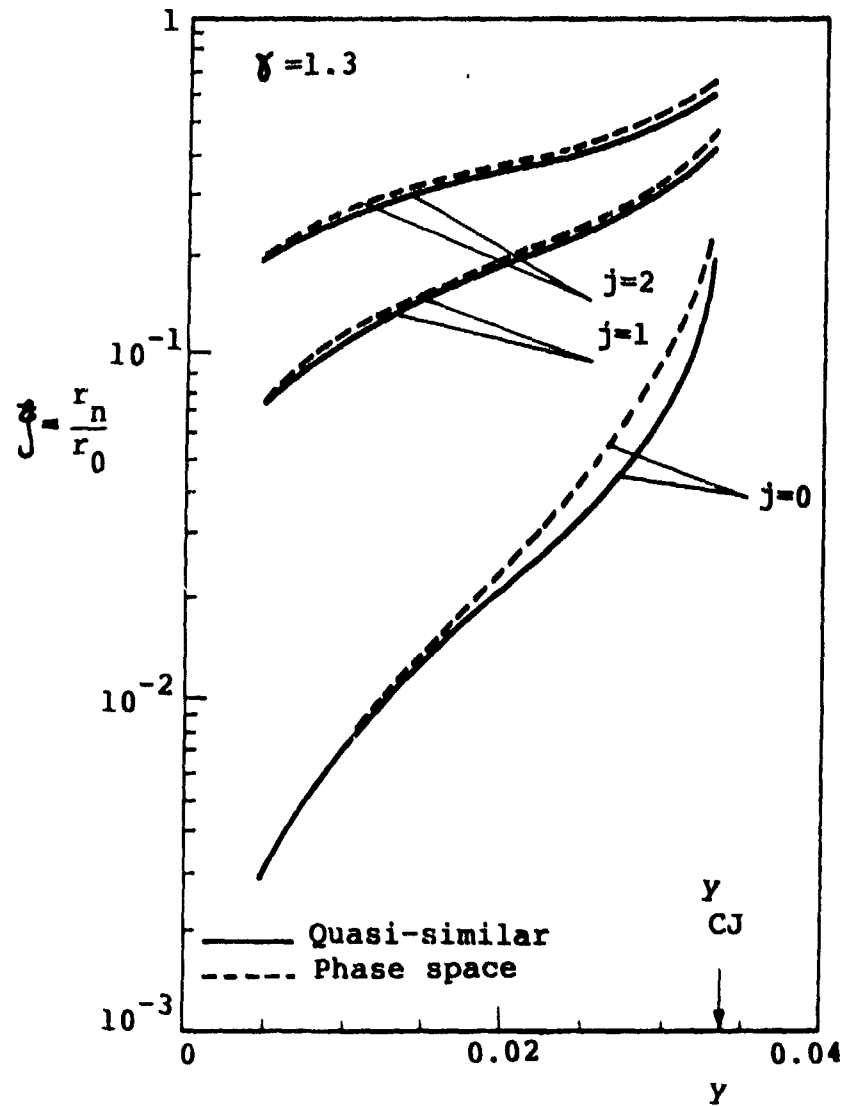
Fig. IV.4.14b

Fig. IV.4.14C

Fig. IV.4.15

Fig. IV.4.16

Fig. IV.4.17

IV.5. ANALYSIS OF REACTIVE BLAST WAVES PROPAGATING THROUGH GASEOUS MIXTURES WITH A SPATIALLY VARYING HEAT OF DETONATION*

i) Introduction

In the actual situation, as occurring during an accidental spill of fuel gases into open air, the initial conditions are no longer uniform and may be very complex. In particular, the concentration of the fuel gases may vary with the distance from the fuel source. This non-uniformity will affect the propagation of any resulting detonation wave considerably and is essential in studying real explosions, Geiger (1979).

In this section, the propagation of reactive blast waves through a medium of spatially non-uniform fuel concentration is analyzed. For simplicity, the fuel gas concentration distribution is assumed to be symmetrical with respect to the center of explosion. With this assumption, blast wave propagation is a spatially one-dimensional problem. In addition, the change in concentration is expressed by the change in energy released at the wave front. The chemical heat release q is determined by the chemical composition and the thermodynamic states of the reactants and products. In this analysis q is assumed to depend only on the initial chemical composition which varies with distance from the explosion center. While the transient diffusion problem may be used to determine the concentration profile, the distribution $q(r)$, with r being the distance from the fuel source is given a priori. For simplicity, changes in concentration due to transient diffusion are neglected since the diffusional velocities are much smaller than the shock wave velocity.

The effect of combustion heat release appears only in the boundary conditions at the wave front and varies as the wave propagates, so that the boundary conditions include the unknown function which controls the propagation of the wave. The formulation of the problem is applicable for the three geometrical symmetries: spherical, cylindrical and planar, while the results are obtained in the case of spherical waves only. The detonating medium is assumed to behave as an inviscid perfect gas with a mean specific heat ratio γ.

---

* This application is based on Ohyagi et al. (1981).

ii) Problem Formulation

At a time $t = 0$ and a point $r = 0$ a finite amount of energy E_i is liberated by some energy source to form a non-steady, symmetrically expanding shock wave, i.e. a blast wave as is shown in Fig. IV.5.1. If the medium is an inert gas, the blast wave decays to sound wave. In exothermic reactive media, if the energy E_i exceeds a critical level, the waves decay to the Chapman-Jouguet wave whose propagation velocity is determined by the chemical energy of the medium.

In this problem, the concentration of the fuel gas changes with the distance from the center of explosion. As noted previously, the distribution utilized here is that of chemical energy instead of that of the concentration. For simplicity, the distribution is assumed to be symmetric with respect to the center so that a symmetrical nature of the propagation is assumed. The chemical energy release at the wave front is given as a function of r_n ,

$$q = q(r_n)$$ (IV.5.1)

Any explosive gas mixture exhibits detonability limits beyond which a detonation can not be established. Here, the chemical reaction is always assumed to be complete at the wave front, and the complex physico-chemical phenomena occurring in the reaction zone is neglected. If the detonatility limits should be taken into account, the value of the limiting concentration or the limiting chemical energy should be given a priori.

In addition to these fundamental assumptions, one may assume that the change in molecular weights of the fuels and the oxidizers do not affect the density and the pressure of the medium ahead of the front.

The governing equations, Eqs. (II.20), (II.22) and (II.24), for a sourceless, inviscid and thermally and calorically perfect with constant specific heats medium, are reduced to

$$\lambda y \frac{\partial h}{\partial y} + (f-x)\frac{\partial h}{\partial x} + h\left(\frac{\partial f}{\partial x} + j\frac{f}{x}\right) = 0$$

$$\lambda y \frac{\partial f}{\partial y} + (f-x)\frac{\partial f}{\partial x} - \frac{\lambda}{2}f + \frac{1}{h}\frac{\partial g}{\partial x} = 0 \qquad\qquad\text{(IV.5.2)}$$

$$\lambda y \frac{\partial g}{\partial y} + (f-x)\frac{\partial g}{\partial x} - \lambda g + \gamma g\left(\frac{\partial f}{\partial x} + j\frac{f}{x}\right) = 0$$

where λ is the decay coefficient defined in Eq. (II.14), which may be rewritten as

$$\lambda = \frac{d \ln y}{d \ln r_n} = -2\frac{d \ln M}{d \ln r_n} \qquad\qquad\text{(IV.5.3)}$$

The boundary conditions of the problem are that of the reactive medium with instantaneous heat release at the wave front of strong detonation, which are given by Eqs. (II.93), (II.54) and (II.85). These equations may be rewritten as follows:

$$f_n = f(1,y) = \frac{1-y+K}{\gamma+1}$$

$$h_n = h(1,y) = \frac{\gamma+1}{\gamma+y-K} \qquad\qquad\text{(IV.5.4)}$$

$$g_n = g(1,y) = \frac{\gamma+y+\gamma K}{\gamma(\gamma+1)}$$

where

$$K = \left[(1-y)^2 - 2(\gamma^2-1)y\bar{q}\right]^{1/2} \qquad\qquad\text{(IV.5.5)}$$

with $\bar{q}$ being the non-dimensional chemical heat release at the wave front, de-

fined by Eq. (II.53) which is, in this case,

$$\bar{q} = \frac{q(r_n)}{a_a^2} \qquad (IV.5.6)$$

The heat release at the wave front, $\bar{q}$, depends on the wave position, r_n, so that it is a function of y.

A condition to be satisfied at the center of symmetry is that the particle velocity must equal to zero for all times, which is given by Eq. (II.112) as

$$f(0, y) =' 0 \qquad (IV.5.7)$$

The problem now is to solve Eqs. (IV.5.2) with the boundary conditions, Eqs. (IV.5.4), as well as the compatibility equation, Eq. (IV.5.7), to find a functional form of $\lambda(y)$ for a given function of $q(r_n)$. For this purpose the relation between r_n and y must be given.

Integration of Eq. (IV.5.3) yields

$$\zeta = \frac{r_n}{r_o} = exp \left(\int_{y_o}^{y} \frac{dy}{\lambda y} \right) \qquad (IV.5.8)$$

where y_o and r_o are arbitrary constants which express the initial condition of the wave Mach number and position, respectively. When the value of y_o is very small, the self-similarity of the flow holds at this initial stage. As defined previously in Eq. (II.72), the initial position r_o is proportional to $E_i^{1/(j+1)}$. By using Eq. (IV.5.3), $\bar{q}$ may be expressed in terms of y. Therefore, the boundary conditions, through $\bar{q}(r_n)$, as well as the basic conditions include the unknown function $\lambda(y)$.

Here, the function $\bar{q}(r_n)$ is assumed to be differentiable. Therefore, the application of the quasi-similar concept yields the following ordinary differential equations for the governing equations, as given by Eqs. (III.23)-

(III.25) where, for a sourceless flow field, all Φ's vanish.

$$(f-x)\frac{dh}{dx} + h(\frac{df}{dx} + j\frac{f}{x}) + \lambda A h = 0$$

$$(f-x)\frac{df}{dx} + \frac{1}{h}\frac{dg}{dx} + \lambda B f = 0 \qquad \qquad \text{(IV.5.9)}$$

$$(f-x)\frac{dg}{dx} + \gamma g(\frac{df}{dx} + j\frac{f}{x}) + \lambda g G = 0$$

where

$$A \equiv \frac{\varphi}{1 - f_n} \qquad \qquad \text{(IV.5.10)}$$

$$B \equiv \frac{\varphi}{f_n} - 0.5 \qquad \qquad \text{(IV.5.11)}$$

and

$$G \equiv \frac{\gamma\varphi + y}{\gamma f_n + y} - 1 \qquad \qquad \text{(IV.5.12)}$$

while

$$\varphi \equiv y\frac{df_n}{dy} = (\frac{-y}{\gamma+1})(\frac{dK}{dy} - 1) \qquad \qquad \text{(IV.5.13)}$$

and

$$\frac{dK}{dy} = \frac{1}{K}\left[(y-1) - (\gamma^2 - 1)\,\bar{q}\,\left(1 + \frac{d\ln\bar{q}}{\lambda\,d\ln r_n}\right)\right] \qquad \text{(IV.5.14)}$$

As an example, a simple exponential form of the function $\bar{q}\,(r_n)$ is adapted. In the non-dimensional form, it is

$$\bar{q}\,(r_n) = \bar{q}_0\,\exp\left(-\beta\,\frac{r_n}{r_0}\right) = \bar{q}_0\,\exp(-\beta\,\zeta) \qquad \text{(IV.5.15)}$$

where $\bar{q}_0$ and β are non-dimensional parameters.

If β is positive, the fuel concentration becomes smaller with the distance from the center and the chemical energy released at the wave front decreases exponentially as the wave propagates.

In the case of Chapman-Jouguet detonation, K equals to zero, see Eq. (IV.5.5), thus

$$\bar{q} = \frac{(1-y)^2}{2\,y\,(\gamma^2 - 1)}$$

To obtain a functional form for the decay coefficient in the case of C-J wave, one may differentiate the above equation with respect to ζ and utilize the definition of λ , given by Eq. (IV.5.3), to get

$$\lambda_{CJ} = \left(\frac{d\ln y}{d\ln \zeta}\right)_{CJ} = \frac{\beta\,(\gamma^2 - 1)\,\bar{q}}{\zeta\,\left[(1-y) + (\gamma^2 - 1)\,\bar{q}\right]} \qquad \text{(IV.5.16)}$$

iii) Solution

The set of simultaneous ordinary differential equations, Eqs. (IV.5.9) is solved

numerically. Since $\lambda(y)$ is not known initially, the value of λ for each y is first assumed and integrations are started from the wave front, $x = 1$, where the boundary conditions are given by Eqs. (IV.5.4) to the center of explosion, $x = 0$, where the particle velocity is equal to zero. If this condition is not satisfied for the assumed value of λ , this value is corrected and the procedure is repeated until Eq. (IV.5.7) is satisfied to the required accuracy.

A difficulty, however, arises because the integrated term of $\lambda(y)$ appears in the boundary conditions. The steps of the solution in this case are as follows:

a) To obtain $\lambda(y)$, y is assumed firstly to be equal to y_0 .

b) From Eq. (IV.5.8), $j = 1$ and $\bar{q}$ is calculated from Eq. (IV.5.6) so that the decay coefficient $\lambda(y_0)$ is obtained by iteration.

c) Next, y is increased by small amount, Δy , and j is calculated by numerical integration of Eq. (IV.5.8) with the trapezoidal rule.

d) Applying the same procedure as described previously leads to the solution $\lambda(y_0 + \Delta y)$.

d) The further solution will be found by repetition of this procedure.

It should be noted here that the error in this procedure can be reduced if the increment Δy is small.

iv) Results and Conclusions

The results obtained here are for the case of spherical wave, $j = 2$. The values of the other parameters used are:
$\bar{q}_0 = 20$, $\beta = 0.001, 0.05, 0.1, 0.15, 0.2$ and 0.5, $y_0 = 0.0001$ and $\gamma = 1.4$.
So, in these calculations, the medium has sufficient chemical energy to support a detonation near the explosion center, with the energy released decreasing exponentially with distance.

It should be noted here that if β is equal to zero, the wave will decay to the

Chapman-Jouguet wave with $y_{CJ} = 0.026$, calculated by using Eq. (II.94), and the problem is reduced to that discussed briefly in section (IV.4).

The step size for the Runge-Kutta integration for x - direction, Δx , is chosen to be 0.01. For the y - direction, the step size Δy is 0.0001.

Figure IV.5.2 shows the decay coefficient $\lambda(y)$ for each β . When y is equal to zero, the self-similar solution is fulfilled so that λ is equal to $j + 1$ = 3. As y increases, λ decreases generally which means that the wave approaches the steady wave. For small values of β , as 0.001, the heat liberated at the wave front is almost constant and the wave behaves as a reactive blast wave in the uniform combustible mixture for the regime where the solution can be found. It seems to decay to the C-J wave (y_{CJ} = 0.026) but the solution can not be found near C-J state because of the singularity at the wave front in the C-J wave. In the C-J wave, the gradients of f , h and g in the y - direction become infinity as indicated previously in section (IV.4). As β increases, $\left| \frac{d\lambda}{dy} \right|$ decreases, and a transition from the reactive blast wave to the non-reactive one occurs with increasing y . For β = 0.05, λ has a minimal value of 1.09 at the value of $y \cong$ 0.05. It appears that the wave, decaying as a reactive blast wave, loses its energy as it propagates and in turn decays more rapidly as a non-reactive blast wave. But for this case, the solution can not be found for $y >$ 0.07 because of the limit of the numerical precision. For β = 0.1, 0.15, 0.2 and 0.5, the complete solutions show the transition from reactive blasts to non-reactive ones. For β = 0.5, the solution is almost identical to that for $\bar{q}_0$ = 0 (or $\beta \rightarrow \infty$), i.e., the non-reactive blast wave except for very small values of y . The values of the decay coefficient for $\beta >$ 1, when $y >$ 0.35, or $M <$ 1.7, are nearly the same because the chemical energy $\bar{q}$, there, is almost equal to zero. The dashed curve shown in this figure represents the Chapman-Jouguet decay coefficient, λ_{CJ} , for β = 0.1, as a function of y which is given by Eq. (IV.5.16). The C-J decay coefficient for β = 0.1 varies with y because the chemical energy $\bar{q}$ changes with ζ , and it can be called as the local C-J decay coefficient.

Figure IV.5.3 shows that the shock Mach number, M , decreases with an increase in the non-dimensional radius, ζ . The curves for all β 's are calculated

with the same initial condition, i.e., for $\mathcal{J} = 1$, $M = 100$. For $\beta = 0.001$, the Mach number M seems to decay to the Chapman-Jouguet value, $M_{CJ} = 6.202$, corresponding to $y_{CJ} = 0.026$. In reality, it decays to the sound wave as the wave propagates infinitely apart from the center. As β increases, M seems to decrease to unity in the far field. From Fig. IV.5.3, it can be seen that for $\mathcal{J} > 25$, M is less than 1.7 for $\beta > 0.1$. Therefore, in the regime $\mathcal{J} > 25$, although $\bar{q}$ is almost zero for those β's, M for larger β is greater than that for smaller β's. It can be said that this is the effect of history which the wave has experienced. The dashed lines in Fig. IV.5.3 indicate the Chapman-Jouguet Mach number obtained by $K = 0$. The C-J Mach number for a certain β varies with $\mathcal{J}$ because $\bar{q}$ is changing and it can be considered as the local C-J Mach number. It is evident that the Mach numbers for all β's decay to their own local C-J values.

Figures IV.5.4 through IV.5.6 show the variations of the peak values, just behind the wave front, of the non-dimensional density, velocity and pressure with respect to $\mathcal{J}$. They change from the values of the strong blast wave limits (i.e. $h_n = 6.0$, $f_n = 0.8333$ and $g_n = 0.8333$ for $\delta = 1.4$) to the values of the C-J wave (i.e. $h_n = 1.683$, $f_n = 0.4508$ and $g_n = 0.4244$ for $\delta = 1.4$ and $\bar{q} = 20$) for the reactive blast wave in the uniform medium, while they approach the values of sound waves (i.e. $h_n = 1.0$, $f_n = 0$ and $g_n = \frac{1}{\delta}$) for the wave in the non-uniform medium. From Fig. IV.5.4, it can be said that in the early stage the peak density at the wave front decays more rapidly for small β than for large β with respect to the distance from the center. In the early stage, M is determined by the initiation energy rather than the chemical energy. For the same M, the peak values for small chemical energy is larger than for large q as is calculated by the Hugoniot relation. In the later stage of propagation, M approaches to the local C-J value and it is determined by the chemical energy. Therefore, the peak density for large β has a tendency to decay more rapidly than that for small β.

Figures IV.5.7a-c show the typical density profiles normalized with respect to the peak values at the wave front for $\beta \rightarrow \infty$ (or $\bar{q}_o = 0$), $\beta = 0.2$ and 0.001. The non-dimensional density near the center increases as $y \rightarrow 1$ for $\beta \rightarrow \infty$ and $\beta = 0.2$ (here, the profiles of $\beta = 0.2$ for $y > 0.25$ are omitted because

they are almost the same as those for $\beta \to \infty$). For $\beta = 0.001$, the non-dimensional density increases very little as $y \to y_{cJ}$ (when $y = 0.022$, $y/y_{cJ} = 0.846$). In these calculations of the point blast wave, the density near the center remains zero, corresponding to the fact that the velocity gradient $\frac{\partial f}{\partial x}$ does not vanish. If it is possible to extend the solution for larger y , the density may increase more near the center.

Figures IV.5.8a-c show the particle velocity profiles. The core in which the velocity vanishes is not accurate in these figures. This is a consequence of the quasi-similarity approximation since it is expected that for $\bar{q}_0 = 0$ and $y > 0.6$ then $f(x)$ has a negative region near the center.

Figures IV.5.9a-c show the pressure profiles for $\beta \to \infty$, $\beta = 0.2$ and $\beta = 0.001$, respectively, where the profiles exhibit the same general trend as in previous cases.

In this model using the quasi-similar approximation, there have to be some inaccuracies in the gasdynamic profiles. However, the decay coefficient obtained seems to be reasonable. In addition, this method permits the use of any model for the heat release function $\bar{q}(r_n)$ and it makes it very convenient to find the decay coefficient for the wave front.

In this example, $\bar{q}$ is taken to decrease exponentially with distance from the center, the nature of wave propagation is determined by the ratio of the characteristic radius of the initiation energy, r_0 , to that of the decreasing initial chemical energy, β , and it is revealed that for small , such as 0.00: and 0.05, the wave front behaves as a detonation wave and for large values of β , such as 0.5, it decays as a non-reactive blast wave.

Figure Captions

Fig. IV.5.1   Configuration of a spherical blast wave.

Fig. IV.5.2   The decay coefficient λ as a function of y for different values
of β with $\gamma = 1.4$ and $\bar{q}_o = 20$ while $j = 2$.

Fig. IV.5.3   The shock Mach number M as a function of the non-dimensional
shock radius $\overline{\overline{J}}$ for different values of β with $\gamma = 1.4$ and
$\bar{q}_o = 20$ while $j = 2$.

Fig. IV.5.4   The density ratio across the wave front as a function of the non-
dimensional shock radius $\overline{\overline{J}}$ for different values of β with
$\gamma = 1.4$ and $\bar{q}_o = 20$ while $j = 2$.

Fig. IV.5.5   The velocity ratio across the wave front as a function of the non-
dimensional shock radius $\overline{\overline{J}}$ for different values of β with
$\gamma = 1.4$ and $\bar{q}_o = 20$ while $j = 2$.

Fig. IV.5.6   The non-dimensional pressure at the wave front g_n as a function
of the non-dimensional shock radius $\overline{\overline{J}}$ for different values of β
with $\gamma = 1.4$ and $\bar{q}_o = 20$ while $j = 2$.

Fig. IV.5.7 (a), (b) & (c)
The density profiles at different values of y for $\beta = \infty$, 0.2
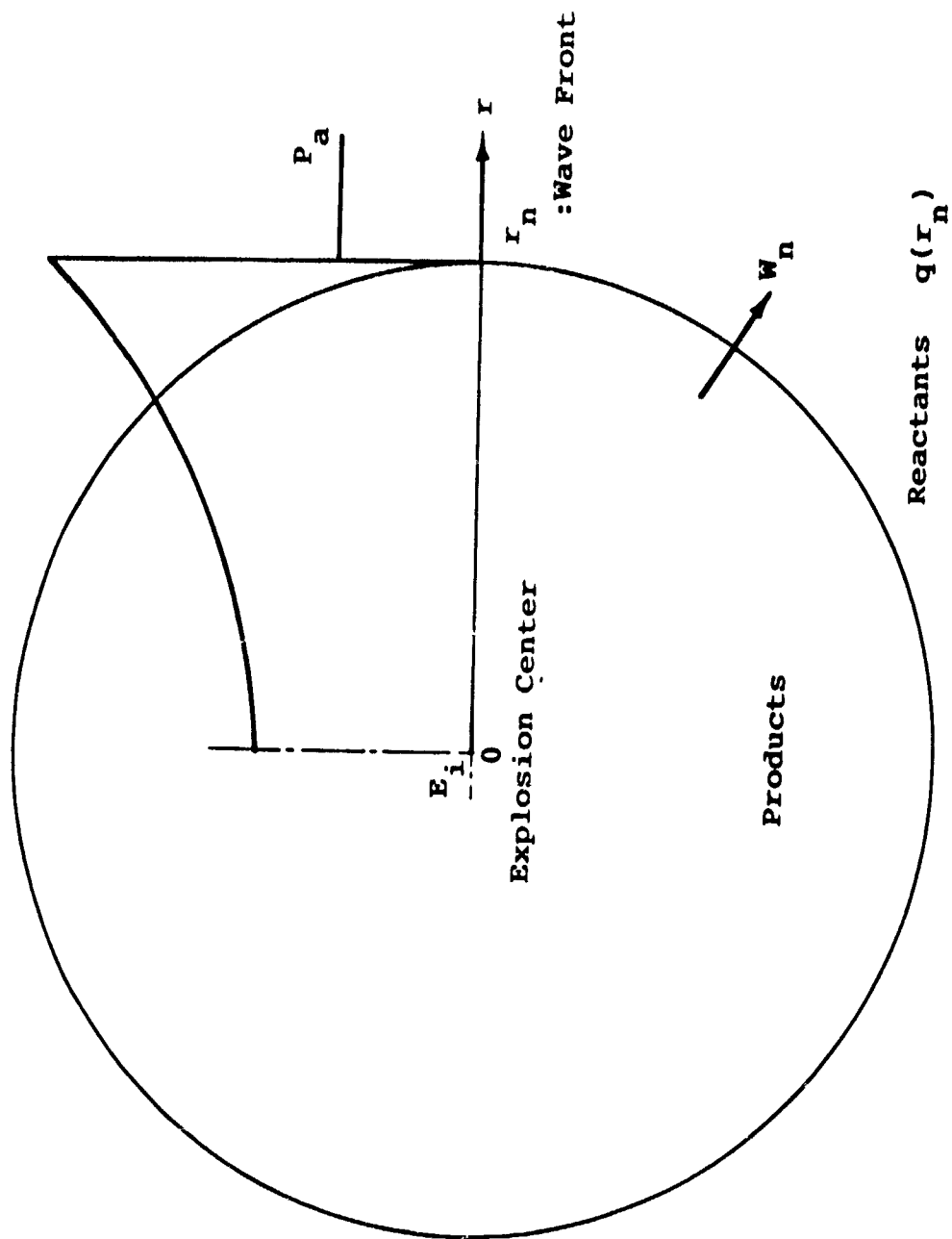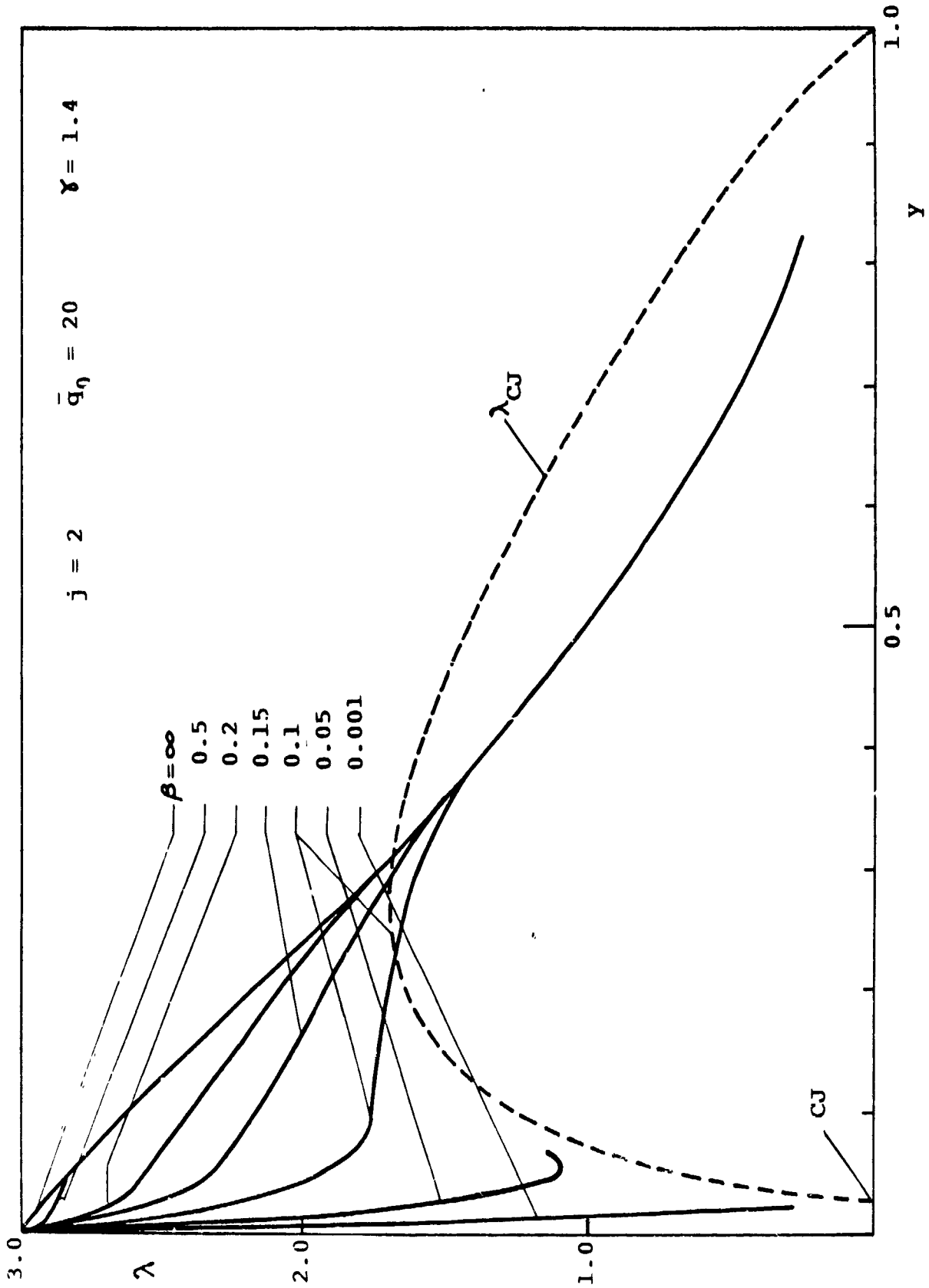and 0.001, respectively, with $\gamma = 1.4$ and $\bar{q}_o = 20$ while $j = 2$.

Fig. IV.5.8 (a), (b) & (c)
The particle velocity profiles at different values of y for
$\beta = \infty$, 0.2 and 0.001, respectively, with $\gamma = 1.4$ and $\bar{q}_o = 20$
while $j = 2$.

Fig. IV.5.9 (a), (b) & (c)
The pressure profiles at different values of y for $\beta = \infty$,

0,2 and 0.001, respectively, with $\gamma = 1.4$ and $\bar{q}_o = 20$ while
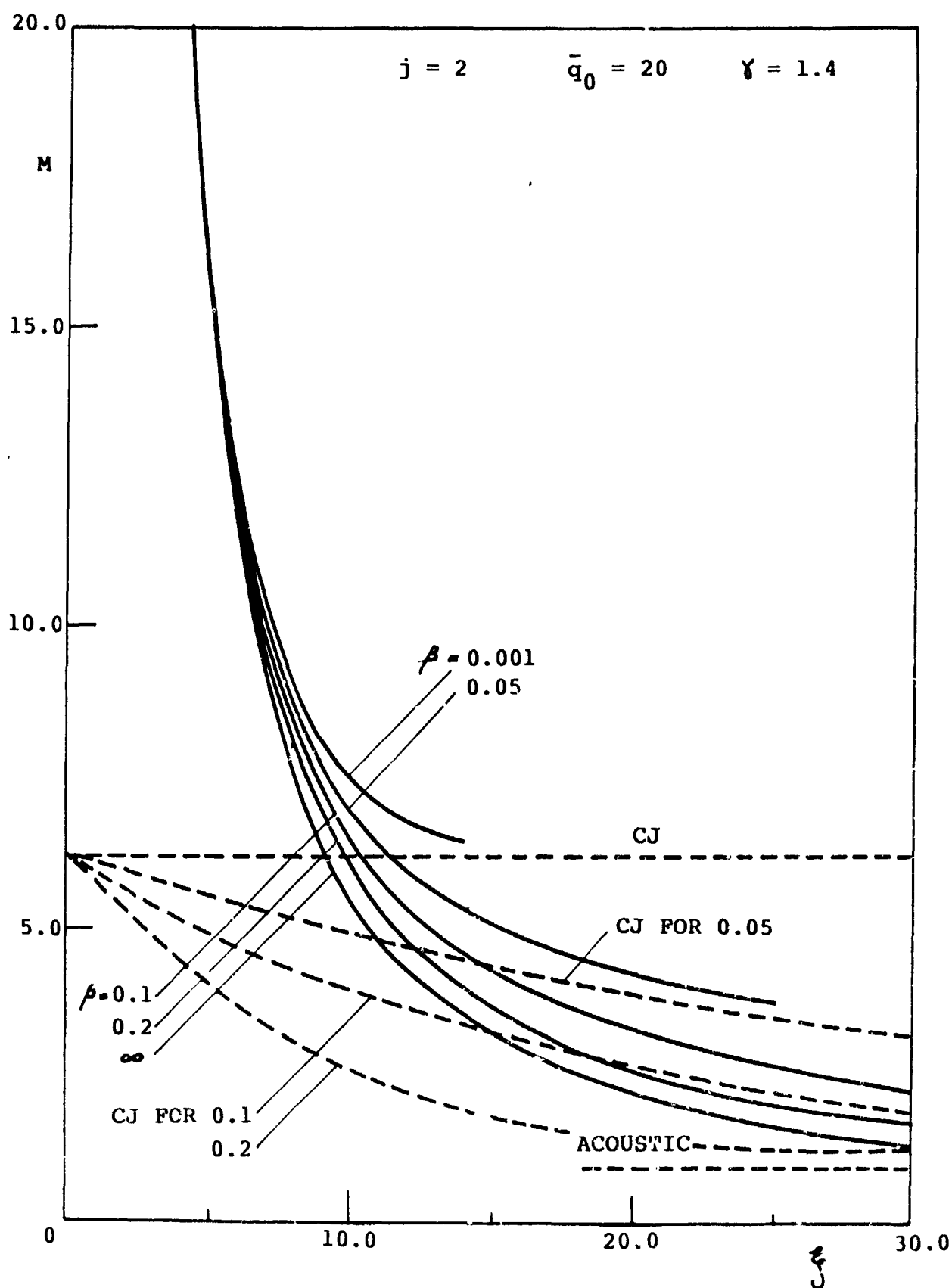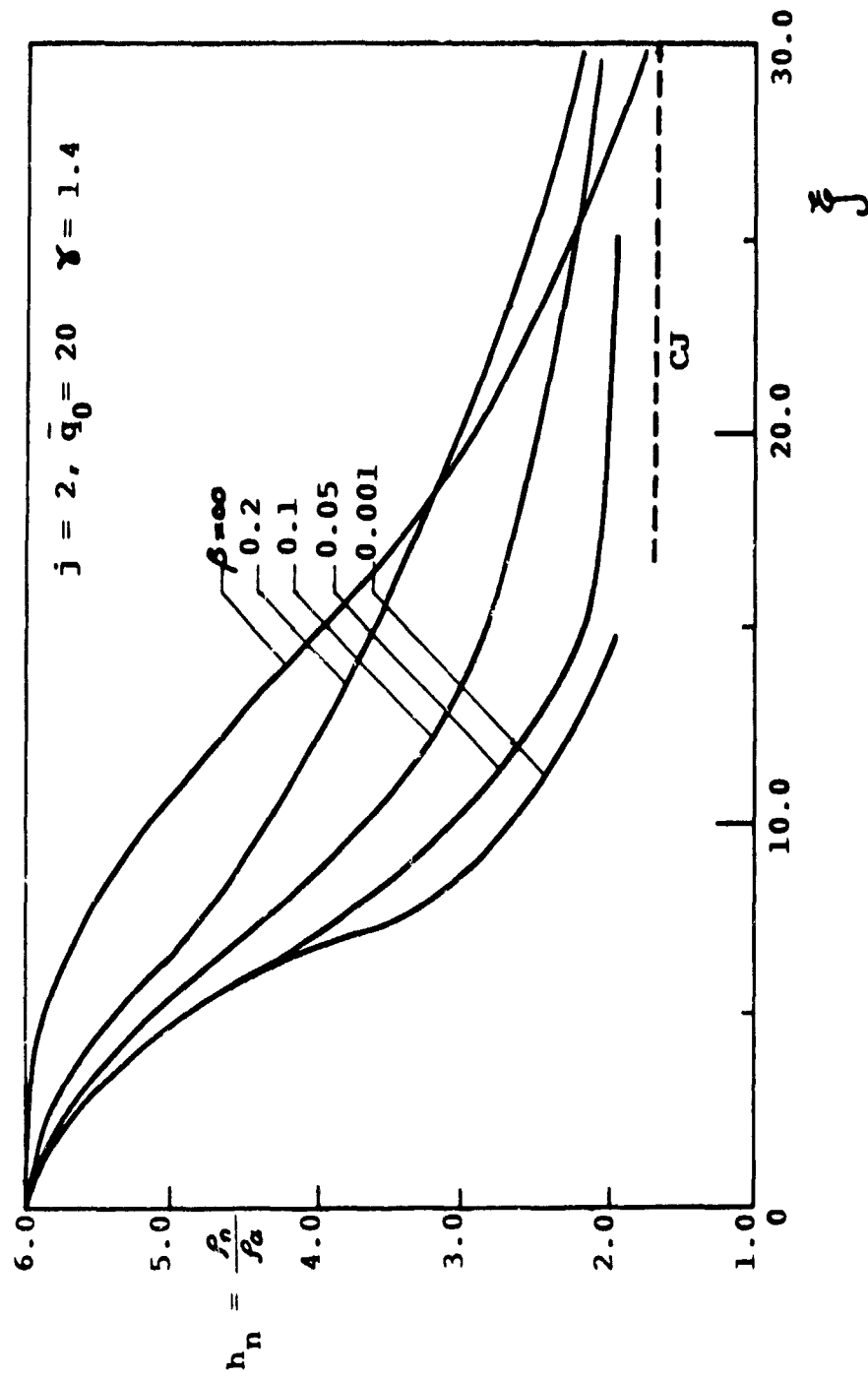$j = 2$.

Fig. IV.5.1

Fig. IV.5.2

Fig. IV.5.3

$j = 2$, $\bar{q}_0 = 20$ $\gamma = 1.4$

$\beta = \infty$
0.2
0.1
0.05
0.001

CJ

$h_n = \dfrac{\rho_n}{\rho_a}$
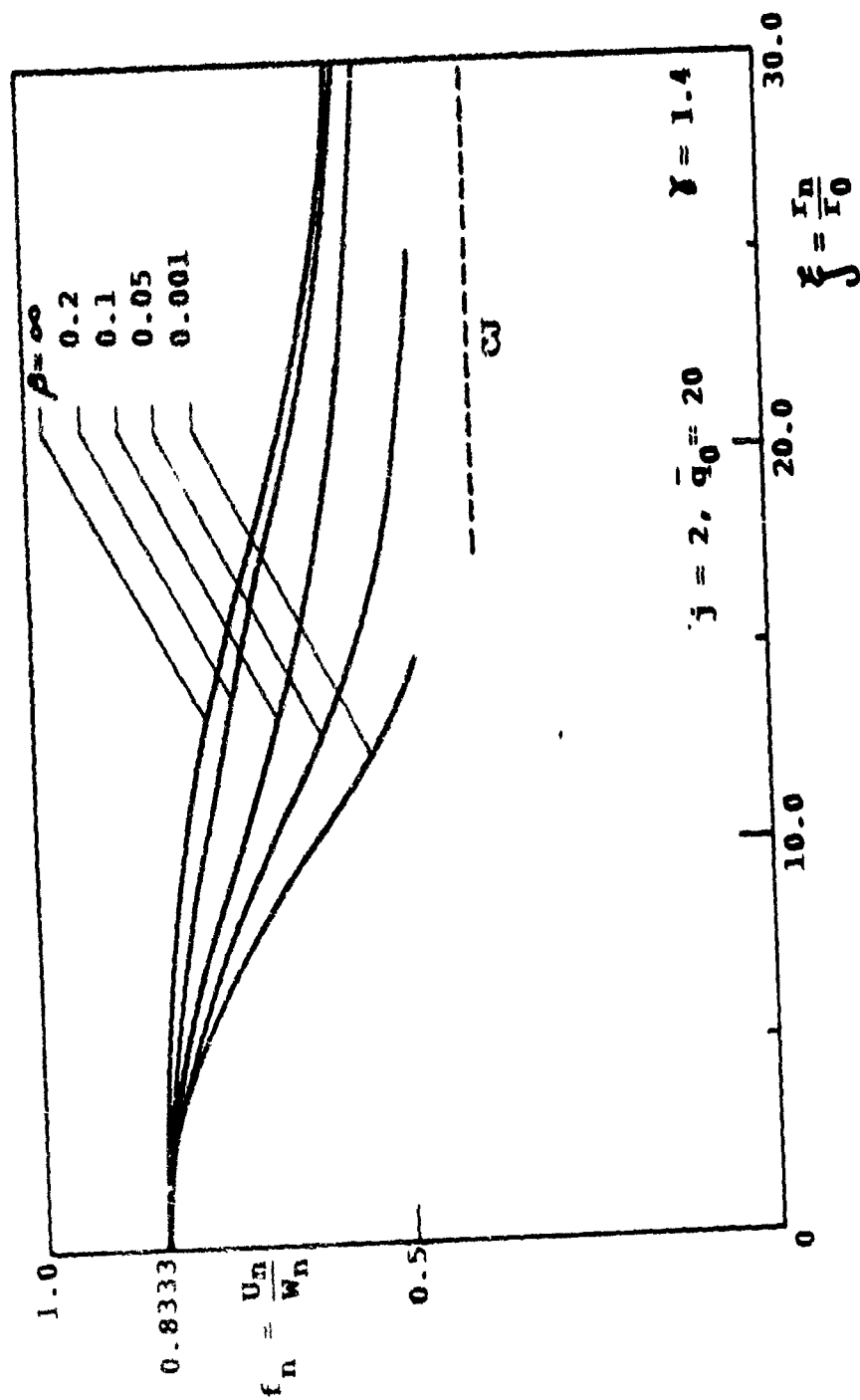
6.0

5.0

4.0

3.0

2.0
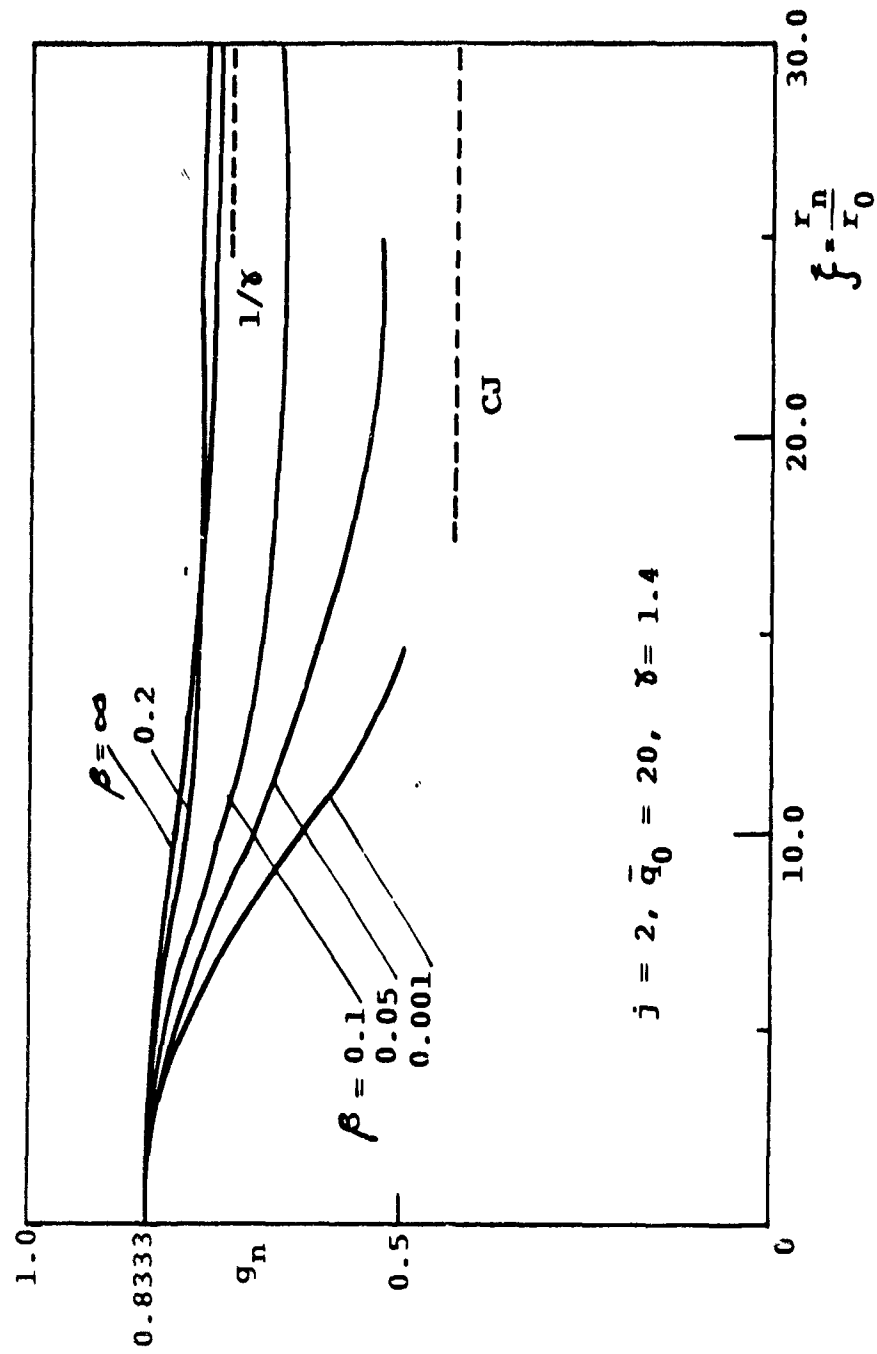
1.0

0

10.0   20.0   30.0
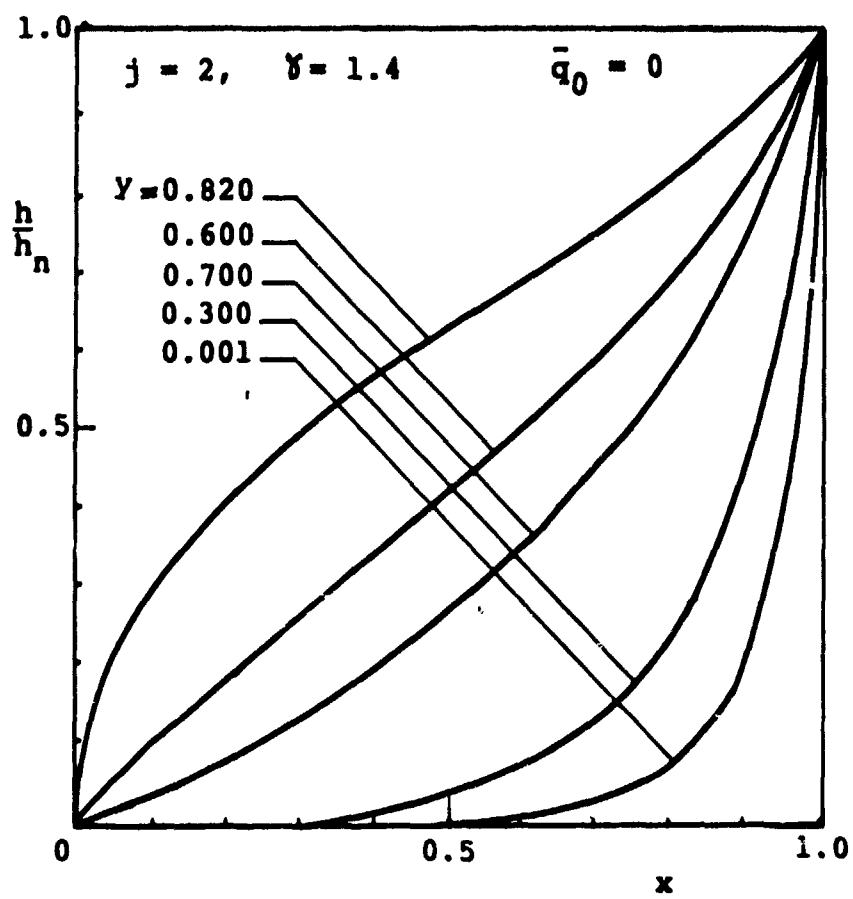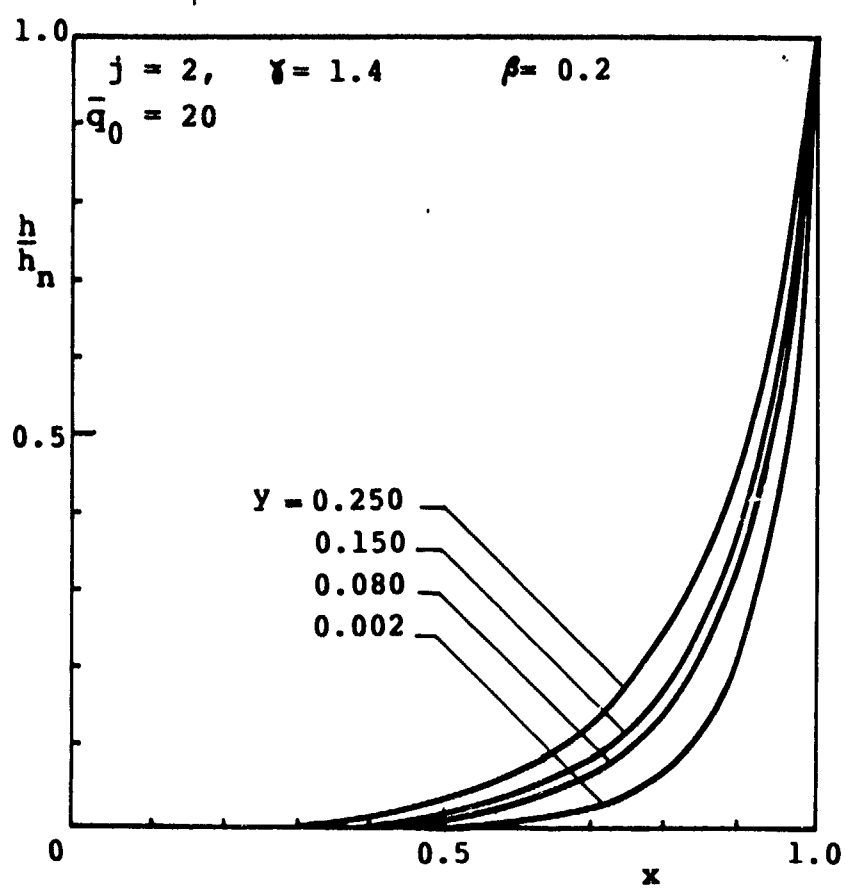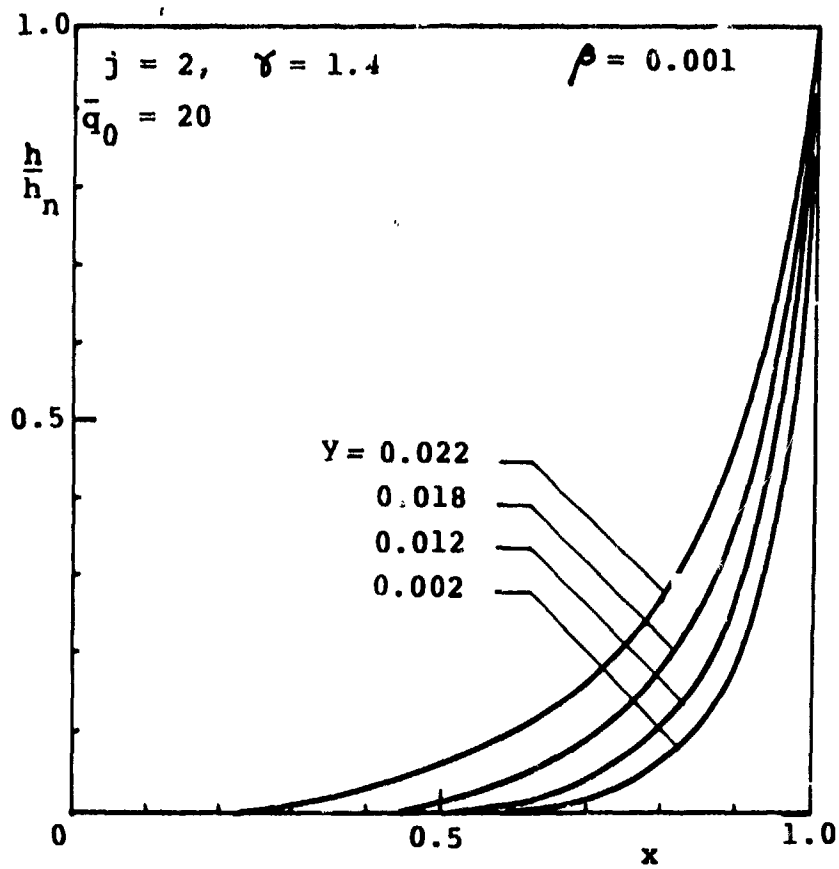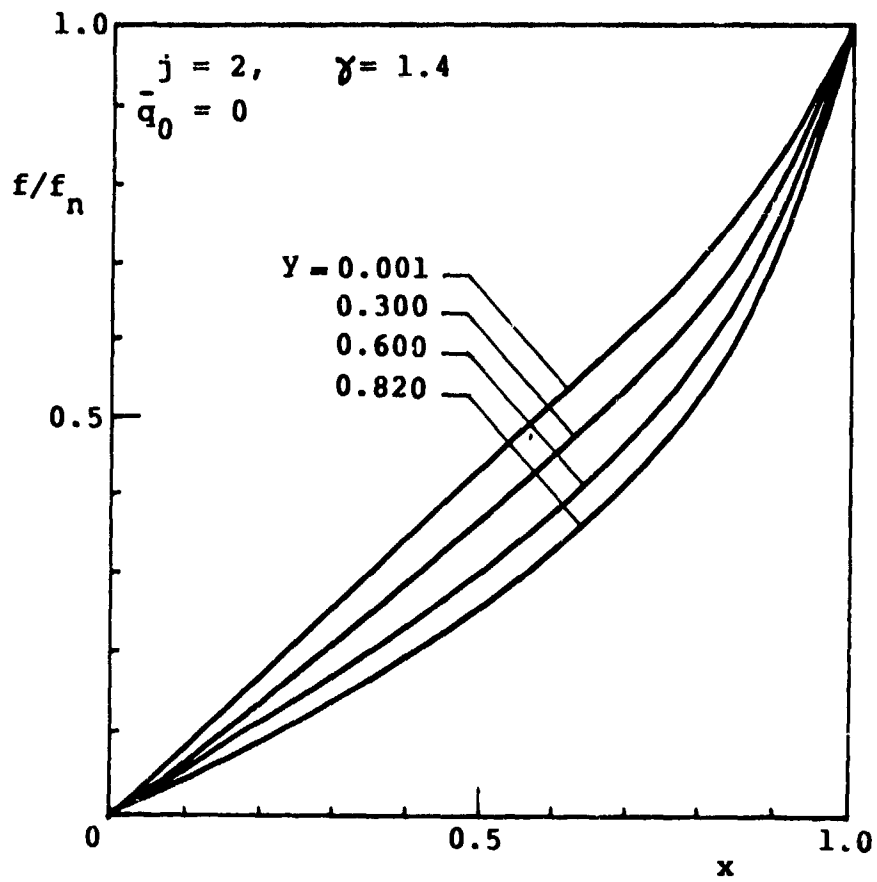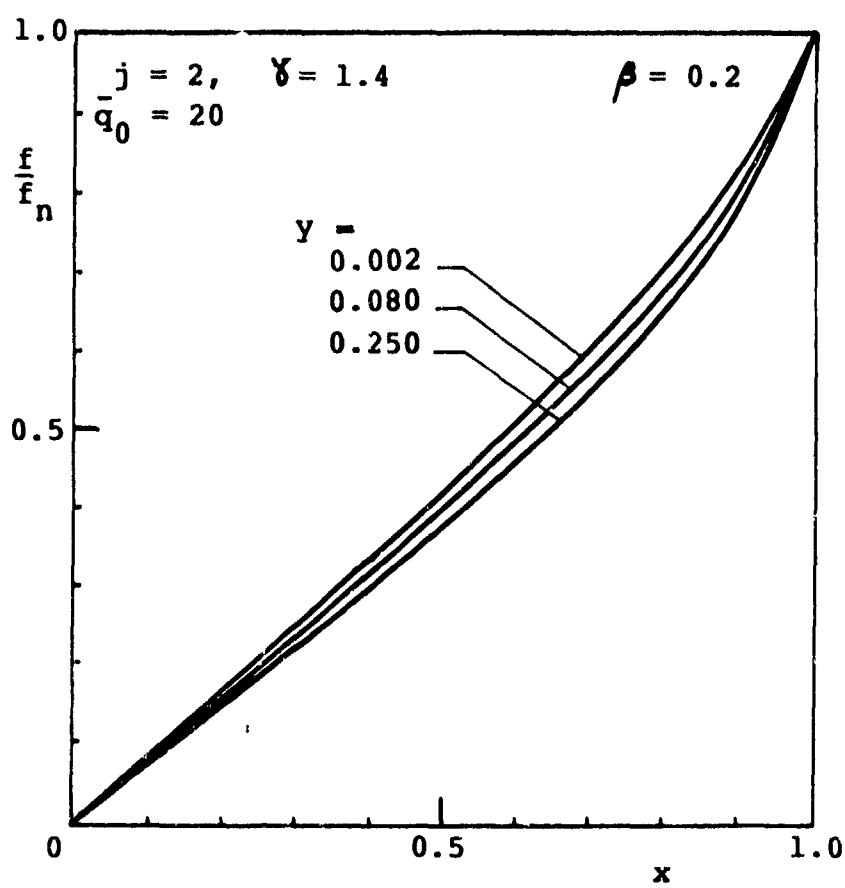
ξ

Fig. IV.5.4

Fig. IV.5.5

Fig. IV.5.6

278

Fig. IV.5.7a

Fig. IV.5.7b

Fig. IV.5.7c
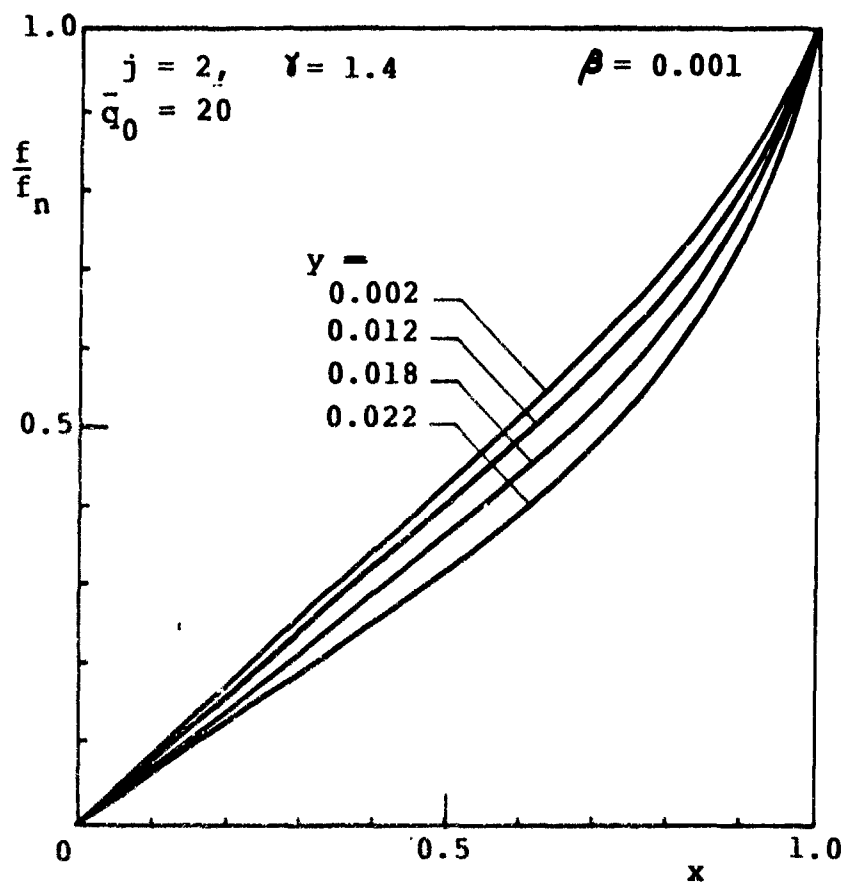
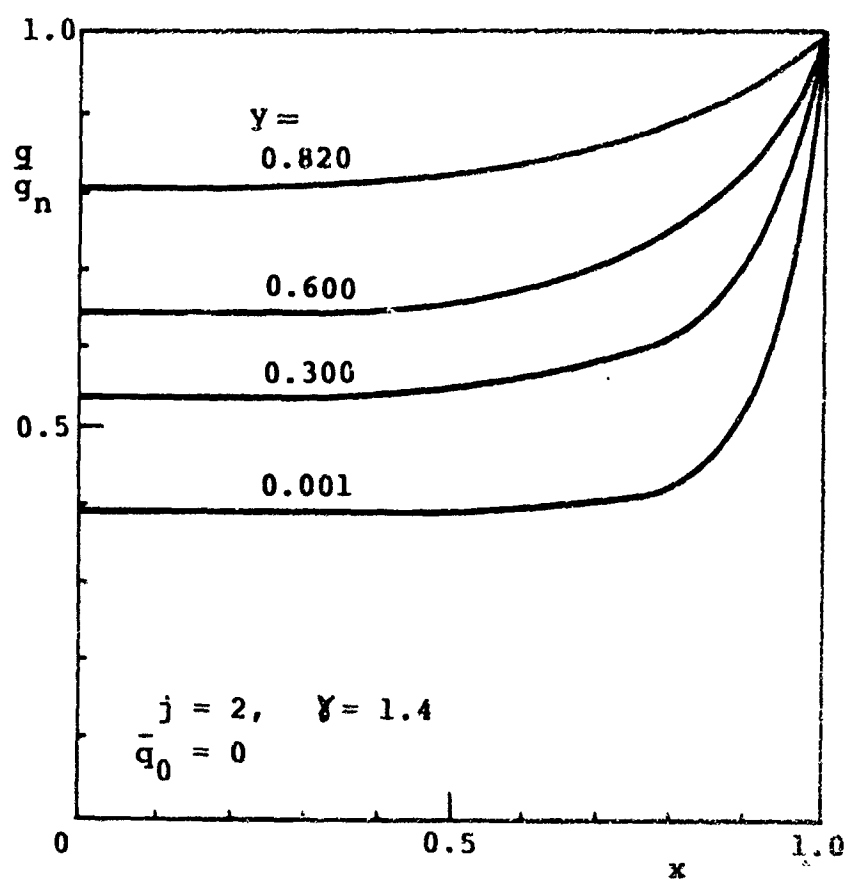Fig. IV.5.8a

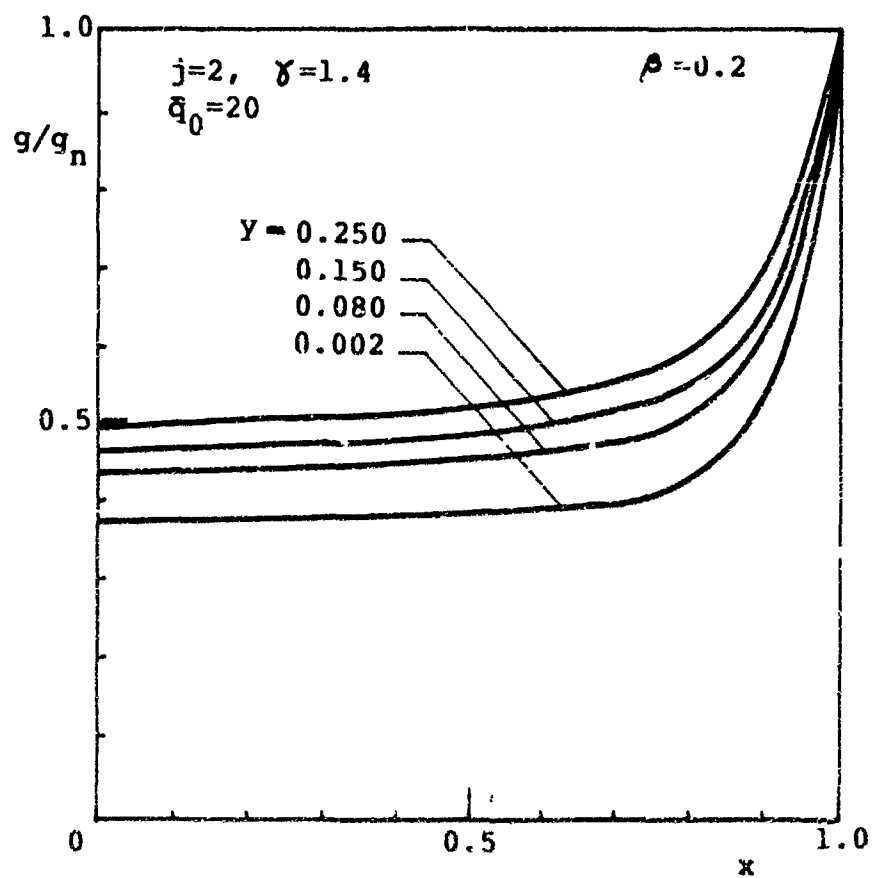Fig. IV.5.8b

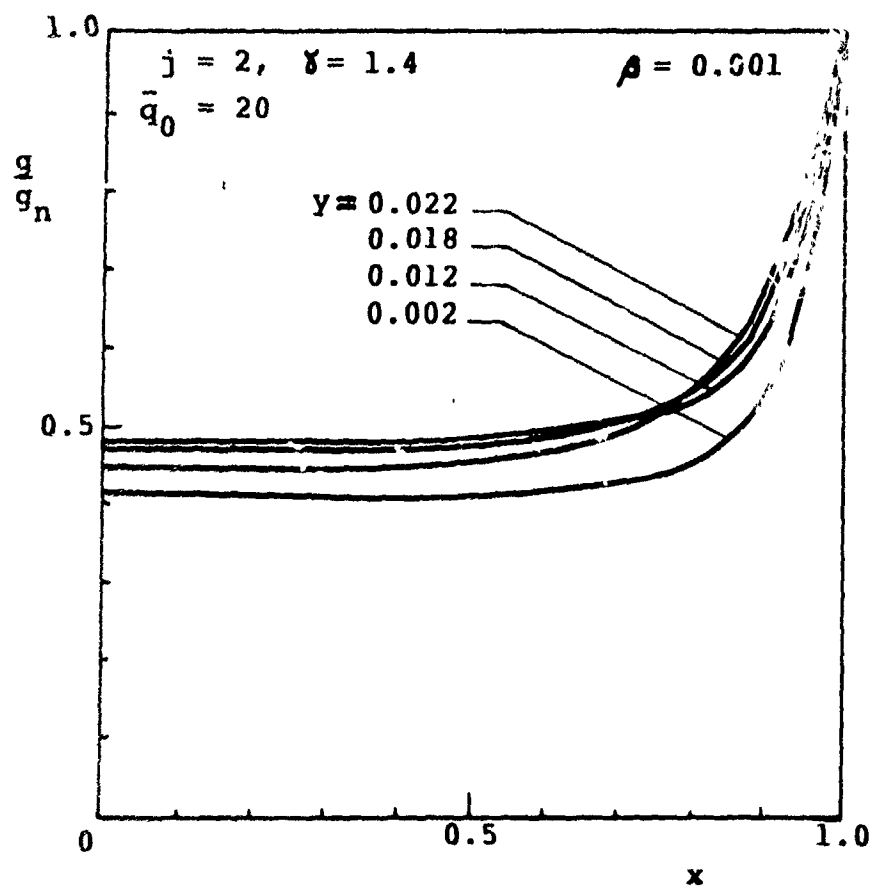Fig. IV.5.8c

284

Fig. IV.5.9a

285

Fig. IV.5.9b

Fig. IV.5.9c

IV.6   BLAST WAVES IN A DETONATING MEDIUM WITH TRANSPORT PROPERTIES TAKEN INTO ACCOUNT*

i)   Introduction

It is evident from previous applications, for both reactive and non-reactive blast waves, that the solution fails near the center of symmetry since the temperature goes to infinity, while the density of the gas tends to zero. In order to improve the solution near the center, one has to take the effects of viscosity, heat conduction and radiation into account.

In this section, the non-self-similar problem of a point explosion in a detonating gas with viscosity, thermal conduction and radiation effects is analyzed. Radiation has been included by assuming a diffusion radiation mode for an optically thick grey gas which, as a consequence, leads to radiation terms that are mathematically similar to those of thermal conduction. The transport coefficients are assumed to be proportional to appropriate powers of temperature. A boundary layer-like region is assumed to exist near the blast origin where all the transport effects are concentrated, thus permitting the rest of the flow field to be treated in the usual inviscid manner. After the inviscid solution has been obtained, series expansions of the gasdynamic parameters are then applied to the inner region equations which, in turn, reduce to algebraic relations. The structure of the non-self-similar flow fields is then fully determined by matching the approximate solution for the inner region with that for the inviscid outer region. The three geometrical symmetries of blast waves are considered and the detonating medium will be treated as a perfect gas with a mean specific heat ratio, γ .

ii)   Problem Formulation

The three conservation equations of mass, momentum and energy, taking into account possible sources of mass, momentum or energy that may affect the flow field, are given by Eqs. (II.1) - (II.3).

For the case considered here, the rate of mass supplied per unit mass of the mixture is zero. Thus

---

* This application is based on Abdel-Raouf (1982).

$$\Lambda_M = 0 \tag{IV.6.1}$$

when taking the effect of thermal radiation, by assuming a diffusion radiation
mode for an optically thick grey gas, thermal conduction and viscous forces
into account, the momentum and energy source terms, as given by Kamel et al.
(1977 a) take the form:

$$\Lambda_F = \frac{4}{3}\frac{\mu}{\rho}\left[\frac{\partial^2 u}{\partial r^2} + \frac{j}{r}\left(\frac{\partial u}{\partial r} - \frac{u}{r}\right)\right] + \frac{4}{3\rho}\frac{\partial \mu}{\partial r}\left(\frac{\partial u}{\partial r} - \frac{j}{2}\frac{u}{r}\right) \tag{IV.6.2}$$

and

$$\Lambda_E = \frac{1}{\rho}\left\{ \frac{4}{3}\mu\left[u\frac{\partial^2 u}{\partial r^2} + \left(\frac{\partial u}{\partial r}\right)^2 - \frac{j(j-1)}{2}\left(\frac{u}{r}\right)^2\right]\right.$$

$$+ \frac{4}{3}\frac{\partial \mu}{\partial r}\left(u\frac{\partial u}{\partial r} - \frac{j}{2r}u^2\right) + \frac{K}{r^j}\frac{\partial}{\partial r}\left(r^j\frac{\partial T}{\partial r}\right)$$

$$+ \frac{\partial K}{\partial r}\cdot\frac{\partial T}{\partial r} + \frac{1}{r^j}\left(\frac{16\,\bar{\sigma}\,T^3}{3\,a'}\right)\frac{\partial}{\partial r}\left(r^j\frac{\partial T}{\partial r}\right)$$

$$\left. + \frac{\partial}{\partial r}\left(\frac{16\,\bar{\sigma}\,T^3}{3\,a'}\right)\frac{\partial T}{\partial r}\right\} \tag{IV.6.3}$$

where T is the absolute temperature and $\bar{\sigma}'$ is the Stefan-Boltzmann constant, while μ, K and a' are the coefficients of viscosity, thermal conduction and absorption, respectively. These coefficients, being thermodynamic properties, are functions of temperature and pressure. However, the pressure is very nearly constant in the inner region near the center of symmetry where the transport properties predominate. Therefore, these coefficients may be considered as functions of temperature only and could be assumed to vary with the local temperature, as given by Kamel et al.(1973a), in the following manner:

$$\mu = \mu_0 \left(\frac{T}{T_0}\right)^{\alpha} \quad ; \quad K = K_0 \left(\frac{T}{T_0}\right)^{\alpha} \quad \text{and} \quad a' = a'_0 \left(\frac{T}{T_0}\right)^{\beta} \quad \text{(IV.6.4)}$$

where α and β are constants, and subscript o refers to some known state.

One may then define the following non-dimensional parameters of the transport properties

$$Re \equiv \frac{r_0 \, a_a \, \rho_a}{\mu_0} \quad , \quad Pr \equiv \frac{\mu_0 \, c_p}{K_0} \quad \text{and} \quad No \equiv \frac{a'_0 \, K_0}{4 \, \bar{\sigma} \, T_0^3} \quad \text{(IV.6.5)}$$

where Re is the Reynolds number; Pr, the Prandtl number; No, the radiation-conduction parameter; c_p the gas specific heat at constant pressure and r_0 is the characteristic length of the explosion.

The basic equations of mass, momentum and energy, in non-dimensional form, Eqs. (II.20), (II.22) and (II.83), with the definitions of Eqs. (II.21), (II.23) and (II.84), under the assumption of uniform ambient atmosphere, are then reduced to

$$\frac{\lambda y}{h} \cdot \frac{\partial h}{\partial y} + \frac{(f - x)}{h} \frac{\partial h}{\partial x} + \frac{\partial f}{\partial x} + j \frac{f}{x} = 0$$

$$-\frac{\lambda}{2} + \frac{\lambda y}{f} \frac{\partial f}{\partial y} + \frac{(f - x)}{f} \frac{\partial f}{\partial x} + \frac{1}{hf} \cdot \frac{\partial g}{\partial x} = \Phi_F \qquad \text{(IV.6.6)}$$

and

$$-\lambda + \frac{\lambda y}{g}\cdot\frac{\partial g}{\partial y} + \frac{(f-x)}{g}\frac{\partial g}{\partial x} + \gamma\left(\frac{\partial f}{\partial x} + j\frac{f}{x}\right) = \Phi_E$$

with

$$\Phi_F = \frac{1}{F}\,\mathcal{A}_F\,\frac{\dot{m}}{w_n^2} \qquad \text{and} \qquad \Phi_E = \frac{(\gamma-1)h}{g}\left(\frac{r_n}{w_n^3}\,\mathcal{A}_E - f\,\mathcal{A}_F\,\frac{r_n}{w_n^2}\right) \qquad (IV.6.7)$$

Substitution from Eqs. (IV.6.2) - (IV.6.5) into Eq. (IV.6.7) yields

$$\Phi_F = \epsilon_1\,\frac{g^\alpha}{f\,h^{\alpha+1}}\left[\frac{\partial^2 f}{\partial x^2} + \frac{j}{x}\frac{\partial f}{\partial x} - \frac{jf}{x^2} + \alpha\left(\frac{1}{g}\frac{\partial g}{\partial x}\right.\right.$$

$$\left.\left. - \frac{1}{h}\frac{\partial h}{\partial x}\right)\left(\frac{\partial f}{\partial x} - \frac{jf}{2x}\right)\right] \qquad (IV.6.8)$$

and

$$\Phi_E = \epsilon_1\,\frac{(\gamma-1)}{g}\left(\frac{g}{h}\right)^\alpha\left[\left(\frac{\partial f}{\partial x}\right)^2 - \frac{jf}{x}\frac{\partial f}{\partial x} + \frac{j(3-j)}{2}\left(\frac{f}{x}\right)^2\right]$$

$$+ \epsilon_2\,\frac{1}{h}\left(\frac{g}{h}\right)^\alpha\left[\frac{-g}{h}\frac{\partial^2 h}{\partial x^2} + \frac{\partial^2 g}{\partial x^2} - \frac{2(\alpha+1)}{h}\cdot\frac{\partial h}{\partial x}\cdot\frac{\partial g}{\partial x}\right.$$

$$\left. - \frac{j}{x}\frac{g}{h}\frac{\partial h}{\partial x} + \frac{j}{x}\frac{\partial g}{\partial x} + (2+\alpha)\frac{g}{h^2}\left(\frac{\partial h}{\partial x}\right)^2 + \frac{\alpha}{g}\left(\frac{\partial g}{\partial x}\right)^2\right]$$

$$+ \epsilon_3\,\frac{g^2}{h^4}\left(\frac{h}{g}\right)^\beta\left[\frac{-g}{h}\frac{\partial^2 h}{\partial x^2} + \frac{\partial^2 g}{\partial x^2} - \frac{2(4-\beta)}{h}\frac{\partial h}{\partial x}\frac{\partial g}{\partial x}\right.$$

$$\left. - \frac{j}{x}\frac{g}{h}\cdot\frac{\partial h}{\partial x} + \frac{j}{x}\frac{\partial g}{\partial x} + (5-\beta)\frac{g}{h^2}\left(\frac{\partial h}{\partial x}\right)^2 + \frac{(3-\beta)}{g}\left(\frac{\partial g}{\partial x}\right)^2\right] \qquad (IV.6.9)$$

where

$$\epsilon_1 = \frac{4}{3} \gamma^\alpha \frac{M^{2\alpha-1}}{Re\ \bar{f}}$$

$$\epsilon_3 = \frac{4}{3} \gamma^{4-\beta} \frac{M^{5-2\beta}}{Re\ Pr\ No\ \bar{f}}$$

(IV.6.10)

and

$$\epsilon_2 = \gamma^{\alpha+1} \frac{M^{2\alpha-1}}{Re\ Pr\ \bar{f}}$$

The boundary conditions of detonating blast wave problems are given by the Hugoniot relations, Eqs. (II.93), (II.54) and (II.85). These equations may be re-written as

$$f_n = \frac{1-y}{\gamma+1} + \left[\left(\frac{1-y}{\gamma+1}\right)^2 - 2\left(\frac{\gamma-1}{\gamma+1}\right) y\ \bar{q} \right]^{1/2}$$

$$h_n = \frac{1}{1-f_n}$$

(IV.6.11)

and

$$g_n = f_n + \frac{y}{\gamma}$$

The reduction of the governing equations, Eqs. (IV.6.6), to self-similarity leads to the determination of the values of the constants α and β, as given by Kamel et al. (1977a), which are equal to:

$$\alpha = \tfrac{1}{2}\left(\frac{j-1}{j+1}\right) \qquad \text{and} \qquad \beta = \tfrac{1}{2}\left(\frac{5j+7}{j+1}\right) \qquad\qquad \text{(IV.6.12)}$$

The coefficients of viscosity, thermal conduction and absorption which vary with temperature as given by Eq. (IV.6.4), must be independent of time, since they are properties of the flowing substance. Therefore, the constants α and β must have the same values, given by Eq. (IV.6.12), that are independent of y which are also valid for the non-self-similar case.

The mass and energy integrals, in the case of inviscid medium, have the forms given by Eqs. (II.65) and (II.96) respectively, which are

$$J_1 = \int_0^1 h\, x^j\, dx = \frac{1}{j+1} \qquad\qquad \text{(IV.6.13)}$$

and

$$J_3 = \int_0^1 \left(\frac{g}{\gamma-1} + \tfrac{1}{2} h f^2\right) x^j\, dx$$

$$= \frac{y}{\gamma}\left(\, \mathfrak{Z}^{-(j+1)} + \frac{1}{(j+1)(\gamma-1)} + \frac{\gamma \bar{q}}{j+1}\right) \qquad\qquad \text{(IV.6.14)}$$

while the decay coefficient λ is given by Eq. (II.97) as

$$\lambda = \frac{(j+1)\, J_3 - \dfrac{y}{\gamma(\gamma-1)} - \bar{q}\, y}{J_3 - y\, \dfrac{dJ_3}{dy}} \qquad\qquad \text{(IV.6.15)}$$

which for self-similar cases, reduces to

$$\lambda = j+1 \qquad\qquad \text{(IV.6.16)}$$

The quasi-similar technique, when applied, reduces the basic equations, Eqs. (IV.6.6), to ordinary differential ones, given by Eqs. (III.23) - (II.25). Noting that $\Phi_M = 0$, these equations in this case reduce to

$$(f-x)\frac{dh}{dx} + h\left(\frac{df}{dx} + j\frac{f}{x}\right) + \lambda h A = 0$$

$$(f-x)\frac{df}{dx} + \frac{1}{h}\frac{dg}{dx} + \lambda f B = f \Phi_F \qquad (IV.6.17)$$

and

$$(f-x)\frac{dg}{dx} + \gamma g\left(\frac{df}{dx} + j\frac{f}{x}\right) + \lambda g G = g \Phi_E$$

where

$$A \equiv \frac{\varphi}{1-f_n}$$

$$B \equiv \frac{\varphi}{f_n} - 0.5$$

and

$$G \equiv \frac{\gamma\varphi + y}{\gamma f_n + y} - 1$$

with

$$\varphi \equiv y\frac{df_n}{dy} = \left(\frac{-y}{\gamma+1}\right)\left[1 - \frac{(1-y)+(\gamma^2-1)\bar{q}}{(1-y)-(\gamma+1)f_n}\right]$$

Solving for the derivatives $\frac{df}{dx}$, $\frac{dh}{dx}$ and $\frac{dg}{dx}$ in Eqs. (IV.6.17), one ob-

tains, as given by Eqs. (III.26) - (III.28) when $\phi_M = 0$,

$$\frac{df}{dx} = \left\{ \frac{j\gamma g f}{x} + \lambda g G + f(f-x)h(\phi_F - \lambda B) - g\phi_F \right\} \Big/ \left[h(f-x)^2 - \gamma g \right]$$

$$\frac{dh}{dx} = \frac{-h}{(f-x)} \left(\frac{df}{dx} + j\frac{f}{x} + \lambda A \right)$$

(IV.6.18)

and

$$\frac{dg}{dx} = -h \left[(f-x)\frac{df}{dx} + \lambda f B - f \phi_F \right]$$

iii) Solution

The solution procedure is divided into two steps. First, the inviscid flow
field is obtained by solving the conservation equations, Eqs. (IV.6.18), ne-
glecting transport effects (i.e. $\phi_F = \phi_E = 0$) and the problem is reduced
to the one discussed previously in section (IV.4). This solution is obtained
in order to determine λ. Then the effect of transport phenomena is accoun-
ted for by assuming the flow field to consist of two regions, namely an outer
region and an inner region, with transport effects existing in the inner re-
gion only (Kamel et al., 1977a). Series expansions for the gasdynamic parame-
t rs are used to obtain the inner region solution which must be matched with
t e or the inviscid outer region.

An order of magnitude analysis to the conservation equations was performed by
Kamel et al. (1977a) to simplify them in the inner region. Two main conclu-
sions were obtained:

  i) The viscosity terms are of negligible contribution and may thus be

dropped from the momentum and energy equation.

b) The momentum equation reduces to:

$$\frac{\partial S}{\partial x} = 0 \tag{IV.6.19}$$

which indicates that the pressure is constant throughout the inner region. The continuity equation remains unchanged, as given by the first of Eqs. (IV.6.6), while the energy equation becomes:

$$-\lambda + \frac{\lambda y}{g} \cdot \frac{\partial g}{\partial y} + \gamma\left(\frac{\partial f}{\partial x} + \frac{jf}{x}\right) = \frac{\epsilon}{hg}\left(\frac{g}{h}\right)^{\alpha}\left[\frac{-g}{h}\cdot\frac{\partial^2 h}{\partial x^2}\right.$$

$$\left. -\frac{j}{x}\cdot\frac{g}{h}\cdot\frac{\partial h}{\partial x} + (2+\alpha)\frac{g}{h^2}\left(\frac{\partial h}{\partial x}\right)^2\right] \tag{IV.6.20}$$

where

$$\epsilon = \epsilon_2 + \epsilon_3$$

For the inner region solution, instead of following the complicated procedure of finding the value of Φ_E which contains second order differentiations by iteration, one can obtain an approximate solution, leading to at least a good qualitative description of the flow field, by assuming that the gasdynamic parameters may be expanded in a power series in the form

$$f = f_o + f_1\,x + f_2\,x^2 + f_3\,x^3 + O(x^4) \qquad\left.\begin{array}{c}\\[3em]\end{array}\right\} \tag{IV.6.21}$$

$$h = h_o + h_1\,x + h_2\,x^2 + h_3\,x^3 + O(x^4)$$

and

$$g = g_o$$

where the coefficients of the powers of x are functions of y only. A compatibility equation which must be satisfied by the correct solution, Eq. (II.112), is that the particle velocity at the center of symmetry must be equal to zero, that is $f(o,y) = 0$. Immediately it is shown that $f_o = 0$. At the center of symmetry, however, one has:

$$\frac{\partial T}{\partial x} \qquad \text{at} \qquad x = 0$$

Equation (IV.6.19) with the above equation may yield:

$$\frac{\partial h}{\partial x} \qquad \text{at} \qquad x = 0$$

If this equation is to be satisfied then h_1 must also vanish. Substituting Eqs. (IV.6.21) into the first of Eqs. (IV.6.6) and Eq. (IV.6.20), and equating the coefficients of the same powers of x to zero, one obtains from the continuity equation:

$$\lambda y \frac{h_o}{h_o} + (j+1) f_1 = 0 \tag{IV.6.22}$$

where the prime indicates differentiation with respect to y, also $f_2 = 0$, $h_3 = 0$ and

$$\lambda y \left(h_2' - \frac{h_2 h_o'}{h_o} \cdot \frac{j+3}{j+1} \right) - 2 h_2 + (j+3) h_o f_3 = 0 \tag{IV.6.23}$$

From the energy equation, one gets

$$-\lambda + \lambda y \frac{g_o'}{g_o} - \gamma \lambda y \frac{h_o'}{h_o} = -\epsilon \left[2 \, (j+1) h_2 \right] \frac{g_o^\alpha}{h_o^{\alpha+1}} \qquad \text{(IV.6.24)}$$

The gasdynamic parameters f and h , given by Eqs. (IV.6.21), are now reduced to:

$$f = f_1 \, x + f_3 \, x^3$$

and

$$h = h_o + h_2 \, x^2 \qquad\qquad\qquad\qquad \text{(IV.6.25)}$$

In addition to algebraic Eqs. (IV.6.22) - (IV.6.24) one has the three equations that match the inner solution to the outer solution, namely

$$f_m = f_1 \, x_m + f_3 \, x_m^3$$

$$h_m = h_o + h_2 \, x_m^2 \qquad\qquad\qquad\qquad \text{(IV.6.26)}$$

and

$$g_m = g_o$$

where x_m is the x boundary of the inner region.

Equations (IV.6.22), (IV.6.23), (IV.6.24) and (IV.6.26) form a system of six equations that may be solved simultaneously for f_1 f_3 , h_o , h_2 , g_o and x_m , for a particular shock strength y .

The derivatives of the coefficients h_o, h_2 and g_o with respect to y can be put in a finite difference form as:

$$h_o')_i = \frac{dh_o}{dy} \cong \frac{\Delta h_o}{\Delta y} = \frac{h_o)_i - h_o)_{i-1}}{\Delta y}$$

$$h_2')_i = \frac{dh_2}{dy} \cong \frac{\Delta h_2}{\Delta y} = \frac{h_2)_i - h_2)_{i-1}}{\Delta y}$$

and

$$g_o')_i = \frac{dg_o}{dy} \cong \frac{\Delta g_o}{\Delta y} = \frac{g_o)_i - g_o)_{i-1}}{\Delta y}$$

(IV.6.27)

To develop the computational procedure, the problem is solved first in the self-similar case by putting y equal to zero in Eqs. (IV.6.22) - (IV.6.24). These equations reduce to

$$f_1 = 0$$

$$f_3 = 2 h_2/[h_o(j+3)]$$

and

$$h_2 = h_o^{\alpha+2}/[2\epsilon g_o^{\alpha}]$$

(IV.6.28)

After some algebraic manipulation, one can easily obtain the following equations for the determination of the coefficients g_o, f_3, h_o and h_2 in terms of the values of the gasdynamic parameters at the matching point g_m, f_m and h_m:

$$g_o = g_m$$

$$f_3 = f_m / x_m^3$$

$$h_o = 2 h_m / \left[(j+3) f_3 x_m^2 + 2 \right]$$

and

$$h_2 = f_3 h_o (j+3) / 2$$

(IV.6.29)

Since all the coefficients depend on the matching point parameters, an iterative procedure is required to find the matching point x_m which satisfies the last of Eqs. (IV.6.28). The latter equation may not be satisfied at a specified step of the numerical integration procedure, x_i . Thus, assuming a linear relation between the residual value of that equation, R , and x , the correct value of the matching point x_m can be obtained by interpolation, as shown in Fig. IV.6.1. In addition, the following relations were used:

$$R = h_2 - h_o^{\alpha+2} / (2 \epsilon \, g_o^\alpha)$$

(IV.6.30)

and

$$x_m = x_i + (\Delta x) \, R_i / (R_i - R_{i-1})$$

(IV.6.31)

where R_i is the residual value of the last of Eqs. (IV.6.28) at x_i .

The corresponding values of the gasdynamic parameters at the matching point are also determined by interpolation, considering straight line relations between their values and x . For an example, Fig. IV.6.2 shows how the particle

velocity at the matching point, f_m , is determined. Thus

$$f_m = f_i + \frac{(f_{i-1} - f_i)(x_m - x_i)}{(\Delta x)}$$

$$h_m = h_i + \frac{(h_{i-1} - h_i)(x_m - x_i)}{(\Delta x)}$$

and

$$g_m = g_i + \frac{(g_{i-1} - g_i)(x_m - x_i)}{(\Delta x)}$$

(IV.6.32)

Once the matching point parameters are determined, the coefficients g_0 , h_0 , h_2 and f_3 are also determined to define completely the inner region solution for the self-similar problem.

One can then proceed to obtain the solution for the non-self-similar problem. At a specified value of $y = y_i$, from Eqs. (IV.6.22), (IV.6.23) and (IV.6.27), after some algebraic manipulations, one may obtain the coefficients g_0 , h_0 , h_2 , f_1 and f_3 in terms of the values of the gasdynamic parameters at the matching point as follows:

$$g_{0_i} = g_m$$

$$h_{0_i} = (b + \sqrt{b^2 - 4ac})/2a$$

$$h_{2_i} = (h_m - h_{0_i})/x_m^2$$

$$f_{1_i} = -\lambda_i y_i \frac{(h_{0i} - h_{0i-1})}{(\Delta y) h_{i}^{(1+1)}}$$

(IV.6.33)

and

$$f_{3_i} = (f_m - f_{1_i} x_m) / x_m^3$$

where

$$a = \lambda_i y_i x_m \left(\frac{i+5}{i+1}\right) + \left[2 x_m + f_m (i+3)\right] (\Delta y)$$

$$b = \frac{2 \lambda_i y_i x_m}{i+1} \left[h_m + (i+3) h_{0_{i-1}}\right]$$

$$+ x_m \left[2 h_m (\Delta y) + \lambda_i y_i h_{2_{i-1}} x_m^2\right]$$

and

$$c = \left(\frac{i+3}{i+1}\right) \lambda_i y_i x_m h_m h'_{0_{i-1}}$$

Equation (IV.6.24) must be satisfied for the correct values of the gasdynamic parameters, and thus one follows the same procedure which is used for the self-similar problem.

The equation which corresponds to Eq. (IV.6.30) will take the form:

$$R = \lambda_i \left\{ -1 + y_i \left[\left(1 - \frac{g_{0\,i-1}}{g_{0i}}\right) - \gamma\left(1 - \frac{h_{0\,i-1}}{h_{0i}}\right)\right]\right\}$$

$$+ 2 \epsilon (i+1) h_{2_i} \left(\frac{g_{0i}}{h_{0i}}\right)^\alpha / h_{0i}^2 \qquad (IV.6.34)$$

Equations (IV.6.31) and (IV.6.32) are used to obtain the gasdynamic parameters at the matching point x_m and thus the coefficients g_0, f_1, f_3, h_0 and h_1.

Having computed all variables at $y = y_i$, one can proceed to obtain the solution at $y = y_{i+1}$ by applying the same procedure. The procedure is then repeated to cover the whole y domain.

iv) Results and Conclusions

In order to obtain a numerical solution, it has been considered that the detonating medium is a stoichiometric methane-air mixture, for which $\bar{q}$ = 20.0231, γ = 1.3 and y_{cJ} = 0.033786 (see section (IV.4)).

The values of the parameters of transport properties which have been used to obtain the inner region solution are $Re = 10^4$, Pr = 1 and No = 1.

Introducing the effect of transport properties inside the inner region, the density at the center of symmetry, as expected, took the non-zero values shown in Figs. IV.6.3 and the temperature took finite values shown in Figs. IV.6.4 for different geometries and the indicated specific values of Re , Pr and No . The dotted range in these curves expresses the continuation of the inviscid solution of the outer region if transport effects were to be neglected. Since the energy inside the flow field is conserved, the solution of the inner region rearranges the temperature distribution inside the inner region only as shown in Figs.IV.6.4. One may expect that the rearrangement of such temperature inside the whole of the flow field can be achieved by considering the transport effects in the outer region, which would have a rather small contribution.

The velocity profiles for $0.005 \leqslant y < 0.033$, as shown in Figs. IV.6.5, extend into negative values of f indicating that the particles, after their initial outward shift due to the passage of the front, returns towards the center of the flow field. This occurs due to the relaxation following the strong explosion which causes nearly all the mass of the blast wave, immediately after explosion, to be concentrated close to the wave front.

It should be noted that the pressure profiles are not different from those of the inviscid case, Figs. IV.4.1. This result is based on the assumption that the pressure is constant throughout the inner region. This assumption was upheld by Kamel et al.(1977a) when he found that the pressure distribution is

insensitive to the effects of both thermal conduction and radiation.

The viscosity and conductivity exponent α is taken to equal its self-similar values of $-\frac{1}{2}$, 0 and 1/6 for planar, cylindrical and spherical geometries, respectively, while the radiation exponent β is considered to equal 7/2, J and 17/6 for the same geometries, as given by Eq. (IV.6.12). Therefore, at a certain temperature, the thermal conductivity is greatest for the spherical wave and least for the planar one, while the absorption coefficient a' must be lowest for the spherical wave and highest for the planar one. This means that the dissipation effects are greatest for spherical waves and least for planar waves.

Figure IV.6.6 shows the thickness of the central inner region, x_m , as a function of the parameter y for planar, cylindrical and spherical geometries. As expected, the thickness of the inner region has a maximum value at $y = 0$, immediately after explosion, with highest heat dissipation and then decreases as the wave front decays. At any specified value of y , the thickness of the inner region is greatest for the spherical case, with its greatest dissipative effects, and least for the planar wave.

Figures IV.6.7 show the integral curves in the $F - Z$ phase-plane, for the inner region, for planar, cylindrical and spherical geometries. As shown in these figures, the integral curves, within the range $0.005 < y \leq 0.033$, extend into negative values of F , the same tendency in velocity profiles.

Figures from IV.6.8 to IV.6.12 give the relations between the coefficients g_0 , h_o , h_2 , f_1 and f_3 and the parameter y , respectively, for different blast wave geometries.

Another important result of this analysis is that, when the mass integral, J_1 , and the energy integral, J_3 , were evaluated with transport phenomena taken into account, they differ very slightly from those of the inviscid medium. This directly indicates from Eq. (IV.6.14) that the shock wave similarity front trajectory remains nearly unaffected by transport phenomena and does not differ from that of the inviscid medium.

The sharp transition between the inner region, where transport phenomena are most important, and the outer inviscid region is associated, of course, with a

physically inadmissible idealization. However, smooth transitions may be
achieved if series expansions of the gasdynamic parameters of higher powers
for the inner region solution are used and if the outer region contains al-
so the transport effects.

Figure Captions

Fig. IV.6.1.   A schematic diagram shows how the correct value of the matching point $\mathcal{X}_m$ is obtained.

Fig. IV.6.2   A schematic diagram shows how the particle velocity at the matching point f_m is obtained.

Fig. IV.6.3 (a), (b) & (c)

Non-dimensional density profiles of blast waves in a detonating methane-air mixture with transport phenomena taken into account for $Re = 10^4$, $Pr = 1$, $No = 1$ and $\gamma = 1.3$ while $j = 0$, 1 and 2, respectively.

Fig. IV.6.4 (a), (b) & (c)

Non-dimensional temperature profiles of blast waves in a detonating methane-air mixture with transport phenomena taken into account for $Re = 10^4$, $Pr = 1$, $No = 1$ and $\gamma = 1.3$ while $j = 0$, 1 and 2, respectively.

Fig. IV.6.5 (a), (b) & (c)

Non-dimensional velocity profiles of blast waves in a detonating methane-air mixture with transport phenomena taken into account for $Re = 10^4$, $Pr = 1$, $No = 1$ and $\gamma = 1.3$ while $j = 0$, 1 and 2, respectively.

Fig. IV.6.6   Non-dimensional thickness of the inner region $\mathcal{X}_m$, as a function of y, of blast waves in a detonating methane-air mixture with transport phenomena taken into account for $Re = 10^4$, $Pr = 1$, $No = 1$ and $\gamma = 1.3$ while $j = 0$, 1 and 2.

Fig. IV.6.7 (a), (b) & (c)

Integral curves in the F-Z phase plane for the inner region, for different values of y, of blast waves in a detonating methane-

air mixture with transport phenomena taken into account for $Re = 10^4$, $P_r = 1$, $No = 1$ and $\gamma = 1.3$ while $j = 0$, 1 and 2, respectively.

Fig. IV.6.1

Fig. IV.6.2

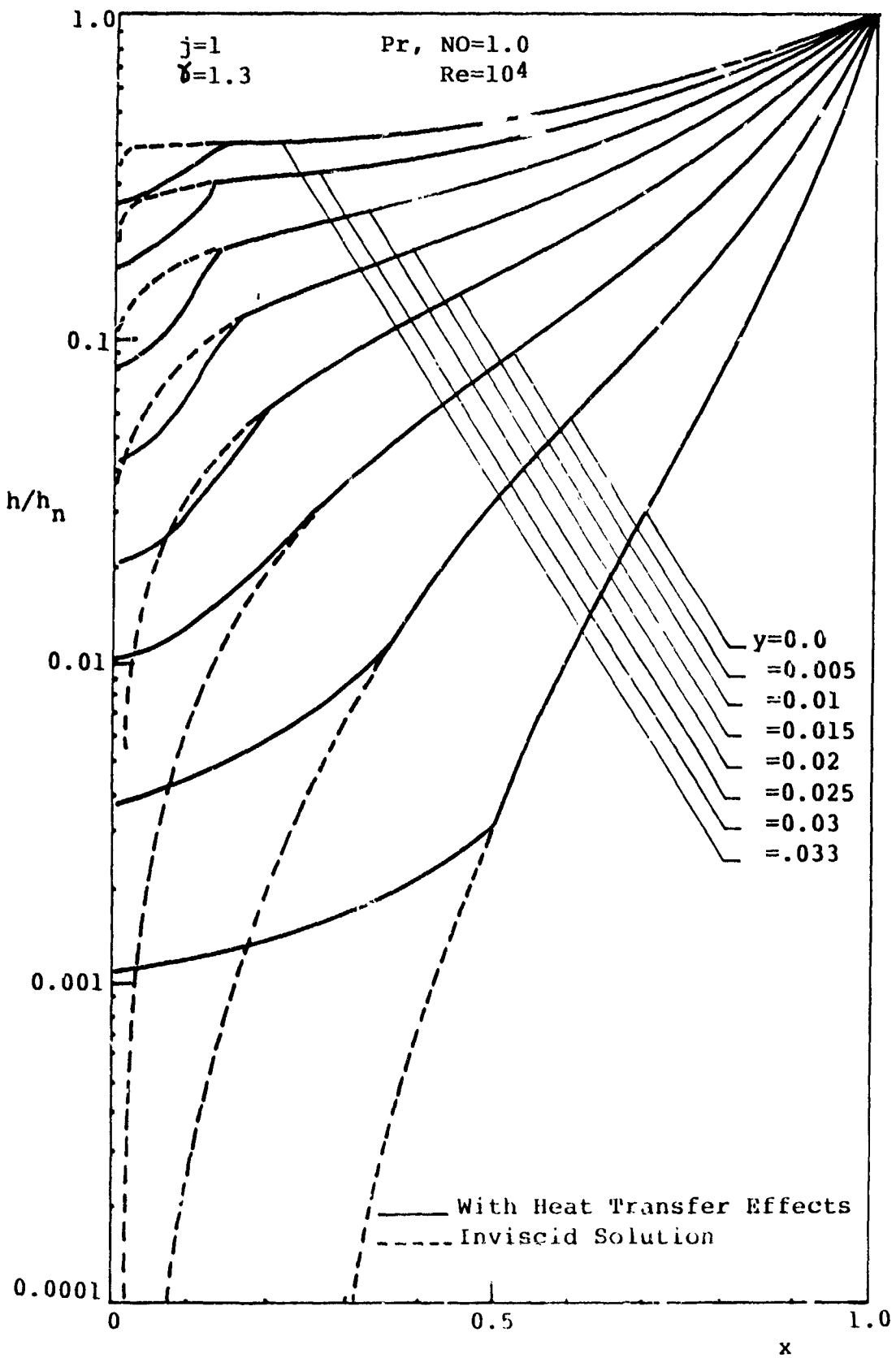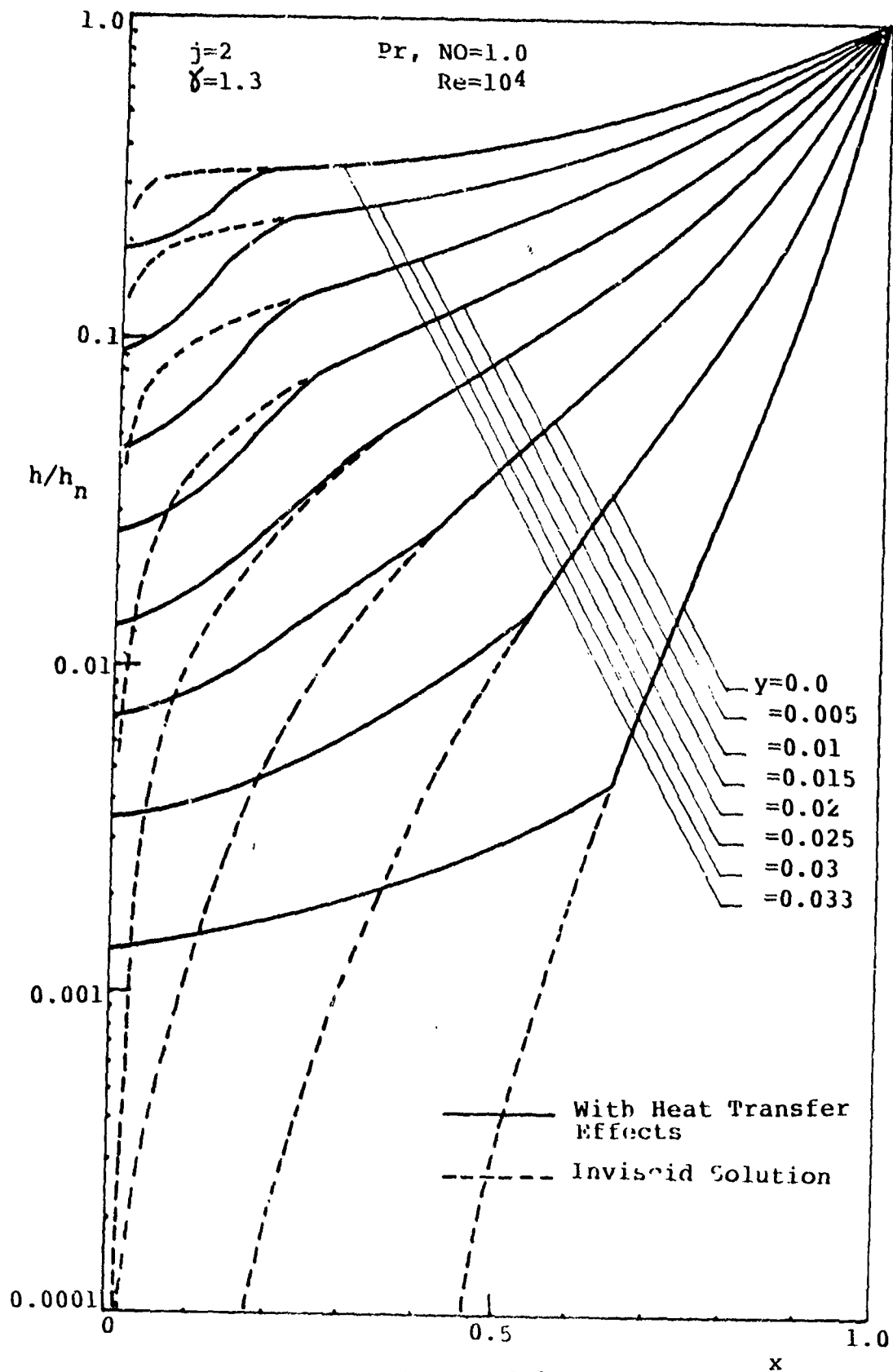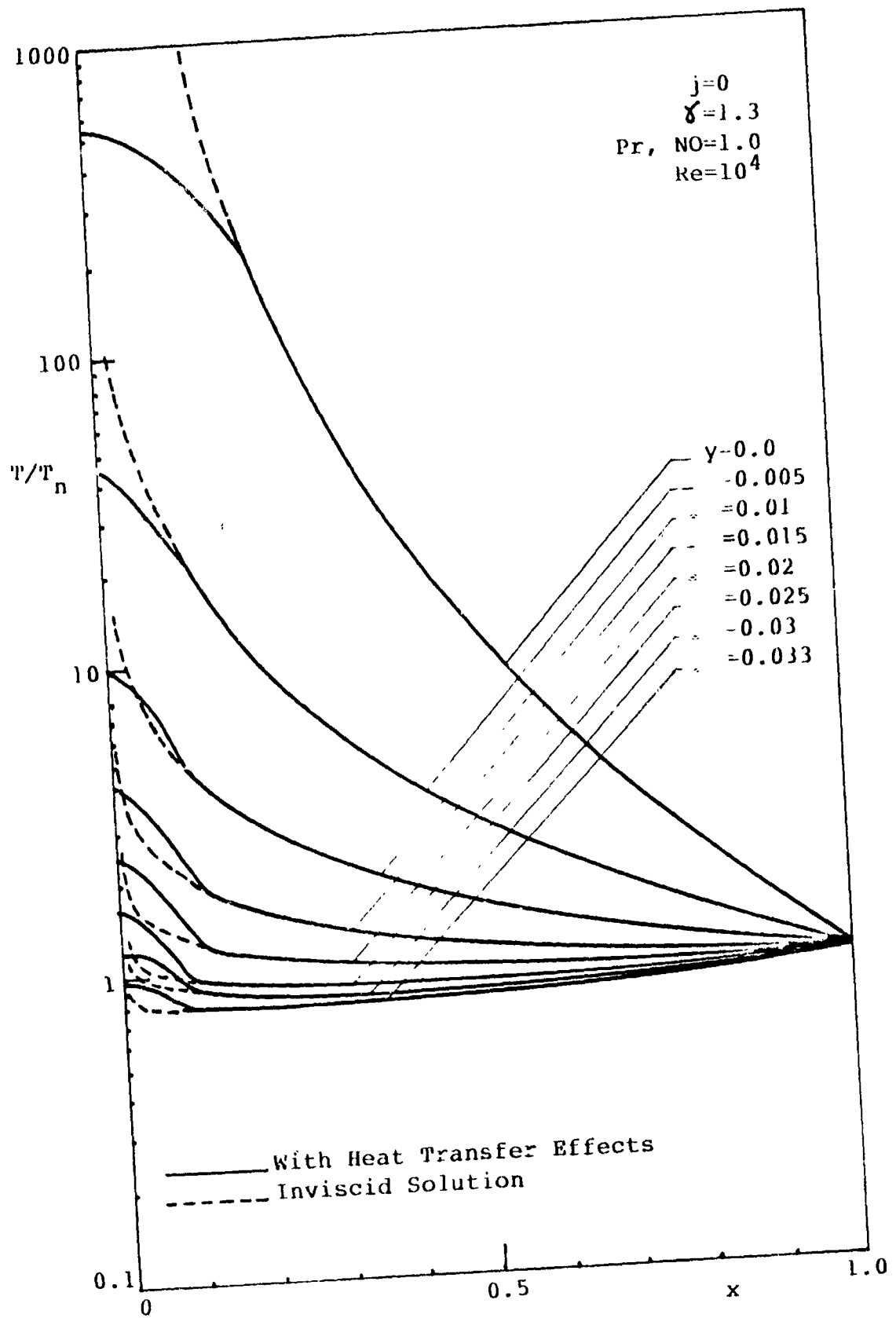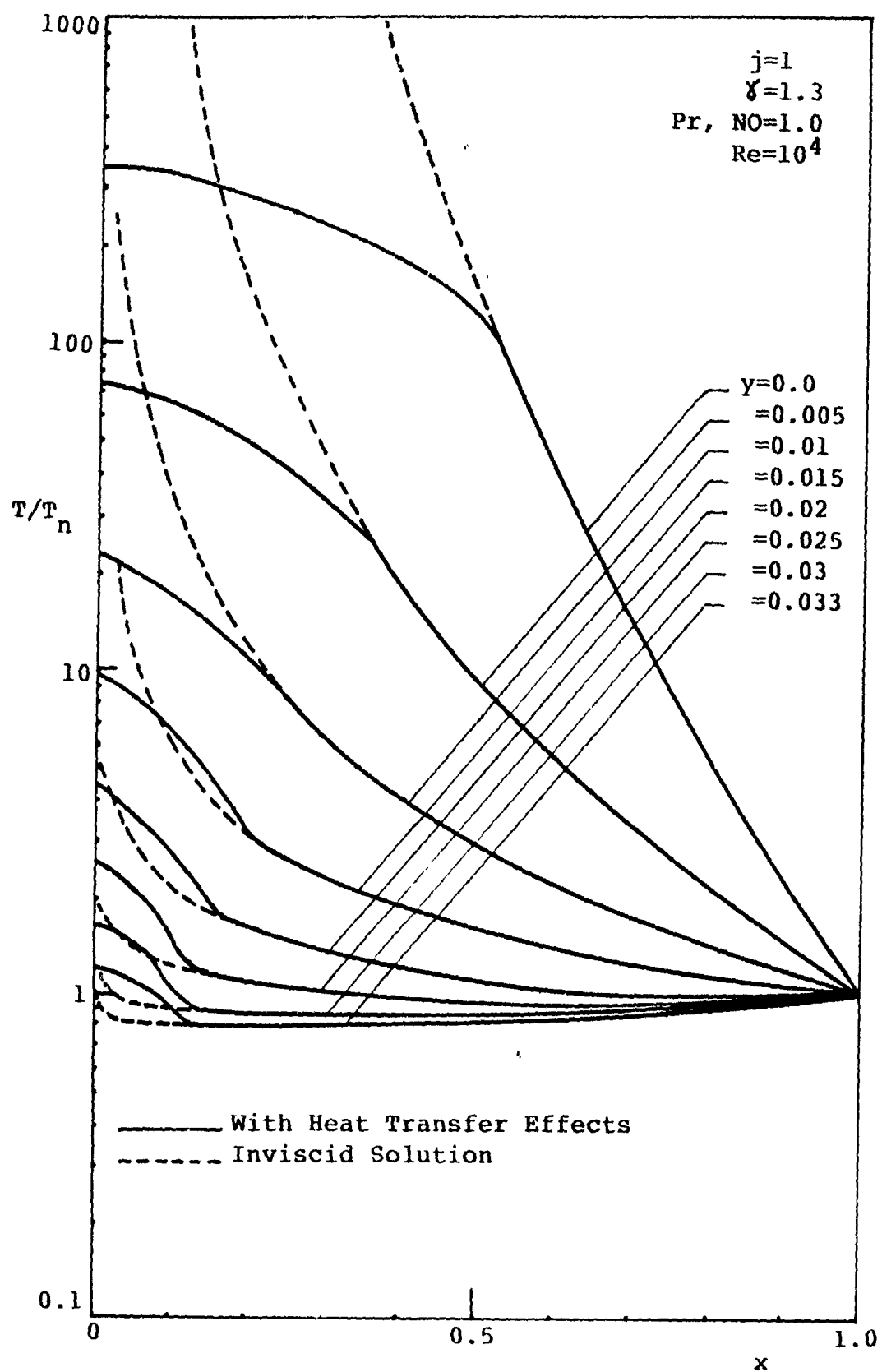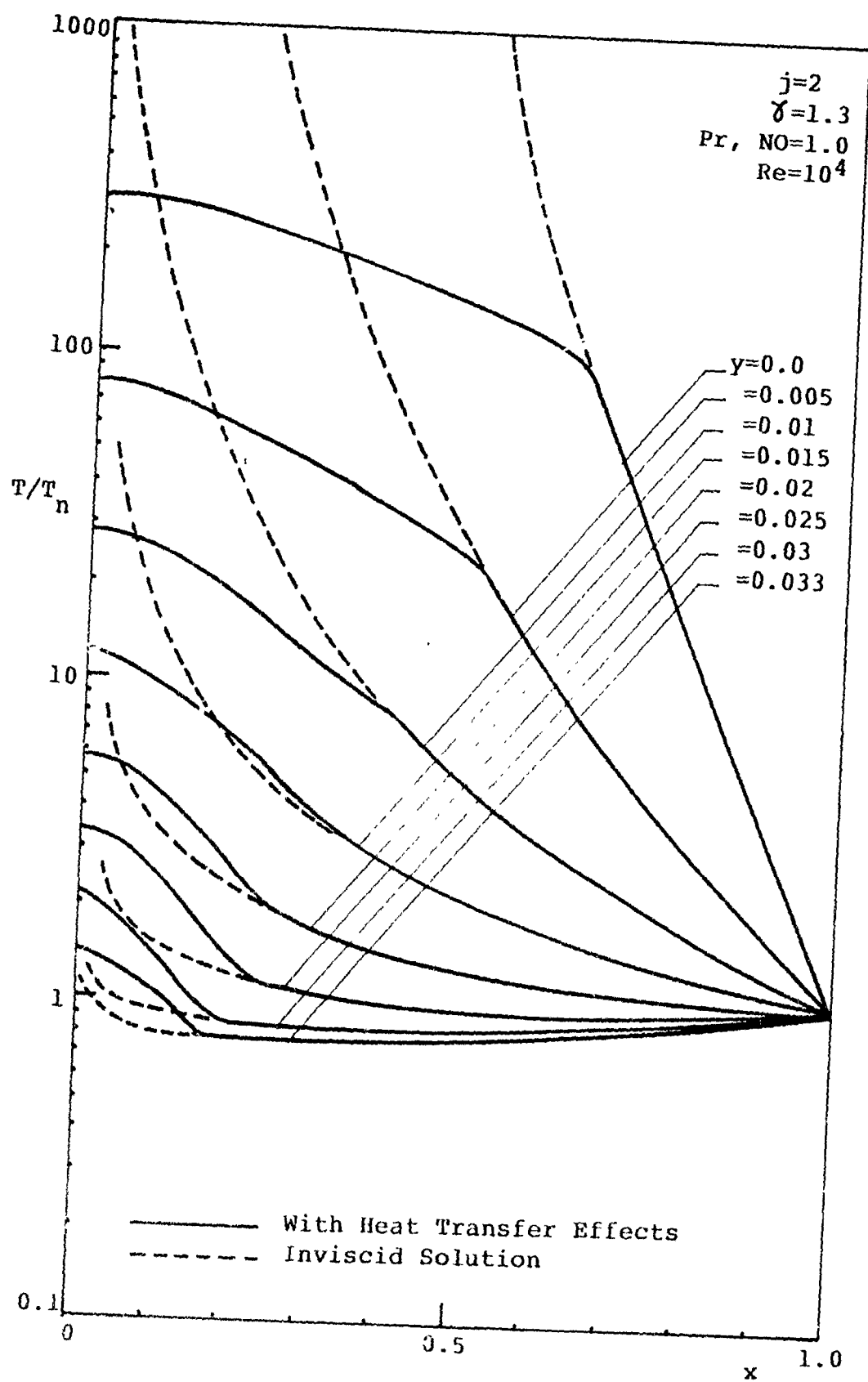Fig. IV.6.42

Fig. IV.6.3b

310
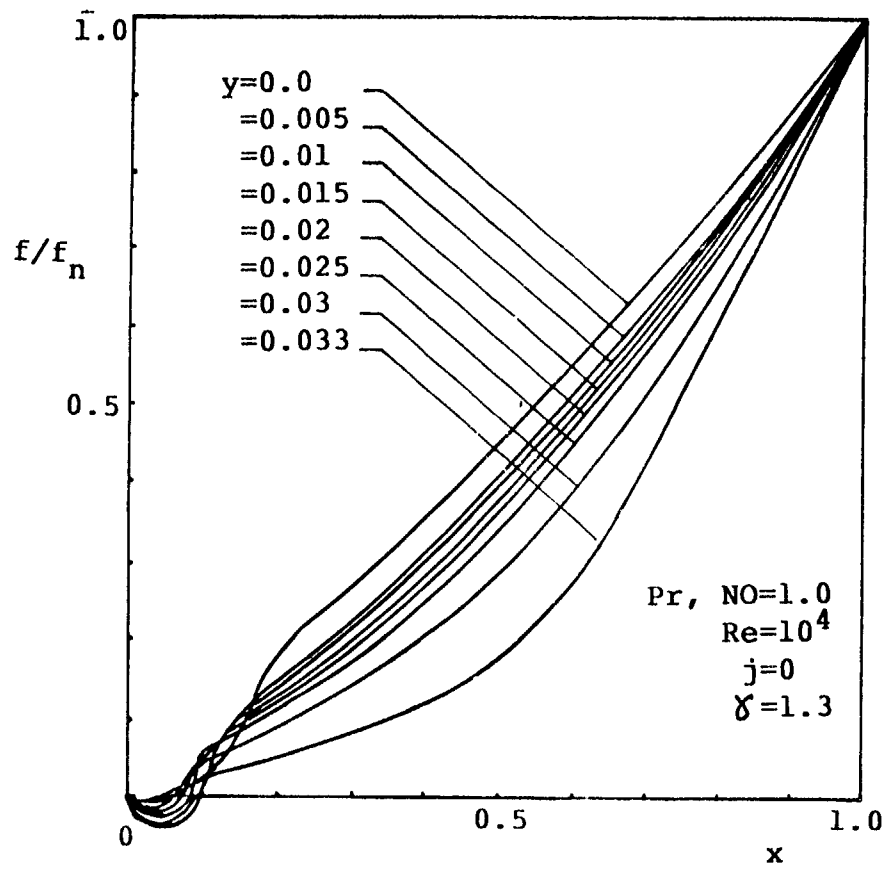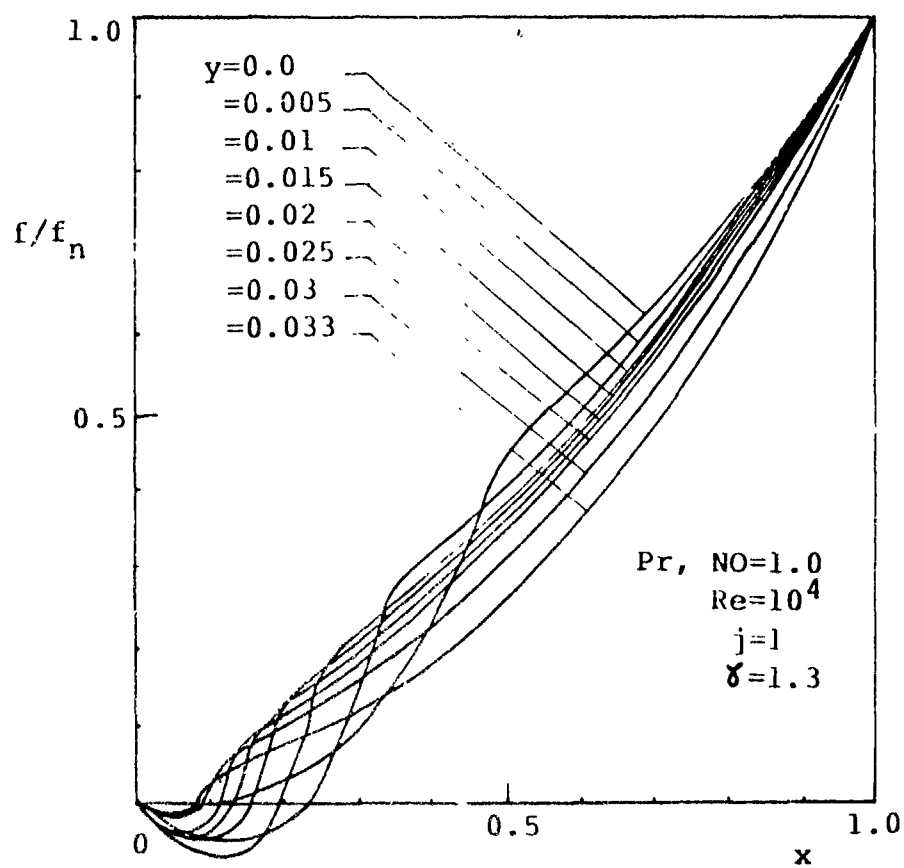

Fig. IV.6.3c

Fig. IV.6.4a
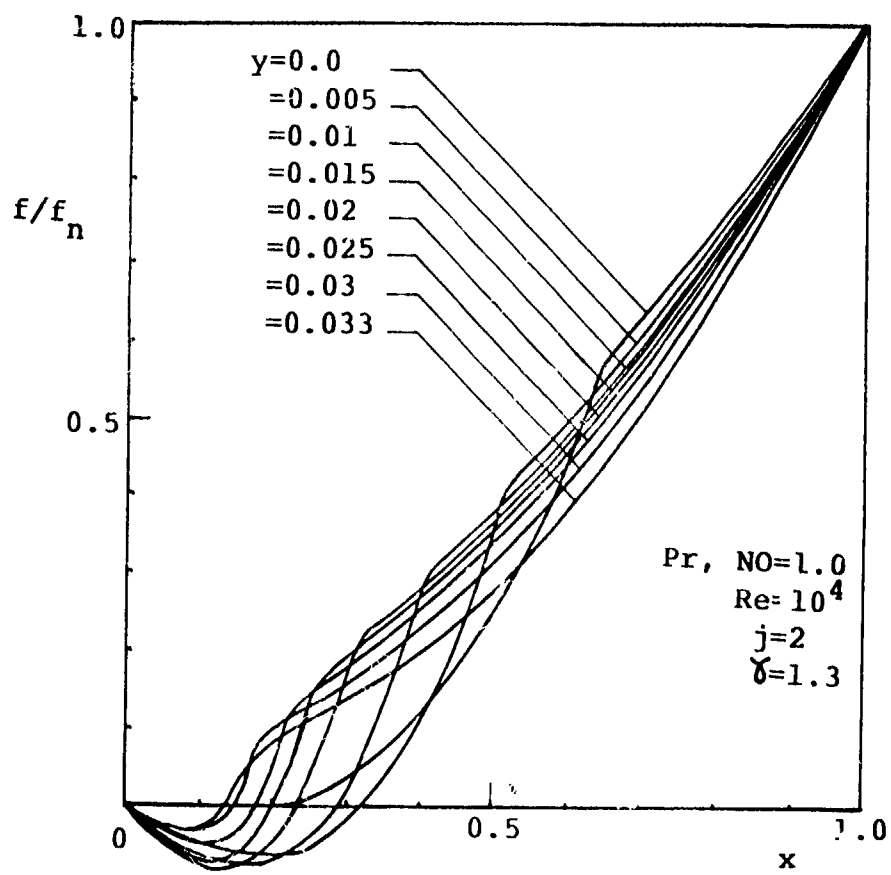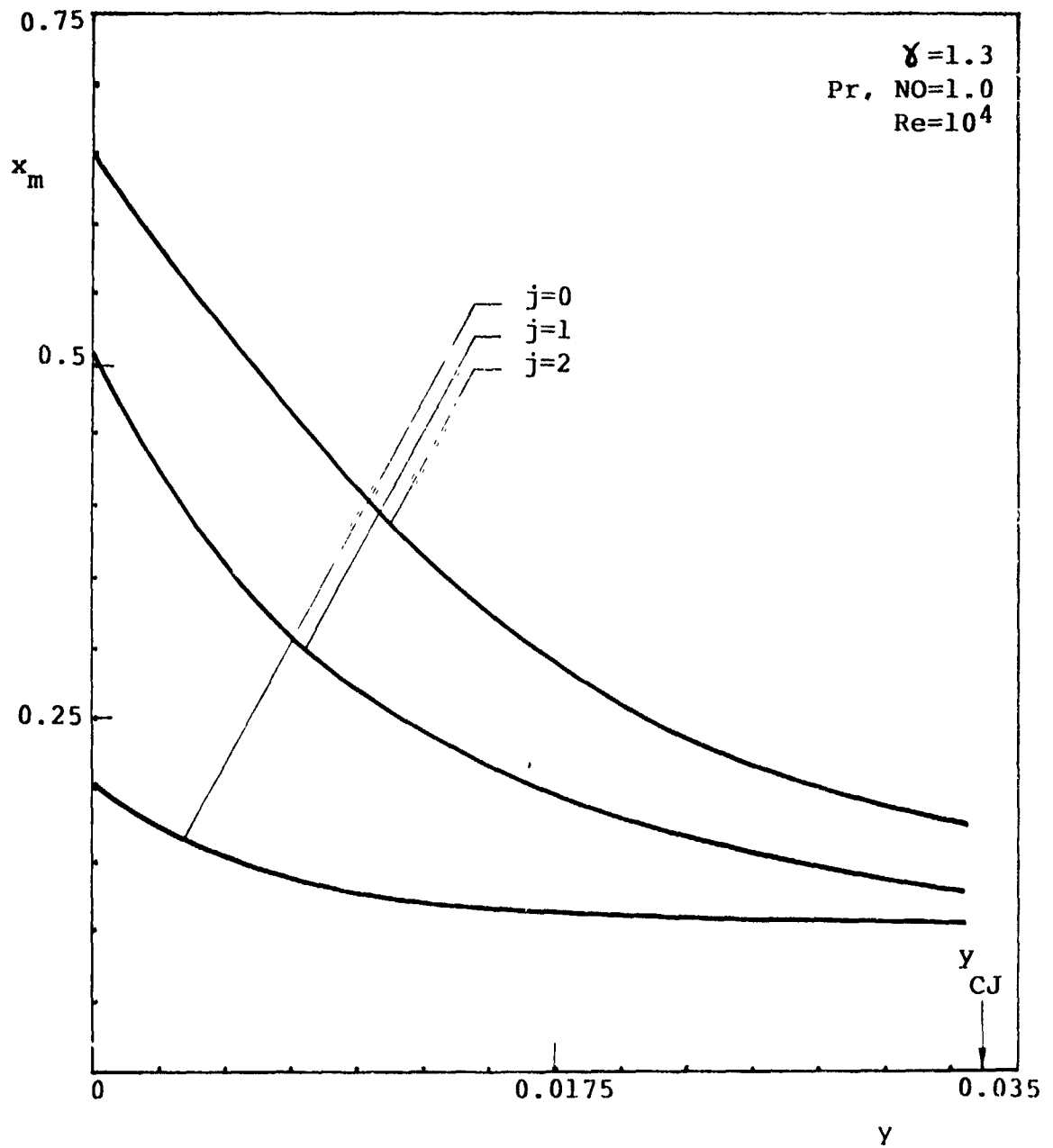
312

Fig. IV.6.4b

Fig. IV.6.4c
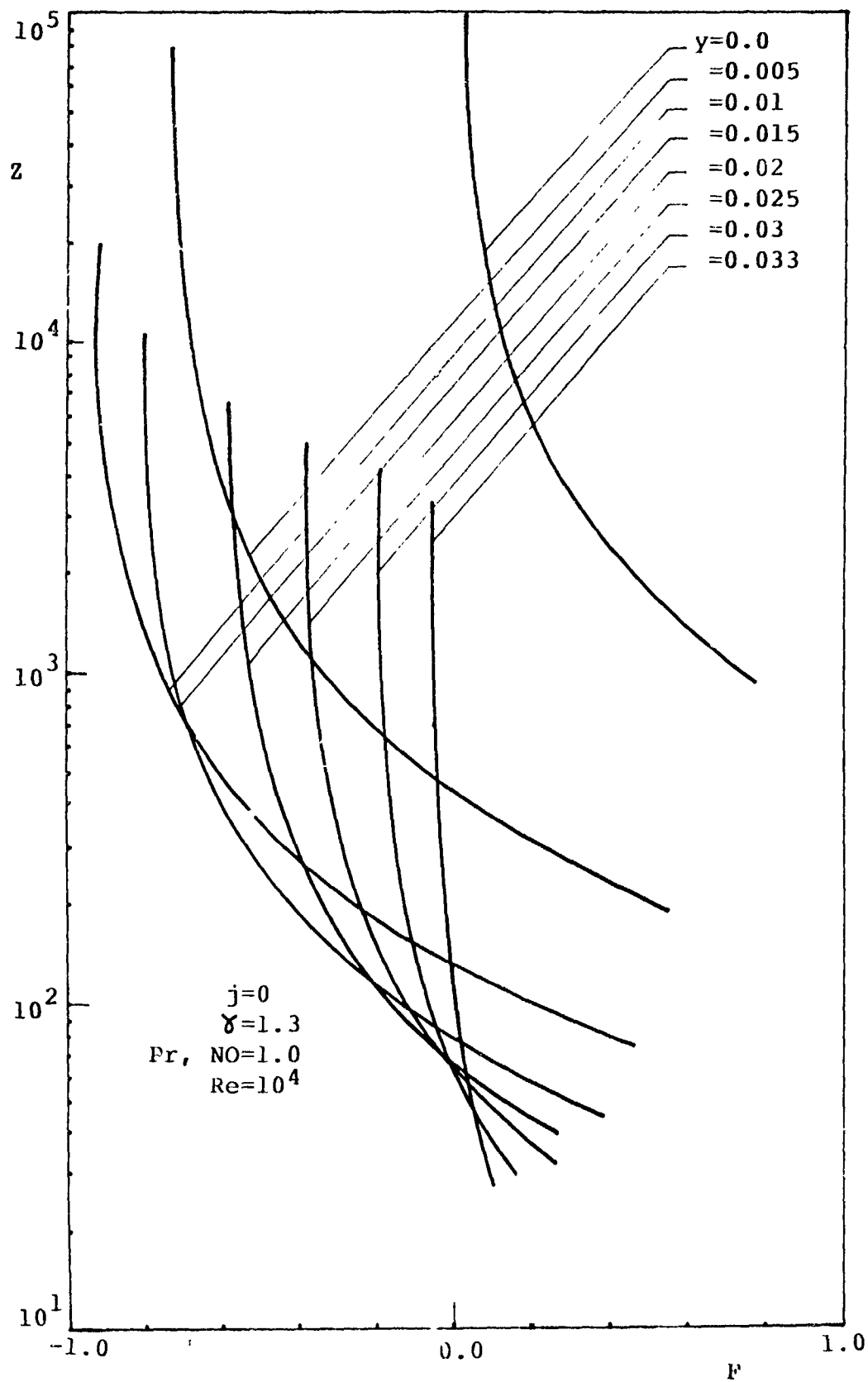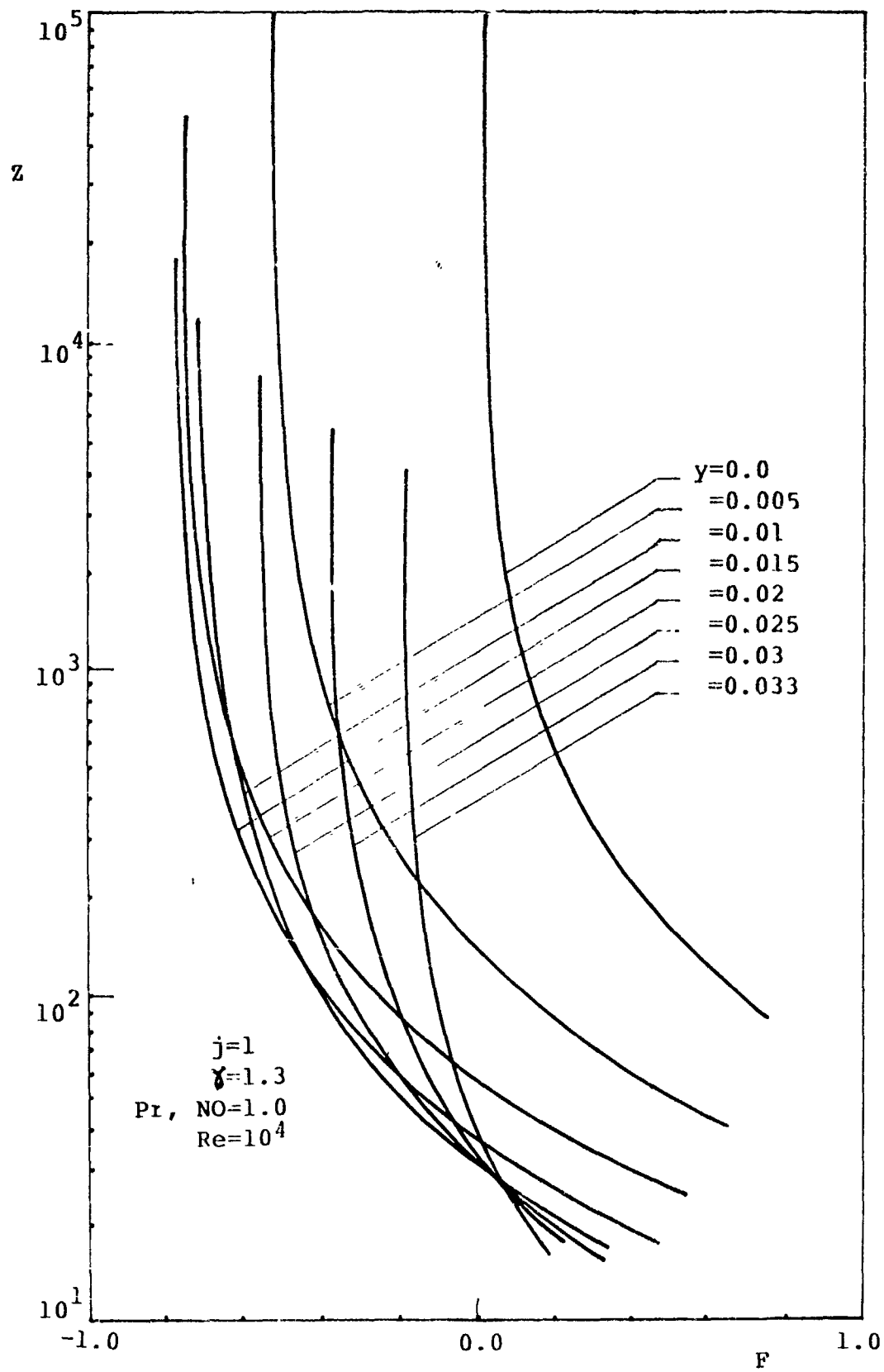
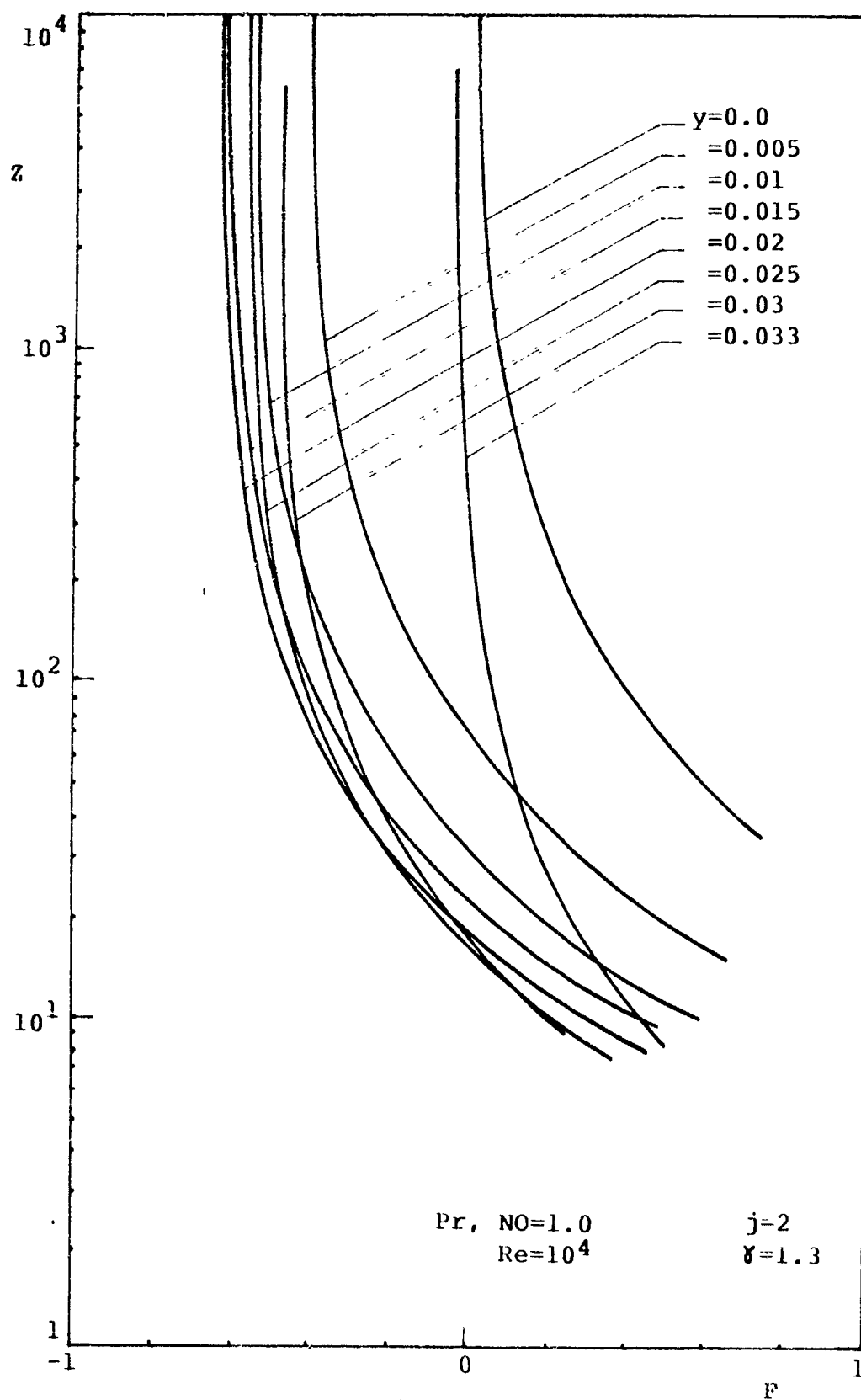Fig. IV.6.5a

Fig. IV.6.5b

Fig. IV.6.5c
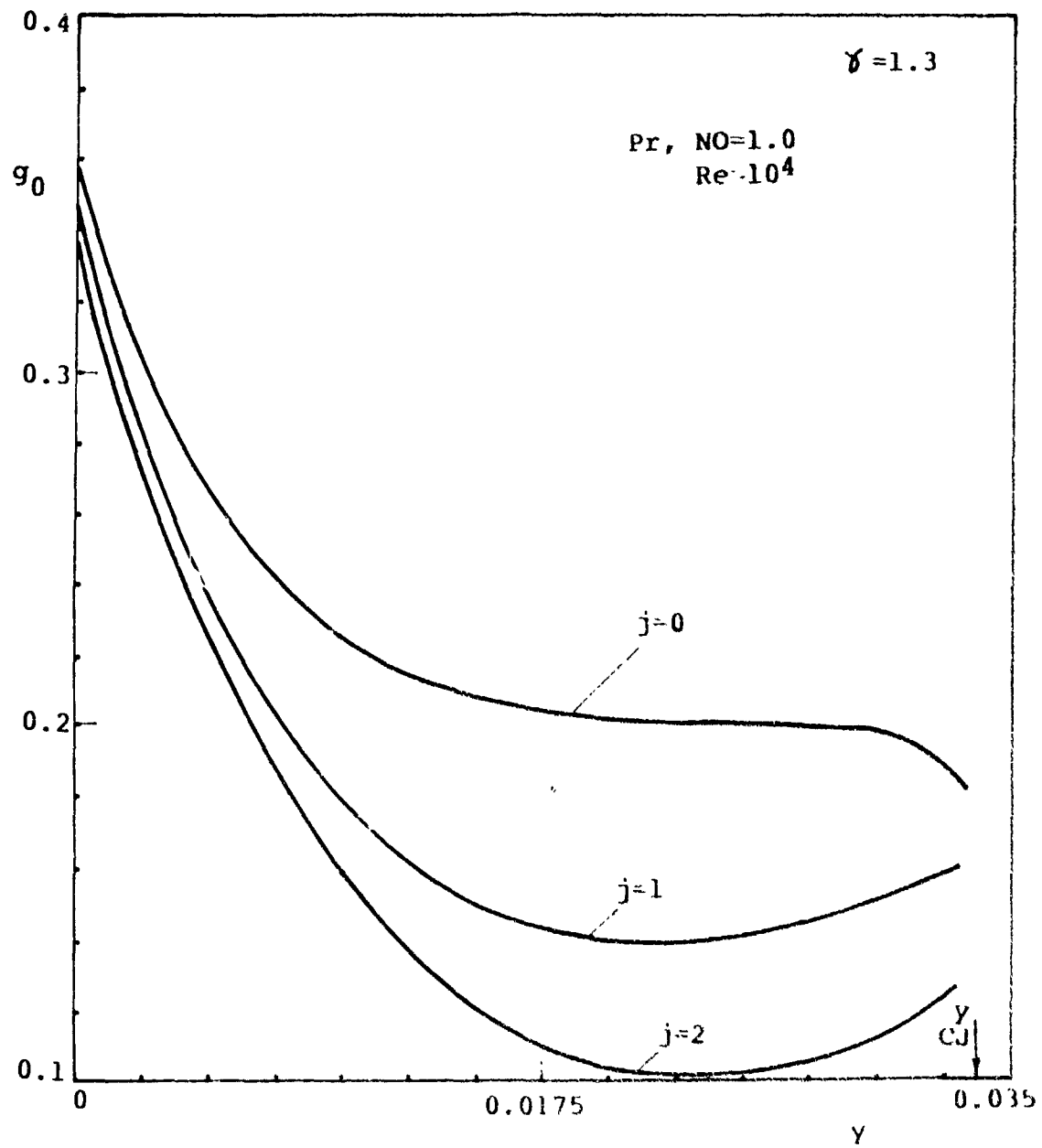
Fig. IV.6.6
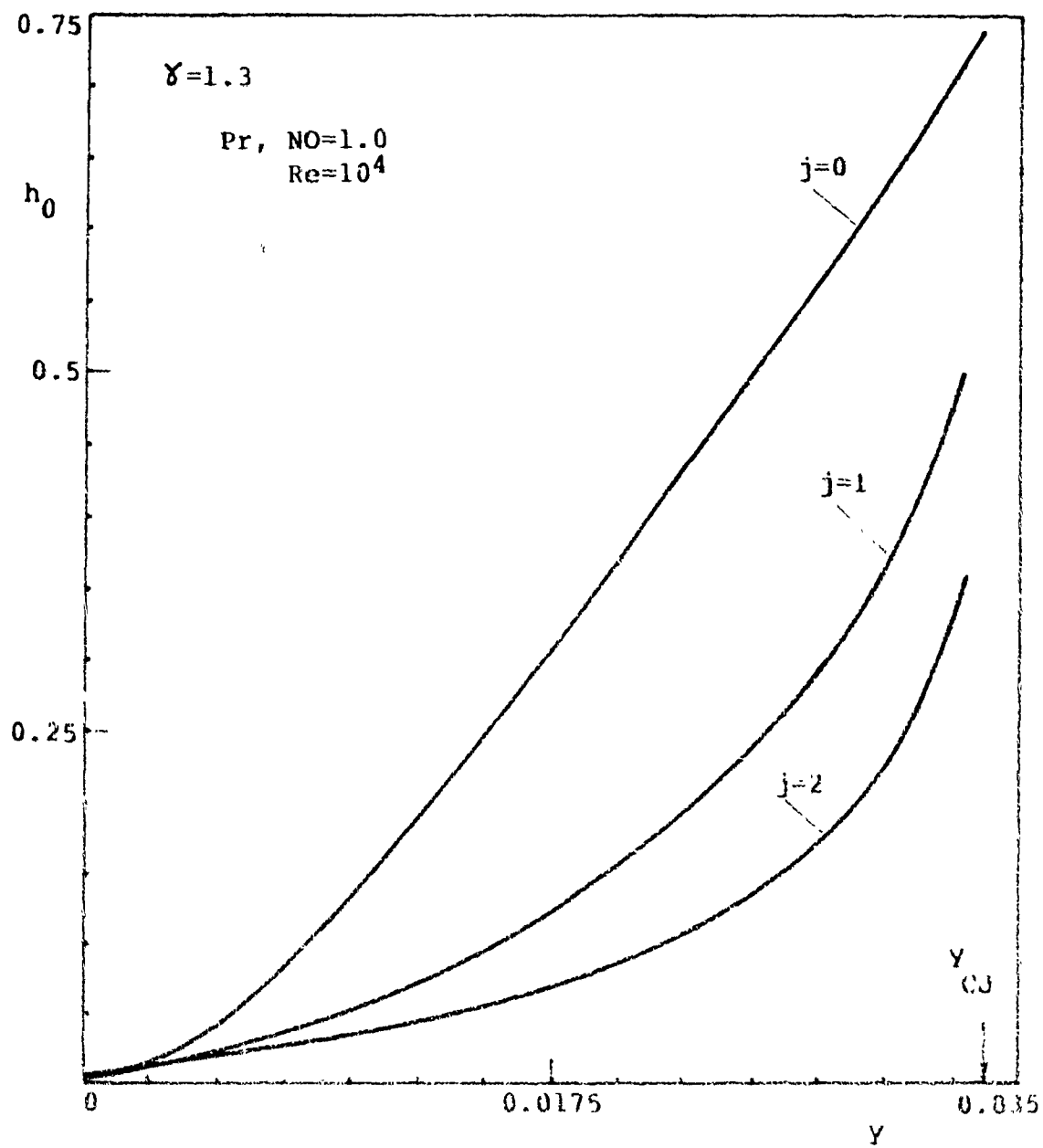
Fig. IV.6.7a
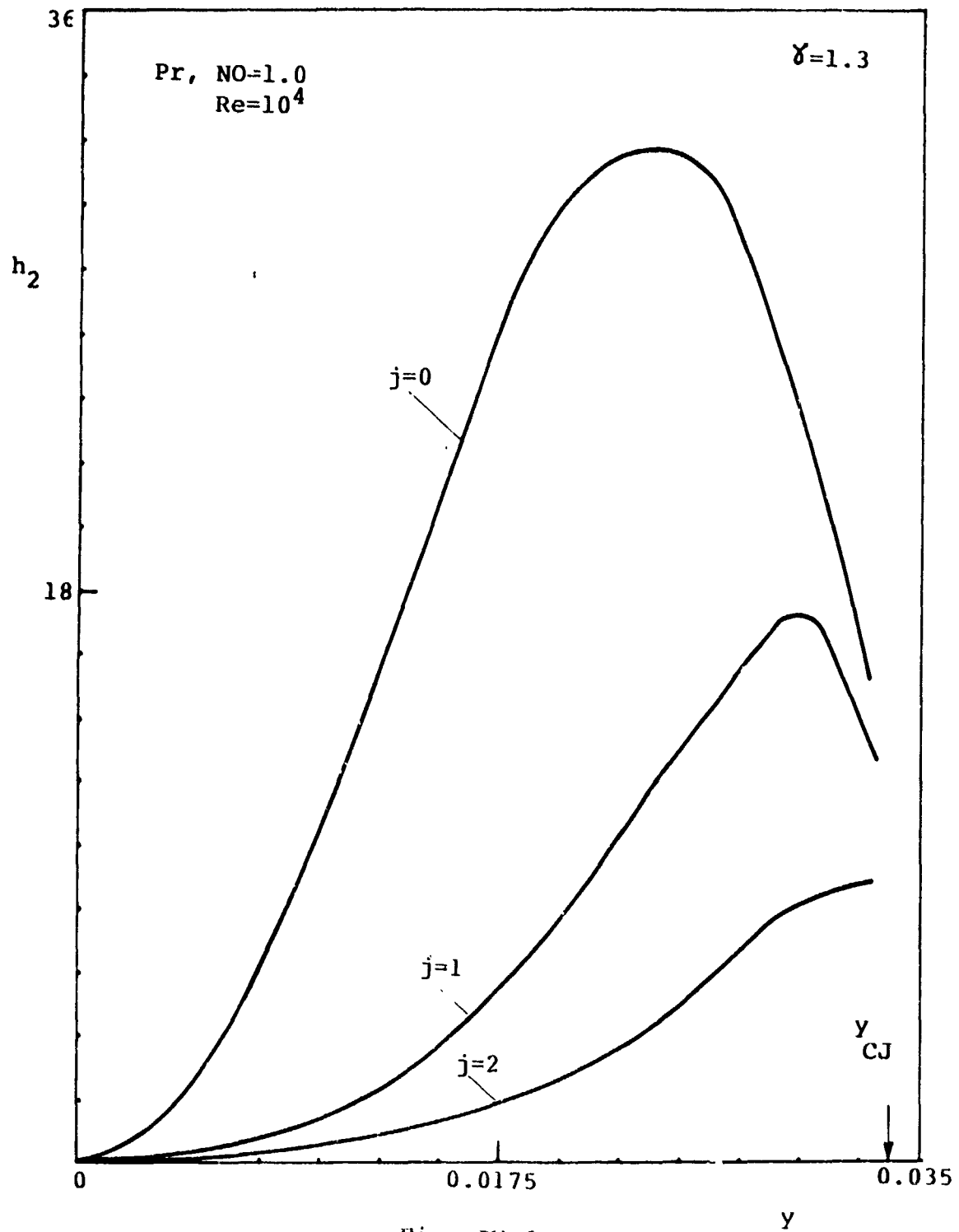
Fig. IV.6.7b
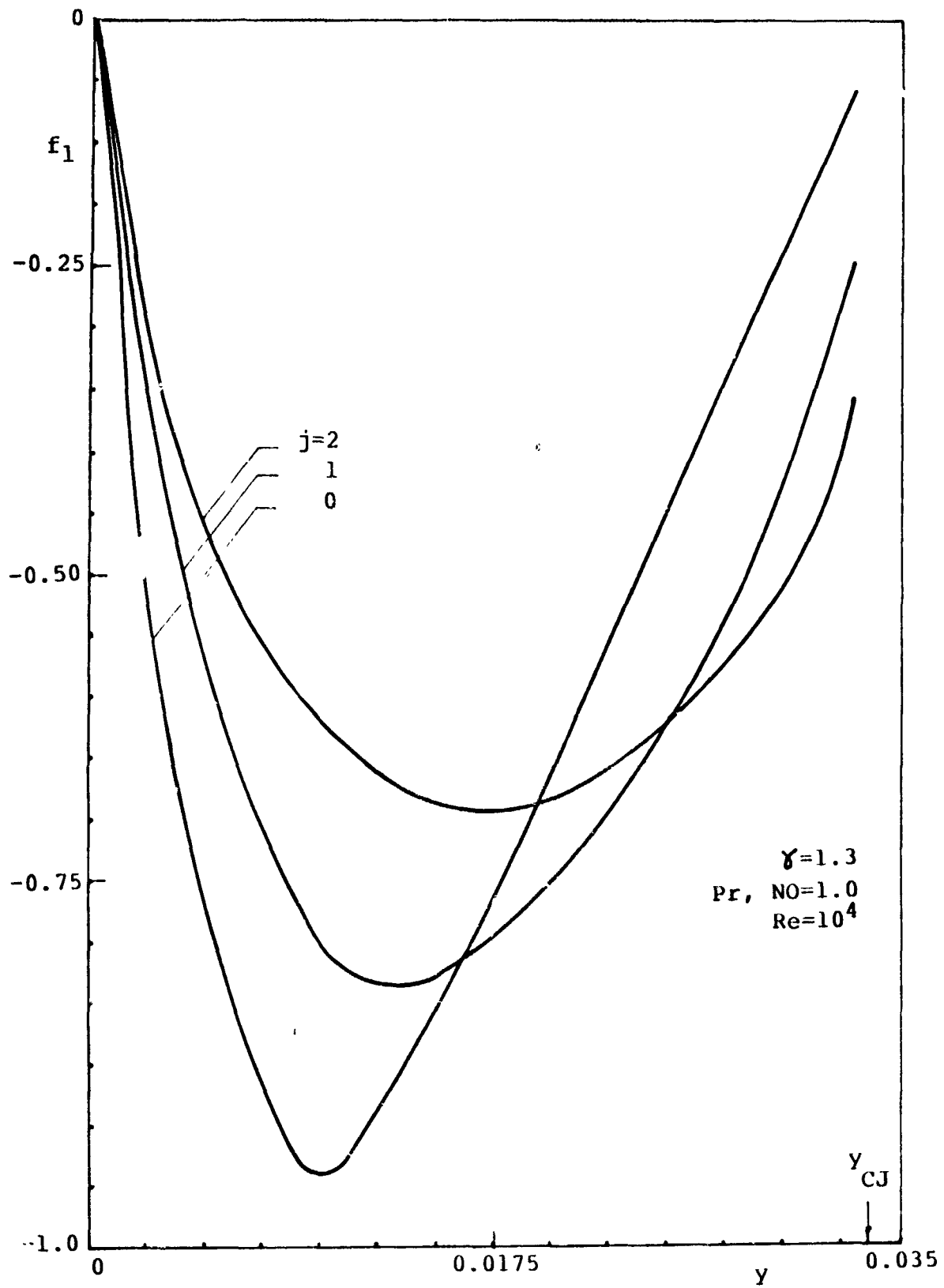
Fig. IV.6.7c
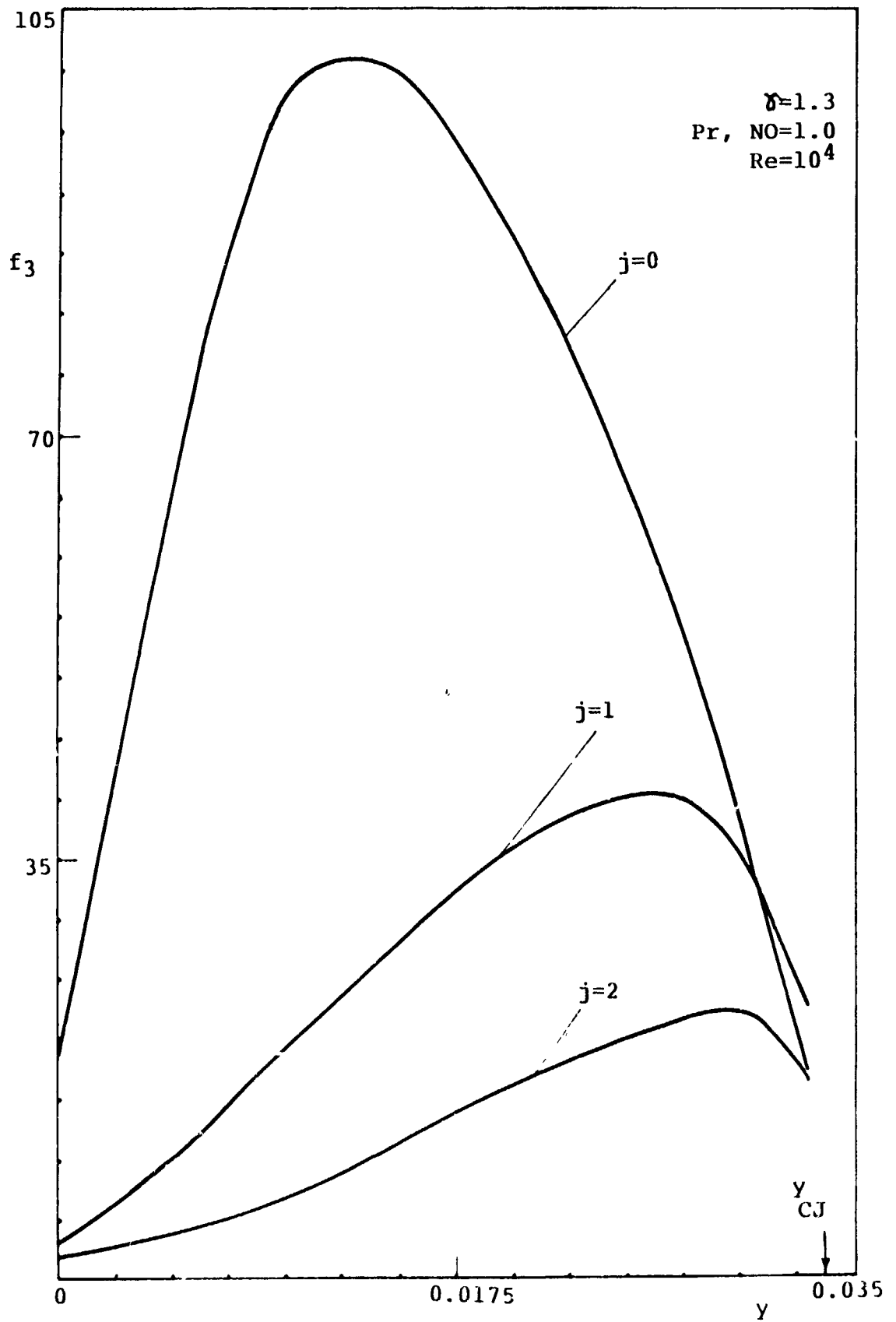
Fig. IV.6.8

Fig. IV.6.9

Fig. IV.6.10

Fig. IV.6.11

Fig. IV.6.12

REFERENCES

Abdel-Raouf, A.M. (1982), "Non-Self-Similar Blast Waves in a Detonating Medium with Heat Transfer Effects", unpublished M.Sc. Thesis, Cairo University.

Attia, Y.M. (1974), "A Study of the Application of Quasi-Similar Solution to the Non-Self-Similar Blast Waves", unpublished M.Sc. Thesis, Cairo University.

Bach, G.G. and Lee, J.H. (1969), "Higher-Order Perturbation Solutions for Blast Waves", AIAA Journal, Vol. 7.

Bach, G.G. and Lee, J.H. (1970), "An Analytical Solution for Blast Waves", AIAA Journal, Vol. 8, No. 2, pp. 271-275.

Benson, R.S. (1967), "Advanced Engineering Thermodynamics", Pergamon Press, London.

Brode, H.L. (1955), "Numerical Solutions of Spherical Blast Waves", J. App. Physics, Vol. 26, No. 6, pp. 766-775.

Brode, H.L. (1959), "Blast Wave from a Spherical Charge", Phys. Fluid, Vol. 2, pp. 230-235.

Camble, A.B. (1963), "Plasma Physics and Magnetofluid-Mechanics", Mc Graw-Hill, New York.

Geiger, W. (1979), "Explosion Hazards of Transport Gases - Research within the Reactor Safety Program of the Federal Republic of Germany. Discussion on Explosion Hazards at the 7th International Collequium on Gasdynamics of Explosions and Reactive Systems, Goettingen, 24. August, edited by H.Gg. Wagner, 49-56.

Ghoneim, A.F. (1975), "Blast Waves in Real Gases", unpublished M.Sc. Thesis, Cairo University.

Grossman, L.M. (1969), "Thermodynamics and Statistical Mecahnics," Mc Graw-Hill, New York.

Kamel, M.M. (1971), "A Study of Gasdynamic Phenomena Associated with Explosive Reaction", Unpublished Ph.D. Thesis, College of Engineering, University of California, Berkeley.

Kamel, M.M.; Kim, K.B.; Berger, S.A.; Korobeinikov, V.P. and Oppenheim, A.K. (1973a), "On Point Explosions in Heat Conducting and Viscous Gases", Sci. Eng. Bull., Cairo University.

Kamel, M.M. and Oppenheim, A.K. (1973b), "Photographic Laboratory Studies of Explosions", L'Aerotecnica Missile e Spasio, No. 2, pp. 122-134.

Kamel, M.M.; Khater, H.A.; Sefien, H.G.; Rafat, N.M. and Oppenheim, A.K. (1977a), "A Self-Similar Solution for Blast Waves with Transport Phenomena", Acta Astronautica, Vol. 4, Nos. 3-4, pp. 425-437.

Kamel, M.M.; Ghoneim, A.F.; Rashed, I.M. and Oppenheim, A.K. (1977b), "Blast Waves in Real Gases", Acta Astronautica, Vol. 4, Nos. 3-4, pp. 439-458.

Kamel, M.M.; Kuhl, A.L.; Guirguis, R.H. and Oppenheim, A.K. (1979), "Point Explosion Waves in a Detonating Gas", Scientific Engineering Bulletin, 1979/3, Cairo University.

Korobeinikov, V.P. and Levin, V.A. (1969), "Strong Explosions in a Combustible Gas Mixture", ZZv. AN SSSR Mekh. Zhid. i Gaza, Vol. 4, No. 6, pp. 48-51.

Korobeinikov, V.P.; Mil'nikova, N.S. and Ryazanov, Ye.V. (1961), "The Theory of Point Explosion", Fizmatgiz, Moscow, (Engl. Transl. U.S. Dept. of Commerce, JPRS:14,334,C50:6961-N, Washington, D.C., 1962).

Lee, B.H.K. (1967), "Non-Uniform Propagation of Imploding Shocks and Detonation", AIAA Journal, Vol. 5, No. 11.

Lee, J.F.; Sears, F.W. and Turcolte, D.L. (1963), "Statistical Thermodynamics", Addison-Wesley, Massachusetts.

Lewis, C.H. (1961), "Plane, Cylindrical and Spherical Blast Waves Based Upon Oshima's Quasi-Similar Model", AEDC-TN-61-157.

Ohyagi, S. and Ohsawa, A. (1981), "Analysis of Reactive Blast Waves Propagating through Gaseous Mixtures with a Spatially Varying Heat of Detonation" Paper Presented at the 8th International Colloquium on Gasdynamics of Explosions and Reactive Systems, Minsk, USSR.

Oppenheim, A.K. (1966), "Gasdynamics of Explosions" , College of Engineering, University of California, Berkeley.

Oppenheim, A.K.; Lundstrom, E.A.; Kuhl, A.L. and Kamel, M.M. (1971), "A Systematic Exposition of the Conservation Equations for Blast Waves", Journal of Applied Mechanics, pp. 783-794.

Oshima, K. (1960), "Blast Waves Produced by Exploding Wires", Aero. Research Institute, University of Tokyo, Rept. No. 358.

Oshima, K. (1962), "Blast Waves Produced by Exploding Wires", Exploding Wires II (ed. W. Chace and H. Moore), Plenum Press, Inc., N.Y., pp. 159-174.

Oshima, K. (1964), "Quasi-Similar Solutions of Blast Waves", Aero. Research Institute, University of Tokyo, Rept. No. 386.

Oshima, K. (1967), Private Communication.

Rae, W.J. and Kirchner, H.P. (1963), "Final Report on a Study of Meteoroid Impact Phenomena", Cornell Aero. Lab., Inc., CAL Rep. No. RM-1655-M-4.

Rae, W.J. (1965), "Non-Similar Solutions for Impact-Generated Shock Propagation in Solids", NASA CR-54251, CAL. Rep. No. AI-1821-A-2.

Rae, W.J. (1968), "Analytical Studies of Impact-Generated Shock Propagation-Survey and New Results", CAL Rep. No. AI-2456-A-1

Rozhdestrenskii, L.B. (1961), "Thermodynamic and Gasdynamic Properties of Flowing Air Downstream a Normal Shock Wave with Allowance for Ionization and Dissociation", Physical Gasdynamics, Engl. Transl., Murray, R.C., Pergamon Press, New York.

Saad, M.A. (1969), "Thermodynamics for Engineers", Prentice-Hall Series, New Delhi.

Sakurai, A. (1954), "On the Propagation and Structure of the Blast Wave, II", Journal of Physical Society of Japan, Vol. 9, pp. 156-266.

Sakurai, A. (1965), "Blast Wave Theory", Basic Developments in Fluid Dynamics, Vol. 1 (ed. M. Holt), Academic Press, N.Y., pp. 309-375.

Sedov, L.I. (1957), "Similarity and Dimensional Methods in Mechanics", 4th edn. Moscow, (Trans. 1959), ed. M. Holt, Academic Press, New York and London).

Thompson, P.A. (1972), "Compressible Fluid Dynamics", Mc Graw-Hill, New York.

Zel'dovich, Ya.B. and Raizer, Yu.P. (1966), "Physics of Shock Waves and High Temperature Hydrodynamic Phenomena", 2nd edn., Izdatl'stuo Nauka, Moscow, (Engl. transl., Hayes, W.D. and Probstein, R.F., eds., Academic Press, New York, Vol. 1, 1967.